Republic of Iraq

Ministry of Higher Education

and Scientific Research

University of Babylon

College of Engineering

Department of Mechanical Engineering

Investigation of Thermal Conditions and Carbon Dioxide in Different Rooms by Adopting Chilled Ceiling Combined with Ventilation System Under Al-Hilla City Conditions

A Thesis

Submitted to the College of Engineering, University of Babylon in Partial Fulfillment of the Requirements for the Ph.D degree in Engineering / Mechanical Engineering / Power

By

Dhuha Radhi Nayyef Omran

Supervised by

Prof. Dr. Ala'a Abbas Mahdi

2023 A.D. **1444 A.H.**

بِسْمِ ٱللَّهِ ٱلرَّحْمَٰنِ ٱلرَّحِيمِ

﴿ وَمَآ أُوتِيتُم مِّنَ ٱلْعِلْمِ إِلَّا قَلِيلًا ﴾

صـدق الله العلي العظيـم

سورة الإسراء: الآية (85)

Supervisors Certification

I certify that this thesis entitled **"Investigation of Thermal Conditions and Carbon Dioxide in Different Rooms by Adopting Chilled Ceiling Combined with Ventilation System Under Al-Hilla City Conditions**" has been prepared by "Dhuha Radhi Nayyef " under my supervision "*Prof. Dr. Ala'a Abbas Mahdi* " at the department of Mechanical Engineering, College of Engineering, University of Babylon as a partial fulfillment of the requirements for the Degree of Doctor of Science in Mechanical Engineering / Power.

I recommend that this thesis be forwarded for examination in accordance with the regulation of the University of Babylon.

Signature

Prof. Dr. Ala'a Abbas Mahdi

Department of Mechanical Engineering College of Engineering

University of Babylon

Data: / / 2023

ACKNOWLEDGMENTS

First and foremost, I am indebted to the all-powerful almighty God, for giving me strength and ability to understand learn and complete this thesis.

I would like to express my thanks and deep gratitude to my supervisor , who has motivated me with constructive comments , unwavering optimism , and academic guidance throughout the current toward the success of this endeavor.

It is pleasure to thank my college of Engineering/Mechanical department in the Babylon university and special thanks and gratitude goes out the Dean of the College of Engineering (Prof. Dr. Hatem Hadi Obeid) for the efforts to overcome the difficulties . I would like to take this opportunity to thank the staff at Babylon University, mechanical engineering department for their support and teaching and staff of laboratories at the College of Engineering .

I am very grateful to my family specially my dear father and mother and my husband for their continuous support in the implementation of my dissertation and to everyone who helped me with a word or advice

Abstract

Due to the global spread of diseases and epidemics, the need to maintain a clean indoor atmosphere has received increasing attention in recent years. Therefore, there will be a need to clearly estimate and define the areas that affect human exposure to pollutants, taking into account the occupied density, which is the primary importance of this research. The capacity of the chilled ceiling combined with mixing ventilation and a personal ventilation system has been studied and compared with the chilled ceiling with mixing ventilation in terms of mean air life, temperature distribution, CO_2 concentration, thermal efficiency, and thermal comfort parameters such as (average Projected Vote (PMV), Percentage Expected Dissatisfied (PPD) and Air Diffusion Performance Index (ADPI) with the best flow rate of the proposed system considering the occupied density in a thermally insulated office room experimentally and numerically in the climate of Iraq – Hilla city (hot climate and dry). It was chosen as a research area for this system and it is located in the center of Iraq at longitude (44.42ºC) and latitude (32.46 ºC).

Computational fluid dynamics (CFD) model was used in a thermally insulated office room that accommodates three people and in a meeting room that accommodates eight people , under cooling loads (445W), (2316W) respectively using AIRPAK software. Twelve tests were carried out for four different cooling loads treated with the chilled ceiling (0, 25, 50, and 80% relative to the total cooling load) at a constant supply air flow rate (46 l/s) with a personal ventilation air flow rates (5l/s and 7.5 l/s) for three cases (case-I, case- II and case-III) that were experimentally studied and numerically analyzed in a thermally insulated office room. Eight tests were also studied numerically in the meeting room for four different cooling loads that were treated with a chilled ceiling (0, 25, 50, 80%) and a constant supply air flow rate (240 l/s) with a personal ventilation air

flow rate (7.5 l/s) for the two cases (case-IV and case-V). The air supply temperature varies for each case depending on the cooling load treated by mixing ventilation , room air temperature (25°C).

It was discovered that in all cases, as the cooling load treated by chilled ceiling (η) increases, the average air age increases with height. As a result of the use of personal ventilation , the percentage of air age drops below a value of (0.34%) compared to the chilled ceiling with mixing ventilation. A value of (14%) improvement in occupant protection from cross infection was observed with higher personal ventilation airflow rates . In all cases it was seen that the values of (PMV and PPD) decreased from (0.33 to 0.36%) ,(0.25 to 0.30%) respectively with the chilled ceiling combined with mixing ventilation and a personal ventilation system compared to the chilled ceiling with mixing ventilation system at(η= 0 to 80%). The heat removal effectiveness increased by (4-5.12%) at (η = 0-80%) in the chilled ceiling combined with mixing ventilation and a personal ventilation system compared with chilled ceiling with mixing ventilation. The highest values for a seated and standing person were seen between (0.8-0.52°C) for a person standing with chilled ceiling with mixing ventilation system .

This study shows that the chilled ceiling combined with mixing ventilation and a personal ventilation system with a flow rate (7.5 l/s) that provides thermal comfort and higher air quality in the occupied area. Based on the values of air exchange efficiency and occupants air exchange efficiency (η_a , η_D) by (75 to 72%),(99 to 93%) respectively at (η = 0 to 80%) . As a result, flow rate (7.5 l/s) is the best option for protecting occupants from direct pollution in the breathing zone and in the surrounding microclimate., as we note that the longer the stay, the less air change for occupants due to the lower ventilation rate.

Nomenclature

List of symbols	Description	Unit
A_s	Surface area	m^2
A_f	Floor area	m^2
C_p	Specific heat of the air at constant pressure.	kJ/kg.K
$C_{1\varepsilon},C_{2\varepsilon}$	Coefficient in the specific dissipation rate	
CL_{MV}	Cooling load of mixing ventilation	W
CL_{CC}	Cooling load of chilled ceiling	W
dx dy dz	Control volume	m
DR	Daily rang for outlet temperature.	^oC
D	Equivalent diameter of panel (4 area/perimeter)	m
O.D	Occupants density	
E_{ij}	The mean rate of deformation tenser	m
f	Ratio of chilled ceiling area respect to the floor area	
g	Gravitational acceleration	m/s^2
$h_{i,o}$	Convection heat transfer coefficient for inside and outside air	$W/m^2.K$
K	Color factor correct	
K_1	Conduction heat transfer coefficient for first layer of wall.	W/m.K
$k_{i,j,k}$	Turbulent kinetic energy at cell (i,j,k)	m^2/s^2
M	Metabolic heat generation	
N	Total number of draft temperature points measured in occupied zone	
N_θ	Number of points of draft temperature measured in occupied zone	
P	Pressure	N/ m^2
Q_{MV}	Supply air flow rate for mixing ventilation	l/s
Q_{PV}	Air flow rate for personal ventilation	l/s
q	Cooling load for the heat conduction through the walls and transmitted solar radiation	W
R	Thermal resistance	$m^2.K/W$

List of symbols	Description	Unit
S	Source term for the rate of thermal energy Production	J/kg
T	Temperature	^oC
U	Total heat transfer coefficient.	$W/m^2.K$
$u_{i,j,k}$	Velocity at cell (i,j,k)	m/s
u,v,w	Velocity component in x,y, and z-directions	m/s
V_{room}	Volume of room	m^3
Vx	Local air velocity	m/ s
x, y, z	Cartesian coordinates	m

Greek symbols

σ	Prandtl or Schmidt number	---
ρ	Air density	kg/m^3
ε	Turbulent energy dissipation rate.	J/kg.s
η	Portion of cooling load treated by chilled ceiling	
Γ	Diffusion coefficient (diffusivity)	m^2/s
α	Thermal diffusivity	m^2/s
α_r	Relaxation factor	
μ_t	Turbulent viscosity	$N.s/m^2$
S	Modulus of the mean rate-of-strain tensor	
ΔT	Temperature difference	^oC
$\alpha_k,\alpha_\varepsilon$	Coefficient in the specific dissipation rate	

Sub-Scripts

a	Air	l	Overhead light
av	Average	o	Outdoor
c	Correct, convection	oe	Occupants and equipment
rd	Room design	p	Person, plate
e	Equivalent	r	Radiation
ex	External	s	Supply
f	Floor	th	Thermal
hf	Head to foot level.	wr	Water return
i	Indoor, location	ws	Water supply

Abbreviations

ACH	Air change per hour
ADPI	Air Distribution Performance Index
ASHRAE	American Society for Heating, Refrigeration, and Air Conditioning Engineers
AUST	Area-weighted temperature of all indoor surfaces of walls, ceiling, floor, windows, doors, etc. (excluding active chilled surfaces)
ATD	Air terminal device
ACB	Active chilled beam
BZ	Breathing Zone
CC	Chilled ceiling
CFD	Computational Fluid Dynamics
CLF	Cooling load factor.
CLTD	Cooling load temperature difference, depend on type of wall.
CLTDc	Correct cooling load temperature difference
DBT	Dry bulb temperature
DMF	Desk mounted fans
DPV	Ductless Personalized Ventilation
DPV ATD	The desktop Personalized Ventilation Air Terminal Device
DV	Displacement Ventilation
EDT	Effective Draft Temperature
IAQ	Indoor air quality
LM	Corrector latitude and month
ID	Occupants stay in a certain region
LMA	Local mean air age
MV	Mixing Ventilation
PAQ	Perceived air quality
PMV	Predicated Mean vote
PPD	Predicted percentage dissatisfied
PPM	Part Per Million
PV	Personal Ventilation
Pr	Prandtl number
RNG	Re-Normalization Group
SBS	Sick Building Syndrome
SC	Shadow coefficient.
SHG	solar heat gain.
UFAD	Under Floor Air Distribution
VATD	Vertical air temperature difference
VAV	Variable air volume

Table of contents

CHAPTER ONE

INTRODUCTION

Chapter One

Introduction

1. General Concept

The health, comfort, and productivity of office workers are all affected by the thermal climate and indoor air quality,**[1].** Heating and cooling systems consume around 40% of a building's total energy. As a result, heating ventilation air condition (HVAC) engineers have a difficult time creating pleasant conditions in low-energy environments, necessitating the development of new technologies,**[2]**. Mixed ventilation (MV) is a traditional system that has been used in many modern buildings since the 20th century .But since the cold supply air is reheated at a large flow rate , the energy consumption of the medium-voltage system was significant**,[3].**

Combining an mixing ventilation system with a radiant cooling system can be an effective way to reduce the energy consumption of an HVAC system because a radiant cooling system can provide some reasonable cooling load to the room, allowing the cold air flow rate to be significantly reduced and directly supplied to the room without reheating **,[3].** Convective heat transfer between cooled surfaces and indoor air as well as system cooling capacity will increase as a result of the combination of chilled ceiling with mixing ventilation**,[4].** But when an mixing ventilation system is combined with a chilled ceiling system, the chilled ceiling will cause a draft slump, which can affect how the air is distributed inside the room **,[4].**

The system chilled ceiling with mixing ventilation also works with a central control system to maintain a unified indoor environment in the occupied area, and this cannot satisfy all passengers as air is provided from a distance from the passengers and is mixed with polluted room air before entering the breathing areas of people**, [5].**

Several review studies have demonstrated that there is strong and sufficient evidence for most diseases to establish the link between ventilation and air movement in buildings and the spread of pathogens such as SARS, highlighting the importance of indoor environmental control **,[6].** As a result, personal ventilation has the potential to achieve efficient air distribution that delivers clean air directly to the breathing areas and allows individual microclimate control at each workstation **,[7].** On the other hand, personal ventilation systems are not able to remove a significant portion of the sensible heat load generated in areas due to low air flow rates and minimum air temperature restrictions**, [7,8].**

Therefore, an experimental comparison of the thermal internal environment produced by chilled ceiling with mixing ventilation and the other system reveals that the chilled ceiling with mixing ventilation can produce a somewhat more uniform thermal environment than chilled ceiling combined with mixing ventilation and personal ventilation **,[9].** Where, with the chilled ceiling combined with mixing ventilation and personal ventilation system, the supplied cold air is well mixed with the ambient air to ensure even and uniform vertical distributions of room air velocity, temperature, and pollutant concentration in the indoor room **,[9,10].**

Previous research has shown that the combination of personal ventilation and mixed ventilation with a cooled ceiling is an effective way to increase thermal comfort and improve perceived air quality in rooms with temperatures above the maximum standard (26°C)**,[10].** Changing from total volume to target air distribution in workstations can also improve the perceived air quality. Most of the previous studies dealt with ventilation and the chilled ceiling system but did not focus directly on the occupied density index. It will be needed to estimate and clearly identify areas affecting human exposure to pollutants.

1.1. Ventilation Systems:

This section discusses two different types of ventilation systems (personal and mixing ventilation).

1.1.1 Personalized ventilation system (PV):

It is an air distribution system that enables occupants to individually control local ventilation, **[10]** as shown in Fig.(1-1). Personal ventilation delivers clean, cool air at a low speed (did not exceed 0.25 m/s in the breathing zone) with minimal turbulence to the occupants' breathing areas . It has been demonstrated that the configuration of the air terminal devices (ATD), its location in relation to the occupant, the supply flow rate, the customized airflow's supply flow volume, as well as the temperature and target area size discrepancy between room air and personalized ventilation airflow, are all factors that affect the amount of personalized air inhaled **,[10].** While it was pointed out that (PV /ATD) can be optimized to achieve (100%) breathing zone air distribution effectiveness, the optimum efficiency for most of the (ATD) has not exceeded (50–60%) of clean air with each inhalation**,[7].**This system is ideal for providing a thermally comfortable atmosphere for occupants of commercial office buildings, and it also has the ability to minimize the possibility of airborne infectious disease transmission in the indoor environment thereby lowering total air conditioning energy demand **,[10].**

i. Personalized ventilation's energy-saving potential

The energy-saving potential of personalized ventilation has been documented in the literature. The following are the primary ways mentioned in the literature to save energy with tailored ventilation **,[11]:**

1. Reducing the exterior airflow rate due to PV's increased ventilation effectiveness.
2. Using PV's ability to generate a controlled microclimate to extend the room temperature comfort limitations
3. Personalized air is only delivered when the occupant is at the desk

ii. Advantages of the personalized ventilation system

PV systems have the following advantages over total volume (TV) systems in terms of mixing ventilation, displacement ventilation, and underfloor air distribution **,[11]:**

1. Possibilities for enhancing the quality of breathed air.
2. increased thermal comfort due to the ability of each occupant to customize and alter the temperature, flow rate (local air velocity), and direction of the specially customized air that is delivered to each location according to personal preferences.
3. Possibility of boosting employee output.
4. Possibilities of reducing the risk of infectious pathogens being spread through the air.

Fig.(1-1) Principles of personal ventilation system **,[10]**.

iii. Disadvantages of the personalized ventilation system

1. Due to smaller airflow rates and limitation of the lowest supply air temperature personalized ventilation systems are not able to remove substantial amount of sensible heat load generated in spaces. In such cases additional cooling system is needed.
2. PV may promote mixing of exhaled pathogens with room air when the infected person uses PV. There may be a risk for other occupants who do not use PV for protection in the same room.
3. Complex airflow interactions in the breathing zone should be considered as they may interfere with the transmission of infectious agents
4. The photoelectric flux interacts with large droplets (>5 μm) and is less effective in the transmission path of small droplets

1.1.2 Mixing ventilation system (MV)

Mixing ventilation was one of the first studies that Boyle Son in 1899, **[10]** , as shown in Fig.(1-2). To maintain a consistent temperature distribution and lower pollutant concentrations throughout the structure, supply air is pumped in from the roof or wall and mixes with the room air**,[10].** Inertia forces the flow for the air supply. In this system his ventilation efficiency is about (51) % indicating a well-mixed environment in the room; the air supply is achieved at a speed of (2–8) m/s and a temperature of (9–40) C **,[6,10].** As a ventilation system, it can be used to cool and heat a room which providing thermal comfort to the occupants .

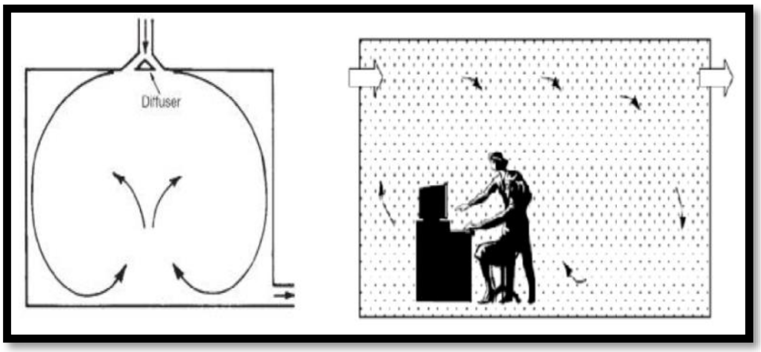

Fig.(1-2) Mixing ventilation system**, [10].**

1.3 Chilled Ceiling System (CC)

It is a technique used to removes sensible heat by convection and radiation as HVAC system or to minimize cooling load Fig.(1-3). Willis Carrier began developing designs for under-sill induction units in the 1920s, which gave rise to the chilled ceiling **,[12]**.The air attaches to the chilled ceiling, gets colder, and then falls to the floor. After that, hot air rises from the heat source in the below region, resulting in a steady passive air movement known as convection, which cools the space chilled ceiling's pipes are installed over metal ceiling plates, and the cooled plates are the source of radiation and convection, **[12]**.

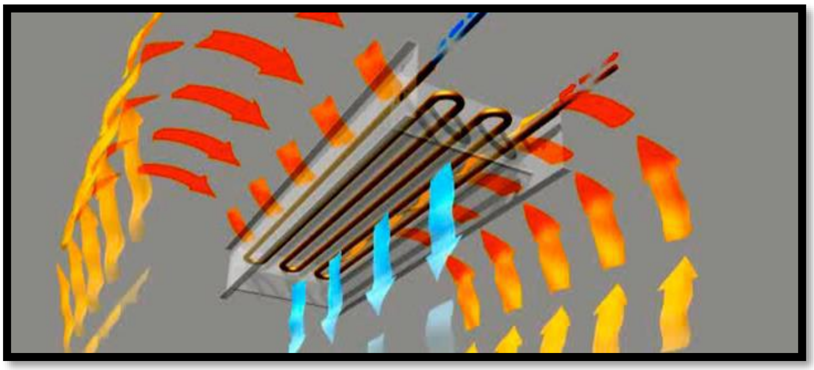

Fig. (1- 3) Natural air circulation with chilled ceiling ,**[12].**

1.3.1 Advantages of chilled ceiling

In comparison to other air conditioning technologies, chilled ceilings equipment offers superior benefits . For example, **[12,13]**:

1. More energy-saving (about 20 %)

2. Chilled ceilings save (27% - 30%) of peak capacity than fan coil units.
3. As compared to fan coil units, chilled ceilings use higher-temperature water flow.
4. Lower life time prices, no moving parts, and quieter operation.
5. Ensure the highest level of thermal comfort.

1.3.2 Disadvantages of chilled ceiling

1. Chilled ceiling systems cannot be used alone in buildings where the ceilings are higher than 2.7 m (8.9 ft), because the air will not properly circulate. A forced-air circulation system must be employed in such cases .
2. If the water temperature is too low or humidity is high, condensation on the beam can occur leading to a problem known as (internal rain)
3. Chilled ceiling systems are not recommended for areas with high humidity (such as theaters, gymnasiums, cafeterias). Because they are less effective at cooling .
4. Hospitals generally cannot use chilled ceiling systems because of restrictions on using recirculated air, cause noticeable air circulation which can make some people uncomfortable .
5. Some designers have found that enlarging the ducts around active chilled ceiling systems to increase air circulation causes echoes in working areas and amplifies the sound of water moving through the pipes to noticeable levels.

1.3.3 Types of chilled ceiling

i. Radiant chilled ceilings

The radiant chilled ceiling is a metal or plaster board surface that includes absorption of heat directly generated from hot surfaces inside the room through radiation and convection via chilled water pipes running through them, as seen in Fig.(1-4). It's ideal for buildings with a lot of vertical space.

The benefits of a sparkling cooled ceiling are summarized as follows**, [13]**:

1. Since insulation is added to the upper side of the cooled roof, the useful ventilation in the room is below the ceiling.
2. Direct absorption of heat radiated from heat sources reduces cooling energy consumption by (15% - 20%).
3. A ventilation system is essential as a separate source of fresh air.
4. Radiant chilled ceiling provides an acceptable architectural look, decent comfort levels due to the low air velocity distribution

ii. Radiant and convective chilled rafts

The cooled water coil is mounted at the back of the big flat panels that are hanging under the roof as seen in Fig.(1-4). Its benefits are summarized in**, [12,13]:**

1. The back of the panel has no insulation added .
2. Sails may be used to provide efficient radiant heating .
3. Heat is transferred to the room through natural convection.
4. The raft receives further natural convection.

iii. Convective chilled ceiling

In this type Fig.(1-4) a collection of fins attached to a chilled water conduit is usually used in these systems. This form has the benefit of**, [13]:**

1. Cooling the fins is accomplished by transferring heat from cooled water to copper and then to aluminum.
2. Heat convection through the angled fins accounted for more cooling air than radiation
3. This system has more cooling than a traditional radiant system, but less than the passive coolant beam

iv. Radiant cooled ceilings (plaster board finishing)

Small-bore plastic capillary coils of this sort, as shown in Figs.(1–4) , are mounted to the wall or ceiling frame and have a plaster finish applied to them.

A specialized thin plaster is required to counteract the effects of decreased thermal conductivity,**[13].**

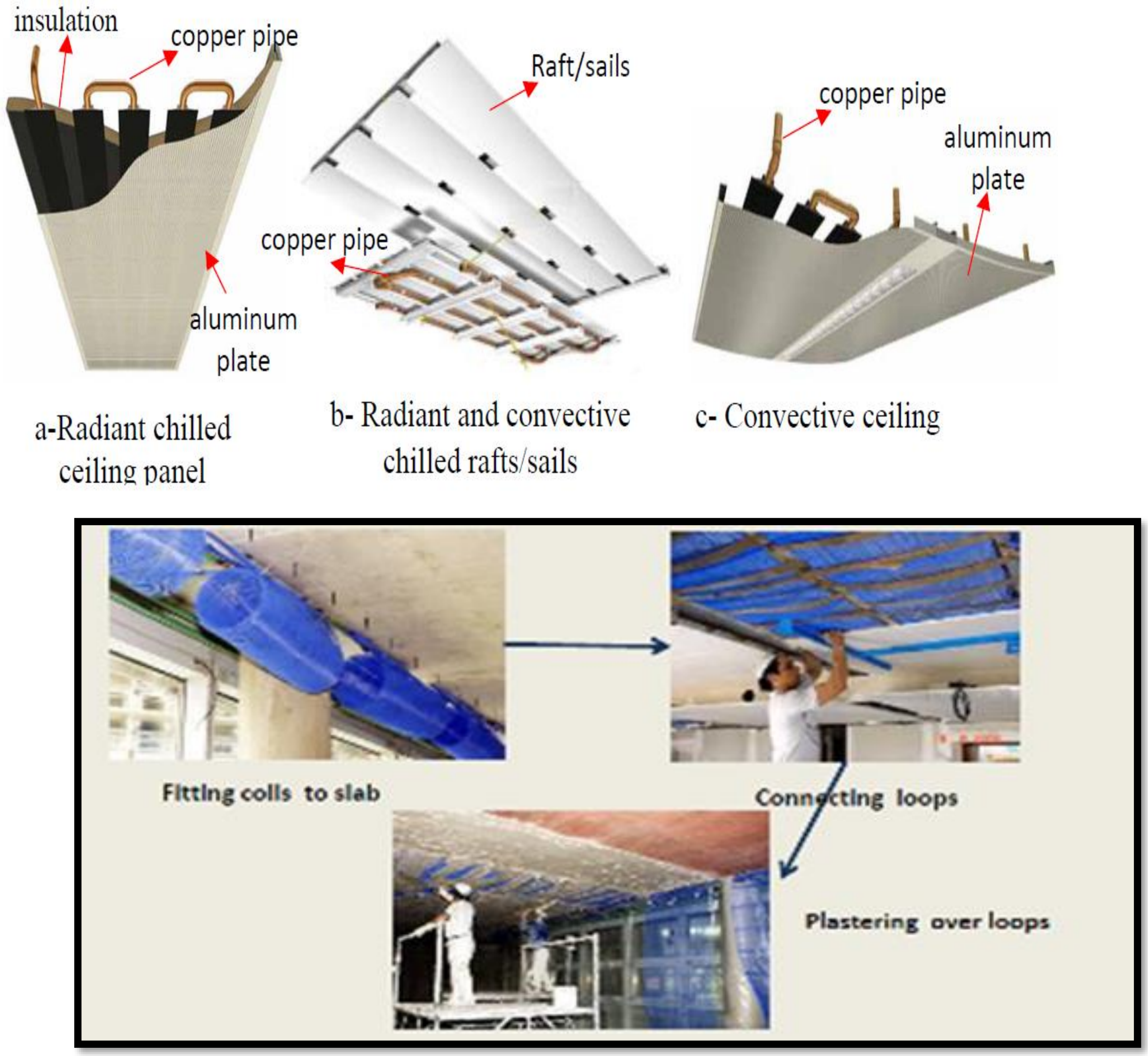

d- Plasterboard with a radiant plate

Fig.(1-4) Illustrate the several types of chilled ceiling, **[13].**

1.4 Age of Air

The age of air was studied in the early 1980s, and a novel technique was adopted as the ability of the ventilation process to replace the old air in a room with fresh air **,[14].** The local mean age (LMA) was regarded as the average time elapsed between entering fresh air and it reaching a certain point in the room, Fig.(1-5). Moreover, the average room air age was defined as the average time required for outside air to reach all local points in the room, and it could be used to measure the overall ventilation performance inside the room. Since the supply air does not blend perfectly with the space air, much of the time the air is exhausted from the room until it is full of indoor pollutants. As a result, varying concentrations will exist in the occupied region, and a higher air supply rate will be needed to reach the threshold limit value,**[14].** If assume the room mean air age. The nominal time constant (an) of a ventilated zone (the ratio of zone volume to the air flow rate supply) **,[14].**

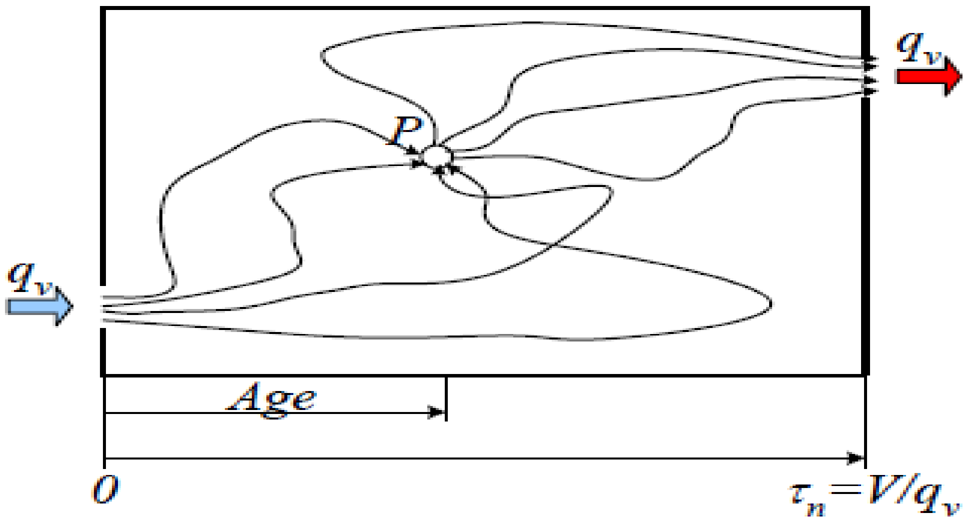

Fig.(1-5) The age of the air in the room**,[14].**

1.4.1 The purpose of calculating the age of air

Calculating the age of air has a specific function. Knowing the age of the air in a closed space will give us a lot of information, such as:

1. Assessing indoor air quality in a confined space .
2. Denotes how effectively the ventilation system swaps out the stale air in the room for brand-new, fresh air**, [14]**
3. Controlling air emissions.
4. Assess the effectiveness of the ventilation system.

5. Indoor air quality improves as the air age decreases.

1.4.2 Method for determining the age of air:

It is important to employ a tracer gas to determine the local air age in a room. To determine the local air age there are three methods, **[14]:**

1- Step down method : at the start of the test, when the injection is discontinued, a uniform concentration of tracer is attained, Fig.(1-6).

2- Step-up method : from the start of the test to the end, the tracer is injected at a consistent rate at the air inlet Fig.(1-6).

3-Tracer pulse method : at the beginning of the experiment, a short tracer pulse is discharged into the air inlet.

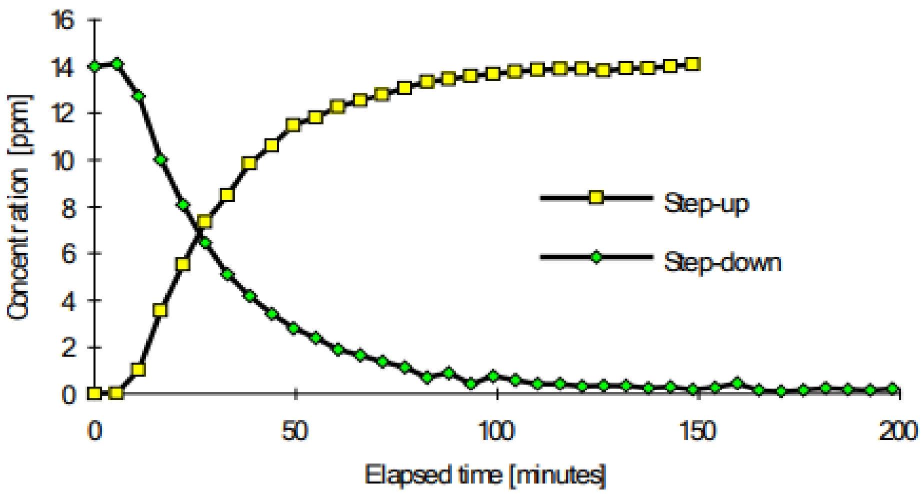

Fig.(1-6) Variation of concentration over time during measurements of air age**, [14]**.

1.5 Combined personalized Ventilation with Chilled Ceiling system

The combined system of the chilled ceiling and personalized ventilation exemplify an effective design framework**, [15].** The combination of (PV) with (CC) has the ability to provide more efficient cooling of occupants because convective and radiant cooling are exacerbated. Its combines between the energy efficiency of personalized ventilation system with energy-saving of chilled ceiling lead to increase ventilation capacity due to the convective and radiant cooling are exacerbated**,[11].**

Ventilation for massive sensible cooling loads is given by personalized ventilation, which can be combined with a cooling ceiling, as shown in Fig.(1-7). Many commercial office designs currently incorporate this combined framework as a design alternative. The cooling capability of the used personalized ventilation system was just about (30–40W/m^2) of floor area,**[15].** Combine external cooling systems, such as a chilled beam or chilled ceiling tiles, to increase the cooling power absorb.

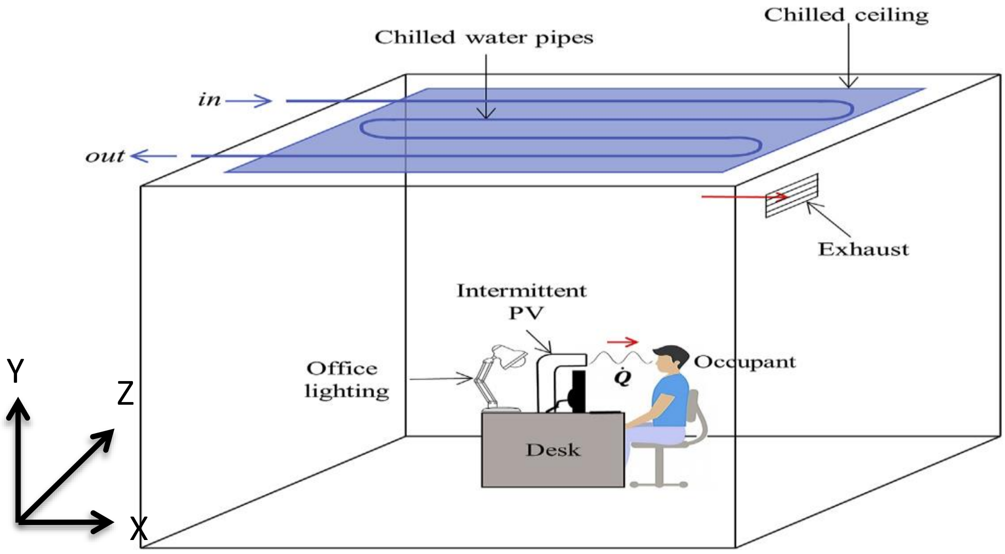

Fig.(1-7) A diagram of an office area with chilled ceiling and personal ventilation system, **[15].**

1.5.1 Energy savings of personalized ventilation and chilled ceiling

A combination system of customized ventilation and cooled ceiling is a viable HVAC solution for hot regions, as shown in Fig. (1-8) , **[15] :**

1. It was demonstrated that the suggested combined system can save a significant amount of energy savings of up to 40% were achieved when compared to a standard variable air volume (VAV) solution.
2. The most efficient technique is to raise the room temperature and provide customized air at (20-22)°C. It provided for a reduction in energy consumption about (48%) compared to reference mixed ventilation cases, as well as a reduction (27%) in room humidity in hot climes.

3. Raising the design room temperature was a successful technique for lowering energy consumption.

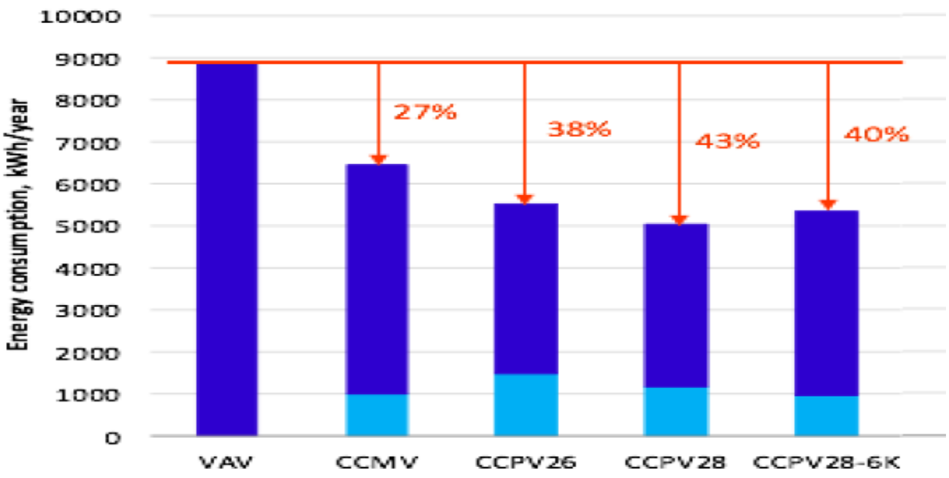

Fig.(1-8) Annual energy use at two levels of solar heat gains, **[15].**

1.6 Ventilation for Air Quality

The term "ventilation" refers to the process of replacing indoor air with clean, new air. Certain compounds were discovered to have higher concentrations inside than outside. This may be because such contaminants are generated internally by inhabitants and their behaviors, or because of other factors. As a result, appropriate amounts of pollutants in outdoor air must be defined for use in building ventilation. Concentrations of many indoor contaminants are mentioned in the ASHRAE handbook of fundamentals, **[2].**

1.7 Thermal Comfort

The word 'thermal comfort' refers to a person's psychological state of mind, and it is most commonly used to describe whether or not they are too hot or cold. Thermal comfort is defined as "a state of mind that reflects happiness with the thermal environment," according to ISO 7730 or ASHRAE**, [2]**.

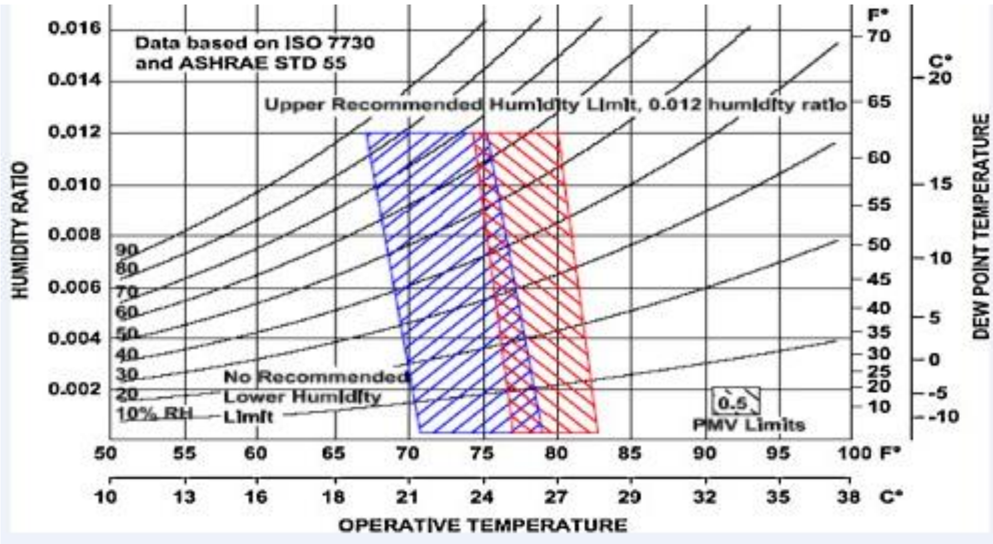

Fig.(1-9) ASHRAE comfort chart for occupants **, [2].**

1.7.1 Predicted Mean Vote (PMV)

Fanger (1970) described the PMV model as an index that predicts the population's average vote on a seven-point thermal sensation scale, from (+3) for cold interior air to (-3) for hot interior air as shown in Fig. (1-10).In accordance with ASHRAE recommendations, the ideal range of (PMV) for sufficient internal comfort is

(-0.5<PMV< 0.5) **,[14].**

1.7.2 Predicted Percentage Dissatisfied (PPD)

(PPD) forecasts the proportion of people experiencing extreme heat discomfort. According to (-0.5<PMV< 0.5) **,[14]**, the maximum PPD for an ideal temperature condition is 10%, as shown in Fig. (1-11).

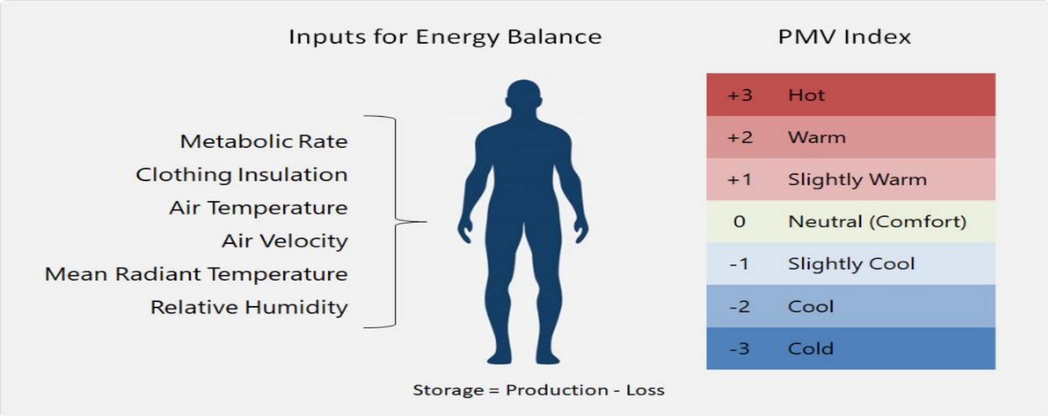

Fig.(1-10) Thermal comfort requirements based on (PMV) ,**[14]**.

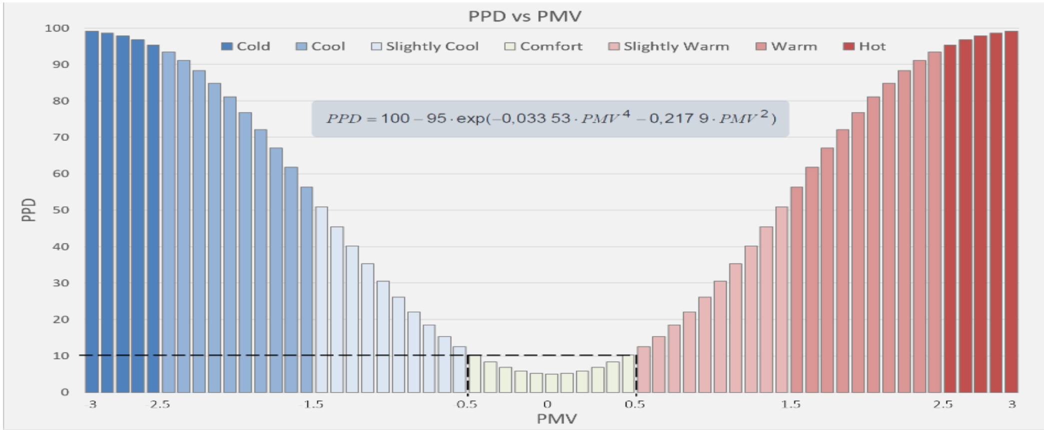

Fig.(1-11) Predicted Mean Vote vs. Predicted Percentage Dissatisfaction,**[14]**.

1.7.3 Air diffusion performance index (ADPI)

An air distribution system's total performance, or the level of comfort it offers, can be measured using the (ADPI) metric. When divided by the total number of temperature points in the same area, it is determined as a percentage of the total number of temperature points in an occupied zone with an EDT value between (-1.7 and 1.1) C ,**[14].** For cooling mode operation, a (ADPI) value of (80)% is often appropriate , **[14].**

1.7.4 Effectiveness of Temperature distribution

The ventilation system that can provide the required level of thermal comfort in a ventilated space is defined by the ventilation efficacy at a local location for the temperature distribution. It must have a value larger than one,**[10].** Because the temperature of the expelled air is higher than the normal interior air temperature,

1.8 Contaminants in Office Room

Many common products used in offices can give off pollutants and odors, as can office equipment such as copiers, printers and fax machines. If any of these items are used in the office environment, adequate and sometimes separate ventilation should be provided. Pollutants and odors (which may or may not indicate a health concern) generated in space may not only bother those in the immediate area, but may enter the building ventilation system and cause problems for other tenants in other parts of the building.

- **Indoor Air Pollutants and Health**

Asbestos.

Building and Paint Products.

Carbon Monoxide.

Carpets.

Cleaning Supplies and Household Chemicals.

Cockroaches.

Dust Mites.

Formaldehyde.

1.9 Contaminants Control

Contaminants management is an important function for ventilation. Understanding the characteristics and importance of primary contaminants and pollutant origins is also important. Indoor contaminants come from both outside and inside outlets, and of these sources necessitate various ventilation management methods to maintain good health and comfort**, [11,9]**. All percentages of CO_2 in indoor air are shown in a table(1-1).

Table(1-1): Classification of Indoor Air Quality **, [9]**.

Category	**Description**	**CO_2-level of indoor air in ppm**	
		Typical range	**Default value**
(I)	High indoor air quality	<400	350
(II)	Medium indoor air quality	400-600	500
(III)	Moderate indoor air quality	600-1000	800
(IV)	Low indoor air quality	>1 000	1200

1.10 Occupancy and Occupants Activity in Buildings

The fundamental aspects of human existence in the built environment," were described and debated by Farbstein,(1974) were: the activity's nature; the performers, i.e. the person or group of people who are conducting the activity; and the time sequence in which the events take place, **[15].** There is a lot of research that the efficacy of building ventilation has a big impact on the efficiency of those who work there**, [9].** Employee efficiency is harmed by poor indoor air quality in the workplace. It has also been found to cause health problems in the household, **[11]**.

1.10 Objectives of the Present Work

The following are the primary goals of this work:

1. Created and constructed an experimental test rig with a chilled ceiling and mixed ventilation with personalized ventilation for various case studies.
2. Investigation experimentally and numerically the effectiveness of the chilled ceilings combined with mixing and personalized ventilation system in terms of contaminants of air and compare it to the chilled ceilings with mixing ventilation system, taking into account the occupied density index, under the climate of Iraq - Hilla city
3. Assessing how the air age and human thermal comfort metrics are affected by the change in the portion of cooling load treated by chilled ceiling.
4. Evaluation of the effectiveness of the personalized ventilation (PV) system and determining the best (PV) air flow rate operation that assists the chilled ceilings with mixing ventilation in terms of thermal comfort and IAQ.
5. Reaching the acceptable situation in terms of air age and human thermal comfort for humans provided by the system's performance under hot and dry conditions

CHAPTER TWO

LITERATURE

REVI

EW

Chapter Two

Literature Review

This chapter's major goal is to summarize some current and previous activities and studies that are directly related to the areas of the (CC/MVPV) system in terms of (indoor air flows, indoor pollutants, and occupants activity , PV/MV systems alone and CC alone) .

So that the knowledge gap is discovered and research hypotheses are developed based on the literature review.

Despite the fact that the cooled ceiling technology predates the development of blend personal ventilation with mixing ventilation, it has recently gained notoriety in commercial applications as well as academic literature. Therefore, there is a growing interest in examining the indoor air quality (IAQ) and thermal comfort of the combined system taking into account occupant activities in space. Experimental measurement and computer simulation are the two main methodologies used to investigate and predict detailed microclimate conditions.

This literature review is subdivided into four main topics:

2.1 Theoretical Studies.

Zhao et. al. (2012), [16] studied numerically occupant air-exchange efficiency by taking into account variable occupancy levels in office room under China-Beijing climate. Three case studies were presented at different types of ventilation system (a large-space ventilation, PV , DV) case with dimensions of (X ,Y ,Z) (3×10 × 5) ,(3 × 2.7 × 5) , (5.16 × 3.65 × 2.43) m with the supply airflow rate were (9,1,5 ACH), the supply air temperature was (13°C). These cases were validated by three dimensional simulations by utilized (STACH-3) software for time-dependent HVAC, the (standard k-ε, Zero equation) turbulence model are utilized to account for the turbulent flow in a room. The PV nozzle was separated from the occupant by (30cm) . The results show that the occupant air-exchange efficiency is a superior metric to employ when evaluating a room's ventilation effect.

Khan et. al. (2017), [17] examined numerically the energy saving potential of radioactive cooling systems for office buildings in four cities in different climatic regions of India. The performance of a radiant cooling system was evaluated in an office building, total area of the building, about (24,000)m^2. The building consists of two symmetrical sides; one side of the building is cooled by the radiant cooling system with a a dedicated outdoor air system (DOAS), whereas the other side uses a variable air volume system. Fresh air is delivered from (DOAS)at a rate of (2.5 l/s per person). The DOAS unit is connected to an energy recovery unit at (25°C). The chiller set point for leaving cooled water is around (7°C) on the conventional side and (15 to 16)°C on the radiant side. The data showed that energy saving for Bengaluru, Chennai ,Ahmedabad, New Delhi respectively of (27,11, 6, 3)%.

Franchesca et. al. (2017), [18]examined the relationship between ventilation efficiency, building layouts and the local air age , which is defined as the time it takes for fresh air to replace old air when it enters a specific zone. The standard (RNG k-Ɛ turbulent model) was used in numerical studies with Fluent software. The calculation domain was set at (x: 1000 m, y: 1000 m, z: 180 m).The results revealed that the local air age is greater in complex areas with a high density of structures than in contrasted locations. Some urban characteristics, such as the fraction of unoccupied land, have been discovered to boost ventilation efficiency.

Gao. et. al. (2018), [19] examined numerically the interrelationship between human thermal comfort and heat exchange between the human body and its surroundings subject to the radiant air conditioning system to master the features of it and improved its design processes a room with dimensions of (4.72 x 3.55 x 2.75) m . The surface temperatures of the cooling ceiling were varied from (16.9 to 24) ºC, the air humidity and velocity have been set to (50% and 0.21 m/s), respectively.. AIRPAK3.0 software was used to solve the radiation heat transfer by using (RNG k-Ɛ turbulent model). The sensible heat loss from a human body under a radiant air conditioning system was essentially linear to the PMV under all simulated situations, according to numerical calculations. Finally, the simplified PMV model is provided, which is based just on the consideration of human thermal balance rather than complex ambient characteristics.

SzczepanikŚcisł. (2018),[20] determined numerically the effectiveness of the personal ventilation system at different flow rates and test if the PV can provide protection for occupants from cross-contamination. Different air flow rate were simulated around the occupants' face of (15, 10, 5 , 1) l/s. Fresh air was provided through a series of (5 mm) holes in the air flow terminal device, which was a round air unit with a diameter of (180mm) and a series of (5mm) holes. The air device was put (70 cm) in front of the test mannequin's face. To see how the velocity altered around the occupant's face, the air flow rate was reduced from (15 to 1) l/s. The findings indicated that the personal ventilation system may not be a reliable cross-contamination defense when the air flow is minimal.

Liu et. al. (2019),[21] compared the thermal comfort, ventilation effectiveness, and energy consumption of a radiant floor cooling system when combined with various ventilation systems, including mixed ventilation (MV), sheet ventilation (SV), displacement ventilation (DV), and personal no-duct ventilation (DPV), in the tested room (3 x 2 x 4) m with two air change rates of (1.2, 2.4) h^{-1}. With two air change rates of (1.2, 2.4) h^{-1}, the (MV, SV, DV, DPV) systems were settled at (20, 22, and 24°C). In the DPV system, a flow rate of (2 l /s) was established for the personalized air system, which was draw out at a suction height of (0.1m).Vertical air temperature differences (VATD) at ankle and head level, the proportion of unsatisfied, and the ankle level draught rate were the main evaluation indices used. According to the research, the (VATD) in (DV) systems can reach up to (5°C), compared to about (2°C) in MV and SV systems. In the DV and DPV instances. A higher draught rate at the ankle level, ranging from (6.55 to 9.99%) , with (2.4 ACH). The lower comparable temperatures for the foot and calf segments occur when the floor temperature is (20°C). The associated whole-body temperature values consistently indicate an appropriate level of thermal discomfort.

Li et. al. (2020), [22] presented a design strategy for radiant cooling systems in low-energy buildings from the perspective of the interior environment's thermal response properties. Two different types of modular radiant cooling systems were investigated: the copper tube radiant cooling (CTRC) and the capillary radiant cooling (CRC) systems. Two energy-efficient office spaces measuring (L,W,H) (5.8 x 3.2 x 3.2 m each) were used for the tests at Tingyi University in Shanghai, China. A total of (16) cases—eight for CTRC and eight for CRC—were investigated, with supply water temperatures ranging from (12 to 19)°C. The findings showed that the temperature of the supply water has a bigger influence on the temperature distribution of the envelope for CTRC than it does for CRC. Additionally, when using CTRC rather than CRC, the thermal response of the envelope is much more sensitive to both lower supply water temperatures (below 16 °C) and higher supply water temperatures (above 15 °C) , raise indoor air's thermal stability speed more quickly than CRC.

Qin et. al. (2020), [23] developed a simplified predicted mean vote (PMV) model and a sensible cooling load equation based on human thermal comfort. The link between thermal comfort qualities, design, and operation parameters was investigated using Airpark simulations. To solve the airflow field, a two-equation k-ε turbulence model was used. The simulated room's overall dimensions were (3.4 x 3 x 3)m, with the north wall serving as the external wall and the air supply intake and outlet, which are (1.2 x 0.6)m and (0.3 x 0.3)m respectively, are also positioned on the south and east walls. In the simulated scenario, the indoor air velocity was less than (0.15 m/s), which met the requirements of the occupied zone's limit values. When the fresh-air supply temperature was (26°C), the ideal radiant surface temperature was (19 to 23) °C. The results revealed that the interior air temperature is connected relatively linearly with radiant surface temperature, fresh-air supply temperature, and the area ratio, with relative humidity having little effect.

Khalil et.al.(2020),[24] examined numerically the impact of employing a hybrid ventilation system equipped with personalized ventilation units on energy consumption saving while maintaining thermal comfort and good air quality of an office floor in Beirut. The PV will be adjusted to (22°C and 10 l/s) to produce the desired cooling effect while preventing thermal draft in an office with a total size of (240 m^2). The macroclimate temperature is predicted to range between (23, 29) °C. Using an indoor air speed, RH of (0.15 m/s, and a 55 %) humidity level, an estimated PMV value of (0.53) was determined for average office workers. The PV-chiller has a rated capacity of (2.7 kW) and a rated input power of (1.42 kW), giving it a rated COP of while operating at full load and at a temperature of around (40°C) (1.9). The new cooling strategy results in the (VC) system running for fewer hours and saving (53%) in energy compared to the base case when using only the (VC) system.

Katramiz et.al. (2020),[25]studied the interaction between human breathing with the intermittent personalized ventilation (IPV) jet, as well as its effectiveness in giving clean breathable air under relaxed background pollutants' concentration conditions in office space were of (3.4 x 3.4 m x 2.8)m equipped with (MV) system as shown in Fig.(2-1) . The breathing air quality of the IPV user was assessed using the tracer gas method at various IPV operation frequencies. Maximum ventilation effectiveness (ε_V) ranges during inhalation were found to be (36.75–86.6)% for nose breathing,(49.6–87.3%)for mouth breathing(42.42–86.93)% when breathing was not considered at an IPV frequency of (0.5 Hz). Due to the stronger dilution given by horizontally exhaled air, the nose breathing mode had the (lowest ε_V), whereas the mouth breathing mode had the highest(ε_V). The average (ε_V) for nose and mouth breathing was nearly identical to that of no-breathing, resulting in acceptable air quality at the (BZ).

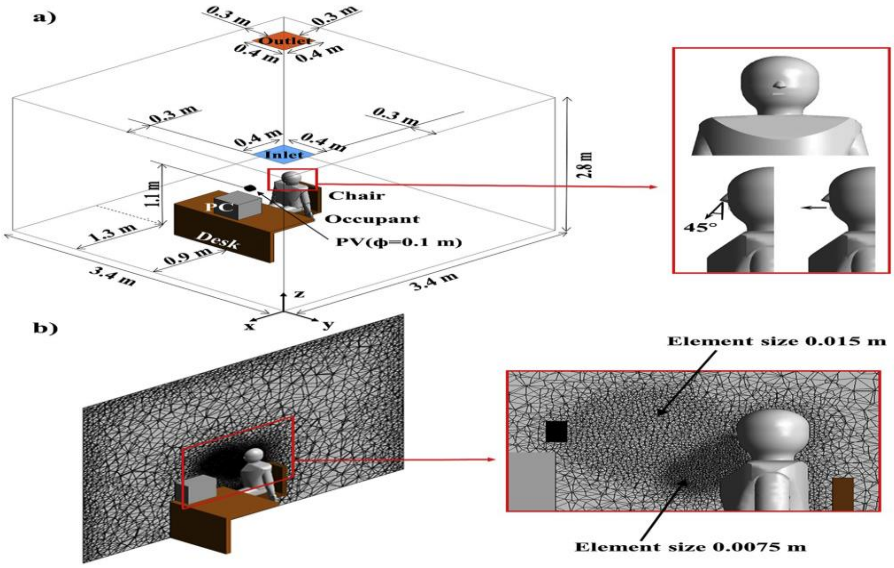

Fig.(2-1) Simulation model by Katramiz et.al.,**[34]**.

Ihab. et. al. (2020), [26] examined the influence of various locations of the intake and outlet air ventilation, as well as their interaction with heat sources and air distribution, on the indoor environment in modeling of an office space with mixed ventilation. ANSYS FLUENT software was used in numerical analyses (RNG k-Ɛ) turbulence model used to simulated turbulent flow. The case study was an office room in Malaysia of dimensions (4.8 x 4.8 x 2.65)m with two inlets and outlets with dimensions of (0.4 x 0.4)m, (0.55 x 0.43)m with one outlet having a diameter of (0.3m).The first inlet was located in the center of the room's upper level. The distance between inlet one and inlet two was (0.19 m), while the distance between the room's middle and the center of outlet one or two was (0.45 m). The study looked at four distinct locations in four separate situations with eight lines , four in different corners and four surrounding the heat source. It also looked at the Air Distribution Performance Index and ventilation efficacy as indicators of air distribution improvement. The results revealed a considerable increase in (ADPI) from (33 to 83)%, as well as an improvement in the indoor thermal environment thanks to the altered inlet and outlet positions.

Al Assaad et. al. (2020), [27]verified numerically and compared the performance of intermittent PVU assisting with chilled ceilings and mixing ventilation for improve comfort and saving energy of two office spaces with dimensions of (3.4×3.4× 2.8)m, total load of (40 W/m^2) . At an average flow rate of (7.5 l/s), the intermittent jet was delivered to an infected occupant. In each case, the duration of the intermittent PV was altered. In the case of a cold ceiling under medium to warm circumstances, the intermittent tailored ventilator was proven to provide higher thermal comfort (14%) increase compared to (MV) systems. Mixing ventilation, on the other hand, saved twice as much energy as chilled ceilings in terms of energy savings. As a result, intermittent (PVU) under (MV) systems is preferable than continuous (PVU).

Itani et. al. (2021),[28] studied numerically thermal comfort correlation in naturally ventilated areas with customized ventilation in a (240 m^2) office space in Beirut was developed statistically using multivariable linear regression while preserving factors based on significance and interdependency. The design temperature and relative humidity for interior air were set at (25^{o}C and 50%) , respectively. On the basis of the correlation, it was determined that the indoor temperature, relative humidity, facial temperature , and its rate of shift were all related. In order to compare simulated and expected (TC very comfortable) at a standard error of (0.4) with a maximum deviation of, sample data from the studies used in constructing the correlation were used (1.0).

Alsaad and Voelker. (2021), [29] evaluated numerically the inhaled pollutant concentrations when using (PV,DPV) system and the effect of the two system on thermal comfort and inhaled air quality in a simulated office room (3×3×2.44)m and total cooling load (55.3W/m^2) with two occupations: a sensitive occupant and a source occupant, indoor air temperature (26°C), Personalized and room ventilation flow rate (10, 20) L/s, (60, 75) L/s respectively. Exhalation/inhalation Constant with a velocity of (0.77m/s) and air temperature of (34°C).The results showed that (DPV) performance better than the desk fan of eliminating exhaled pollutants, but desk fan better of eliminating pollutants released from a passive source above the floor level. Both of systems are highly dependent on the location of the pollutant source.

2.2 Experimental Studies

Lipczynska. et. al. (2015), [30]studied experimentally contaminants distribution and inhaled air quality by using ventilation systems (PVCC,MV,MVCC, MVCC/PV) for two thermal manikins, a heat gains of office room (66-72) W/m^2 was simulated at room air temperature between (26 , 28) ºC .The suspended ceiling of the chamber was fitted with (18) radiant panels and dimension of each one (1190×590×20) mm, fully occupied (75%) of the floor space as shown in Fig.(2-2). At a temperature of (25°C), air was delivered by individualized ventilation. The total flow rate supplied varied between (26,82)L/s. Results show that (PV/CC) can in decrease of pollutants concentration in the inhaled air by (12.4 - 84.4) % and of the airborne infection risk by (35.4-80.9) % comparing to (CCMV and TVMV).

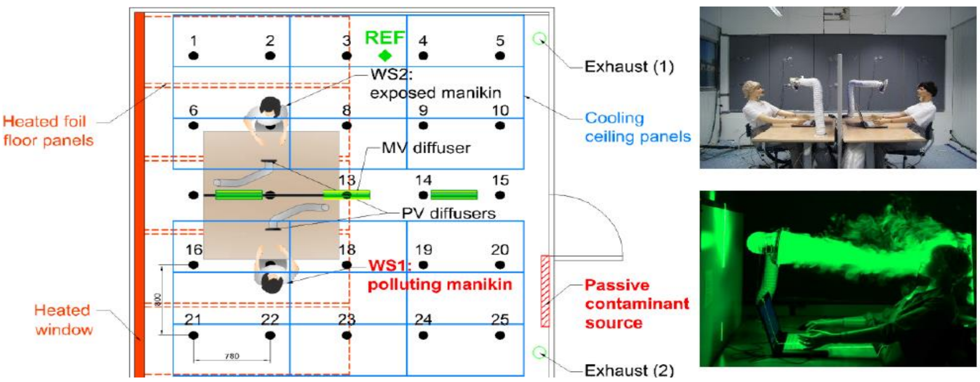

Fig.(2-2) Tested room: plane view with measurement points (1-25) and reference point (REF); on the right – view of the test room by Lipczynska. et. al. ,**[40].**

Yuan et. al. (2015), [31] developed a simplified relationship between heat flux and temperature differential to obtain the limiting values of total heat transfer coefficients of tested room with area of (15.12 m^2) located at Tongji university. The height of the internal cooling ceiling was (2.4 m) and covered the ceiling area (49%). The walls of the room tested were made of stainless steel with windows on the south wall. The temperature of all walls was controlled using water pipes, only the south wall is insulated and the other walls are simulated as if exposed to outside weather at a temperature of (1040ºC). Three cases were investigated as a function of three different plate structures with a surface temperature of (1420 ºC) . The total heat transfer coefficient fluctuated slightly in the absence of strong solar radiation, with the internal heat source evenly distributed.

Lestinen et. al. (2019), [32] studied compared indoor air thermal conditions and draft discomfort for diffuse ceiling ventilation (DCV), chilled beam (CB), and chilled ceiling with mixing ventilation (CCMV) systems on thermal conditions and draft discomfort at various heat loads. Experiments were conducted in two office rooms of (L,W,H) (4.1 x 4.2 x 2.9),(5.5 x 3.8 x 3.2)m , the heat gain strength was increased from a typical level of (37-40 W/floor-m^2) to a peak load level of (57-64W/floor-m^2) at the desired interior air temperature was 26 ºC). The cooling panels of the (CC/MV) system were installed at a height of (2.9 m) in the suspended ceiling, the cooling panels took up (77%) of the ceiling space. To distribute supplied air in two directions to the test chamber, two linear diffusers of (Lx H) (472 x 20) mm were placed. At a height of (2.5 m), the (CB) system placed an exposed chilled beam and a coil with a total length of (3.0 m) and a coil length of (2.1 m). The findings show that at a typical load, the air temperature, air speed, and draft rate were all acceptable, but increased marginally at peak load. For the studied systems, the thermal conditions were identical, (CC/MV) system, on the other hand, may minimize draft discomfort slightly more than (10%).

Wu et. al. (2020), [33]focused experimental on evaluated the influence of ceiling surface temperature on indoor air flow characteristics with (MVCC) system , as the internal and external sensible cooling loads increased from (41.5 to 69.5) W/m^2 in tested room (3.7 x 2.8 x 2.6)m equipped with the (CC) system consisted of (11) metal radiant panels (600x600)m with a coverage rate of around (76%).When increase the cooling load, lead to increase the average vertical air temperature difference, turbulence intensity, and contaminant removal effectiveness were (30-36) %. Results found that in a space with mixing airflow, the chilled ceiling had a minor effect on the indoor air circulation. With various internal or external cooling loads, it was discovered that a slight vertical air temperature discrepancy corresponded to significant turbulence strength and contaminant removal effectiveness**.**

Tian et. al. (2020), [34] studied experimentally and numerically the occupant thermal comfort utilizing radiant ceiling cooling and an overhead air distribution system (RCF) in a hot and humid summer, an office building in Suzhou .With five rounds of survey and measurements at varied indoor temperatures. Over the summer, (135) data sets were obtained from (44) participants. The results showed that the whole-body thermal sensations with the radiating roof and the upper air system deviated from the (PMV) model in the operating temperature range (23.6-28.6) ºC in summer, and the neutral temperature with the (RCF) around (26ºC), passenger preferred temperature was around (25.3ºC) with RCF. The pre-computed percentage rate of dissatisfied (PPD) is (13.9%), but the actual thermal environment dissatisfaction rate was (8.3%) with an acceptance rate of only (1.5%), which is much better than the calculated (PPD).

Xu et. al. (2020),[35]evaluated experimentally the effectiveness of (PV) on the risk of cross infection between two occupants in close proximity (less than one meter) of tested room with dimension (5 x 3.5 x 2.5)m equipped with (MV). The temperature of the supplied air was set at (16.5 ºC) and the conditioned supply air kept the room air temperature and humidity at (25.5 ºC and 36 %).The air change rate was set to (2 h) and which corresponds to a (24.3 l/s) air flow rate. There were three different flow rates used (3, 6, 9)l/s with initial turbulence intensity of the nozzle jet less than (5%) and the length of the clean air core was (3–4) times the diameter of the nozzle (50.8 mm). For starters, applying (PV) to the source resulted in almost (90%) of the target being exposed indirectly. Second, the direct exposure of the target was increased by nearly (50%)

due to the (PV) jet's direct entrainment from the infectious exhale. These results show that (PV) may only be an infection-prevention strategy if it is maintained with high ventilation efficiency at the inhalation zone, which may

be accomplished by decreasing infectious flow entrainment and boosting clean air volume.

Chakroun et.al. (2020),[36] studied experimentally the capacity of (CPV) system with (DF/CF) to provide thermal comfort to occupants was studied. Climatic chambers are equipped with ceiling personalized ventilation (CPV) system assisted by chair fans (CF) and desk fans (DF) in two experiments. Experiment participants were placed in a transitional setting with traditional mixed ventilation (MV) at (24 °C) and a RH of (50%.When the fresh air flow rate was (20 CFM), (93) % of the participants felt thermal comfortable during the first (30 min) at temperatures from (21-22 ℃). Because the overhead temperature decreased to (19.5) °C, most participants didn't feel comfortable at high flow rates of (25 and 30) (CFM).

Auerswald et. al. (2020), [37] investigated experimentally the effectiveness of push-pull ventilation aerators. Performed (15) tests a tracer gas analysis in room with dimension (2.77×2.70×5.00)m with two push-pull devices with Summer, winter, and isothermal supply air conditions are all included in the testing because this parameter variation has been missing in push-pull devices up to this point. The results revealed that air exchange efficiency varies depending on boundary conditions, always falling below the range of $(0.5 < \eta_a < 1)$, suggesting a lack of air exchange including short circuiting, It increases with increasing heat load Depend on the distance between the interior apertures and the temperature differential between inside and outside, local air exchange values imply inhomogeneous air renewal.

8] investigated experimentally the impact of the **3Shin et. al. (2021), [** open-type installation and air circulators on the cooling capacity and energy performance of the CRCP system with dimensions were (3.8 x 3.7 x 2.9 m). On the ceiling of the test chamber, twenty-five (CRCPs) were mounted. Each CRCP had a (0.6x 0.6)m footprint and was made out of a perforated aluminum panel (thickness = 3 mm), a chilled water pipe, and a heat conduction plate. The ceiling surface was (14.06 m^2) and the (CRCP) surface was (9.0 m^2)Compared to a conventional CRCP system, the cooling capacity of an open-type CRCP system with air circulators increased by up to (26.2) %, and its cooling energy consumption decreased by up to (26.4) %.

2.3 Experimental and Numerical Studies.

Chludzinska and Bogdan(2015), [39] investigated experimentally the minimizing exposure to indoor contaminants by applying a wearable personal ventilation at (23) °C The tested were carried out in a climatic chamber (2.5 x 3.0 x 3.0)m with the help of (20 participants) , simulated ambient temperature similar to that of an office working environment. The ambient temperature (T_a) was kept at (18, 20, 22, 24, 26, 28) ºC during the winter and summer months, the relative air humidity was kept constant at (50%).Controlling the flow interaction near a person's face by injecting a decreased volume of clean air at velocity (0.2–0.6 m/s) into the breathing zone is crucial to the customized ventilation device's efficiency. The quality of the inhaled air improved by (94)% when using wearable PV. In addition, over six times decreased the number of secondary infected travelers compared with (MV)

Ning et. al. (2016), [40]evaluated experimentally and numerically energy savings performance, surface temperature distribution and cooling capacity for cooling radiant ceiling panel(CRCP) of test room with dimensions were (2.4 x 1.8 x 1.9)m. To increase the cooling capacity, three enhanced (CRCP) types with a thin air layer were presented had a uniform surface temperature distribution, for condensation control in China's hot and humid climate. The cold water temperature was (12ºC), the flow rate was (0.107 m^3/h), and the cooling load capacity was about (85.9W / m^2).The thickness of the thin air layer between the aluminum plate and the copper tube was (1 mm). In comparison to the original CRCP, cooling capacities have improved by (43- 46) %, while surface temperature distribution remains uniform.

Mahdi and Hassan (2016), [41]evaluated the performance of ventilation (displacement and mixing ventilation system) with regard to indoor air quality and air flow distribution in room under Iraqi Climate . The inside dimensions (length, breadth, and height) of the test chamber were (4 x 3.5 x 3.75)m at indoor temperature (25-28) °C as and 1bar as pressure, during three weeks in May 2015. The air conditioning system was turned on until the temperature in the test rooms reached (23°C). The results show that compared to the mixing ventilation, the use of floor displacement ventilation reduces the concentration of pollutants in the breathing area, but indoor spaces are more prone to disturbance due of high temperature.

Al Assaad et. al. (2017), [42] investigated and improves the performance of sinusoidal flow PV system combined with mixing ventilation (MV) system to predict thermal comfort and IAQ. Experiments was tested in a climatic room were dimensions of (2.75 x 2.5 x 2.8)m. The velocity, temperature, and CO2 fields around the occupant microclimate were assessed using CFD and validated with experiments. Average PV flux of

(7.5 L / s at 0.94 Hz) was ideal for (MV) temperature of (26) °C and a PV temperature of (22) °C. In optimum conditions, a comfort level of (0.95) was obtained and a ventilation efficiency of(77)%. PV energy cost reduced by (21.34)% compared to static PV system with equal thermal comfort.

Al Assaad et. al. (2018), [43] presented experimentally study of the ability of intermittent personalized ventilation (PV) system equipped with chilled ceilings to shield occupants from active particulate matter as a result of an indoor pollution source. The velocity, thermal, and particle concentration fields in the space were calculated using (CFD). The experiments were conducted in a climate chamber with dimensions of (2×2.75×2.8)m at an average personalized ventilation flow rate of (7.5 L/s) and (CC) covers (80%) of the ceiling surface area as shown in Fig.(2-3). It was found that intermittent personalized ventilation does not increase comfort or air quality at lower chilled ceiling temperatures (16°C), hence steady flow personalized ventilation is advised. Intermittent individualized ventilation working at (0.5 Hz), as opposed to continuous tailored ventilation, improved comfort at typical chilled ceiling temperatures of (20°C). In comparison to a stable system and a standalone chilled ceiling under identical comfort conditions, the intermittent (PV) was able to save (7.52, 15.04)% of energy, respectively.

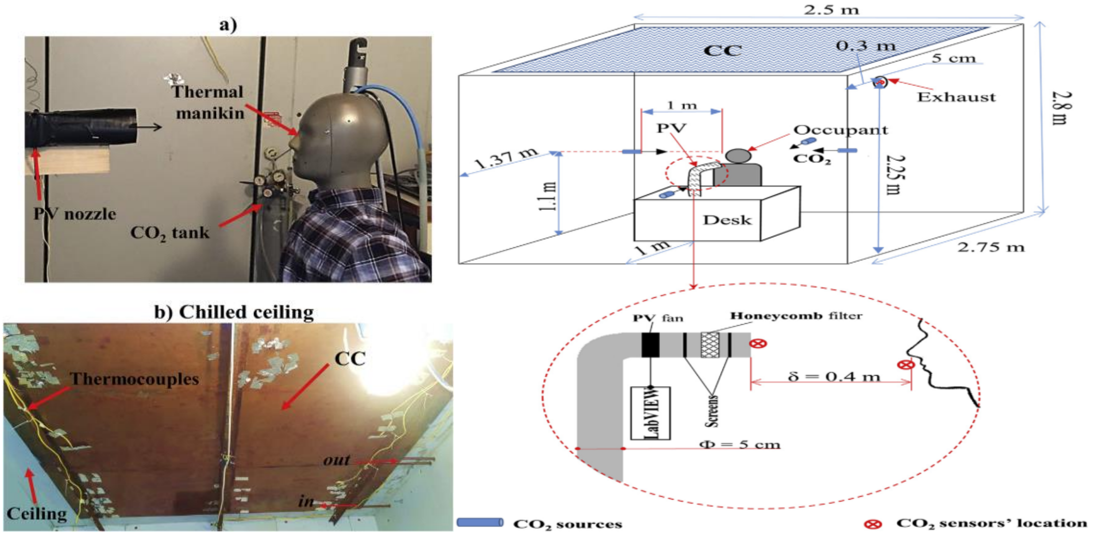

Fig. (2-3) Tested room studied by Al Assaad et. al.,**[73].**

Al Assaad et. al. (2018), [44] studied experimentally and numerically the efficiency of intermittent periodic personal ventilation combined with mixing ventilation in terms of its ability to keep occupants safe from pollutant in the space. Use the CFD model to assessed velocity, temperature, and particle concentration. The CFD model and the tests agreement well. The size of the office room (3.4m x 3.4m x 2.8 m) . It was discovered that an average flow rate of (7.5) L/s and an operational frequency of (0.86) Hz offered appropriate intake fractions and deposition rates in the breathing zone and a thermal comfort (0.87), ventilation (77.1 %).

Cao. et. al. (2018), [45] investigated experimentally and numerically the effect of vent inlet size (ratio D/L) on ventilation efficiency with regard to indoor air flow pattern and pollutant dispersion for five configurations with various inlet sizes under three different air change rates by using a dimensionless time scale ratio (proportional to (Ri /α), Richardson number (Ri/ α)(mass flux ratio) at dimension of test room (1×1×1)m with the ventilation intake and outlet are (0.18 ×0.05 m) (length x width) as shown in Fig.(2-4).When (CO_2) leaves the bucket at (20°C), it quickly exchanges heat with the surrounding air. Under three distinct (ACHs), studies were conducted for five different configurations with varied inlet sizes (D/L ratios of 0.2, 0.4, 0.6, 0.8, 1) (4, 10, 16) ACH. The results showed that (Ri / α)is smaller for cases with a small size ratio (critical value ≤ 10^{-3}) than for cases with larger ones, indicating superior pollutant removal performance. The data demonstrated that (Ri / α) is less for cases with a small size ratio (critical value 10-3) than for cases with larger ones, indicating greater pollutant removal efficacy. These insights can simplify and improve the basic ventilation plan of a building.

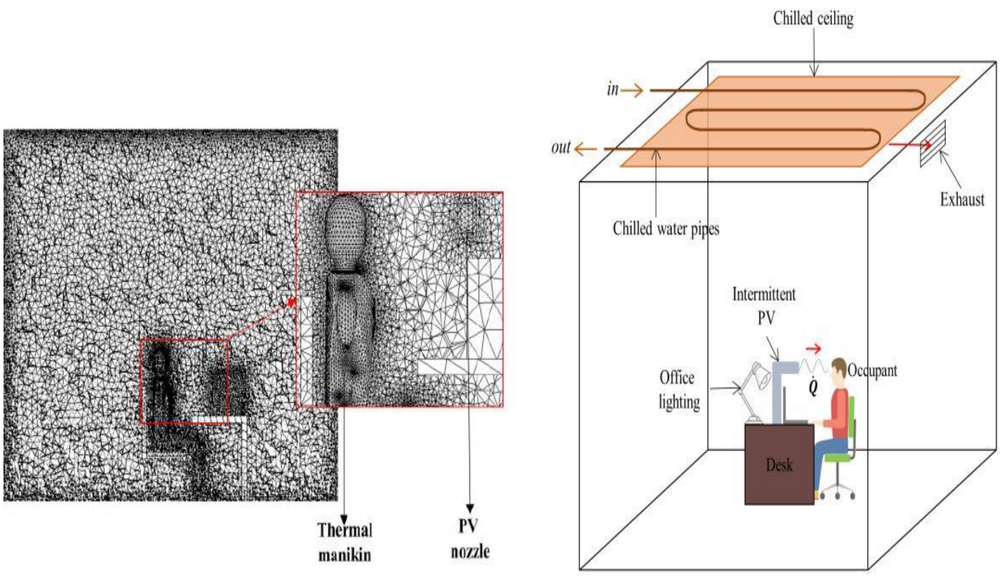

Fig.(2-4) Simulation model by Cao. et. al.,[76].

Yuan et. al. (2019), [46] studied experimentally and numerically the relation between the total heat flux and the radiation system's surface temperature area . The radiant system's operating limit zone was discovered and suggested by graphing crucial parameters like supply water temperature, operating panel surface temperature, and total heat flux density on a single surface as shown in Fig.(2-5). The supply water temperature was allowed to fluctuate between (14,20)°C and (34,40)°C, whereas the designed interior operating temperature increased from (24 to 30)°C in cooling mode and (16 to 24)°C in heating mode. Following steady state for at least 1800 seconds for each experiment, the inner surface temperatures of the climate chamber were maintained constant (within 0.5°C). It was discovered that not every point within the operating limit region was appropriate for practical application in order to prevent the possibility of water condensation in the cooling mode and significant temperature variations in a vertical direction in the heating mode in the heating position.

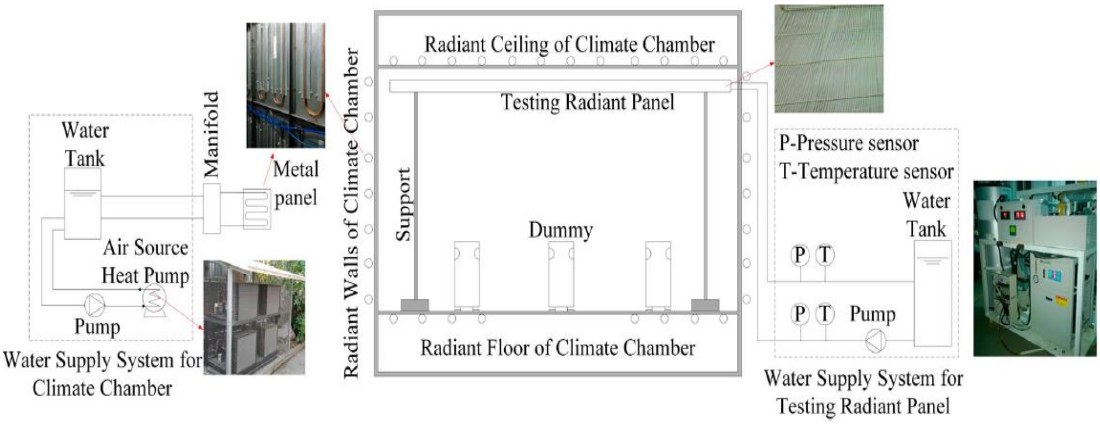

Fig (2-5) Tested room studied by **Yuan et. al. ,[77].**

7] investigated the difference of temperatures on the **4Su et. al. (2019), [** whole cooling panel surface, as well as a basic specification map for the new (CRCP) system and validated by a comparison analysis with the experimental data. The experiment was carried out in Zhuhai, China, in a room with measuring(8.18 x 6.55 x 2.33)m. The chilled water flow rate was roughly (0.22 m^3/h), the exterior diameter of copper pipes is (10mm), and the center-to-center distance between two adjacent parallel copper pipes was(0.20m). For cooling panels to provide a uniform surface temperature distribution, computer calculations suggest a thickness of (4-5 mm). Additionally, enhancing flow disturbance in the air layer to improve heat transfer between aluminum sheets and cooling panels is feasible, which will help to lower the initial cost by utilizing less pipe materials in the (CRCP) system.

Csáky et.al. (2020), [48] verified experimentally and numerically of the developed personal ventilation system (ALTAIR PV) by testing eleven different pneumatic terminal devices and proving that only five devices generate disturbance intensity less than (20%). The apparatus has (160) duct fan with continuous speed control .The diameter of the air duct was lowered from (160 to 100) mm to allow for the connection of air terminal devices at (10, 20, 30, 40, 50) cm from the ATDs, airflow was set to (30, 40, 50 m^3/h) . For these ATD classes, the mean turbulence intensities were (15.56, 7.36, and 7.52)%. The turbulence was quite high for the other six ATDs: (74.72, 59.52, 68.04%). It was demonstrated that the thermal comfort experience can be significantly enhanced when indoor temperatures are high. The amount of background noise and the noise produced by the unique ventilation system were measured using a variety of techniques. It was established that the air distribution system has to be improved.

Jin et. al. (2020), [49] investigated the dynamic change of surface temperature of radiant ceilings in regulation the supply water flow. Dimensions of the test room (5 mx 3m x 2.4m height) . It was found that condensation on the radiant ceiling panel surface easily avoided when the cooled water source is turned off .The ceiling panel was comprised of nine U-shaped capillary metal radiant plates. The capillary had outer diameter and inner diameter (2.7, 4.3)mm, and a (10mm) tube spacing, chilled water at temperatures between (7,12)°C. Size of the air supply outlets, which were (200 x 200) mm, situated on the east wall. According to simulation results and statistical analysis, the surface temperature for fixed source water flow is primarily affected by three variables: the equilibrium temperature of the non-cooling surface, the indoor air temperature, and the internal surface temperature of the outside window. (47.6, 39.2, and 10.1%) of the total is attributable to these variables.

Xie et. al. (2020), [50] studied numerically and experimentally the effect of water supply temperature, mass flow rate, heat load distribution, and radiant roof capability on radiant roof capacity and thermal comfort conditions . In tested room (45.6) m^3 with capillary ceiling radiant cooling plates, increases in water temperature and air supply velocity are used to produce uniform ceiling surface temperature distribution as shown in Fig (2-6). The test room's two side walls were installed with air supply inlets and air return outlets that were (0.4x0.2)m, and (0.7x0.2)m, respectively, in size. The average surface temperature of the ceiling rose from 16.9 to 21.5 C when the ventilation system was shut off, while the temperature of the inflow water rose from 16.9 to 20.1. The relation between indoor air temperature and internal heat load was beneficial, however the association between indoor air temperature and air supply velocity is adverse.

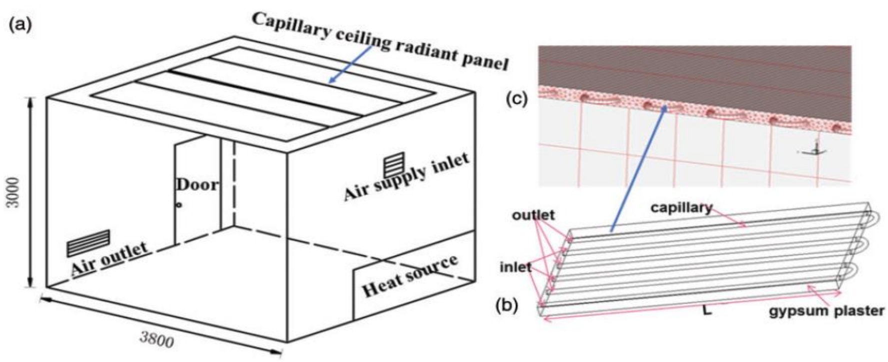

Fig.(2-6) (a) Tested room with a C-CRCP system, (b) a U-type capillary matting, and (c) an unstructured computational grid by Xie et. al**.,[82].**

Ye et. al.(2020), [51] investigated numerically and experimentally compared to (RCCP) system without ventilation, the cooling performance and indoor thermal comfort of the (RCCP) system with forced ventilation. (2.7 x 2.7 x 2)m is the size of each chamber. The right chamber, the test cell, has four radiant ceiling panels that measure (1.782 x 0.583)m and were suspended (0.19 m) below the ceiling. The left chamber's temperature is adjusted to (40°C). The space is inside heated by four fake cylinders, while the exterior is heated by heat gain from the left room. Energy is produced at a rate of (59.8W/m^2) by each cylinder. The chiller controls the fluid's flow rate and temperature to (18°C, 1.7 L/min). The ANSYS FLUENT multi-physics model is used to resolve the relationship between fluid flow and heat transfer inside a closed enclosure. The turbulent kinetic energy is calculated using the conventional k-Ɛ turbulence model. The results show that CFD model had a good agreement with the experimental results and the ventilation system is effective to decreases the indoor air temperature by (1.2)°C and enhanced the cooling performance of the RCCP and saves more energy.

Khail (2020),[52] created a self-contained, autonomously controlled personalized ventilation (PV) device that can be used in a naturally ventilated (NV) office space to maintain appropriate thermal comfort (TC) under a variety of indoor circumstances and activity levels of an office floor in Beirut. The NV-office space was (240 m^2) in size, with fifteen inhabitants (90W/occupant). Indoor temperature has a temperature range of (25 to 33°C) with a relative humidity of (55 to 80 %). The PV closer to the body (typically at 40 cm from the occupant) to ensure that PV flow reached the face at the temperature close to the PV supply conditions were (22 to 26°C) and (0 to 15 l/s) for PV (the velocity of the air near the face might vary between (0.2 and 1 m/s). The new cooling strategy results in the (VC) system running for fewer hours and saving 53% in energy compared to the base case when using only the (VC) system.

Zhang et.al. (2020), [53] studied numerically and experimentally the variations in indoor air quality and thermal comfort between four ventilation methods (ceiling supply, return to ceiling, ceiling supply, return on side wall , side wall supply and return to ceiling) (SSW-RC) and supply on side wall and back wall side were tested numerically and experimentally .The office's dimensions were (9.45m × 7.8m × 3.5m) m. when the outside air temperature ranged from (10 to 3)°C. In numerical investigations, the k-epsilon turbulence model was employed with ANSYS FLUENT software. Room air inlet and outlet (16,32) °C, (15 ACH) .Results reveal that according to the indoor average PM2.5 concentration, SSW-RSW may give the best indoor air quality. SSW-RSW and SSW-RC can improve interior thermal comfort by (29–36)%.

Katramiz et.al. (2021),[54] investigated experimentally and numerically the impact of individual flow control of PV on the risk of cross-pollution in the workplace for two occupants sitting in tandem(either face to face or back to face) with two contaminant sources (breathing, coughing) with an office room of dimension(3.4×3.4×2.6)m conditioned by a (MV/PV) system, and the PV flow rate control range from (0 to 13) l/s, ensuring that thermal comfort . Utilize CFD to calculate the inhaled intake fraction (iF)index, which compares the mass of pollutants ingested by a healthy individual to the mass exhaled by an infectious person, to identify cross-contamination. When (PVi 4 l/s) in tandem and (PVi > 9 l/s) in facing orientations, a modest exposure for healthy people. The average (iF) of facing seating was lower than that of tandem seating by (31% coughing) and (86% breathing).

Al Assaad . et. al. (2021), [55] focused experimentally and numerically on the PV systems' impact on reducing inhalation exposure to indoor particles is weighed against their contribution to particle deposition contamination of garments of typical office tested were of (3.4×3.4×2.6)m was estimated to be conditioned by an MV system, which was served by its own air handling unit in this study (AHU). It brought conditioned external clean air in through a rectangular grille diffuser (0.45 ×0.25)m in the ceiling and discharged it through a ceiling diffuser (0.45×0.25)m. Inhalation exposure (iF) and garment pollution performance (DFr) of three PV ATDs (computer mounted panel (CMP), vertical desk grill (VDG) and round movable panel (RMP). An experimentally tested 3D CFD model of an office with MV + PV was created. Main conclusion was: As opposed to standalone MV, CMP decreased iF by up to (89 %) and DFr by up to (72% at 5 l/s). As compared to MV, VDG reduced iF by up to (91%) while increasing DFr by up to(12 % at 10 l/s) .As compared to MV, RMP decreased iF by up to (97 %) while increasing DFr by up to (80 %at 10 l/s)

Shbeeb .(2021), [56] studied experimentally and numerically the impact of air supply diffuser shape on air age and thermal comfort characteristics , the time required to remove pollution (such as CO_2) by using combined displacement ventilation and chilled ceiling system (DV/CC) in the office room at dimension of (3×2.5×2.5m) under Babylon (Iraq) climate. AIRPAK3.0 software was utilized to simulate office room (RNG k-ε turbulent model). The major findings revealed that as the cooling load treated by the chilled ceiling grew, the local air age increased CO_2 concentrations in the (CC/DV) system rise with height, but this effect fades as the proportion of cooling load treated by chilled ceiling rises. The semi-circle diffuser had advantages in terms of decreasing CO_2concentration and air age. When compared to a rectangle diffuser, it tends to improve (PMV), (PPD), and (ADPI) while also providing improved thermal comfort.

Table (2-1) Summary of numerical studies

Reference	Year	Place of study	Main focus	Findings
Zhao et. al. [16]	2012	Tsinghua University (China)	Occupant air-exchange efficiency	Used occupant air-exchange efficiency to boost the ventilation effect assessment criteria
Khan et. al. [17]	2017	Centre for Energy (India)	Energy saving potential of radioactive cooling systems	The largest energy savings from an energy recovery wheel were reached (6,3,and 8%) Ahmedabad, New Delhi and Chennai, respectively
Franchesca et. al. [18]	2017	Osaka University (Japan)	Concept of air local age	Local age of air in complex sites is greater than in contrasted sites
Gao. et. al. [19]	2018	Xi'an University (China)	Interrelationship between human thermal comfort and heat exchange	The sensible heat loss from a human body under a radiant air conditioning system is essentially linear to the PMV
SzczepanikŚci sł. [20]	2018	Cracow University (Poland)	Effectiveness of the PV system	When the air flow is low, PV may not be effective in protection From cross contamination
]1Liu et. al. [2	2019	Shandong University (China)	Design concept for radiant cooling systems in low-energy buildings	For CTRC compared to CRC, the temperature of the supply water has a bigger effect on the temperature distribution of the envelope.

]2Liu et. al. [2	2019	Shandong University (China)	Compared performance of radiant floor cooling system combined with different ventilation system	In all cases thermal discomfort that is tolerable according to the body's comparable temperature levels
]3Qin et. al. [2	2020	Southeast University (China)	Developed a simplified (PMV) model and a sensible cooling load equation based on human thermal comfort	the interior air temperature is connected relatively linearly with radiant surface temperature, fresh-air supply temperature, and the area ratio, with relative humidity having little effect
Khalil et.al.]4[2	2020	American University (Lebanon)	The effects of using a hybrid ventilation system with PV units	The new cooling method reduces the amount of time the VC system is in operation and saves 53% of energy.
Katramiz]5et.al.[2	2020	American University (Lebanon)	Effective the IPV+MMV system performance	IPV MMV units reduced the number of AC operating hours while maintaining thermal comfort
Ihab. et. al.]6[2	2020	Tun Hussein University (Malaysia)	Impacts of inlet and exit air locations on air distribution, thermal comfort	Improvement in the indoor thermal environment due to the altered positions
Al Assaad et.]7al. [2	2020	American University (Lebanon)	Compared the performance of intermittent PVU assisting with CC and MV	The intermittent PVU was found to offer better thermal comfort of 14 % as compared to MV system.
Itani et. al.]8[2	2021	American University (Lebanon)	Multivariable linear regression to develop TC in (NC with PV) system	For a number of different hierarchical thermal environments, the presented technique can be used to derive TC correlations.
Alsaad and Voelker. [29]	2021	Bauhaus-University (Germany)	Performance comparison DPV and DF	DPV performance better than the desk fan of eliminating exhaled pollutants

Table (2-2) Summary of Experimental Studies

Reference	Year	Place of study	Main focus	Findings
Lipczynska et.al. [30]	2015	Silesian University (Poland)	Contaminant distribution and inhaled air quality by using ventilation systems (PVCC, MV, MVCC and MVCC/PV)	(PVCC) can in decrease of pollutants concentration in the inhaled air by (12.4-84.4 %) and of the airborne infection risk by (35.4-80.9)% comparing to (CCMV and TVMV).
Yuan et. al. [31]	2015	Tongji University (China)	A simplified correlation between heat flux and temperature difference	The size of the heat flux can be determined separately in different radiation systems
Lestinen et. al. [32]	2019	Aalto University (Finland)	Compared of (DCV), (CB), (CCMV) systems of thermal conditions	For the studied systems, the thermal conditions were identical , CCMV, on the other hand, may minimize draft discomfort slightly .
Wu et. al. [33]	2020	Dalian University (China)	Influence of ceiling surface temperature on indoor air flow characteristics with MV+CC	In a space with mixing airflow, the chilled ceiling had a minor effect on the indoor air distribution
Tian et. al. [34]	2020	Hunan University (China)	The thermal comfort of passengers with RCF	At the same operative temperature range, the RCF system for thermal comfort greater comfort conditions than with traditional air conditioning
Xu et. al. [35]	2020	China University (China)	effectiveness of (PV) on the risk of cross infection between two occupants	(PV) may only be an infection-prevention strategy if it is maintained with high ventilation efficiency at the inhalation zone, which may be accomplished by decreasing infectious flow entrainment and boosting clean air volume.
Chakroun et. al. [36]	2020	American University (Lebanon)	Capacity of a CPV system with DF/CF	93 % of the participants felt thermal comfortable during the first 30 min at temperatures from 21-22 ℃
Auerswald et. al.	2020	Offenburg	Effectiveness of push-	Air exchange efficiency varies depending on

[37]		University (Germany)	pull ventilation aerators	boundary conditions.
Shin . et. al. [38]	2021	Pukyong University (Korea)	Cooling capacity and energy performance of the CRCP system	Cooling capacity of the open-type CRCP system increased while reducing energy consumption.

Table (2-3) Summary of Experimental and Numerical Studies

Reference	Year	Place of study	Main focus	Findings
Bolashikov and Bogdan [39]	2015	Warsaw University (Poland)	Determined optimum airflow direction using PV	The face and upper body portions were particularly sensitive to changes in the direction of provided airflow
Ning et. al. [40]	2016	Hunan University (China)	Energy savings performance , surface temperature distribution and cooling capacity for cooling radiant ceiling	A cooling radiant ceiling was found to have consistent temperature distribution and improved cooling capability by 43-46 %
Mahdi et. al. [41]	2016	Babylon University (Iraq)	Performance of ventilation and air flow distribution	Use of floor DV reduces the concentration of pollutants but more prone to disturbance
AlAssaad et. al. [42]	2018	American University (Lebanon)	Performance of sinusoidal flow (PV /MV) system to predict thermal comfort and IAQ	When compared to a constant PV system with the same thermal comfort, PV energy costs were lowered by (21.34 %)
Al Assaad et. al. [43]	2018	American University (Lebanon)	Capacity of an intermittent PV CC for IAQ	Intermittent PV CC improved comfort and IAQ and saved 7.52 % of the energy
Al Assaad et. al. [44]	2018	American University	The ability of (PV/MV)protecting	PVM system operating at a frequency range of (0.78–0.94) Hz will provided ventilation

		(Lebanon)	occupants from indoor contaminants accumulation	efficiency of about (77%) as well as a (16.1%) reduction in energy costs
Cao. et. al. [45]	2018	Aalborg University (Denmark)	Effect of vent inlet size on ventilation efficiency using a dimensionless time scale	The lower the intake size higher the inlet ventilation at ACH constant, at the outlet the higher the ACH, the lower the average CO_2 concentration
Yuan et. al. [46]	2019	(Ireland)	Characteristics of radiant ceiling system	Not all points within the operating limit area were suitable for practical application in order to avoid the risk of water condensation in the cooling mode and large temperature differences in heating
Su et. al. [47]	2019	(France)	Difference of temperatures on the whole cooling panel surface,	A thickness of (4-5 mm) for cooling panels is recommended to obtain a consistent surface temperature distribution
Csáky et. al. [48]	2019	Debrecen University (Hungary)	Developed personal ventilation system (ALTAIR PV)	ALTAIR PV system saves energy compared to conventional refrigeration systems and improves the thermal comfort sensation
Jin et. al. [49]	2020	Tianjin University China	Dynamic change of surface temperature of radiant ceilings	Condensation on the radiant ceiling panel surface easily avoided when the cooled water source is turned off.
Xie et. al. [50]	2020	South China University China	Effect of water supply temperature, mass flow rate, heat load distribution, and radiant roof capability on radiant roof capacity and thermal comfort conditions	The air supply temperature and internal heat load have a favorable relationship with indoor air temperature, but the air supply velocity has a negative relationship
Ye et. al. [51]	2020	Hokkaido University (Japan)	Thermal comfort of the RCCP system with forced ventilation	(RCCP) system provide thermally and Economically effective, but it cannot prevent hot air from escaping through individual

				windows.
Khail [52]	2020	American University (Lebanon)	created a self-contained, autonomously controlled (PV)	The new cooling strategy results in the (VC) system running for fewer hours and saving 53% in energy compared to the base case when using only the (VC) system.
Zhang et.al. [53]	2020	Tianjin University (China)	Four different ventilation techniques have different effects on the thermal comfort and indoor air quality.	SSW-RSW might provide the highest level of indoor air quality, based on average indoor PM2.5 concentration.
Katramiz et.al. [54]	2021	American University (Lebanon)	Impact of individual flow control of PV on the risk of pollution	When PVi < 4 l/s in tandem and PVi > 9 l/s in facing positions a low exposure for healthy people
Al Assaad . et. al. [55]	2021	American University (Lebanon)	Inhalation exposure (iF) and garment pollution performance(DFr)	1.CMP decreased iF and DFr at 5 l/s. 2. VDG reduced iF while increasing DFr at 10 l/s. 3. RMP decreased iF while increasing DFr at 10 l/s
Shbeeb et. al. [56]	2021	Hilla (Iraq)	Compare two types of supply diffusers with the used (CC/DV) system to determine air age and thermal comfort characteristics.	With increased cooling load treated by the chilled ceiling, the local air age increased. CO2 concentrations rise with height, but this effect fades as the proportion of cooling load treated by chilled ceiling rises. The semi-circle diffuser had benefits in terms of lowering air age and CO2 content.
Present work	2023	Hilla (Iraq)	studying the impact of the mean age of air , and PV air flow rate and supply air temperature on the PVMVCC performance .	

2.5 Scope of the present work.

The current study will concentrate on the following topics:

1. Studying of the performance of the chilled ceiling combined with mixing ventilation and personalized ventilation(CC/MVPV) system under Iraq climate (Hilla city) in terms of air age and thermal comfort, considering occupant density experimentally and numerically .

2. Comparing the air age and thermal performance for the chilled ceiling combined with mixing ventilation and personalized ventilation(CC/MVPV) with chilled ceiling combined with mixing ventilation (CC/MV) considering occupant density

3. Evaluation the effected by the change in the portion of cooling load treated by chilled ceiling on air age and human thermal comfort metrics .

4. Examining the effect of PV air flow rate on acceptable value of the age of air and distribution of air temperature and determining the best flow for (PV) system operation to improve thermal comfort and protect occupants from negative pollutants.

5. Studying human response to system in terms of (thermal sensation, perceived air quality, work performance).

2.6 Originality Points of the Present Work

The present work study the effectiveness of the (CC / PVMV) system with portion of cooling load treated by chilled ceiling (η) in terms of air age, air temperature distribution, CO_2 concentration, and indoor air quality parameters (PMV, PPD, and ADPI) and compare it with the system (CCMV), taking into account the density index occupied in an office room under the climate of Iraq - Hilla city. The data will be collecting by using experimental work and compare results with numerical data obtained by adopting appropriate turbulence model in computational fluid dynamics(CFD).

The originality of the current work can be summed up as follows:

1. There are few studies that discuss combined mixing ventilation and personalized ventilation with chilled ceiling systems to attain the capacities required in numerous enclosed space applications under hot and dry climates (such as the Iraq climate in Hilla city) taking into account the density index occupied.

2. Using AIRPAK.3.0.16 software in the numerical study , one of the new systems, and a scientific addition to our current study, as most of the previous studies did not address this technique.

3. Using an active self controller for the compressor operation and cut off , breathing cycle through experimental tests of the system.

CHAPTER THREE

MATHEMATICAL MODELLING AND NUMERICAL ANALYSIS

Chapter Three

Mathematical Modeling and Numerical Analysis

The performance of the (CC/MVPV) system was investigated using Computational Fluid Dynamics modeling. The major goal of the (CFD) analysis is

- Determination of the effect of average air age, thermal comfort parameters, PV air flow rate, and air temperature on associated system performance as studied in experiments but in more detail
- CFD data can be used to visualize air transmission and pollution in other rooms.
- Comparison of the optimal system with mixing ventilation in terms of average air age, temperature distribution, CO_2 concentration, and thermal efficiency, which will be addressed later in the results and discussion.
- The numerical simulation seeks to solve mathematical equations based on basic conservation laws (continuity, momentum, and energy equations) for the research case**,[57]**. Five numerically cases are studied as listed in Table(3-1)

Table (3-1) Description of the numerical cases studied

Cases		Q_S (W/m^2)	Q_{MV} (L/s)	Q_{PV} (L/s)	Case study	Description
Case-I	CCMV	59.33	46	------	Experimental and numerical study	Isothermal office room at different value of (η)
Case-II	CCMV/PV	59.33	46	5	Experimental and numerical study	Isothermal office room at different value of (η)
Case-III	CCMV/PV	59.33	46	7.5	Experimental and numerical study	Isothermal office room at different value of (η)
Case-IV	CC/MV	132.34	240	------	Numerical study	Non-isothermal meeting room at different value of (η)
Case-V	CCMV/PV	132.34	240	7.5	Numerical study	Non-isothermal meeting room at different value of (η)

3-1 CFD Models

3.1.1 CFD software

CFD simulations using (AIRPAK.3.0.16) are primarily utilized to capture the velocity and heat fields, as well as the carbon dioxide concentration field,**[57].** The design and analysis of ventilation systems that are necessary to provide indoor air quality, thermal comfort, pollution control solutions are made simpler by the use of AIRPAK, an accurate, rapid, and simple to use design tool. Together with FLUENT's quick, accurate, and tried-and-true unstructured solver engine, it is possible to quickly build and automatically mesh ventilation system problems. It had been used by a number of researchers to analyze the performance of ventilation in indoor environments such as **Gao [58] and Liang [59]**.

3.1.2 Conservation of thermal energy

The assumptions for solve Reynolds Average Navier_stokes equations (continuity, momentum and energy equations) as steady, constant density, 3D, Newtonian, incompressible liquid, without chemical reaction, turbulent flow liquid**,[60]**.

(A) Conservation of mass:

The incompressible steady three dimensional flow is expressed as following:

$$\frac{\partial}{\partial \mathrm{x}}(\mathrm{u})+\frac{\partial}{\partial \mathrm{y}}(\mathrm{v})+\frac{\partial}{\partial \mathrm{z}}(\mathrm{w})=0 \qquad \ldots.(\mathbf{3-1})$$

(B) Conservation of momentum (Navier–Stokes equations):

The conservation equation of momentum for three dimensional flow is as following:

X-direction (U-momentum)

$$\frac{\partial}{\partial x}(\rho uu)+\frac{\partial}{\partial y}(\rho uv)+\frac{\partial}{\partial z}(\rho uw)=-\frac{\partial p}{\partial x}+\frac{\partial}{\partial x}\left(\mu\frac{\partial u}{\partial x}\right)+\frac{\partial}{\partial y}\left(\mu\frac{\partial u}{\partial y}\right)+\frac{\partial}{\partial z}\left(\mu\frac{\partial u}{\partial z}\right)+\frac{1}{3}\frac{\partial}{\partial x}\left[\mu\left(\frac{\partial u}{\partial x}+\frac{\partial v}{\partial y}+\frac{\partial w}{\partial z}\right)\right]+\frac{\partial}{\partial x}(-\rho u'u')+\frac{\partial}{\partial y}(-\rho u'v')+\frac{\partial}{\partial z}(-\rho u'w')+\rho\, g_x \quad \ldots.(\mathbf{3-2})$$

Y-direction (V-momentum):

$$\frac{\partial}{\partial x}(\rho uv)+\frac{\partial}{\partial y}(\rho vv)+\frac{\partial}{\partial z}(\rho vw)=-\frac{\partial p}{\partial y}+\frac{\partial}{\partial x}\left(\mu\frac{\partial v}{\partial x}\right)+\frac{\partial}{\partial y}\left(\mu\frac{\partial v}{\partial y}\right)+\frac{\partial}{\partial z}\left(\mu\frac{\partial v}{\partial z}\right)+\frac{\partial}{\partial x}\left(-\rho\overline{u'v'}\right)+\frac{\partial}{\partial y}\left(-\rho\overline{v'v'}\right)+\frac{\partial}{\partial z}\left(-\rho\overline{v'w'}\right)+\rho\, g_y \quad \ldots.(\mathbf{3-3})$$

Z-direction (W-momentum):

$$\frac{\partial}{\partial x}(\rho uw)+\frac{\partial}{\partial y}(\rho vw)+\frac{\partial}{\partial z}(\rho ww)=-\frac{\partial p}{\partial y}+\frac{\partial}{\partial x}\left(\mu\frac{\partial w}{\partial x}\right)+\frac{\partial}{\partial y}\left(\mu\frac{\partial w}{\partial y}\right)+\frac{\partial}{\partial z}\left(\mu\frac{\partial w}{\partial z}\right)+\frac{\partial}{\partial x}\left(-\rho\overline{u'w'}\right)+\frac{\partial}{\partial y}\left(-\rho\overline{v'w'}\right)+\frac{\partial}{\partial z}\left(-\rho\overline{w'w'}\right)+\rho\, g_z \quad \ldots.(\mathbf{3-4})$$

The terms ($\rho\overline{v'w'}$,$-\rho\overline{w'w'}$,$\rho\overline{u'v'}$,$\rho\overline{v'w'}$,$\rho\overline{u'w'}$ …etc.) are the turbulent Reynolds shear stress (τ_t) and ($\rho g_{x,y,z}$) is body force.

(C) Conservation of thermal energy:

The energy equation per unit volume for steady three dimensional flow

$$\frac{\partial}{\partial x}(\rho UT)+\frac{\partial}{\partial y}(\rho VT)+\frac{\partial}{\partial z}(\rho WT) = \frac{\partial}{\partial x}\left(\Gamma\frac{\partial T}{\partial x}\right)+\frac{\partial}{\partial y}\left(\Gamma\frac{\partial T}{\partial y}\right) + \frac{\partial}{\partial z}\left(\Gamma\frac{\partial T}{\partial z}\right) \quad \ldots.(\mathbf{3-5})$$

where (Γ) is the diffusion coefficient (diffusivity), which can be calculated as follows

$$\Gamma=\frac{\mu}{\sigma} \quad .\ldots(\mathbf{3-6})$$

Where the Prandtl number **(Pr)** $= \frac{\vartheta}{\alpha} = \frac{C_p\mu}{K}$ $\quad .\ldots(\mathbf{3-7})$

3.1.3 The turbulence model

The numerical prediction of the air flow inside the test chamber is done using the(RNG k-ε) model turbulence model **[61]**. Using the (RNG k-ε) method, the model was developed from the instantaneous Navier-Stokes equations, and includes low Reynolds number effects for processing the flow near the wall regions. With low turbulence levels, (RNG k-ε) model shows the best accuracy for forced mixing and convection**, [61].** Compared with other turbulence models, the (RNG k-ε) model model is more suitable for simulating air temperature and air flow (Shbeeb and Mahdi**, [62],** Chen**, [63].** As a result, (RNG k- ε) model turbulence model was used in this investigation due to its accuracy and somewhat superior computing efficiency. The discrete coordinated radiation model was used to calculate the transfer of radiant heat between surfaces. The Boussines eq model took into account the effect of buoyancy. In a general sense, the models can be written as follows,**[64]:**

- A term was added in the dissipation equation(ε) to relate the disturbance dissipation to the mean shear
- The effect of eddies on turbulent flow had been addressed.
- Analytical formula for turbulent Prandtl number.
- the differential formula for effective viscosity analysis.

Predictions are improved as a result of adding an additional term to the dissipation equation, by:

- streamline curvature and high strain rate
- Transitional flow , mass transfer and hot walls.

The spreading of a round jet is still not accurately predicted by equations.

TKE equation,**[64].**

$$\underbrace{\rho U_i \frac{\partial k}{\partial x_i}}_{\text{Convection}} = \underbrace{\mu_t S^2}_{\text{Generation}} + \underbrace{\frac{\partial}{\partial x_i}\left(\alpha_k \mu_{eff} \frac{\partial k}{\partial x_i}\right)}_{\text{Diffusion}} - \underbrace{\rho\varepsilon}_{\text{Dissipation}} \quad \dots (3-8)$$

Convection Generation Diffusion Dissipation

$$S \equiv \sqrt{2S_{ij}S_{ij}}, \quad S_{ij} \equiv \frac{1}{2}\left(\frac{\partial U_j}{\partial x_i} + \frac{\partial U_i}{\partial x_j}\right) \quad \dots (3-9)$$

Where Dissipation rate equation:

$$\underbrace{\rho U_i \frac{\partial \varepsilon}{\partial x_i}}_{\text{Convection}} = \underbrace{C_{1\varepsilon}\left(\frac{\varepsilon}{k}\right)\mu_t S^2}_{\text{Generation}} + \underbrace{\frac{\partial}{\partial x_i}\left(\alpha_\varepsilon \mu_{\text{eff}} \frac{\partial \varepsilon}{\partial x_i}\right)}_{\text{Diffusion}} - \underbrace{C_{2\varepsilon}\rho\left(\frac{\varepsilon^2}{k}\right)}_{\text{Destruction}} - \underbrace{R}_{\text{Additional term Related to mean strain\& turbulence quantities}} \quad \dots (3-10)$$

As shown in the dissipation equation (3–11), the (R) term is represented by

$$R = \frac{\eta^3 \rho\, C_\mu\, (1 - \frac{\eta}{\eta_0})\varepsilon^2}{(1+\beta\eta^3)K} \quad \text{Where } \eta = \frac{SK}{\varepsilon} \qquad \ldots(\mathbf{3-11})$$

The values of the model's constants were $C_{1\varepsilon}$=1.42 and $C_{2\varepsilon}$=1.68, $\beta = 0.012$, $\eta_0 = 4.38$, $C_\mu = 0.0845$

3.1.4 Structure of the software AIRPAK

The four basic phases of the AIRPAK program are as follows**,[57]**:

1. Build model: Objects are created based on predefined elements (rooms, people, blocks, fans, etc.) in addition to defining the boundary conditions of the model.
2. Generate mesh : The form is divided into individual parts. The equations regulating heat transfer and flow within these elements will be solved using Airpak software.
3. Calculate the solution: Once the solution is calculated, Airpak checks the model, saves the project, and starts preparing portfolio equations for each node in the model.
4. Examine the results: After the solution is captured, the results (air temperature, air velocity, PMV, PPM, ADPI, etc.) can be analyzed. The main AIRPAK framework appears as indicated in Fig.(3-1)

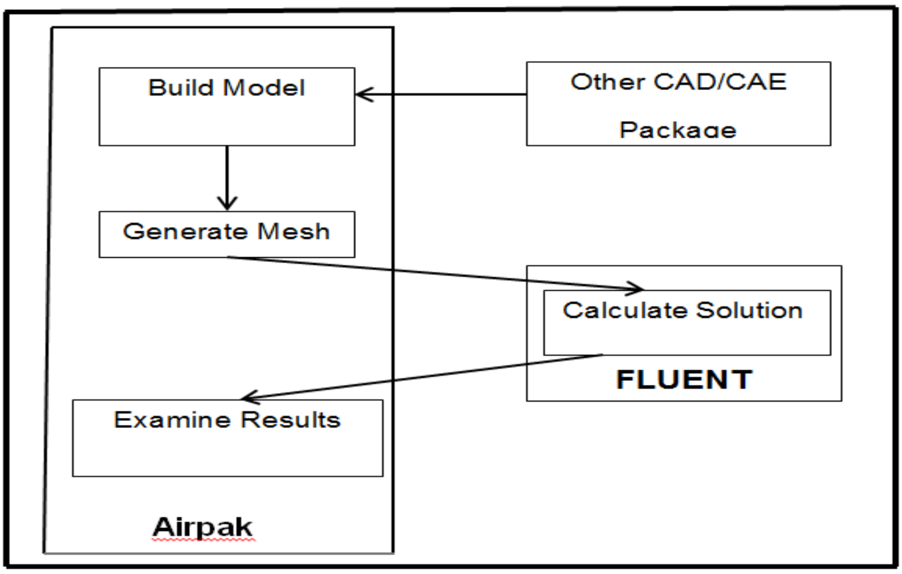

Fig.(3-1) Structure of the basic program

3.2 Numerical Cases Study

At the beginning, Simulation results are compared with experimental measurements to validate the two systems (CC/MV, CC/MVPV) for four tests under three conditions (I, II and III). To describe local air movement, velocity vectors of air dispersion around the manikin are shown. Following the validation of the CFD model, it is utilized to simulate a parametric study in meeting room under Iraq climate (Hilla city), to determine the effectiveness of the two (CC/MV,CCMV/PV) systems in offering acceptable indoor air quality and thermal comfort .The numerical findings for meeting room cases are compared to ASHRAE standard data by using AIRPAK.3.0.16 software is used.

3.2.1 Case-I , II and III (insulated office room with CC/MV and CCMV/PV)

The numerical model was used to simulate office room with the dimensions (3 x 2.5 x 2.5) m^3 as indicated in Fig.(3-2), Fig.(3-3), which corresponds to the same size of the experimentally office room in which the model validation study was conducted for three persons, with chilled ceiling and two ventilation system as mixing ventilation (air supply is located in the upper part of the room and air exhaust at the lower part of the room as shown in (Case-I) and personalized ventilation (The PV nozzle is located at (1.1 m) breathing height, and is separated from the occupant by (0.4)m as shown in (Case-II and III). In three cases, the chilled ceiling served as two walls.

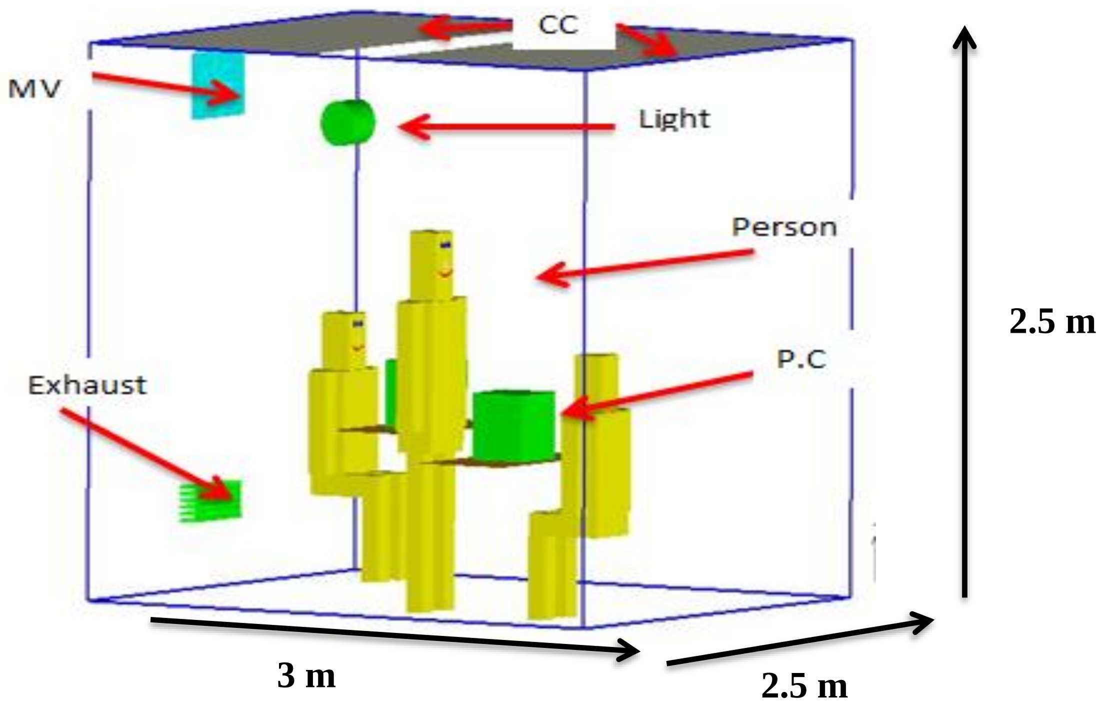

Fig.(3-2): Illustration of an office room with CCMV, (Case-I)

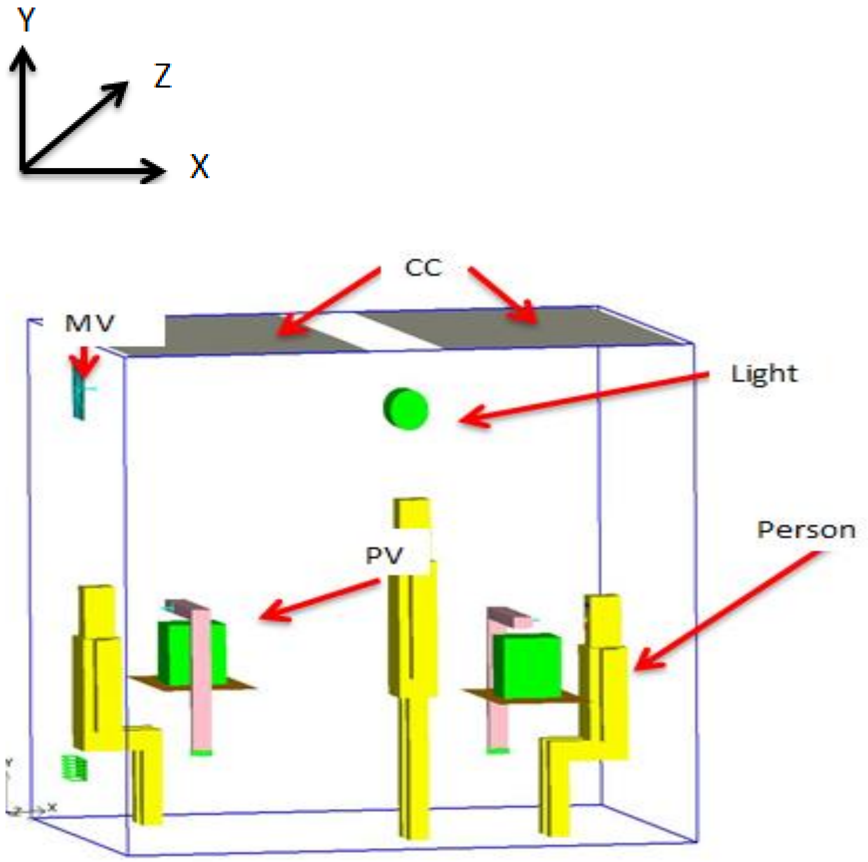

Fig.(3-3): Illustration of an office room with CCMV/PV, (Case- II and III)

3.2.2 Boundary conditions

Boundary conditions for simulating an isolated office room for the three cases (Case I, Case II and Case III), as shown in Table (3-2) and Table(3-3).

Table (3-2): A description of the simulated systems and their boundary conditions

Part	Details
Ventilation systems (MV, PV)	Constant inlet velocity and temperature for MV V_{MV}= 2.5 m/s T_{MV} = 17 °C **, [65]** Constant inlet temperature T_{PV} = 22 °C **, [65]** Average air flow rate Q_{PV} = 5 l/s, 7.5 l/s Room air temperature T_{rd} = 25°C Outdoor air temperature T_0 = 47°C **, [65]**

	Turbulence intensity = 10% Discrete phase modeling of (MV,PV) = Reflect
Exhaust grille	Pressure: Outlet, gauge pressure = Zero Discrete phase modeling: Escape
Thermal manikin, walls, Table floor, chair	Wall: Stationary, No slipping Sidewalls, ceil and floor : Zero heat flux Occupants, computers, lights : Constant heat sources Discrete phase modeling = Trap
Manikin (Human Body)	Constant skin temperature of body for all parts
CO_2 source	Constant inlet velocity ,Turbulence Intensity = 7.7 % Constant inlet value of concentration C_{in} = 1000 ppm

Table(3-3) The boundary conditions for the (Case I, Case II and Case III).

Parts	**Boundary condition**	**Equation**
rectangle air supply diffuser	inlet velocity	$\vec{u}=\vec{u}_x$
Walls	no penetration and no slip condition	$\vec{u}=0$
sidewalls, ceil and floor	zero heat flux	$\frac{dq}{dx}=\frac{dq}{dy}=\frac{dq}{dz}=0$
exhaust grill	constant air flow rate	$V_{in}=V_{out}$
Occupants, computers and lights	constant heat sources	q=constant
chilled ceiling	constant temperature	T=constant

3.2.3 Mesh strategy creation

Due to the presence of the (CCMV/PV) systems, complex airflow field behavior is seen in this study. The (MV) , in reality, creates a complex flow with recirculation zones and mixing. The (CC) creates a temperature gradient in space, which causes unstable stratification and buoyancy, resulting in high turbulence intensities. Furthermore, the PV adds to the turbulence in the microenvironment around the occupant. In addition, there are a number of heat sources in space that cause thermal plumes. Variables in the airflow field, such as temperature, age of air, velocity , containments concentration are affected. As a result, to resolve these various fields , in addition to calculate heat removal effectiveness (εt, ADPI) , the simulation was performed using (RNG k- ε) turbulence model**,[59].**

AIRPAK simulation software to simulate airflow, pollutants, and thermal comfort rapidly and precisely. The use of the premier computational fluid dynamics program, to ventilation problems is made easier with AIRPAK software**, [60].** to solve the equation for mass, energy, and air momentum conservation. For the purpose of solving flow equations, the (RNG k-) turbulence model was adopted. Hexa Cartesian geometry was used to discretize the (CC/ MVPV) mesh, which had (945393, 1120235) element and node numbers, respectively, at (η = 0 to 80%) and (0.07) size elements. For this function, the space needs to be properly meshes in order to make accurate predictions about flow behavior Fig.(3-4a). Simulations were performed until the results were stable, as indicated in the picture, at a level of approximation (10^{-5}).

A mesh improvement study was also carried out in order to detect and reduce the mistake caused by the estimate.

3.2.3.1 Mesh independence study

The grid independence test played a crucial part in the simulation study in determining mesh quality. The grid was meant to solve the boundary layer and capture thermal environment behavior on all sides of the occupants and other objects. To put it another way, the mesh has no bearing on the answer. After that, the five sites used to record the simulation results of air age and temperature were chosen (2.75, 1.1, 0.5). Two of them P1 and P2 are located at two different heights in front of the supply distributor, while P3 and P4 are located in the breathing area near three of the passengers. Figs. (3-3) and (3-4) show the air life and temperature profiles of five Different specific node numbers.The grid size in this study was determined by comparing the simulation results for various mesh sizes as listed in Table (3-4).

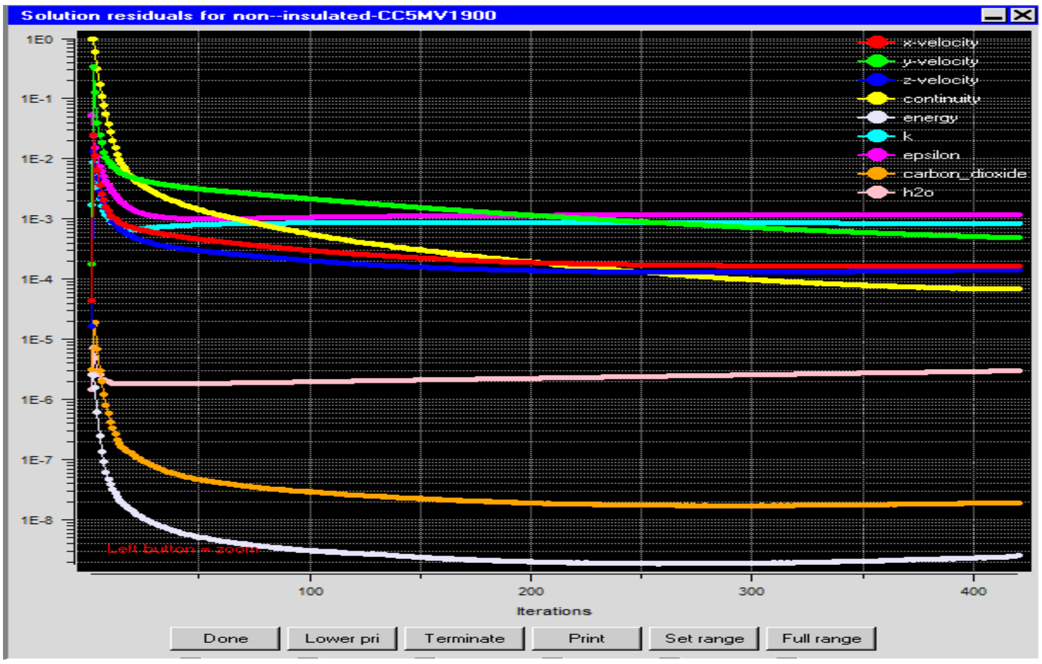

a- Residual error monitor

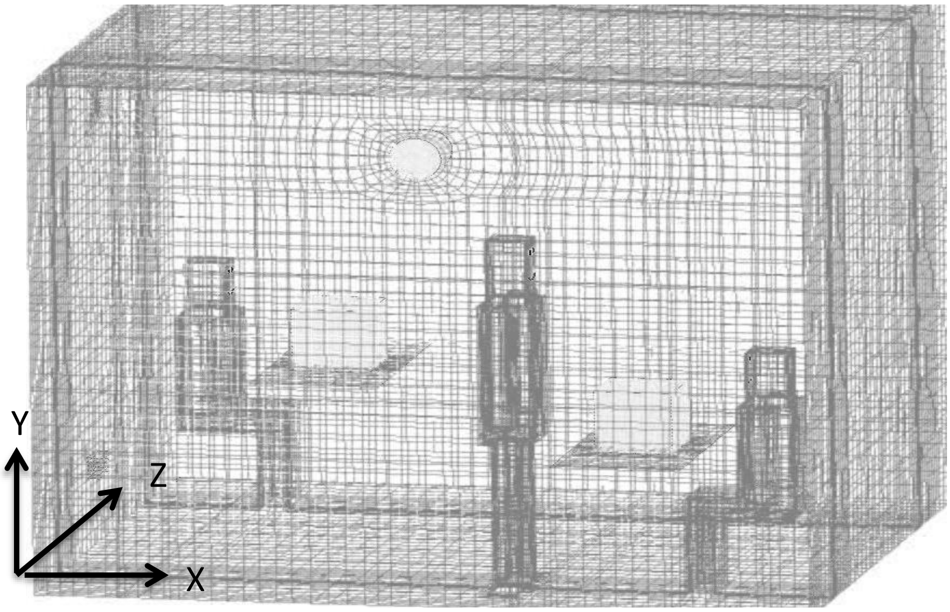

b- Case-I CCMV

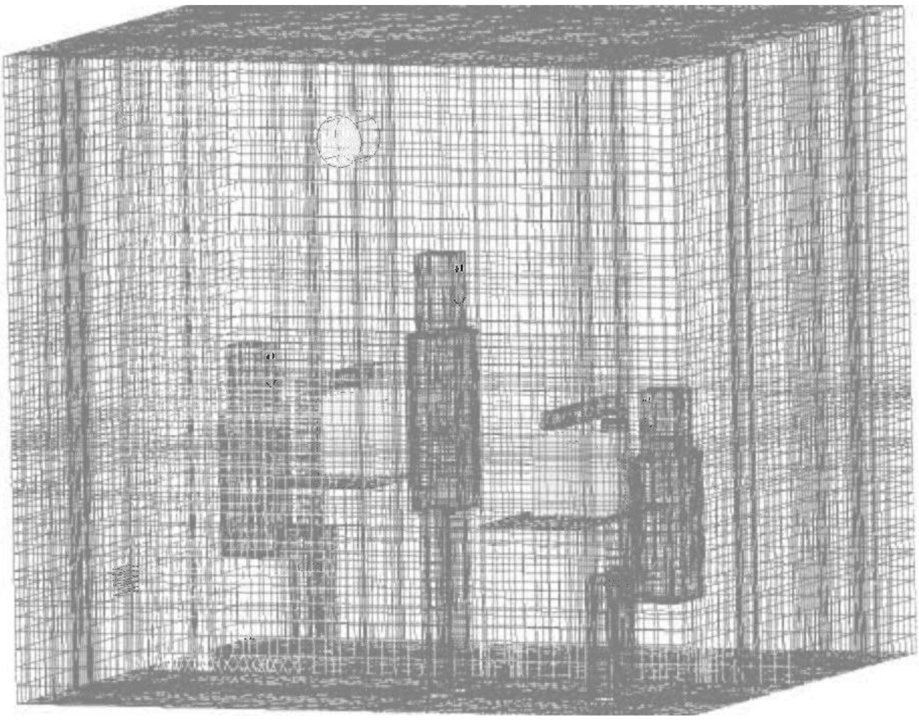

c- Case-II and III CCMV/PV

Fig.(3-4) Illustration of the meshed model for three cases

Table (3-4) Mesh strategy for an office room (Case I, Case II and Case III)

Case	η%	Element No.	Node No.	Size element (X,Y, Z)	global settings		
					Mesh parameter	Max size ratio	Min elems on cyl face
Case-I	0	314657	329321	0.07	Normal	2	4
	25	334923	343678	0.07	Normal	2	4
	50	334923	343678	0.07	Normal	2	4
	80	334923	343678	0.07	Normal	2	4
Case-II	0	366549	377768	0.07	Normal	2	4
	25	382089	402618	0.07	Normal	2	4
	50	382089	402618	0.07	Normal	2	4
	80	382089	402618	0.07	Normal	2	4
Case-III	0	442088	456633	0.07	Normal	2	4
	25	446587	468617	0.07	Normal	2	4
	50	446587	468617	0.07	Normal	2	4
	80	446587	468617	0.07	Normal	2	4

3.2.4 Calculation of error for validated cases

The average error was calculated using the following equation to compare the experimental and simulated results **, [64]**.

$$\boldsymbol{E} = \sum_{\mathbf{i=1}}^{\mathbf{n}} \frac{\left|\mathbf{X}_{\mathbf{CFD}}^{\mathbf{i}} - \mathbf{X}_{\mathbf{EXP}}^{\mathbf{i}}\right|}{\left|\mathbf{X}_{\mathbf{EXP}}^{\mathbf{i}}\right|} * \mathbf{100} \qquad \ldots\ldots(\mathbf{3-12})$$

Where (X) represents the variable value , $\left|\boldsymbol{X}_{\boldsymbol{CFD}}^{\boldsymbol{i}} - \mathbf{X}_{\mathbf{EXP}}^{\mathbf{i}}\right|$ denoted the exact difference between the simulated and experimental values for variable (X), and (n) is the number of measurements.

3.3 Numerical Study for Meeting Room (Cases-IV and V)

In this section, the goal of this study was to determine the thermal environment and age of air and contaminate concentration and temperature distribution in meeting room for eight occupants with chilled ceiling with mixing ventilation and personal ventilation (CC/MVPV) system, and to compare them with mixing ventilation and chilled ceiling (CC/MV) under Iraqi- Hilla city climate with various cooling load ratios treated by chilled ceiling (25 %, 50 %, and 80%).

Ventilation in office spaces have been extensively researched, but there have been few studies comparing the thermal environment achieved with chilled ceilings combined with mixing ventilation and personal ventilation system into meeting room. In order to effectively implement demand-driven solutions in buildings, it is critical to use extensive fine-grained occupancy data. Therefore requires the greater research into the meeting room ventilation system is needed. The results were compared to data from the American Society of Heating, Refrigeration, and Air Conditioning Engineers (ASHRAE standard data**) [65, 4].**

3.3.1 Cases description

The numerical model was implemented in a meeting room of the dean of the College of Engineering with dimensions of (7 x 2.5 x 4.5) m^3 under the Iraqi climate in the summer season at (47°C**) ,[66]** as shown in Figs. (3-5)and(3-6). The ceiling was fitted with radiant cooling panels that covered (80%)of the surface area. The room has a total heat load of (2311W) distributed between (occupants, computers and lighting, tables), two glass windows are fixed to one of the long walls of the room, as shown in Table (3-5), details of equipment and people in the meeting room. The walls of the room consist of several layers of different thickness, indicated in Fig.(3-7) and Table (3-6). The cases were created in accordance with the recommendations of EN 15251 Standard for indoor climate settings,**[67]**.

Table(3-5) Dimensions and thermal load of the internal components for the meeting room(Case-IV and Case-V)

Items	**No.**	**Dimensions of the room (m)**			**Sensible heat, [68]**
		X(m)	**Y(m)**	**Z(m)**	
Person	8	0.35	1.1	0.2	75 W per person
Desktop computer	1	0.3	0.3	0.3	60
Desk	1	3	0.1	3	------
Window	2	1.5	1	0	------
door	1	0.1	2	1	
Supply	1	0	0.2	0.475	-----
Exhaust	1	0	0.2	0.36	------
Lights	4	0.15	0.1	0.1	320
T.V Display Screen	1	1	0.5	0.1	150
Chilled ceiling	2	3	0	4.4	------

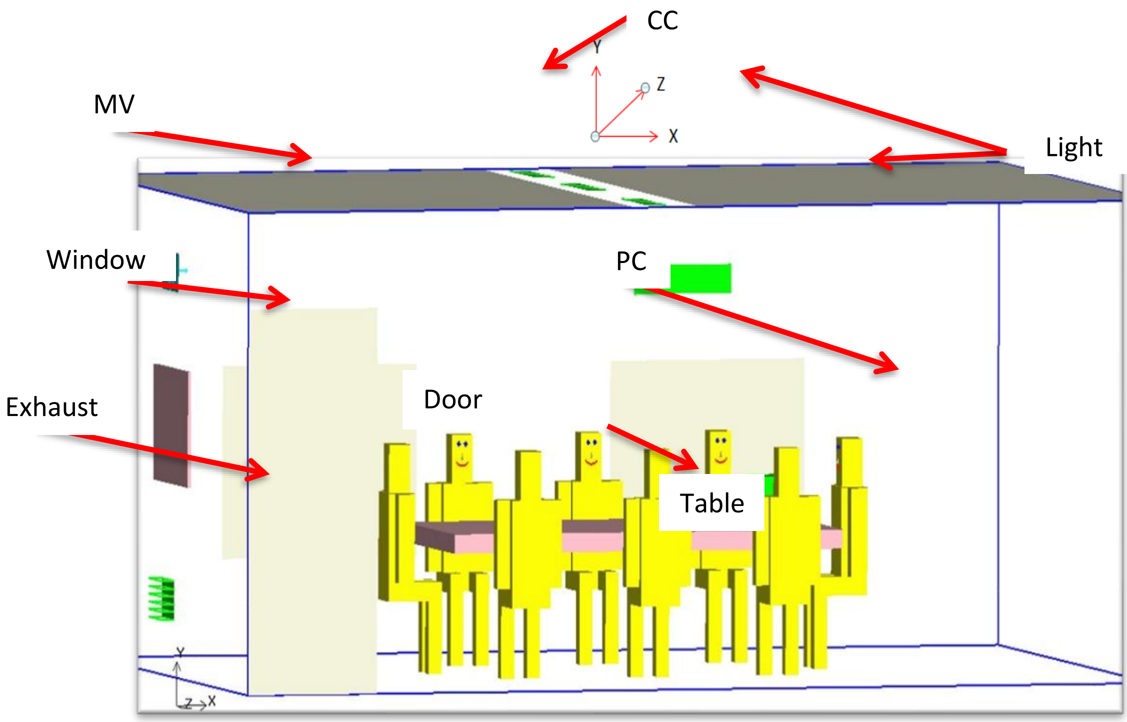

Fig.(3-5): Illustration of an meeting room with CCMV, (Case-IV)

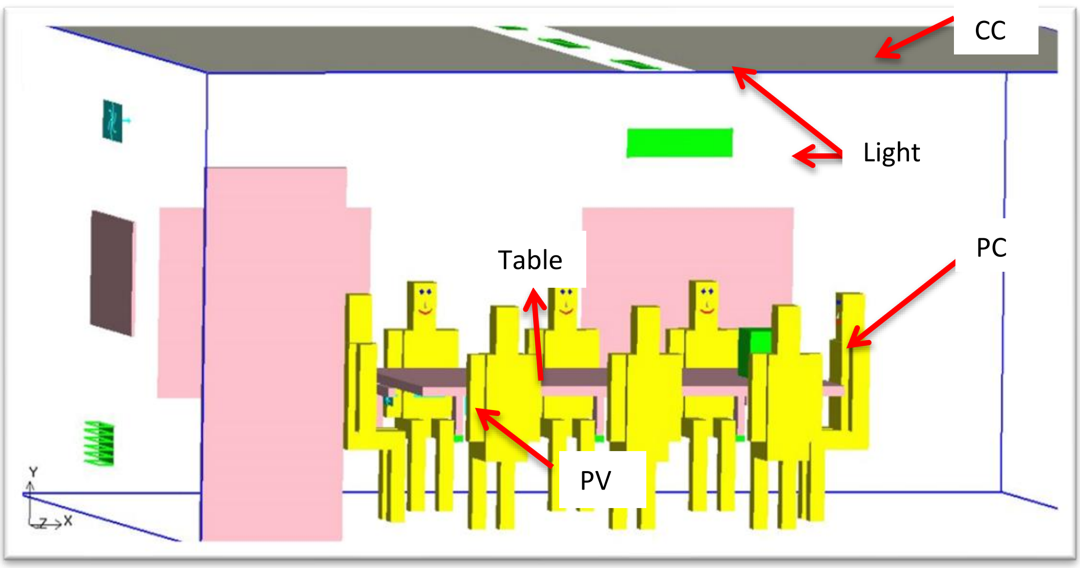

Fig.(3-6): Illustration of an meeting room with CCMV/PV, (Case- V)

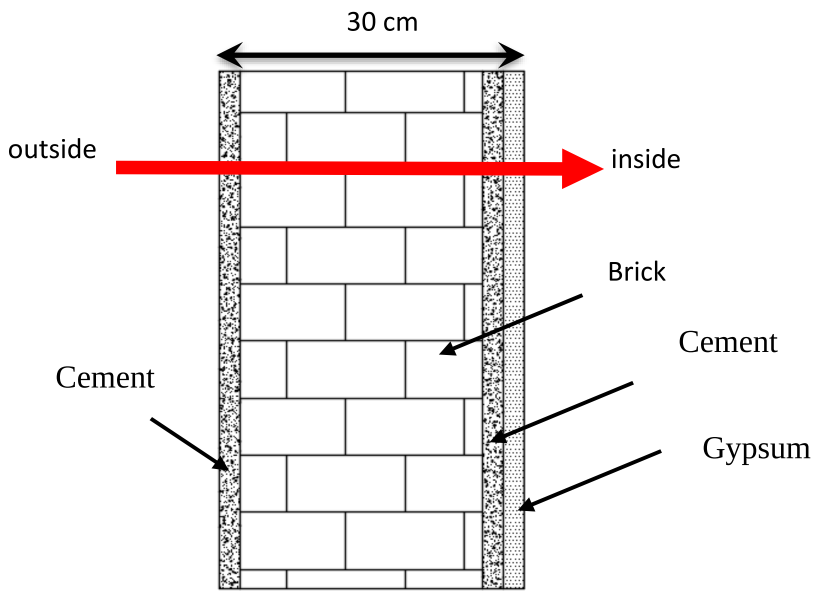

Fig.(3-7) The side walls and their components that transfer heat.

Table (3-6) Details of thermal properties for materials , thickness and walls for insulated office room .

Material	Thickness (m)	Thermal conductivity (W/m.°C), [67]
Brick	0.24	0.72
Gypsum	0.02	0.42
Cement	0.02	0.72
Wood	0.03	0.17
glass	0.006	1

3.3.2 Theoretical analysis

3.3.2.1 Calculation of meeting room cooling load

The method for calculating cooling loads was detailed in the ASHRAE Handbook, 2013**, [68].** As shown in the table, the heat gain is separated into two portions, the first due to occupant heating, lamps, computers, and other heat sources in the room zone. The second part is heat acquisition from the outside, which occurs due to heat transfer through windows, walls, and doors.To calculate heat transfer from the walls, door, and window, apply the cooling load temperature difference approach equations (13 to 20):

$$Q = U \times A \times CLTD_C \qquad \ldots.(\mathbf{3-13})$$

$$U = \frac{1}{R_{th}}$$

$$R_{th} = \frac{1}{h_i} \qquad \ldots.(\mathbf{3-14})$$

$$U = \frac{1}{h_i} + \frac{1}{k_i} + \frac{1}{h_o} + \frac{1}{h_o} \qquad \ldots.(\mathbf{3-15})$$

$CLTD_C$ is computed as follows**:**

For the interior walls:

$$CLTD_C = (CLTD + LM) \times K + (25.5.5 - T_i) + (T_m - 29.4) \ldots.(\mathbf{3-16})$$

$$T_m = T_o - \frac{DR}{2} \qquad \ldots.(\mathbf{3-17})$$

For the door and window:

$$CLTD_C = CLTD + (25.5.5 - Ti) + (Tm - 29.4) \qquad \ldots.(\mathbf{3-18})$$

The heat gain from solar-generated heat transfer through the window is calculated as follows:

$$Q = A \times SC \times SHG \times CLF \qquad \ldots.(\mathbf{3-19})$$

The corridor temperature**, [68]** can then be calculated using equation (9):

$$T_{corridor} = T_i + \frac{2}{3}(T_i - T_o) \qquad \ldots.(\mathbf{3-20})$$

The HAP program was used to determine the overall cooling load for the non–insulated office room, which came to be equivalent to (2311W).

3.3.2.2 HAP-4.5 software

Carrier's Hourly Analysis software (HAP) is a tool that helps engineers in designing heating, ventilation and air conditioning systems. (HAP) had two tools. First, it is a tool for calculation cooling or heating load and design systems. The second tool used to simulate building costs and energy.

3.3.2.3 Supply air temperature and flow rate for (CCMV/PV) System

The thermal loads inside the room are broken down into two parts: the first is caused by the heating of the person, lighting, computers, and other heat sources in the room's vicinity. The second component is heat gain from the exterior, which is brought on by heat transfer through walls, doors, and windows, as explained in (ASHRAE Stander, 2017) **, [65]** using the following equations:

$$CL_{MV} = q_{oe} + q_l + q_{ex} \qquad \ldots.(\mathbf{3-21})$$

Determination of supply air temperatures for MV systems using room air temperature as the design parameter as suggested in (EN 15251 and EN ISO 7730), **[69,70].** Calculating the supply air flow rate (Q_S) according to the following eq:

$$CL_{MV} = m^{\bullet} \times cp \times \Delta T \qquad \ldots.(\mathbf{3-22})$$

$$Q_{MV} = m^{\bullet} \times \rho \qquad \ldots . (\mathbf{3-23})$$

3.3.2.4 Selection of air supply diffuser

Calculating the surface area of the rectangular diffuser for the air according to the following equation:

$$Q_S = V_X \times A_S \qquad \ldots . (\mathbf{3-24})$$

where $V_X = 2.5$, [**71**]

$$\mathrm{ACH} = Q_{MV}\,\mathrm{Vroom} \times 3600 \qquad \ldots . (\mathbf{3-25})$$

Where: V_x: local air velocity (m/s); As follows: The area of the exhaust grills is approximately (80%) of the surface area of the air supply unit (m^2) **,[71,68].**

3.3.2.5 Design of Chilled Ceiling

Heat exchanged through natural convection with the room air and thermal radiation with other inside surfaces on the radiant cooling panels' surfaces during the test. The Stefan-Boltzmann equation can be used to determine radiant heat transfer**,[72]**.

$$q_c = 2.42 \frac{|t_p - t_a|^{0.31} (t_p - t_a)}{{D_e}^{0.08}} \qquad \ldots . (\mathbf{3-26})$$

$$q_r = 5*10^{-8}[(t_p + 273.15)^4 - (AUST + 273.15)^4] \qquad \ldots . (\mathbf{3-27})$$

$$Q_{cc} = q_r + q_c \qquad \ldots . (\mathbf{3-28})$$

The cooling load (CL_{CC}), eliminated by the radiant panels was computed by measuring the airflow rate and the supply and return air temperatures**,[72]**.

$$CL_{CC} = m_{ws} cp_{pw} \ (T_{wr} - T_{ws}) \quad \text{.... (3 - 29)}$$

The (η) is the ratio of the cooling load removed by the chilled ceiling to the overall cooling load (CL_{CC}), it is calculated as follows.

The chilled ceiling surface temperature was calculated using an empirical equation (3-30), **[72].** Table (3-7), present the values of (T_s) and (T_{CC}) at various value of (η).

$$\eta = \frac{CL_{CC}}{(CL_{MV} + CL_{CC})} \quad \text{.... (3 - 30)}$$

$$T_{CC} = T_{rd} - \left(\frac{CL_{MV}/CL_{CC}}{8.92\, f\, A_f}\right)^{0.9} \quad \text{.... (3 - 31)}$$

$$\text{Where } f = \frac{\text{chilled ceiling area } (A_{CC})}{\text{floor area}(A_f)} = 0.8 \quad \text{.... (3 - 32)}$$

Table (3-7): Operating settings and experimental conditions for(Case-VI and Case-V)

η (%)	CL_{PVMV} (W)	CL_{CC} (W)	Q_{MV} (L/s)	Q_{PV} (L/s)	Ts (°C)	Øs (%)	TC(C) (°C)
0	2311	0	240	7.5	17	85	0
25	1733	577.8	240	7.5	19	75	23
50	1155.5	1155.5	240	7.5	21	65	21.39
80	462	1848.8	240	7.5	23	58	19.45

3.3.3 Boundary conditions

The boundary conditions for the two insulated office room cases are shown in Table (3-8). (Case-IV and Case-V).

Table (3-8): A description of the simulated systems and their boundary conditions

Part	Details
Ventilation systems (MV, PV)	Constant inlet velocity and temperature V_{MV}= 2.5 m/s T_{MV} = 17 °C **,[65].** Constant inlet temperature T_{PV} = 22 °C **,[65].** Average air flow rate Q_{PV} = 7.5 l/s Room air temperature T_{rd} = 25°C Outdoor air temperature $T_{\circ}$ = 47°C **,[65].** Turbulence intensity = 10% Discrete phase modeling of (MV, PV) = Reflect
Exhaust grille	Pressure: Outlet, gauge pressure = Zero Discrete phase modeling: Escape
Thermal manikin, walls, Table floor, chair	Wall: Stationary, No slipping Ceil and floor : Zero heat flux Walls, window , door (1181 W) Thermal manikin (75 W) , lamp (320 W) Comp (60 W) T.V screen (150 W) Discrete phase modeling = Trap
Manikin (Human Body)	Constant skin temperature of body for all parts
CO_2 source	Constant inlet velocity ,Turbulence Intensity = 7.7 % Constant inlet value of concentration C_{in} = 1000 ppm

3.3.4 Mesh strategy creation

As previously explained in section (3.2.3), Table(3-9) shows the number of elements and nodes, the size of cells that are appropriate for meeting room after applying the mesh technique to the meeting room generated by the AIRPAK software. Parts of the meshed model for (Cases IV and V) are shown in two cases in Fig.(3-8) .

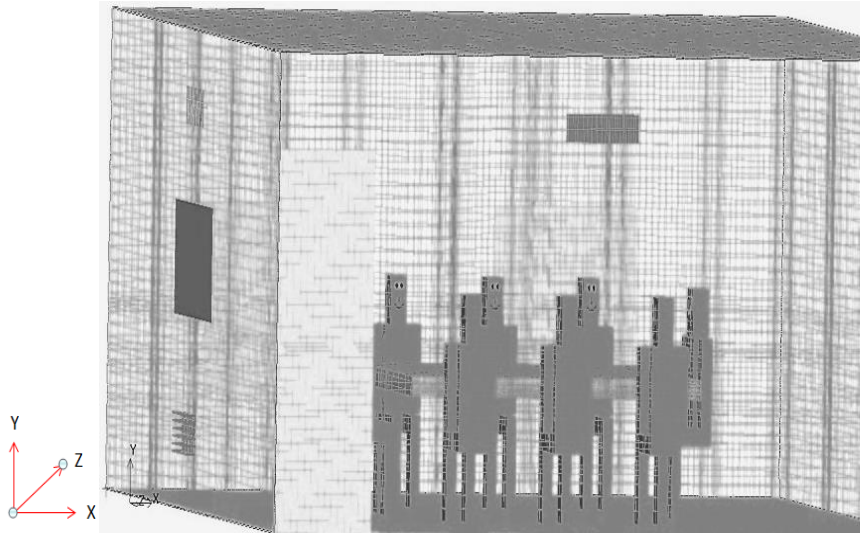

a- Case-IV **CCMV**

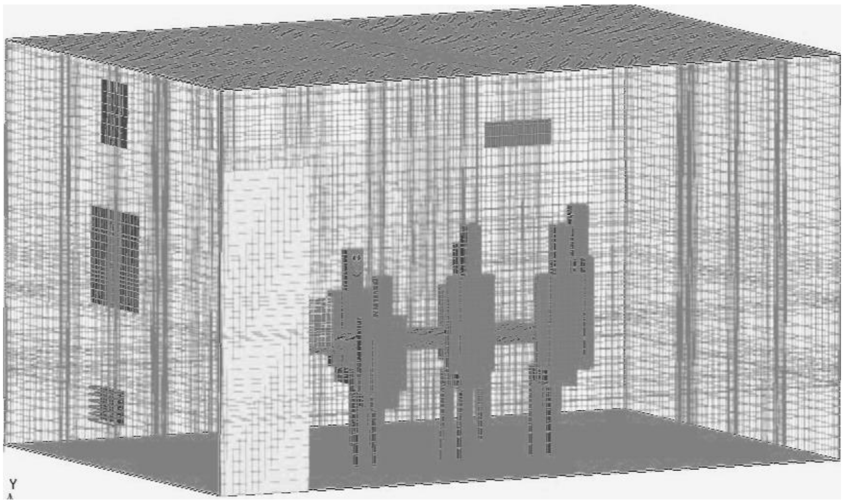

b- Case-V **CCMV/PV**

Fig.(3-8) Illustration of the meshed model for three cases

Table (3-9) Mesh strategy for meeting room (case V, case VI)

Case	η%	Element No.	Node No.	Size element (X,Y,Z)	global settings		
					Mesh parameter	Max size ratio	Min elems on cyl face
Case-V	0	945393	955640	0.07	Normal	2	4
	25	1120235	1121930	0.07	Normal	2	4

	50	1120235	1121930	0.07	Normal	2	4
	80	1120235	1121930	0.07	Normal	2	4
Case-VI	0	1367881	1431392	0.07	Normal	2	4
	25	15519055	1667121	0.07	Normal	2	4
	50	15519055	1667121	0.07	Normal	2	4
	80	15519055	1667121	0.07	Normal	2	4

3.4 Procedures for Numerical Solution

This section contains thorough information on the processes used in the numerical solution of the six situations under consideration four cases.

3.4.1 Properties of the working fluid

In all simulations, the simulated fluid is a mixture of air and CO_2 , H_2O serving as relative humidity. The values of the air characteristics are listed in Table (3-10).

Table (3-10) lists the characteristics of air and CO_2 ,**[73]**.

Parameter	**Air**	**CO_2**
Density (ρ) (Kg/m^3)	1.225	1.7878
Thermal Conductivity (k), (W/m.K)	0.0242	0.0166
Specific Heat (Cp), (J/kg.K)	1005	871
Viscosity (ϑ), (kg/m.s)	1.7894×10^{-5}	1.495×10^{-5}

3.4.2 Boundary conditions of momentum

The momentum boundary conditions for the areas of the model tested room are shown in Table (3-10) for the five cases (Case-I, Case-II, Case-III, Case-IV, Case-V). The equations of general boundary conditions are given in Table (3-11) and Table (3-12).

Table(3-11) Momentum boundary conditions.

Part	**Type**	**Momentum condition**	
		Wall Motion	Shear

			condition
Persons, computer, side wall, tables and lights	Wall	Stationary	No slipping
Rectangle air supply diffusers	velocity inlet	magnitude (normal with X-direction)	
Extract grills	out flow	flow rate weighting ($\frac{V_{in}}{V_{out}}$) =1	

Table(3-12) Boundary conditions equations

Boundary	Velocity (m/s)		Temperature (°C)	Heat flux (W/m²)
Inlet	$U = u_s$		$T=T_s$	-
Outlet	$U = u_s \frac{A_{in}}{A_{out}}$		$\frac{\partial T}{\partial X} = 0$	-
No slip at wall	For six cases	U=0, V=0, W=0	-	q_{wall}/A_{wall}

3.4.3 Controlling the solution

The RNG k-model was utilized to model turbulence due to the (MV/PV), and CC causing turbulence**, [57].** Table (3-13) shows the discretization techniques for the various variables (momentum, energy, k, species ...) For all quantities, numerical convergence is achieved with scaled residuals of less than (10^{-5}).

Table (3-13): Setup of the numerical model and solver

Flow	3D Pressure based, steady state, incompressible fluid, without chemical reaction, frictionless and implicit formulation
Turbulence model	RNG k- model, enhanced wall treatment, full buoyancy effect

Methods of solution	Semi Implicit (SIMPLE Scheme)for pressure and velocity . PREssure Staggering Option (PRESTO) for pressure, Second order upwind for velocity, temperature , H_2o, CO_2 .

The relaxation factor (α) is used to control the updating of the variables' value (Ø)which is computed at each iteration using the equation:

$$\phi_n = \phi_{old} + \alpha\Delta\phi \qquad \text{....}(\mathbf{3-33})$$

This means that all equations are associated with an under relaxation factor. For each variable in the (AIRPAK) software, there is a default under relaxation factor; these default values are near ideal and adequate for many difficulties and the vast majority of cases **,[57].** Table (3-14) lists the under relaxation factors that were employed .

Table (3- 14) factors of under-relaxation

Properties	**Under-Relaxation factor**
viscosity	1
Momentum	0.7
Temperature	1
Body force	0.1

Turbulent Viscosity	1
Pressure	0.3
Turbulent Kinetic Energy	0.5
H_2O	1
Turbulent Dissipation Rate	0.5

3.4.4 Criteria for Convergence

At the end of each iteration, the residual error (RE) for each variable (Ø)is calculated using the equation:

$$R_E = \phi_n - \phi_{n.old} \qquad \text{....}(\mathbf{3-34})$$

The solve will terminate when the residual error for continuity, velocities, energy, H_2O, CO_2, turbulent dissipation rate, and turbulent kinetic energy equations reaches the values presented as shown in Table (3-15) . The residual error is inversely proportional to the numerical results' precision.

Table(3-15) Residual error for tested cases.

Equation	Continuity	X-velocity	Y-velocity	Z-velocity	Energy	K	ε	H_2o	Co_2
R. error	10^{-5}	10^{-5}	10^{-5}	10^{-5}	10^{-6}	10^{-5}	10^{-5}	10^{-5}	10^{-5}

3.5 Prediction of Human Comfort and Air Quality Parameters

The air temperature and velocity distributions, (ADPI), (PMV), (PPD), can all be anticipated after AIRPAK program had completed its analysis.

The following equations can be used to compute the (PMV), (PPD), and (ADPI), **[69,70,74].**

$$PMV = [0.303 \exp(-0.036M) + 0.028]L \quad \ldots.(\mathbf{3-35})$$

$$\mathrm{PPD} = 100 - \exp[-0.03353(\mathrm{PMV})^4 - 0.2179(\mathrm{PMV})^2] \quad \ldots.(\mathbf{3-36})$$

$$\mathrm{ADPI} = (N_\theta/\mathrm{N}) \times 100 \quad \ldots.(\mathbf{3-37})$$

The mean age of air , ventilation effectiveness index ε_t , Air exchange efficiency of occupants which allows for analytical IAQ measurement, was also used,**[16]**.

$$\tau_n = \frac{V}{Q_{MV}} \quad \ldots.(\mathbf{3-38})$$

$$\eta_a = \frac{\tau_n}{2(\tau)} \quad \ldots.(\mathbf{3-39})$$

$$D_i = \frac{\sum_{i=1}^{N} ID_i}{N} \quad \ldots.(\mathbf{3-40})$$

$$\langle\tau\rangle_D = \sum_i \langle\tau\rangle_i D_i \quad \ldots.(\mathbf{3-41})$$

$$\varepsilon_t = \frac{T_o - T_i}{T_m - T_i} \quad \ldots.(\mathbf{3-42})$$

$$\varepsilon_c = \frac{C_o - C_i}{C_m - C_i} \quad \ldots.(\mathbf{3-43})$$

CHAPTER FOUR

EXPERIMENT ALWORK

Chapter Four
Experimental Work

The goal of the experimental chapter is to generate performance data for (CC/MVPV) system under controlled settings. This information will then be utilized to create (CC/MVPV) system performance models for use in system simulation software. Comprehensive parameters are measured under various operating situations (indoor age of air, air distribution temperature) to determine (temperature distribution effectiveness (ε_t), temperature different between heat and foot (ΔT_{hf}) for occupants and air exchange efficiency (η_a).

Practical the tests were carried out in the laboratory building of Mechanical Engineering Department in University of Babylon under the climate of Iraq (Hilla City). Hilla city is located in latitude (32.46 ^{o}C). and longitude (44.42^{o}C)**, [75]** .In the summer, the city is known for its hot and dry climate .

This was accomplished by calculating the overall cooling load and estimating the real size of the supply air flow rate as well as the supply air temperature required for optimal ventilation. Set up and build a chilled ceiling to investigate the impact of heat sources on air age and air temperature distribution around people. All of the experimental tests were conducted as primary tests in June, with the results coming in July , August and September.

4.1 Experimental Facility and Configuration

4.1.1 Description of the tested room

Experiments were performed in office room of dimensions (3x2.5x2.5)m, equipped with mixing ventilation and personal ventilation placed on each desk and with a cooled ceiling (CC), as indicated in Fig.(4-2). Tested room is adiabatic, the wall layers and ceiling are made from insulated materials(sandwich panel with a thermal conductivity of 0.161 W/m.K) ,**[76]**.The total heat load to be removed of (445 W/m^2) due to occupants:(75 W/manikin); computers: (60 W/computer); lighting: (100 W). The (MV) system with its own air handling unit (AHU) provides (100%) filtered recirculated air to the office. The air supplied by the (MV) system at ceiling level from an end north wall. Exhaust diffuser was located in the north wall near the floor. The (PV) system was comprised of a computer-mounted panel that supplied conditioned clean air horizontally to the inhabitants and was served by a separate (AHU). Chilled ceilings are installed at height (2.5m) above the ground and account for (80%) of the total floor surface, **[77]**.

Fig.(4-1) Tested room from outside (at laboratory building)

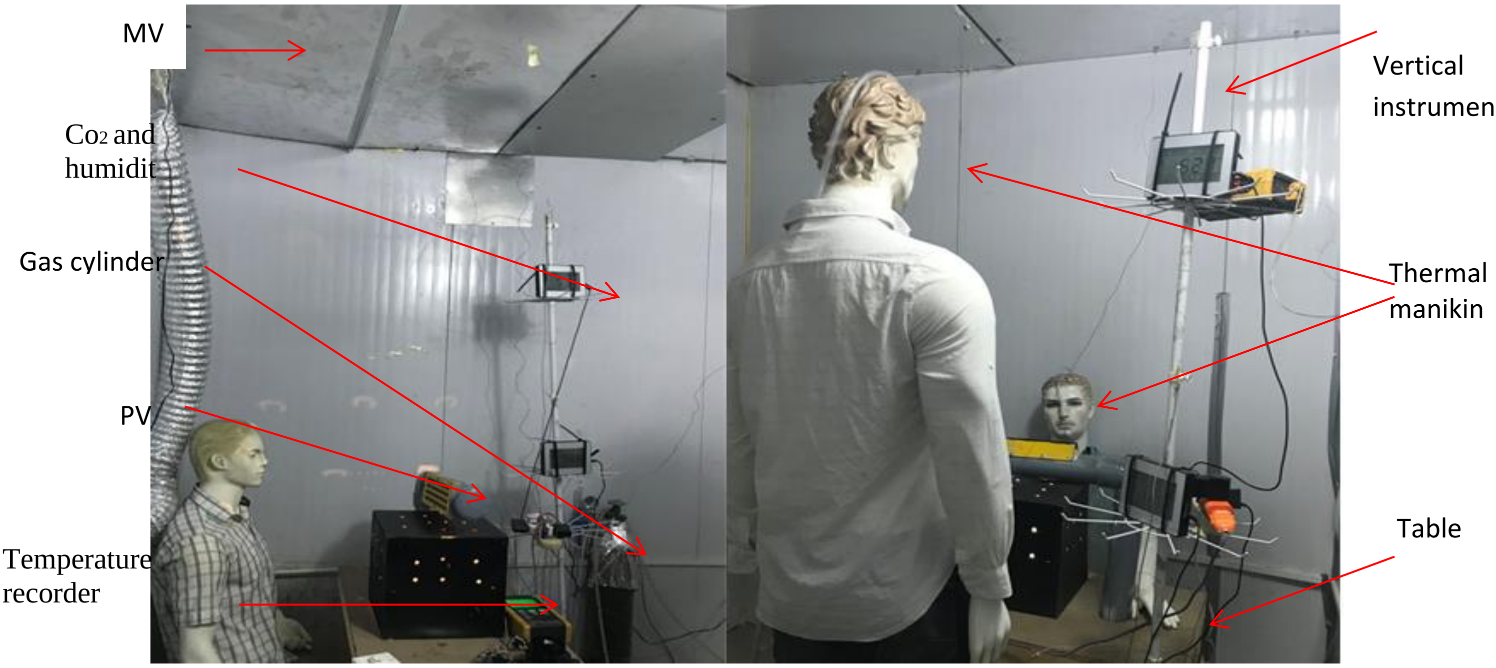

a- inside the testing room with the equipment's b- thermal manikin with instrument

Fig.(4-2) Photos of the experimental setup in an office room

All of the equipment from outside and inside of the tested room was utilized to run and regulate the (CC/MVPV) system as shown in Fig.(4-3), Table(4-1) .

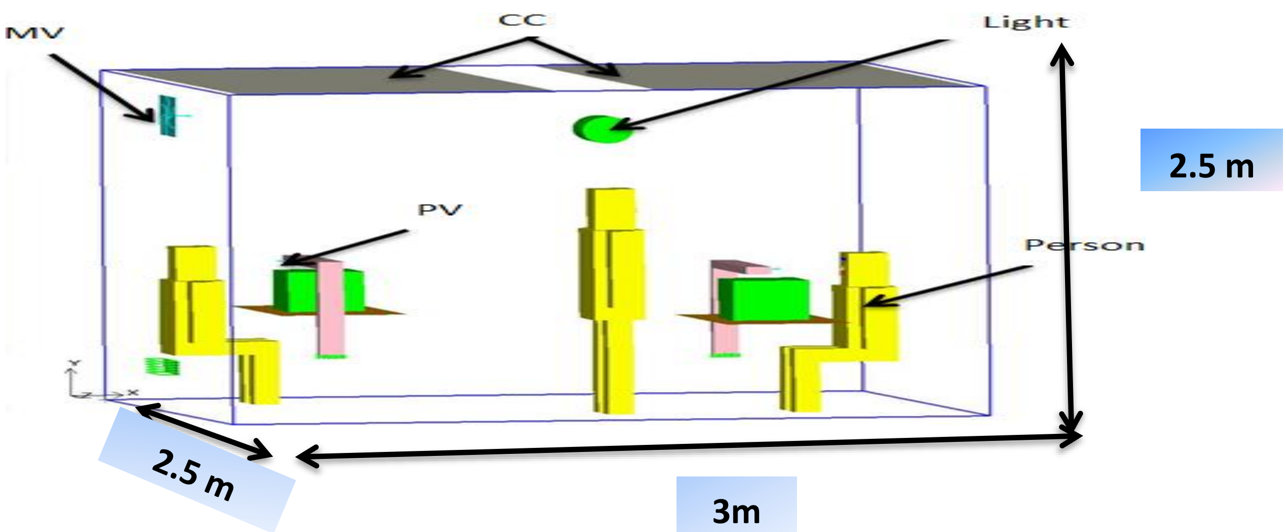

Fig.(4-3): Illustration of an office room with CC/MVPV

Table (4- 1) Room configuration for CCMV/PV for

thermally insulated room.

Item	Location (m)						Sensible heat (W), [78]
	Start			End			
	X	Y	Z	X	Y	Z	
Room	0	0	0	3	2.5	2.5	-----
Mixing device	0	2.1	1.15	0.1	2.2	1.35	-----
Exhaust grille	0	0.3	1.17	0	0.4	1.33	-----
Person no.1	0.25	0	0.5	0.45	1.1	0.9	75
Person no.2	2.75	0	2	2.95	1.1	2.2	75
Person no.3	1.75	0	2	1.95	1.1	2.2	75
Computer_no.1	0.6	0.7	0.3	0.9	1	0.6	60
Computer_no.2	2	0.7	1.7	2.4	1	2	60
Light	1.45	2.4	2.3	1.55	2.45	2.5	100
Computer desk 1	0.5	0.7	0	1	0	1	-----
Computer desk2	2	0.7	1.5	2.5	0	2.5	------
Personal device1	0.6	1.05	0.38	0.7	1.1	0.62	-----
Personal device2	2.2	1.05	1.88	2.3	1.1	2.12	-----
Total cooling load							**445W 59.3W/m^2 of floor area**

All Configuration of the test room were described as the following:

- **Two computers**: the computers were mimicked using two wooden boxes with many holes and an electric bulb to generate heat of around (60W) for each one As illustrated in

Fig.(4-4), a single light fluorescent lamp was positioned immediately below the ceiling in the middle of the room's western side .

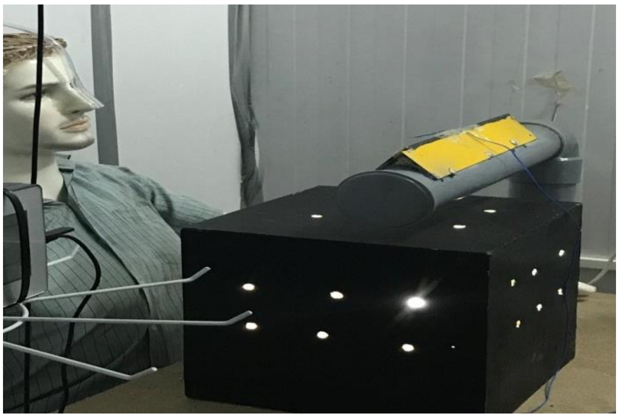

Fig.(4-4) Simulation of a computer using lamp to generate heat

- **Thermal manikin**

To simulate occupiers, three thermal manikins dressed in summer clothes (total insulation with chair of 0.59 clothes) were utilized in the experiment, and produced (75W) by putting a heat source(electric lamp) inside each thermal manikin,**[78]**.

As shown in Fig.(4-5), two manikins are seated, their hands are on the table in front of them, and one manikin with a standing height of (1.68m) is used to imitate a typical male . The breathing mode was utilized for the pollutant transportation study inside the room. The three manikin-equipped artificial lung was utilized to mimic human breathing. The manikin's lung system operated as a closed-circuit delivery and recovery system for respiratory air, and it was attached to the outside of its body by flexible tubing. The lung was regulated to simulate a typical inactive person doing light breathing exercises.

Two seconds of inhalation, two seconds of expiration, and one second of pause were used in each trial's breathing cycle. Two seconds of intake, two seconds of expiration, and one second of pause made up the testing breathing cycle. With a pulmonary ventilation rate of (6 l/min) for each breath, the breathing rate was roughly (12) breaths per minute. (0.5l / 2s =

0.25 l/s = 15 l/min) was used to compute the instantaneous flow,**[79]**. The exhaled air used in this study was not humidified, but it was heated to a density of roughly (1.144 kg/m^3) , which is believed to be comparable to that of exhaled air from a human subject based on presumptions regarding exhaled air properties. When the room air temperature was between (25)°C and the relative humidity was around (95%), assumed that exhaled air comprised (78.1 N_2, 17.3 O_2, 3.6 CO_2, and 0.9 air) vol.% ,**[79]**.

a- thermal manikin

b- breathing cycle

Fig.(4-5) Pictures of thermal manikin (standing and sitting) and breathing cycle.

- **Pollution source**

In this study, the (CO_2) tracer gas was employed to simulate contaminants inside tested room .To provide tracer-gas into the room, a put of (CO_2) gas cylinder and mass flow controller were placed and the injection tube in a side position of the room, as indicated in Fig. (4-6).

Trace gas (pollutant source) is supplied into the office room using a (CO_2) gas cylinder, some pipe connections, and a mass flow control unit. The trace gas passes through the gas supply tube and then is injected in front of the breathing zone of each dwarf for uniform distribution of the trace gas emissions from the gas cylinder. This setup allows the tracer gas to escape through human respiration, to simulate emission. A pressurized tank that contained a flux meter with a spherical suspension floating probe and a pressure adaptor made of stainless steel was used to supply (CO_2) .

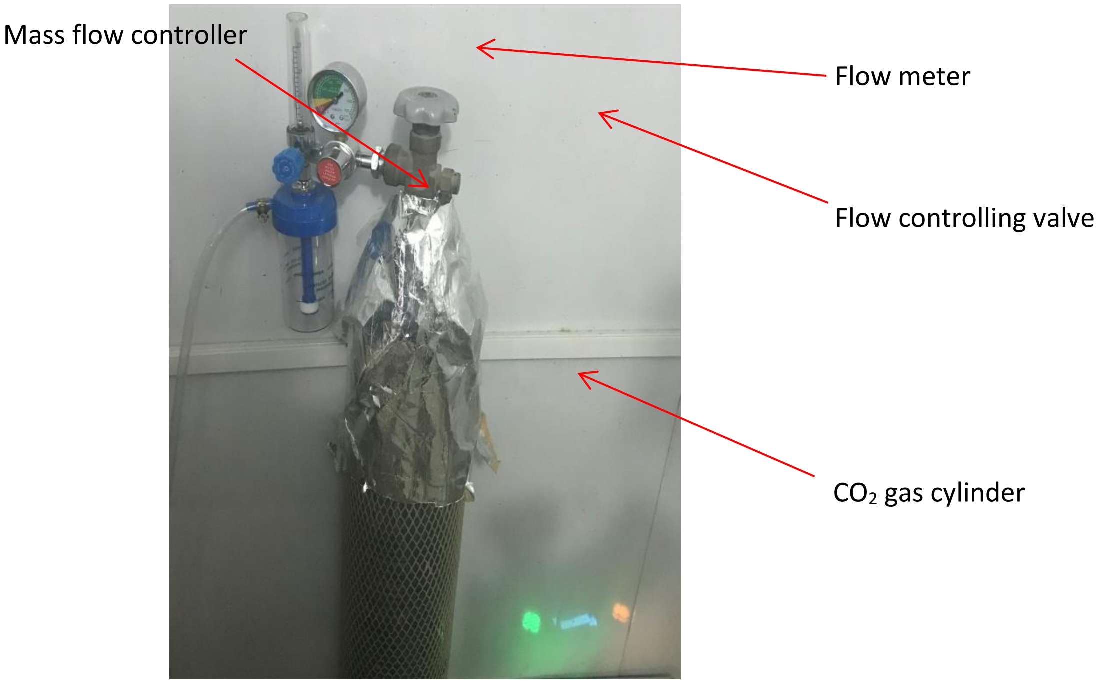

Fig.(4-6) Tracer gas channel with regulator

- **Chilled Ceiling**

Fig.(4-7) shows the hydraulic circuit schematically, four ceiling panels made of an aluminum metal comprising corresponding copper pipe meshes are installed in a parallel installation and fed directly from an unpressurized water tank. Flexible (1/2in) diameter reinforced copper pipes transfer water to the panels and return it to the tank. Two T-shaped pipe fittings are also installed at the panels' inlet and exit to provide for the aforementioned parallel flow.

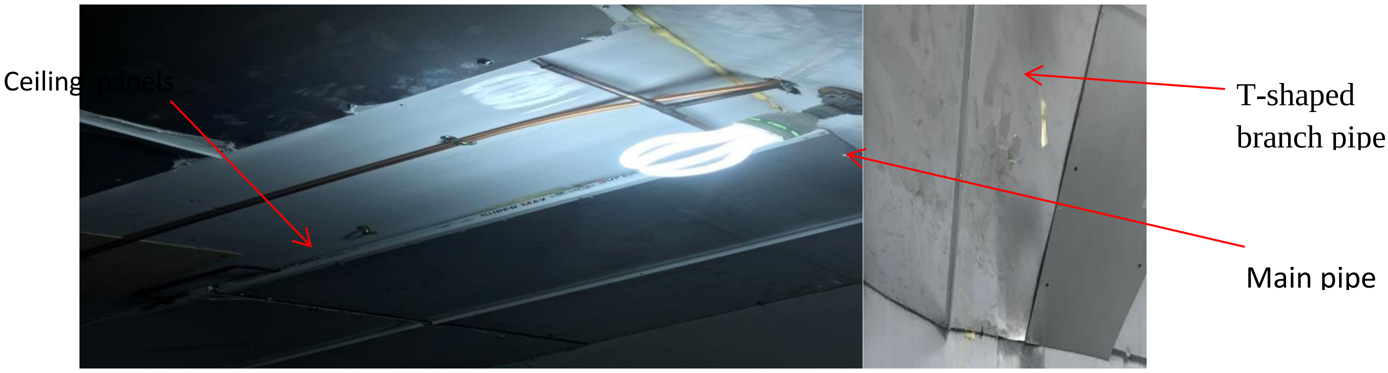

Fig.(4-7) Top of ceiling panels with copper pipes(main and return pipes)

The chilled ceiling is made up of copper coil fastened to an aluminum metal plate, according to ASHRAE standard, **[80]** as shown in Fig.(4-8) . Because the aluminum plate and copper tubes have high thermal conductivity ((237 W/m.°C) for (Al) and (390W/m.°C) for (Cu)**, [80]),** as well as corrosion resistance and ease of installation, so Then these existing materials are a viable option for chilled water use. Copper pipe has a diameter of (1/2 in)**,[77 and 80]** .The chilled ceiling plates cover around (80%) of the ceiling area. At the ceiling, there are four plates. The dimensions of each plate are (L×W) (1.25m x1.2m) and (0.1m) thickness. Aluminum sheeting and glass wool insulation cover the rear of each plate

.

Fig.(4-8) Bottom ceiling panel (copper coil pipe, aluminum metal plate)

Flow meter was also attached in the supply pipe, as shown in Fig.(4-9). This setup allows you to tune the mass flow rate anywhere between (2 and 7) kg/min.

Fig.(4-9) Flow meter

As shown in Fig. (4-10) , metallic adhesive tape was used to secure the water pipe mesh to the metal sheet over each individual tube. To further ensure virtually ideal heat conduction between the pipes and the metal sheet and to reduce heat transfer from the cold water to the air in the top zone, glass wool insulation and aluminum sheeting were carefully placed over the pipes. An aluminum sheet initially reflected the majority of the heat radiation it encountered since the surface that was facing down had a relatively low emissivity rating. This surface's emissivity was raised to (0.8) by using an acrylic matte spray to paint it. This value was determined using surface measurements that matched thermographic camera photos

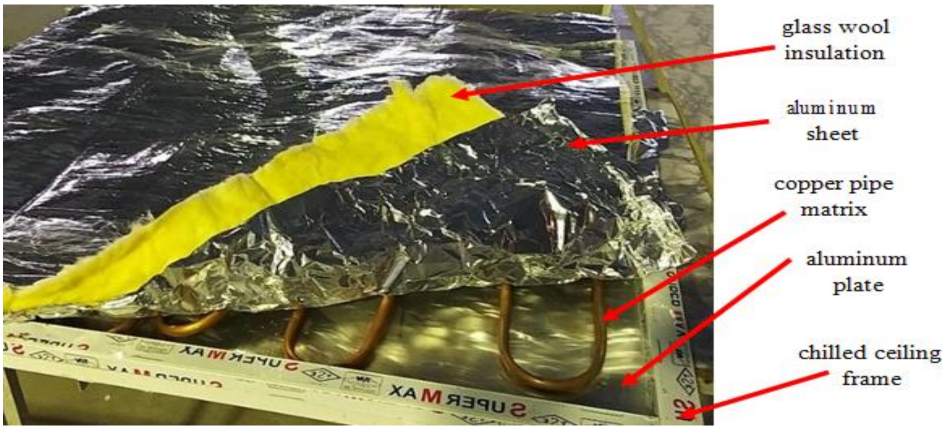

Fig.(4-10) Bottom ceiling panel (aluminum sheeting , glass wool insulation)

Cold water is produced using a vapor compression refrigerator with an evaporator submerged in the water tank, as depicted in Fig. (4-11) . The supply temperature can be regulated within a certain range by controlling the refrigerator with an external signal. This on/off signal is produced by a straightforward controller that is connected to the compressor using a power contactor. The chilled ceiling specification is described in Table (4-2).

Condenser

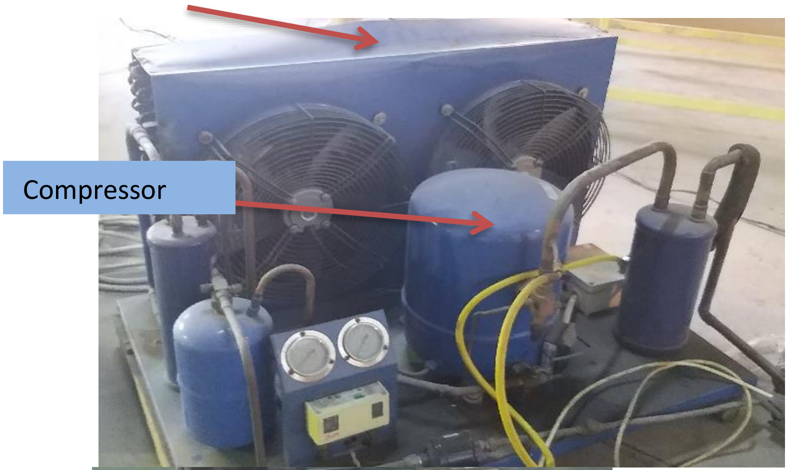

a- condenser unit **b-** evaporator unit

Fig.(4-11) Vapor compression refrigerator with an evaporator immersed in the water tank**.**

Table(4-2) Detailed chilled ceiling specification

	specification
Chiller	Model MT64-4VI Manufacture Danfoss Co./France Refrigeration gas F_{22}
Panel	four plates fixed at ceiling and cover about (80%) of the ceiling area
Pipe	main pipe at diameter (½ in) and (15m) length branch pipe at diameter (½ in) and (20m) length for each plate in ceiling . thermal conductivity (K= 390W/m.°C)

Plate	Dimensions of each plate (1.25 x 1.2) m , (1mm) thickness thermal conductivity (K= 237W/m.°C) insulation (glass wool) (K= 0.04W/m.°C)

4.2 Ventilation systems

Two systems (MV and PV) were used to ventilate the isolated office room. The central control system regulates the supply air temperature for the different cooling load . During the experiments, the MV air flow rate was kept at (46 l/s) and the PV air supply rate is fixed at (5and7.5 l/s). Fig.(4-12), Fig .(4-13) depicts the PV and MV air terminal devices.

4.2.1 Air supply device

Two ventilation devices were utilized in the experiment: mixing ventilation, personalized ventilation. At (2.2m) high, the mixing station was positioned at the top of the wall.The location of the mixing device, which was inserted in the low level of the wall, as seen in Fig.(4-12).

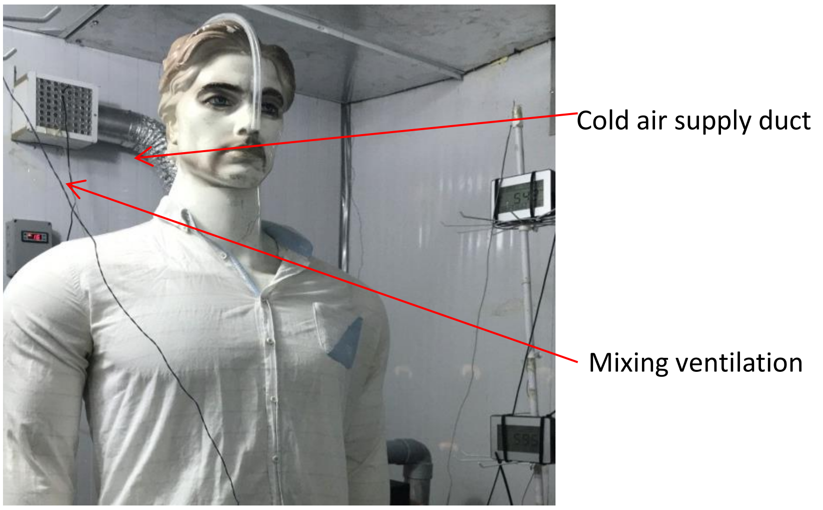

Fig.(4-12)Location of mixing devise

For (MV) system, air diffuser was manufactured in accordance with guide of mixing ventilation air distribution design .The diffuser face is made of aluminum plate with dimensions of (37cm width and 42cm height) and (100) holes with a diameter of (1.6 mm) on its surface, as illustrated in Fig.(4-13). To guarantee consistent air distribution over the effective air supply region, an aluminum plate with holes is covered with a metal mesh with small holes, they are mounted to the wooden frame to create the rectangle .To ensure that the cold air does not escape, all of the side vents were covered. The upper side of the wooden frame has an entrance air duct.

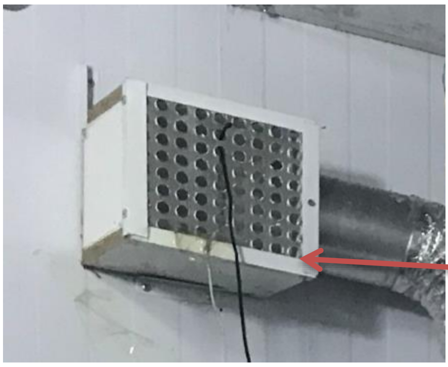

Fig.(4-13) Mixing ventilation

Air conditioning temperature controller type (elitech kibnt STC-200+)

It is a universal and high-efficiency performance that has been used in the cooling system used in the test chamber for temperature regulation. The supply air temperature inside the tested room is controlled by sensors installed in supply device for change supply air temperature (T_S) change with varied the value of cooling load treated by mixing ventilation (CL_{MV}).

Parameter set:

The set condition is pressing the "set" button for more than (2 s), which enters the user settings state, where the time setting indicator and digital tube display the current temperature value,.

Temperature setting: in the user's Settings state, press the "Δ" or "∇" keys to adjust the temperature up or down. Each click the adjustment (1°C) , hold (2 s) above, to quickly adjust. Table.(4-3) shows all setting for device

Table .(4-3) List for device settings

Setting item	Paramater setting range	Default	Code
Temperature differential setting	-1º C - 1 ºC	3 ºC	**F0**
Compressor delay time	0-9 Minute	3 Minutes	**F1**
Temp lower limit setting	-40 º C Set temerature	-20 ºC	**F2**
Temp upper limit setting	70 º C Set temerature	20 ºC	**F3**
Mode optional	1: refrigeration 2:heating 3: alarm	1	**F4**
Temerature calibration	-5 ºC- 5 ºC	0	**F5**

Refrigeration mode:

• Reset the temperature difference relay and start the refrigeration process when the compressor delay time or sensor temperature exceeds the settings for either of those variables.

• When the sensor temperature drops below the predetermined level, the relay is turned off, which stops the refrigeration process.

Dimensions and other technical details:

- The machine measures 77.0 x 34.5 x 65.5 mm.
- The holes for attachment are 70.5 x 28.5 mm.
- The temperature range for operation is -5 to 60 °C.
- The temperature range for storage is -30 to 85 °C.
- The relative humidity fluctuates between 20% and 85%.

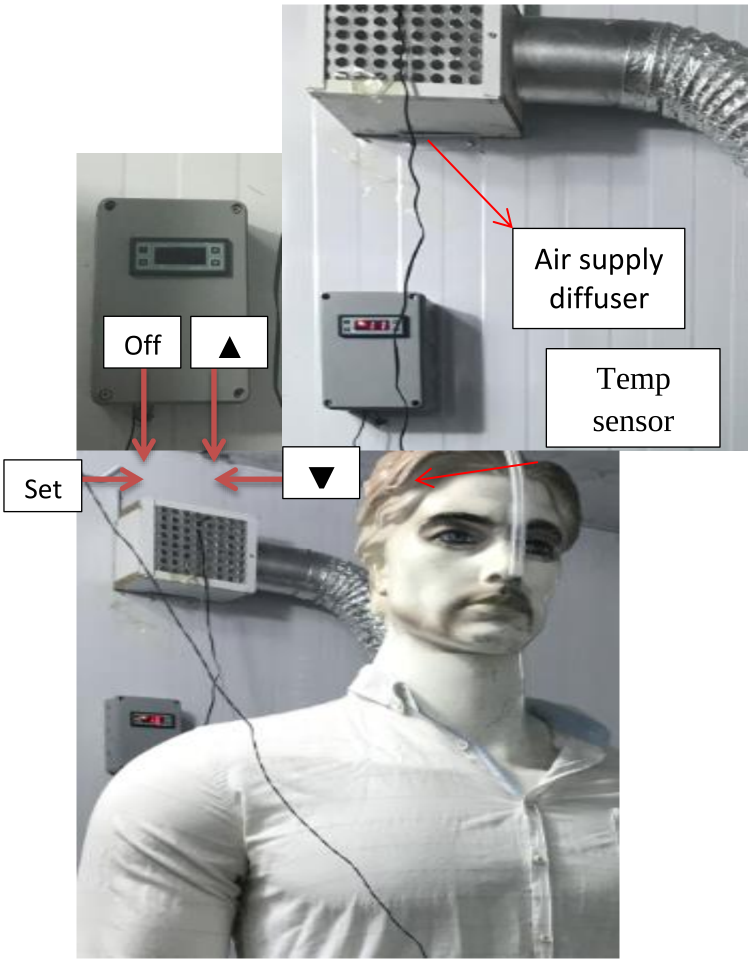

Fig.(4-14) The temperature regulator installed on the MV

For (PV) system , air diffusers were manufactured according to the recommendations for PV made in Melikov (2004) and Kaczmarczyk et al. (2004) ,**[81, 82]**. the personal ventilation system comprises of an air terminal device (ATD), an air intake section (suction fan), and flexible connection tubes put before and after the fan, as well as individual flow control. The air terminal device has (48) holes with a diameter of (1.5cm) spread equally and with similar dimensions over its surface area. Whereas (the total number of holes divided by the total area of each hole). A regulator controlled the amount of air absorbed by the fan. Personal ventilation systems gather air from a height of 0.4 m and deliver it to the seated person's breathing zone at a height of (1.1 m) as illustrated in Fig. (4-15).

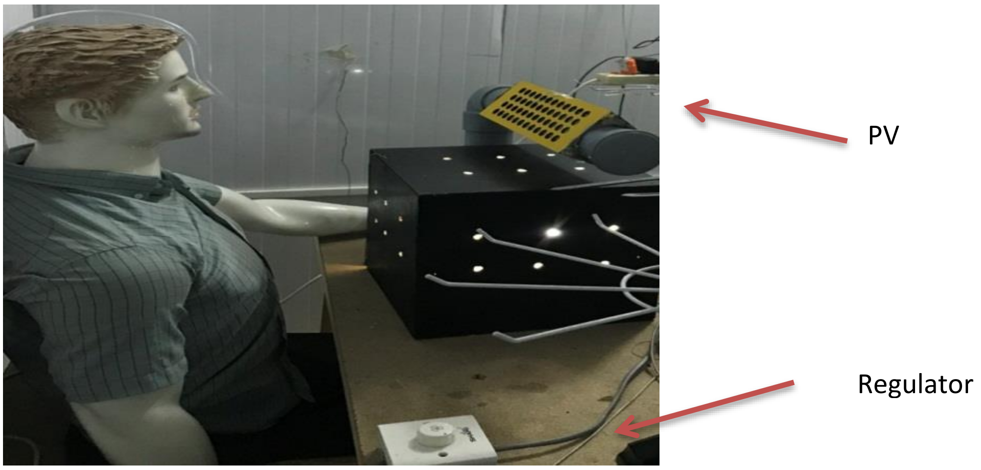

Fig.(4-15) Photo of thermal manikin with PV system

4.3 The experiment's protocol

1. All of the room's heat sources, (MV) and (PV) systems were turned on.
2. The temperature and MV flow rate are set to keep the room at (25 °C).
3. To reduce body temperature asymmetry, the inlet temperature of the PV supply was (3 °C) lower than the ambient temperature (25 °C) and the air flow rate was kept constant **,[82].**
4. The valve that directs cold water from the chiller to the ceiling pipes must be fully opened in order to switch on the (CC) system.
5. After performing the experiment for three hours, the room temperatures stabilized, and the particle generator was turned on.

6. Once the CO_2 emission sources were activated, they reached a quasi-steady state in (3min).

4.3.1 The water pump and piping size

Pipe sizes are determined by two major elements (velocity of water flow and friction loss). Erosion, noise, pumping, and installation costs all limit pipe system maximum and minimum velocities. If the pipe is too small, it creates excessive velocity, which causes noise, erosion, and pumping costs. The size of the pipe must be chosen to avoid the effect of high velocity and to decrease the initial cost, while if the pipe size is too large, the installation cost appears,**[13].** The chart published by ASHRAE 2009 is used to evaluate pressure loss in copper pipes, **[83].** This chart is suitable for water temperatures ranging from (15.5 to 93.3)°C.

The value of the pressure drop in copper pipes can be calculated using Eq.(4-1)and table (4-4), which shows Pressure droop in copper pipes and plastic pipes, depending on the piping system diagrams (fracture loss of water in a copper pipe) , **[84].**

Table.(4-4) Pressure droop in copper pipes and plastic pipes

pipe and fitting	**Length (m)**	**Diameter (mm)**	**mass flow rate (L/s)**	**pressure loses (N/m^2)**
Copper pipe	60 m	12.5	0.039	6500

Copper elbow	46 elbow	-	0.039	455200
Copper main pipe	3 m	14	0.156	7500
			Total	469200

From computed total pressure loss in pipes and mass flow rate, the minimum powerrequirement for the pump needed in this study can be calculated by used, **[84]**:

$$P_{loss} = \frac{\text{water flow rate x pressure}}{\text{water flow efficiency}}$$
….(4-1)

By assuming the efficiency of water pump is (80%), then the pump power is (98W).

4.4 Experimental conditions and assumptions

1. The temperature in the interior room is set at (25 °C).
2. The PV inlet temperature is set at (22 °C), and airflow is set at (5 l/s , 7.5 l/s).
3. The flow rate of MV is set at a constant value of (46 l/s).
4. The supply air for mixing ventilation is set at a constant flow rate and velocity(46l/s , 2.5 m/s).
5. The flow rate of the chiller water supply in the main pipes is set at (0.156 l/s) while the flow rate through each sub-circuit of the chilled water system varies at (0.039 l/s) , at (η) varies from (25% to 80%) .
6. In order to calculate the time required to achieve the usual concentration measured outside the room, the initial CO_2 concentration in the testing room at its maximum value is set at (1000 ppm) for each value of.
7. The chilled water and air supply temperatures are adjusted based on the cooling load eliminated by the chilled ceiling.

4.5 Describe of cases study

The performance of two types of installed (CC/MVPV),(CC/MV) systems were investigated in a steady state and under various operating settings , then presented set of data on air age, CO_2 content, and air temperature distribution .

4.5.1 Cases study

Eight different instances were tested for CC/MV and CC/MVPV systems in this study. Exact details about the testing circumstances and system functioning parameters are listed in Table.**(4-5) ,(4-6).**

4.5.1.1 Case-I (with CC/MV only)

This case includes four tests for each system at various cooling load removal ratios using chilled ceilings (0%, 25%, 50%, and 80%). At a constant air flow rate (46 L/s) and design room temperature, and the supply air temperature (T_s) changing with varying cooling loads, the value of the cooling load treated by mixing ventilation (CL_{MV}) can be determined as indicated in Appendix-A.1. Table (4-5) presents the operating conditions for each test in Case I, where (T_s, RHs, $T_{w,s}$, $T_{w,r}$, V_{ws}, and T_{CC}) are measured on the experimental days and adjusted based on the cooling load eliminated by the chilled ceiling.

Table.(4-5) Operating conditions for (Case-I)

Case		**η (%)**	**CL_{MV} (W)**	**CL_{CC} (W)**	**Q_{MV} (L/s)**	**Q_{PV} (L/s)**	**T_s (°C)**	**$Ø_s$ (%)**	**T_{CC} (°C)**
Case -I	CC/MV	0	445	0	46	-----	17	89	0
Case -I	CC/MV	25	333.75	111.25	46	-----	19	75	23
Case -I	CC/MV	50	222.5	222.5	46	-----	21	65	21.39

Case -I	CC/MV	80	89	356	46	-----	23	58	19.45

4.5.1.2 Case-II and Case-III (with CC/MVPV system)

This case includes four tests for each system at various cooling load removal ratios using chilled ceilings (such as 0%, 25%,, 50%, and 80%). At a constant air flow rate (46 L/s) and design room temperature, the supply air temperature (Ts) changes with the value of the cooling load treated by mixing ventilation and personal ventilation (CC/MVPV).

PV-supplied air temperature and flow rate were set to (22 °C, 5 l/s, and 7.5 l/s) [25], which can be determined as indicated in Appendix-A.1. Tables (4-6) present the operating conditions for each test in Case II, where (T_s, RH_s, T_{ws}, T_{wr}, V_{ws}, and T_{cc}) are measured on the experimental day.

Table.(4-6) Operating conditions for(Case-II and Case-III)

Case		**η (%)**	**CL_{MV} (W)**	**CL_{CC} (W)**	**Q_{MV} (L/s)**	**Q_{PV} (L/s)**	**T_s (°C)**	**$Ø_s$ (%)**	**T_{CC} (°C)**
Case -II	CC/MVPV	0	445	0	46	5	17	89	0
Case -II	CC/MVPV	25	333.75	111.25	46	5	19	75	23
Case -II	CC/MVPV	50	222.5	222.5	46	5	21	65	21.39
Case -II	CC/MVPV	80	89	356	46	5	23	58	19.45
Case-III	CC/MVPV	0	445	0	46	7.5	17	89	0
Case-III	CC/MVPV	25	333.75	111.25	46	7.5	19	75	23
Case-III	CC/MVPV	50	222.5	222.5	46	7.5	21	65	21.39
Case-III	CC/MVPV	80	89	356	46	7.5	23	58	19.45

4.5.2 Local air age measuring

The decay method was utilized in this study to calculate the mean age of the air in the room using a tracer gas, and it is an important component in determining the quality of ventilation and different ventilation effectiveness indices: local air change index, air exchange efficiency, and temperature effectiveness**,[85].** The principle of the decay method is based on marking the air in the ventilated room with the tracer gas and evaluating the time necessary to replace the marked air with unmarked air (ISO 16000–8: 2007) **,[86]**.The tracer gas (CO_2) was injected at a height of (1.8) m in various points of the test room to improve mixing, and minutes were allowed to pass to ensure thorough mixing. The minimum flow rate and the duration of the(CO_2)introduction were established in compliance with the standard**, [79]** as a function of the volume of the room. The presence of people in the test room is a carbon dioxide source, so its concentration was recorded before the tracer gas introduction in order to have a reference value for the mean age of the air calculation. The tracer gas injection was halted after an acceptable concentration was achieved. Each condition was tested, and all tests were performed a minimum of three times. By recharging the chamber with tracer gas numerous times for each condition and reanalyzing the decay, the precision of the test procedure was determined.

Advantages of decay method ,[79]:

- It works best for sampling a single zone.
- A uniform initial tracer gas concentration in the space can be created quite easily.
- Additionally, it's the easiest approach to monitor current ventilation conditions. When the air exchange rate is less than 10 h^{-1} (ASTM 2001), the decay approach can be utilized .
- Fast, simple, economical and accurate method. Also, do not cause any inconvenience, during working hours.

4.5.3 Measurement Locations Arrangement

Three vertical instrument stands were used to measure the temperature distribution in the test office room, which located in three different places . Each stand has seven points for mounting the measuring instruments, which are positioned at various heights (0.1, 0.4, 0.8, 1.1, 1.4, 1.8 and 2 m) from the room's floor as shown in Fig.(4-16).

The temperature, humidity and tracer gas concentration is measured the manikin(at 1.1 and 1.8m for sit and stand occupant), at the supply air, and at the exhaust air, while others represent the ambient air temperatures around and above the seated manikin **,[65],** the temperatures of supply air from mixing and personal ventilation are likewise measured as well as the exhaust air .The thermo-couples on the floor surface measure the temperatures of the inner surface of the wall, the ceiling, and the floor. The thermocouples, temperature recorder devices, CO_2 and humidity measurement equipment were carried by the three stands to cover the environment in the occupied zone.

As indicated in Fig. (4-17) instrument stands were placed in three different places within the test room. The first poles (stand-1) in front of the supply diffuser, while the second and third stands (stand-2 and stand-3) are close to the thermal manikins. This strategy of instrument stand distribution provides sufficient data to comprehend air characteristics and pollutants concentration behavior in occupied zones and near people **,[65].**

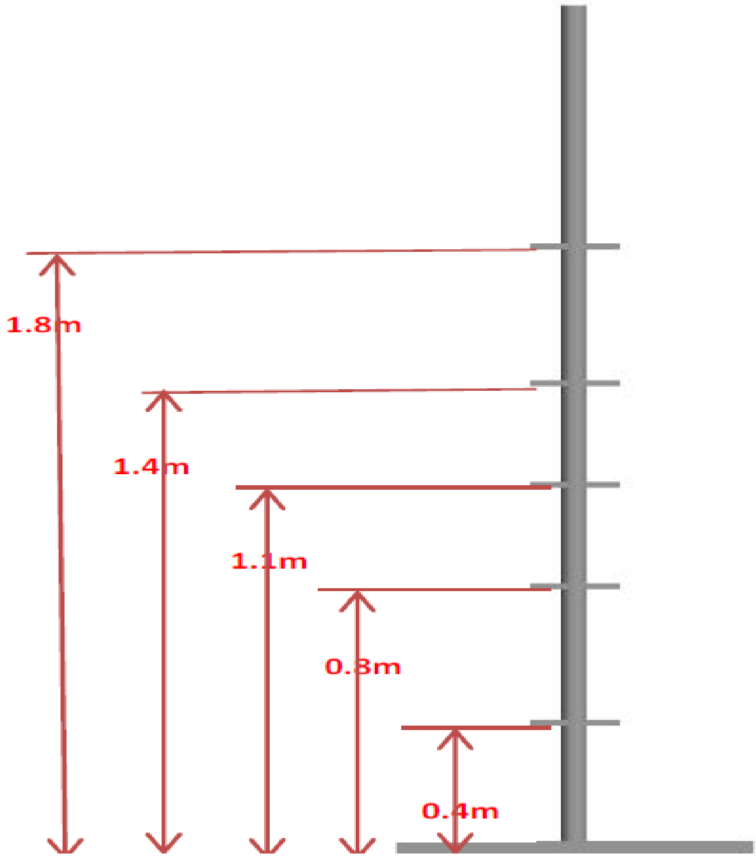
1.8m
1.4m
1.1m
0.8m
0.4m

a- photo of instruments stand b- schematic diagram of instrument stand

Fig.(4-16) Distribution of the measurement devices on instruments stand

.46 Measurement Instruments

There were three basic systems for measuring devices:

1- Measurement system for air, walls, and chilled ceiling Surface temperature.
2- Measurement system for CO_2 concentration and relative humidity.
3- Measurement system for water flow rate and air supply velocity.

4.6.1 Measurement system for air, walls, and chilled ceiling Surface temperature.

This system is built around a set of K-type thermocouples that are permanently installed in the test room. As shown in Figure (4-18), The K-type thermocouple (Nickel Chromium/ Nickel Aluminum) coupled to three data temperature recorder devices (BTM4208 SD) each with twelve channels , which stores the observed temperatures in RAM which is subsequently read by a computer.The temperatures are recorded in RAM, which is subsequently read by a computer. Table(4-5) summarizes the characteristics of the temperature recording device .The thermocouple's calibration and uncertainty are shown in Appendix (B.1).

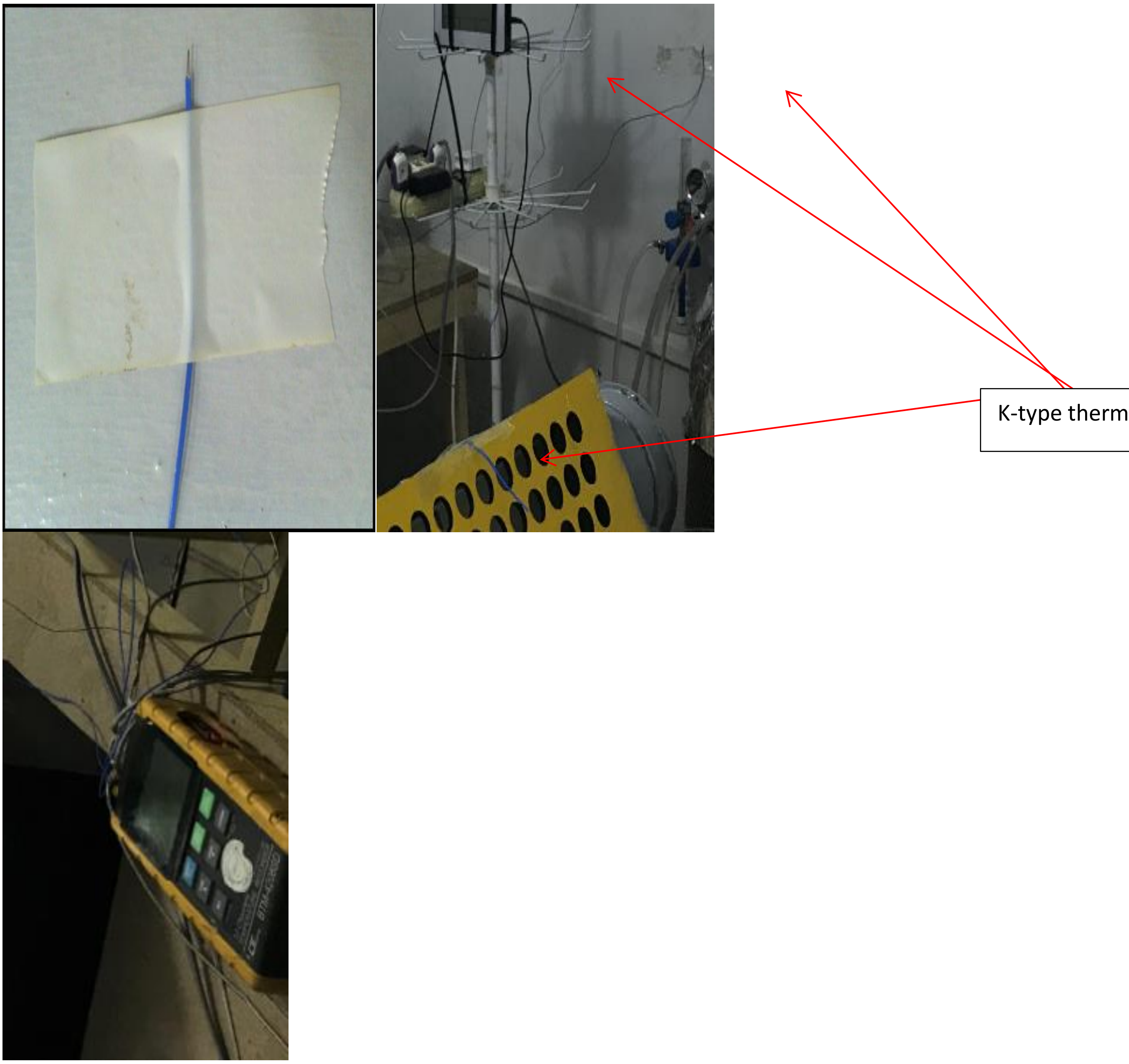

(a) K-type thermocouples (b) recorder devices

Fig(4-18) K-type thermocouples with recorder

Table(4-7) Properties of temperature recorder device

Parameter	Range	Accuracy ,Resolution

Type K thermcouple	-100 to 1300 ºC. 1 to 3600 seconds	0.4% , $\frac{0.1}{1}$ ºC

thirty- four thermocouple sensors were distributed during experiment tests:

nineteen sensors are installed on the sidewalls and the floor (ten sensors for the walls , four sensors are attached to the chilled ceiling surface and three sensors are attached to the exhausted grill of mixing ventilation and personal ventilation, two sensors are attached in the front of BZ for each manikin)as indicated in Fig. (4-19) .The average temperature of the three thermocouple temperature records was used to calculate the temperature of the chilled ceiling.

Fifteen sensors are installed on three vertical instruments poles to allow vertical temperature dispersion in the tested room (each poles includes five thermocouple sensors at various heights (0.1, 0.4, 1.1, 1.8, and 2.4m) as indicated in Fig.(4-19).

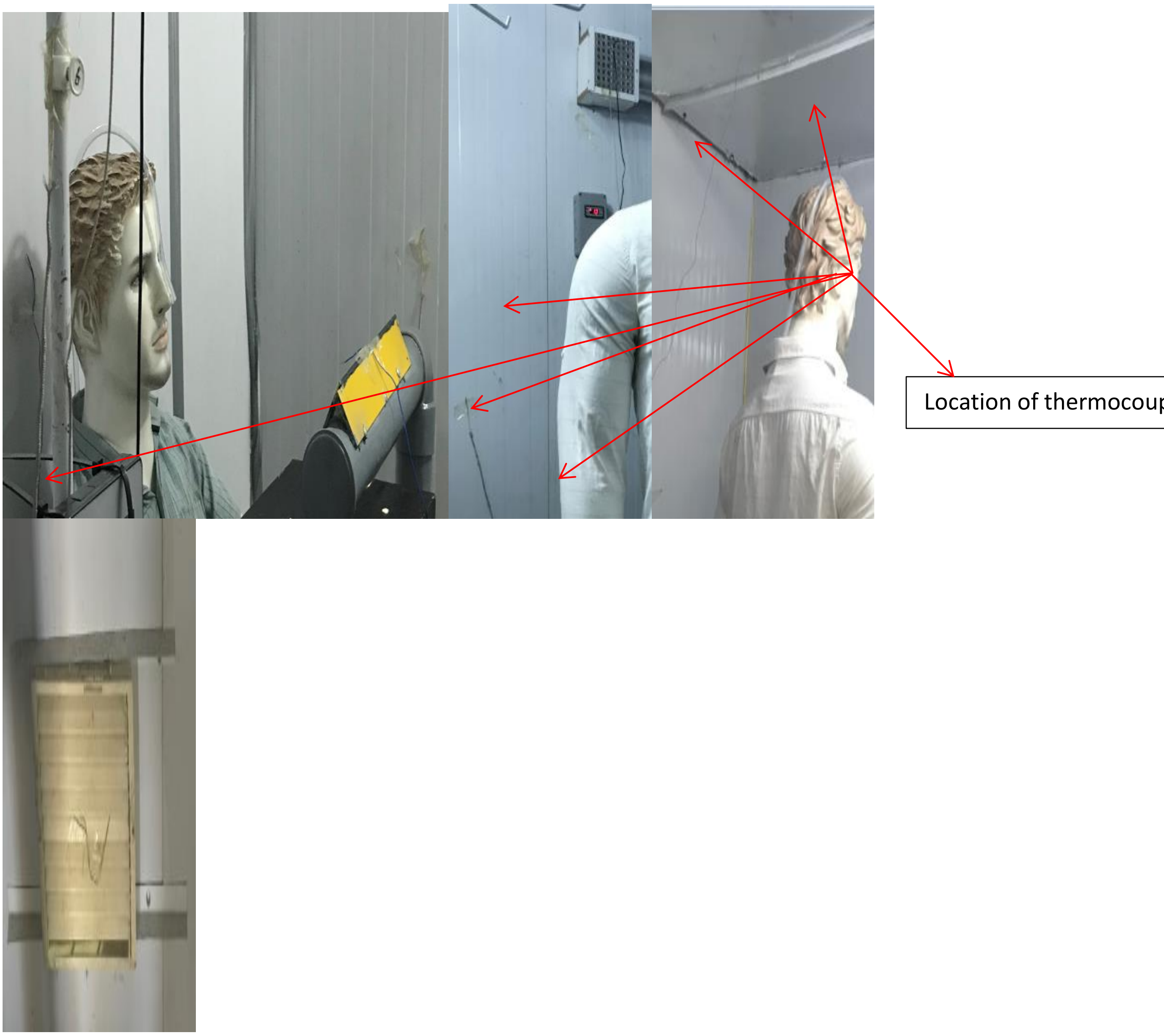

Fig.(4-19) Locations of thermocouple fixed on (stands, PV, wall ,MV, CC, exhaust)

Temperature controller (STC-200): Controlling the temperature of the cooling air in the tested room using a temperature sensor placed against the mixing ventilation through the sensor as shown in Fig.(4-20). The temperature is changed and reset at each cooling load.

Table(4-8) summarizes the characteristics of temperature controller.

The calibration of the flow meter device is shown in Appendix (B.2).

Table(4-8) Properties of temperature controller (STC-200)

Temperature controller (STC-200)	Range of temperatures: -50 to 99 °C Resolution: 1 Precision for temperature control and measurement: ±1 ℃ Relay contacts have a (10 A at 250 VAC) capacity.

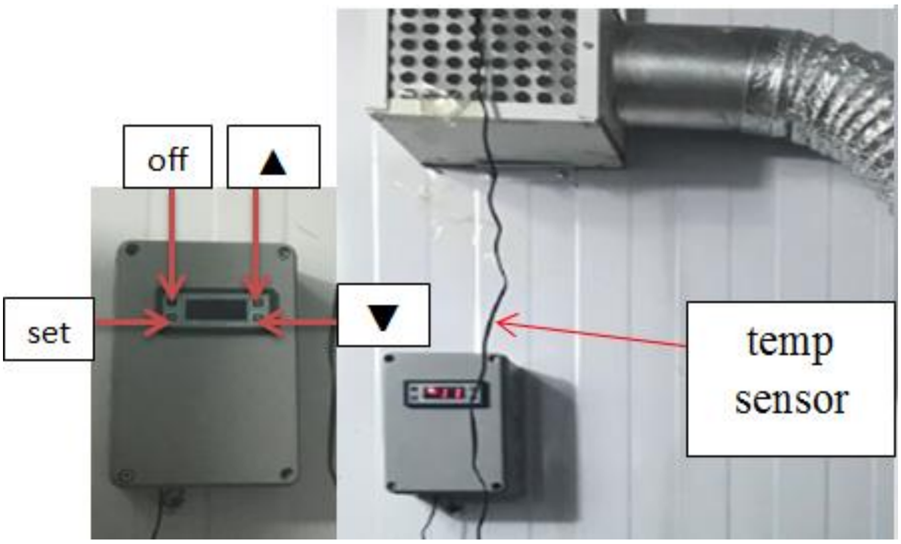

Fig.(4-20) Locations of temperature controller fixed on MV

4.6.2 Measurement system for CO_2 concentration and relative humidity.

Air quality has been evaluated using (CO_2 and humidity recorder devices). Table(4-6) summarizes the characteristics of various devices. All recorder data can be downloaded to the computer through USP cable using special software that came with the device, the information is organized in a table format (Excel). This device allows you to set the time between each reading interval. In Appendix, you'll find the certificate of compliance (B.3). Six CO_2 devices were installed throughout the room , at height of (1.1m, 1.7m) were selected to represent possible presence of a sitting and standing person. As illustrated in Fig.(4-21) , these points are classified into the following categories: (0.5, 1.1, 1.25m), (0.5, 1.8, 1.25m), (1.85, 1.1, 0.4m), (1.85, 1.8, 0.4m), (2.1, 1.1, 1.85m), (2.1, 1.8, 1.85m), (2.1, 1.8, 1.85m), (2.1, 1.8, 1.85m), (2.1, 1.8, 1.85m), (2.1, 1.8, 1.85m).

Table.(4-9) Properties of CO_2 and humidity recorder devices

Parameter	Range	Accuracy, Response time
Carbon Dioxide reading	0-9999 (ppm)	±5 (ppm) ,10 sec
Humidity reading	0- 99.9 (%)	±2 %

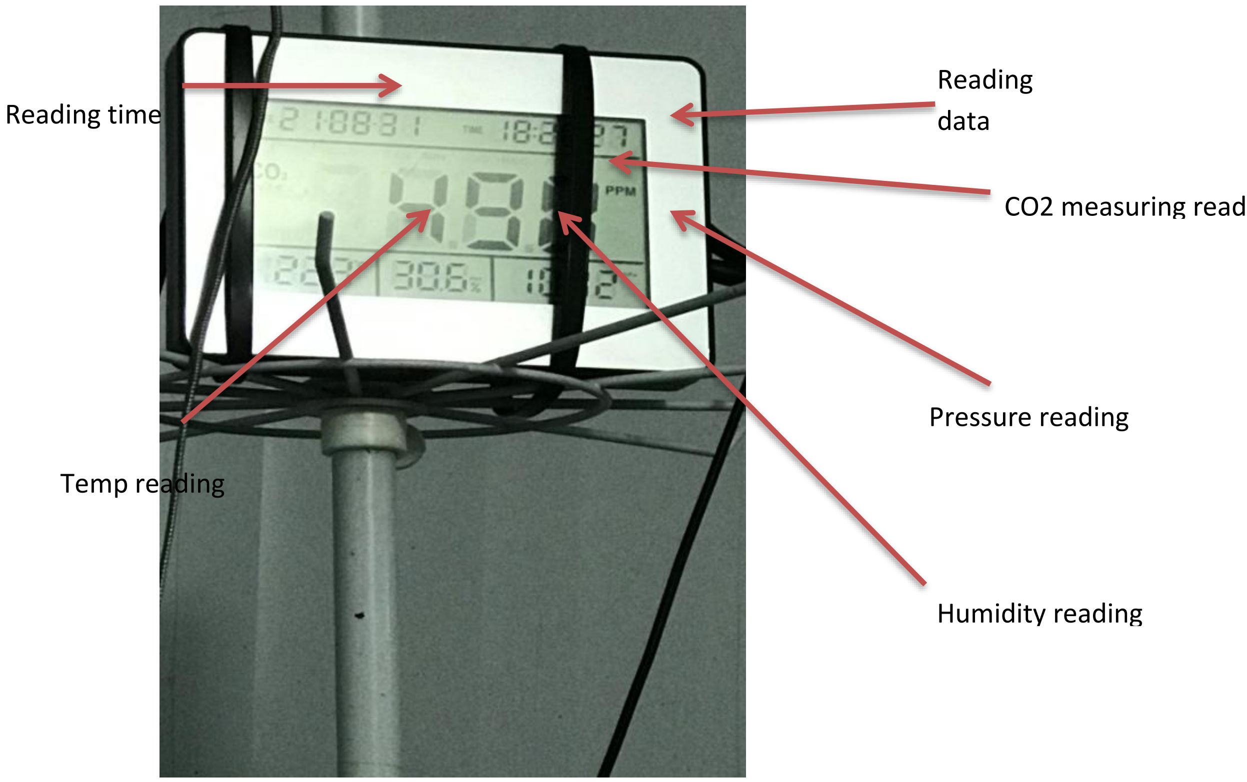

(a) recorder devices

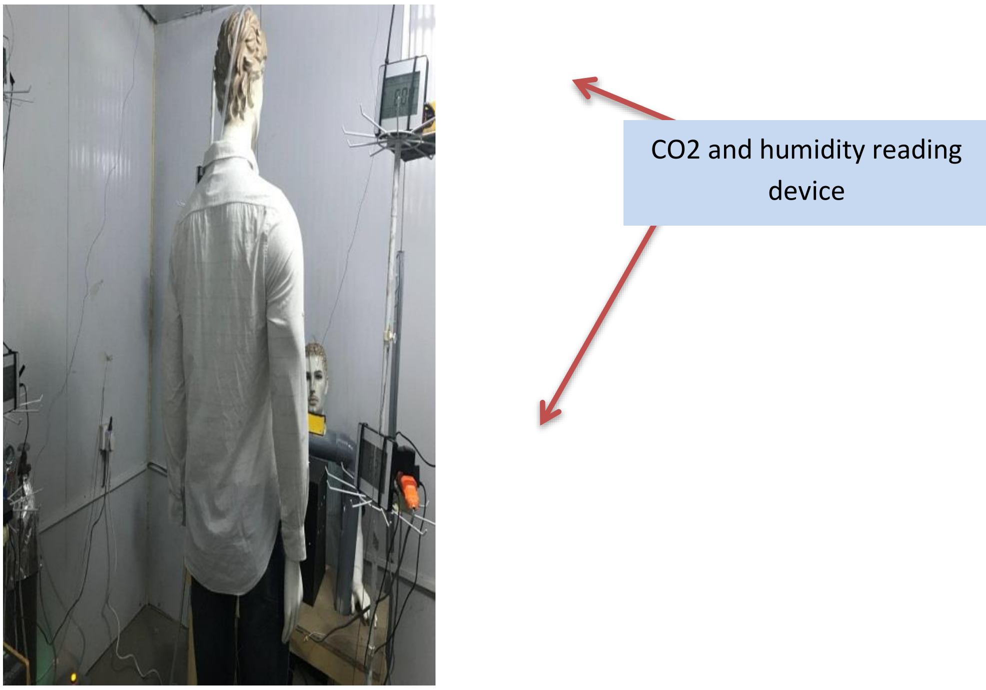

(b)installing the devices on the stands

Fig.(4-21) Recorder devices for CO_2 and relative humidity

4.6.3 Water flow rate and air supply velocity measurement system

4.6.3.1 Flow meter device

A flow meter(Platon type) is a device that measures the amount of water flowing through a pipe and delivered to the chilled ceiling. After the water pump, the flow meter was connected to the main plastic pipe in a series configuration. The required water flow rate for each value of is adjusted using a control water valve(η).A flow meter is a device that measures the amount of gas CO_2 flowing through a cylinder and delivered to the person's nose . After the gas pump, the flow meter was connected to the main plastic pipe in a series configuration. The required water flow rate for each value of is adjusted using a control gas valve(η) as seen in Fig. (4-22).

The calibration of the flow meter device is shown in Appendix (B.2).

Fig.(4-22) Flow meter for gas Co_2

4.6.3.2 Thermos-anemometer instrument

The temperature, air flow and velocity of the air supply were measured using the (thermos-anemometer 8901) instrument, which was placed in front of the air supply diffuser as illustrated in Fig (4-23). For air velocity, the accuracy and resolution are (2% and 0.01m/s) respectively with a response time of (1s). For air temperature, the accuracy and resolution are (0.6°C) and 0.1 (°F/°C). This device is situated in front of the air supply diffuser and waiting until the reading to reach steady state conditions for the air velocity and temperature are measure. Table(4-10) summarizes the characteristics of various devices.

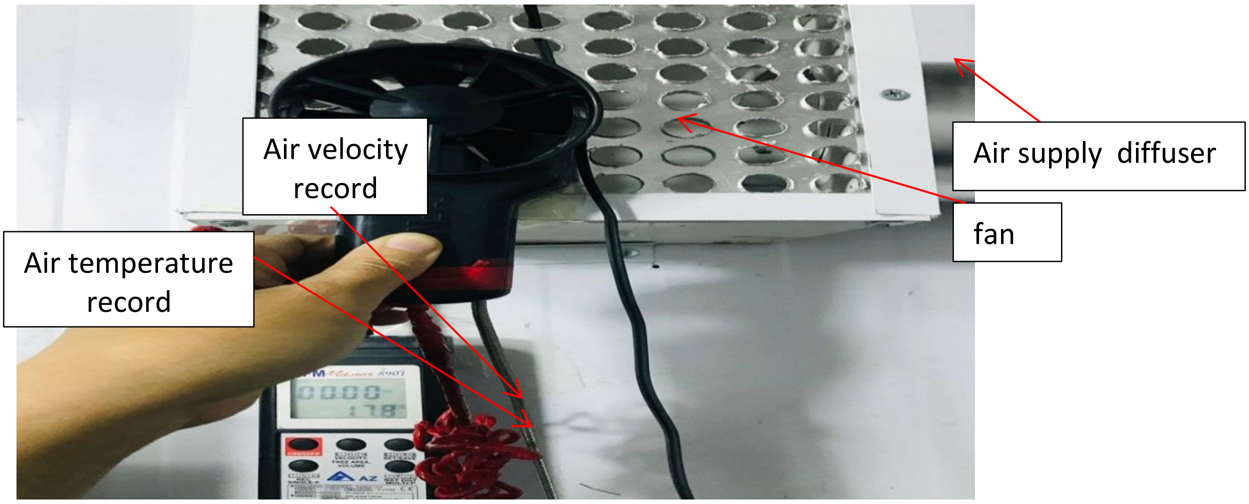

Fig.(4-23) Thermos-anemometer instrument

Table.(4-10) Properties of flow meter and thermos-anemometer devices

flow meter	**Range**	**(0-10L/min)**
	Accuracy	(±1.25%).
thermos-anemometer (Velocity , Temperature)	Range	(0.01m/s)
	Accuracy	±2% (±0.6°C)
	response time Resolution	(1s) 0.1 (°F/°C.).

4.7 Measurements Procedures

1. In all of the experiments work carried out in this research, recording of measurement data after operating the system directly and pollutant injection and begin attaining a stable condition(approving the data recorded after approximately 3 hours) .
2. All the data from the objective measurements was recorded in the same time .
3. Temperatures with height were measured at (34) points distribution and varied locations in the occupied zone.
4. The relative humidity was measured at (six) points in the office room
5. The decay approach was utilized to determine the local mean age of air in the research state. The air age determines how long it takes to register the concentration. The tracer gas was supposed to behave similarly to air in this manner.
6. The carbon dioxide concentration was measured every (100 sec.) starting at (1000 ppm) when the (CC/MV ,CC/MVPV) system

attained steady state to observe the one-of-a-kind time to reach the natural concentration supply via air diffuser (ambient concentration). This approach ,[58] provides a good estimate of the system's effectiveness in eliminating contaminants.

7. To avoid errors, each parameter is measured three times.
8. After collecting the appropriate trial findings, the thermal comfort metrics such as temperature effectiveness, air temperature distribution, (ADPI), (PMV), and (PPD) can be analyzed.

CHAPTER FIVE

Results & Discussion

Chapter Five

Results and Discussion

The experimental and numericall results were studied and discussed of the chilled ceilings system with mixed ventilation and personal ventilation (CC /MVPV) and compared them with mixed ventilation ceilings (CC/MV) in an isolated office room and a meeting room located in Iraq (Hilla City) in the summer (hot climate dry). To achieve the goals of this research, this chapter was organized in three sections. In the first section, the experimental results were discussed to perform each cooling system and compared to the data provided within the test room. The second section is to discuss the numerical results of the isolated test room using (ANSYS AIRPAk.3.0.16). The third section discusses the numerical results of the meeting room analyzed using (ANSYS AIRPAk.3.0.16).

5.1 Experimental Results

The study was conducted experimentally for a system of mixing ventilation and personal ventilation with chilled ceilings in an isolated office room in the months of (July, August and September / 2021), and the ambient temperature at that time ranged between (40-45°C) in the city of Hilla **,[106].** The work started in (June 2020), but the initial test was conducted in (July 2021) month, due to the presence of many laboratory problems during the laboratory experiments.

The proposed system (CC/MVPV) was compared with the system (CC/MV). Four tests were performed for four different cooling loads treated with a chilled ceiling of (0, 25, 50, and 80) %, with a total cooling load of (26, 53, and 85) W/m^2 of floor area. The chilled ceiling surface temperature ranged from (0 to 23, 21, 39, and 19)°C, and the supplied air temperature of the mixing ventilation from (17, 19, 21, and 23)°C at a constant air flow rate of (46) l/s with PV air flow rates of (5 and 7.5) l/s and an indoor room air temperature of (25°C). The mean age of air, temperature distribution, (CO_2) concentration, and thermal efficiency with the best flow rate from the proposed system were determined, and they related to mixing ventilation and chilled ceilings (CC/MV), which were the four categories into which the experimental results were subdivided. The results obtained after four hours since the operation of the system (CC/MVPV) reaching the stable condition (i.e. in the separation period between (1:00-2:30)pm. Primary measurement metrics collected on experimental test days are listed in Table (5-1).

Table (5-1) The main measurement and operating parameters collected during experimental tests.

Case		Test day	η %	T_{av} (ºC)	RH_{av} (%)	Q_T (W)	T_S (ºC)	T_e (ºC)	Q_{CC} (W)	T_{ws} (ºC)	T_{wr} (ºC)	Q_{ws} (m^3/h)	T_{CC} (ºC)
Case I	CC/MV	10/7/2020	0	25.3	54.3	445	17	24.63	0	0	0	0	0
	CC/MV	14/7/2020	25	25.64	54.65	333.75	19	24.74	111.25	19.7	20.2	0.189	22.6
	CC/MV	17/7/2020	50	25.92	54.2	222. 5	21	25	222.5	17.2	17.9	0.266	20.3
	CC/MV	20/7/2020	80	26.26	56.8	89	23	25.5	356	16.4	16.75	0.771	18.6
Case II	CC/MVPV_1	1/8/2020	0	25	55.1	445	17	24.44	0	0	0	0	0
	CC/MVPV_1	10/8/2020	25	25.3	54.4	333.75	19	24.5	111.25	19.7	20.2	0.189	22.6
	CC/MVPV_1	15/8/2020	50	25.61	54.7	222. 5	21	24.87	222.5	17.2	17.9	0.266	20.3
	CC/MVPV_1	22/8/2020	80	25.95	55.5	89	23	25.35	356	16.4	16.75	0.771	18.6
	CC/MVPV_2	1/9/2020	0	24.75	56.1	445	17	24.36	0	0	0	0	0
	CC/MVPV_2	5/9/2020	25	25.15	54.9	333.75	19	24.48	111.25	19.7	20.2	0.189	22.6

Case III	**CC/MVPV_2**	**11/9/2020**	**50**	**25.5**	**54**	**222.5**	**21**	**24.9**	**222.5**	**17.2**	**17.9**	**0.266**	**20.3**
	CC/MVPV_2	**20/9/2020**	**80**	**25.81**	**53**	**89**	**23**	**25.28**	**356**	**16.4**	**16.75**	**0.771**	**18.6**

5.1.1 Local mean age of air results

A comparison was made between the studied systems, as shown in the following forms. The highest local air values were measured in the case of (CC/MV), as it noticed a noticeable decrease in the average amount of air in the breathing area and the surroundings of the room, which means that the air in the breathing area is renovated faster in the case of using the PV system, which leads to an increase in the individual's thermal comfort compared to case-I (CC/MV). As a result, the use of the (PV) reduces the age of air from(440 to 482 s) to (336 to 347 s) at a rate of (0 to 80%) when compared to the use of the (CC/MV), and the decrease in the focus is primarily dependent on the location of the source of pollution in relation to the person who is sitting or standing and on the rate of air flow (PV), so we note that the local air age is less than in (case-III) compared to (cases I and II)

Fig. (5-1) shows the relationship between average local air and the height of three measuring stands with different loads (η: 0 %, 25 %, 50 %, and 80 %). The air age values were recorded at the breathing level of a person sitting and standing for three thermal manikins using the previously shown method of decomposition in Chapter 3. In the three cases of different values (η), local air at the level (1.1 m) is higher than the value at the level (1.8 m) due to increasing the distance from the air supply distributor, where it is noted that the average age of the air increases with the height and then returns to decrease near the devices (ATD) for personal ventilation as well as air supplies (MV device).

The air age in (measuring stand -2) is lower than in other parts of the room (measuring stands 1 and 3), because the air in this region is hotter (due to its proximity to heat sources in the room and its location in front of the air distributor), resulting in an increase in air velocity, as Reese and Evis [6] demonstrate. Because (measuring stand-1) is more vulnerable to cold air from the supply, it has a high air speed, a low air age, and a high concentration of pollutants in space. With the (CC/MV) system, the local air age at (1.8 m) in (measuring stand-2) is (470 s) at (η = 80 %), while with the (PV) system, it is (340 s). This result gives a good idea of the effect of air supply distribution on the local age of air .

The relationship of mean air age with the different values of (η) for three case studies. The effect of the chilled ceiling temperature is visible as the average age of the air increases with increased coolant load treated by the cooler ceiling with two airflow values. This result shows the effect of the cold air movement down due to the thermal load of the cooled ceiling and the effect of the height of the hot air, which leads to a decrease in the speed of the air. In fact, the increased disorder increases the effect of mixing, which increases the spread of pollutants from the sources of carbon dioxide generation in the general climate as shown in Fig(5-2).

Compared to other indoor parts of the room, the three people had the least difference in the concentration of the air between the studied systems and observed the highest carbon dioxide concentrations in the air inhaled with the (CC/MV) system. When compared to the (CC/MV) system, using (PV) airflow rates reduces local air temperature by (30-38%) and (22-24%) at (η = 0 to 80%) .Also, the mean local air age is decreased by 38% with a higher (PV) air flow rate of (5 to 7.5 l/s) compared with (CC/MV).

Fig.(5-3) shows the relationship between the average air age at different breathing levels (1.1m and 1.8 m) for three case studies. The average age of the air for each level of the office room increases with the increase in the treated cooling load and the height of the chilled ceiling (η), because the hot air rises from the lower area and the cold air descends from the upper area after being cooled by the ceiling cooling due to convection, resulting in a decrease in air velocity. The (IAQ) for (CC/MVPV) was higher than for (CC/MV), according to (Table 5-1).Thus, (PV) provides a higher (IAQ) when assisted by a (CC) system with higher surface temperatures.

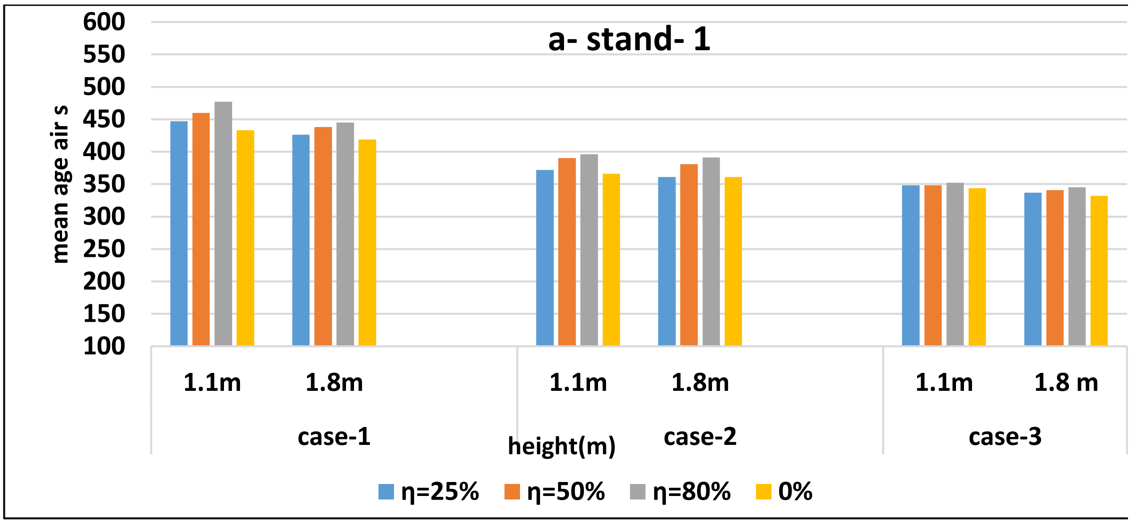

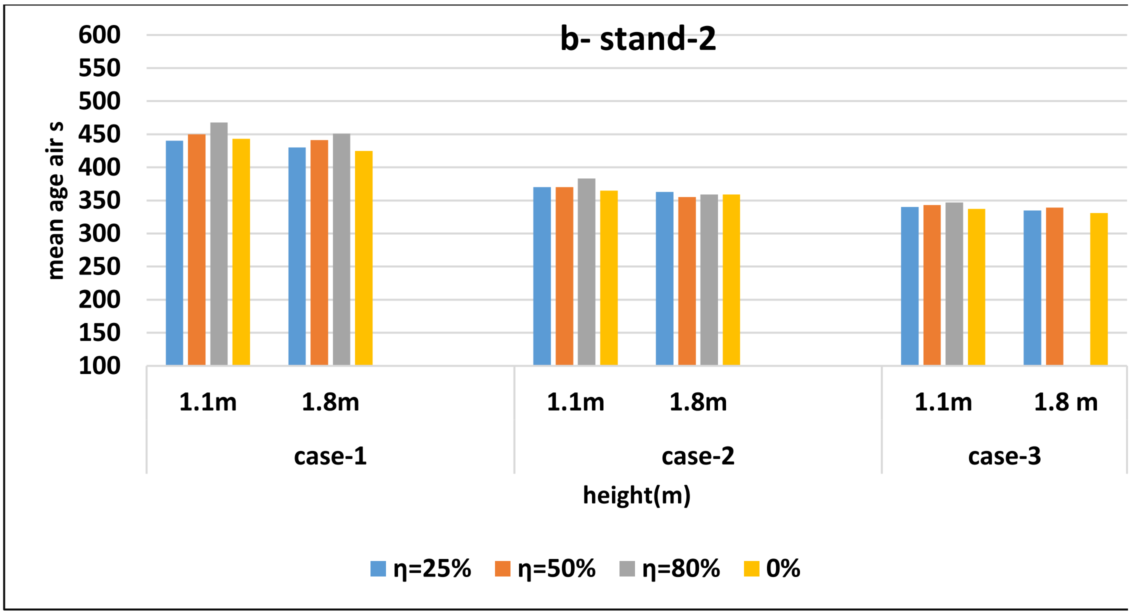

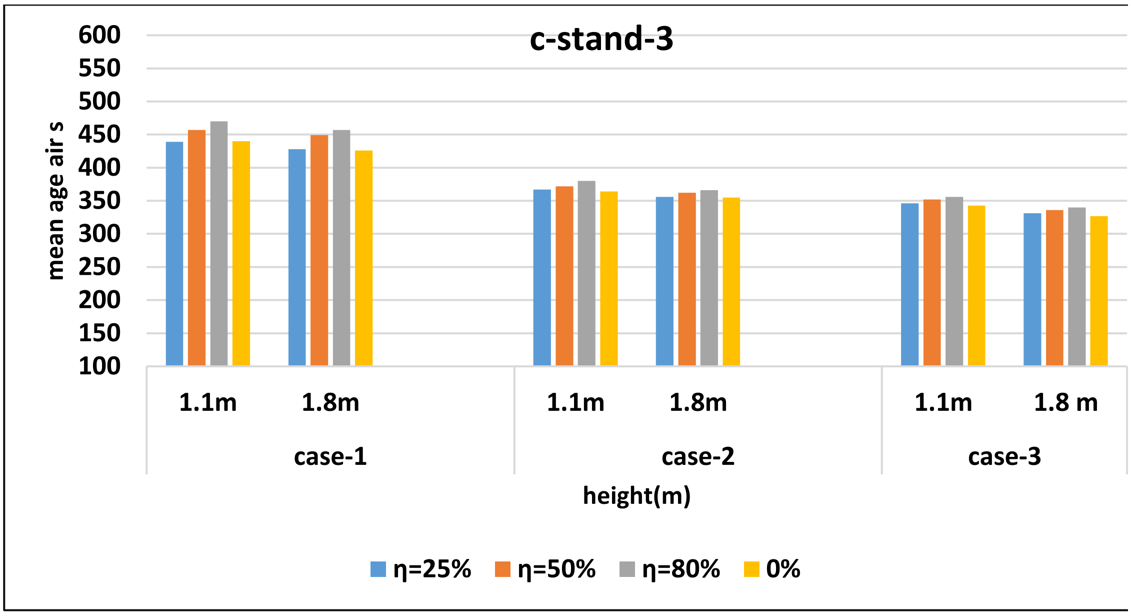

Fig.(5-1) Local mean age of air at heights (1.1m) and (1.8m) for three instruments stands at varies values of (η) for three cases (case-I ,II and III).

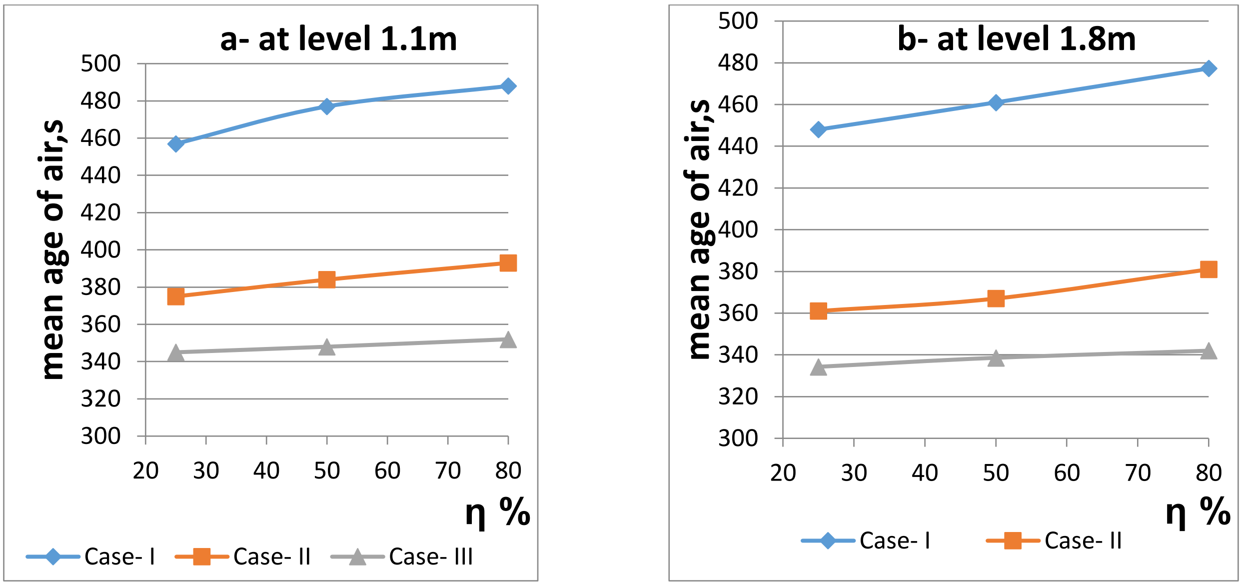

Fig.(5-3) Mean age of air at levels (1.1m , and 1.8m) for different values of (η) and three case studies (I , II and III).

5.1.2 Air temperature distribution results

Figure 5-4 depicts the relationship between air temperature distribution and various values of (η) for three cases and three tests. It is noted that the temperature increases with the height and with the increase of (η), and that the average room temperature increases with the increase in the temperature of the feeding air due to the decrease in the cooling capacity of the air. As it passes through heat sources and moves upward due to buoyancy effects, it returns to a low level near the breathing zone (MV) due to the cold air currents coming from the personal ventilation devices (ATD) as well as the air supply distributor (MV) device installed above the room wall. The temperature difference from head to foot was less than (2°C), which is within an acceptable range as defined by ASHARE standards. It was noted that the lowest temperature inside the room was at a level (0.1 m) above the room floor within the occupied area due to the absence of this level of heat sources. The air enters from a height of (0.4 m) to be supplied to the person's breathing area, and the air outlet is below the diffuser at a height of (0.3 m) from the room floor. The air exit velocity is higher than the air velocity.

In all case studies, the temperatures recorded in (stand-2) were lower than those in stands (1 and 3), due to its proximity to the heat sources inside the room and its location in front of the air distributor. (Stand-1) also experienced higher temperatures because (Stand-3) is more susceptible to the cold air coming from the diffuser. When comparing the distribution of air temperature with room height between the three cases (Case I, Case II, and Case III), the distribution of air temperature with height (at the three measuring mounts) using (CC/MVPV-2) (Case III) is lower compared with (CC/MV) and (CC/MVPV-1) (Case I, Case II), regardless of the value of the chilled ceiling (η), especially when (measuring stand -2) is located in front of the air supply distributor as shown in Fig. (5-5). It has been shown that when using the personal ventilation system in cases II and III, the average room temperature will decrease by (0.5 to 0.8°C) at a range of (0% to 80%) compared with (CC or MV), the temperature distribution will become more uniform, and this will lead to improved thermal comfort. It is seen that increasing the air flow rate of the (PV) system in (case III) for three stands results in a decrease in temperature of (0.3–0.5 °C) at (η = 0 to 80%) , and a higher air flow rate of the (PV) system prevents heat columns from the PCs from reaching the breathing area. Then, at > 1.8 m, the air temperature is affected by the temperature of the cooled ceiling, which leads to convergence of air temperature values in the upper region of the three cases.

Figs.(5–6) show the vertical air temperature difference (VATD) between the head and ankle levels of a seated and standing person with the chilled ceiling temperature for three cases. The chilled ceiling temperature is inversely related to VATD (increasing the chilled ceiling temperature means lowering the portion of the cooling load that is handled by the chilled ceiling). In all three cases, the vertical air temperature difference (VATD) for the seated and standing person was between (1 and 0.6°C) and (0.7 and 0.4°C), respectively, at (η = 0 to 80%), and these differences are considered to be less than the (2°C) maximum allowed for the thermal environment [33].

The highest values for a seated and standing person were seen between (1 and 0.7 °C) for a person standing with (CC/MV) . It is noted that the values of the temperature difference between the head and feet of the seated person decrease with the increase in the cooling load processed by the cooled ceiling, as shown in Figs.(5–6). For the three consecutive cases, the temperature difference between the seated person's head and feet decreases by (0.6 to 0.4)°C with (CC/MVPV-2) between (η= 0 to 80%).This means that the temperature difference between the head and feet levels is the lowest in the third case study when compared to the rest of the cases due to the ability of the (CC/MVPV-2) system to deliver cold air faster to the human body.

According to ISO 7726 [35], the vertical distribution of air and globe temperatures meets the requirements for uniformity at each measurement site.

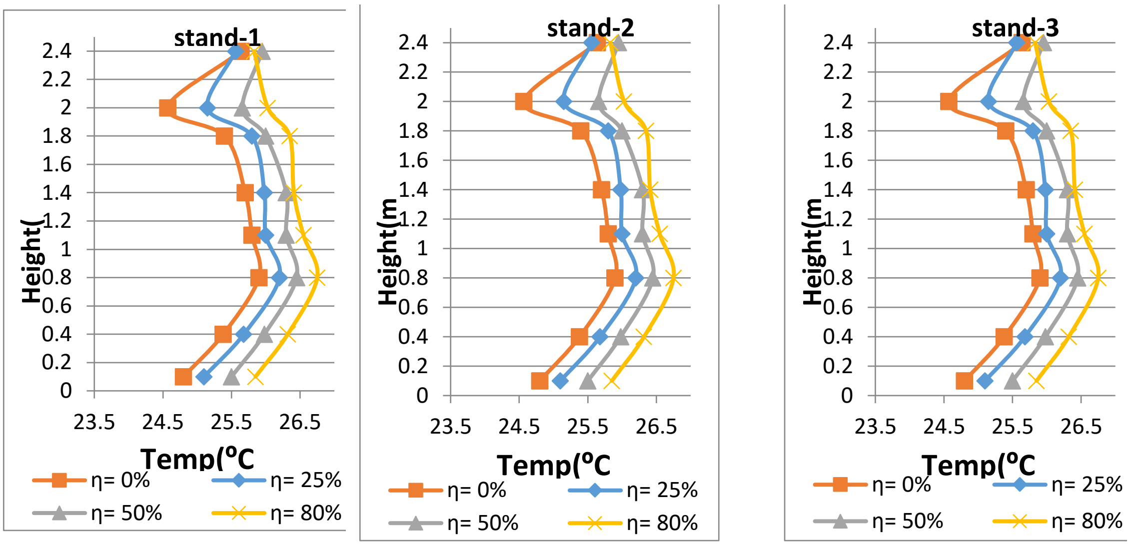

a- Case-I

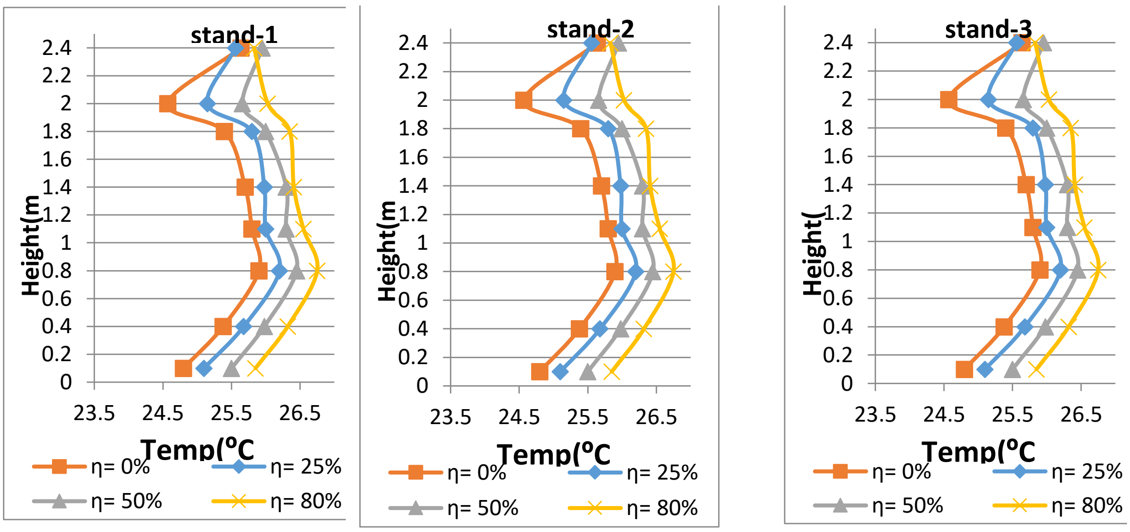

b- Case-II

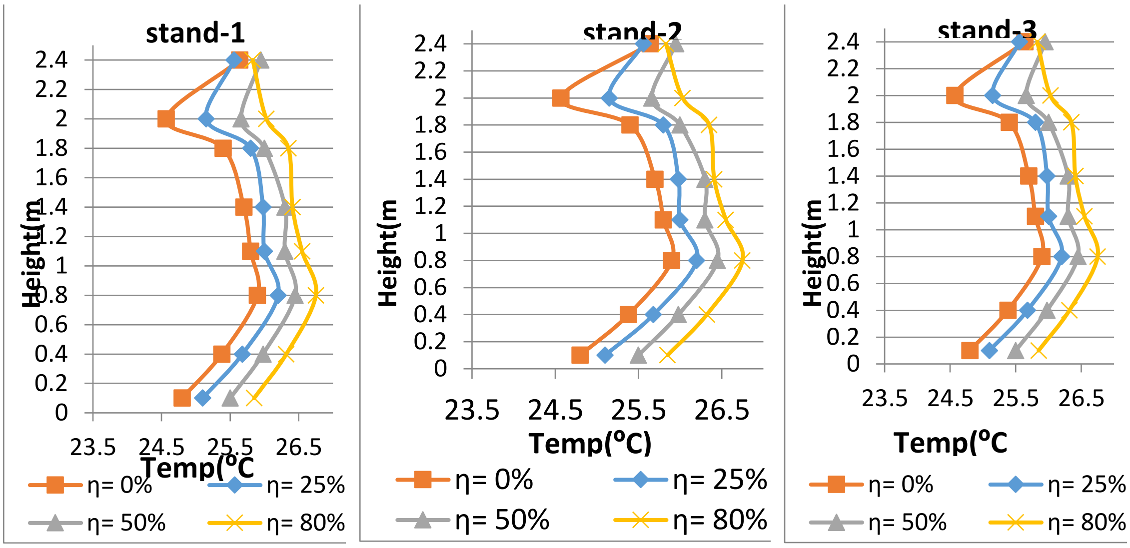

c- Case-III

Fig.(5-4) Distribution of air temperature with height at various values of (η) for three measuring stands in three cases (I, II, and III) .

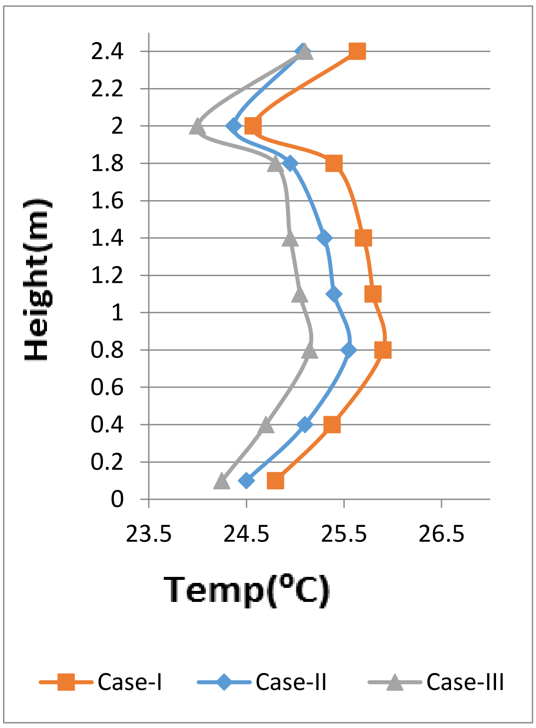

η =0 %

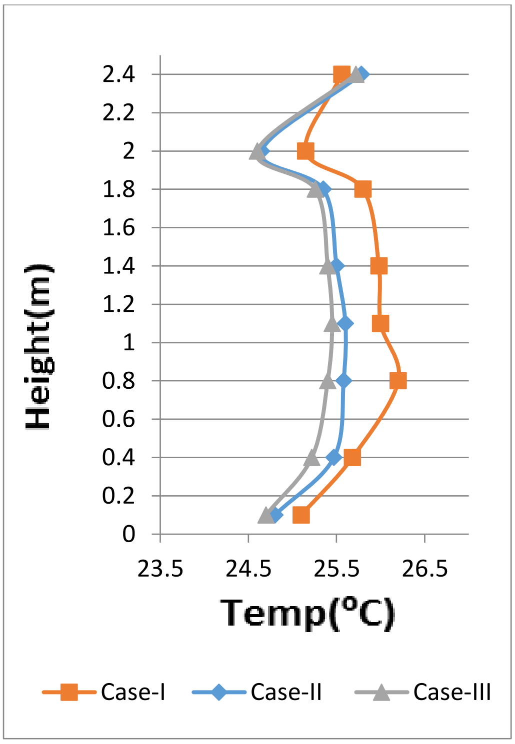

η =25 %

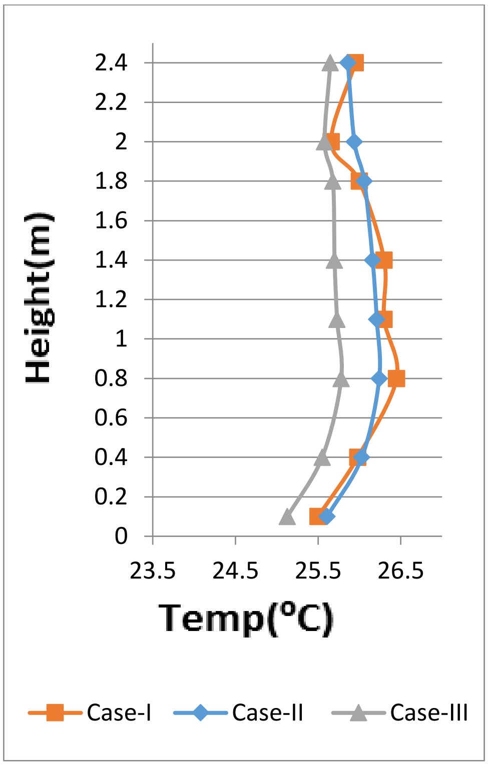

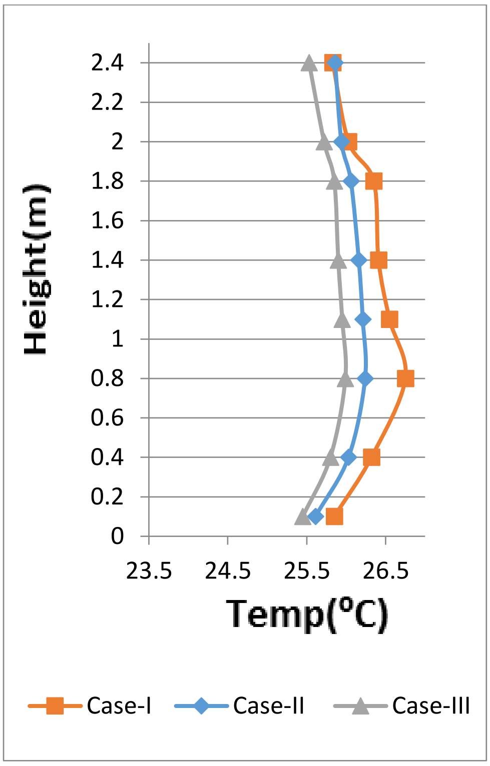

η =50 %

η =80 %

a- measuring stand-1

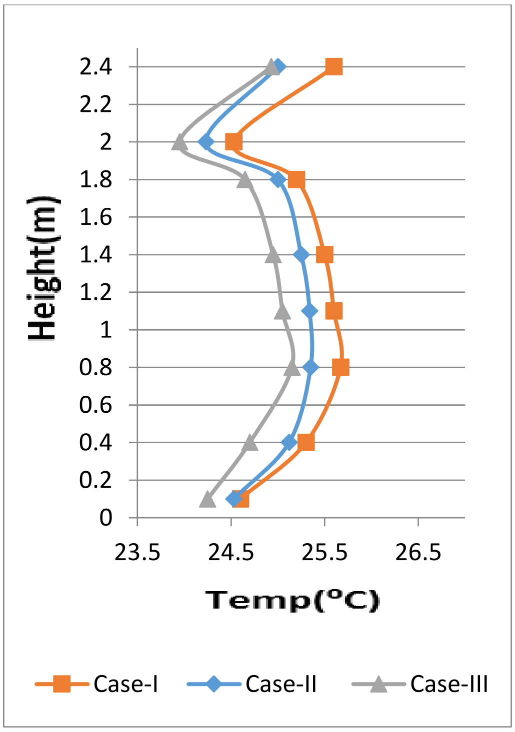

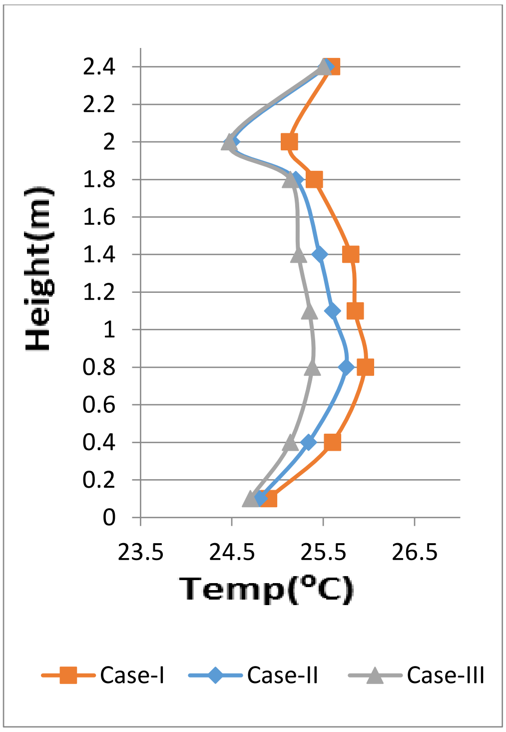

η =0 %

η =25 %

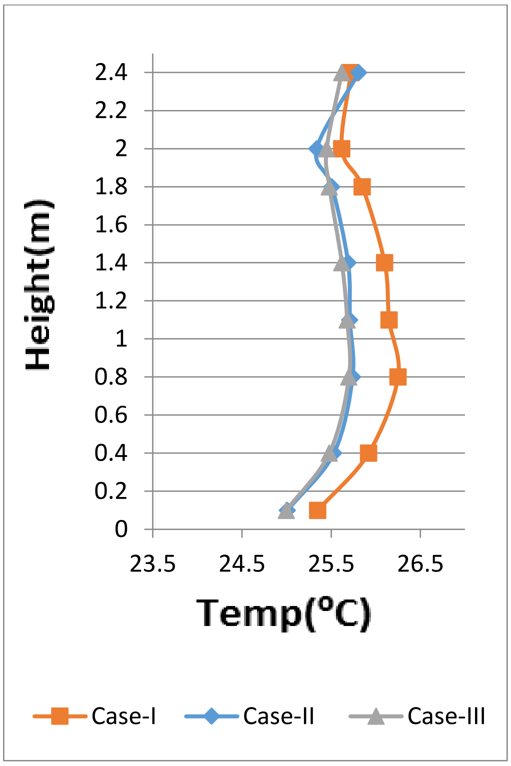

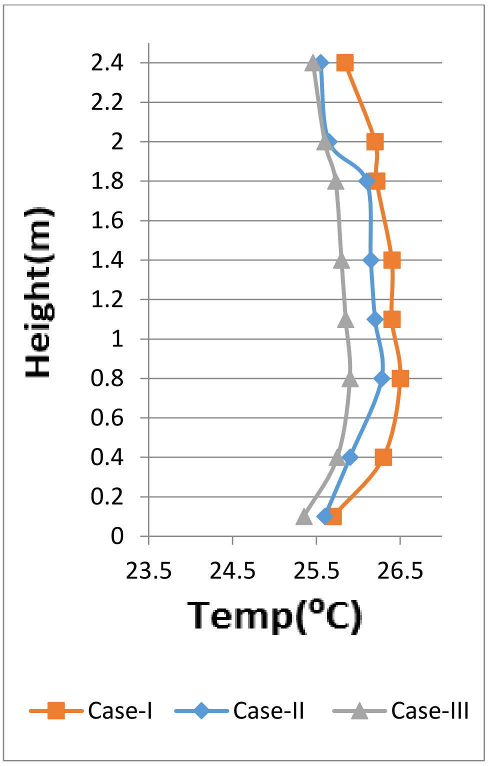

η =50 %

η =80 %

b- measuring stand-2

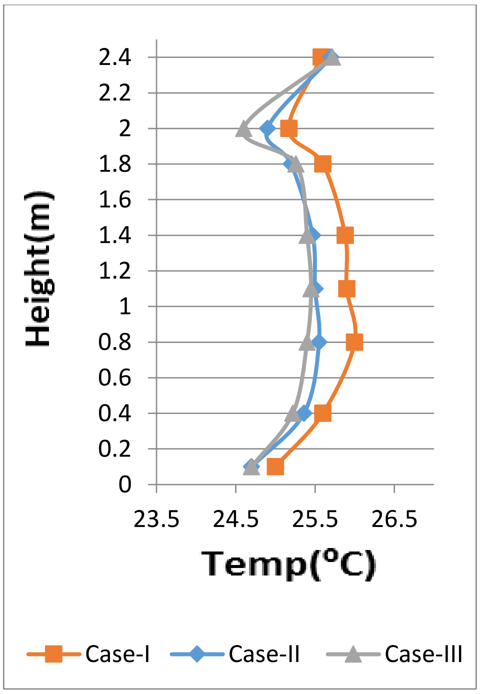

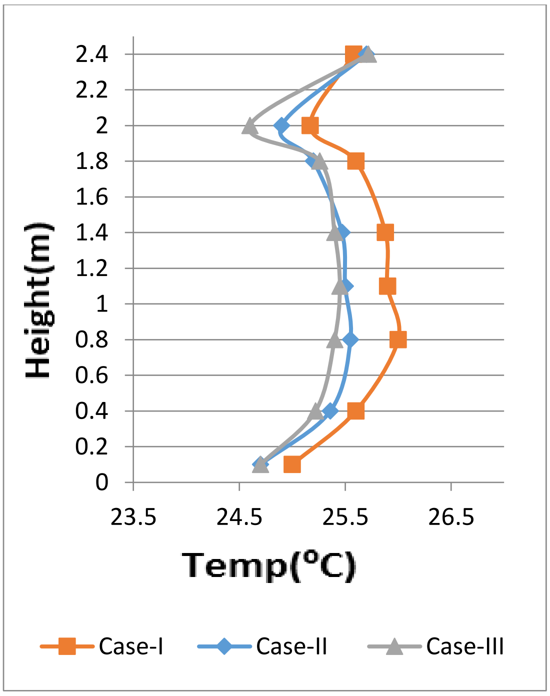

η =0 %

η =25 %

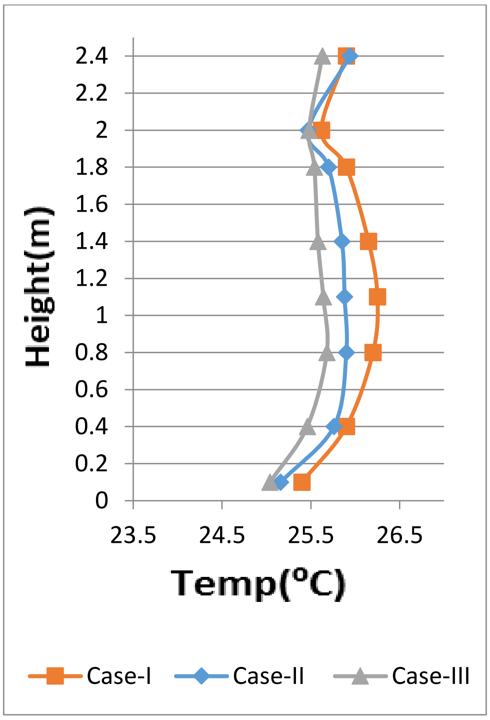

η =50 %

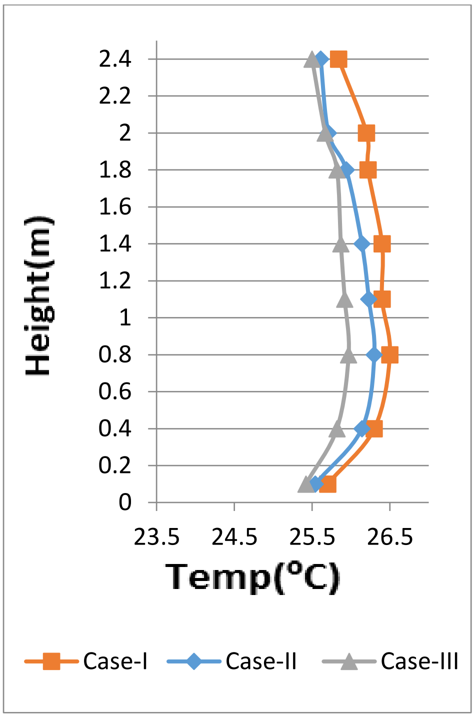

η =80 %

c- measuring stand-3

Fig.(5-5) Distribution of air temperature with height at various values of (η) for three measuring stands .

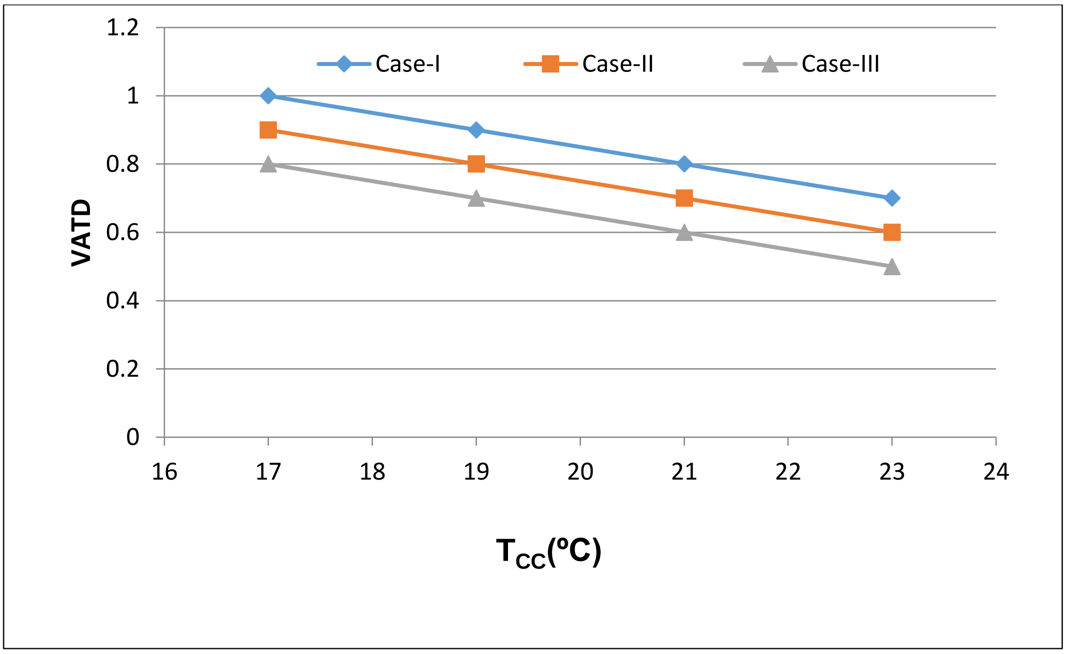

a- sitting person

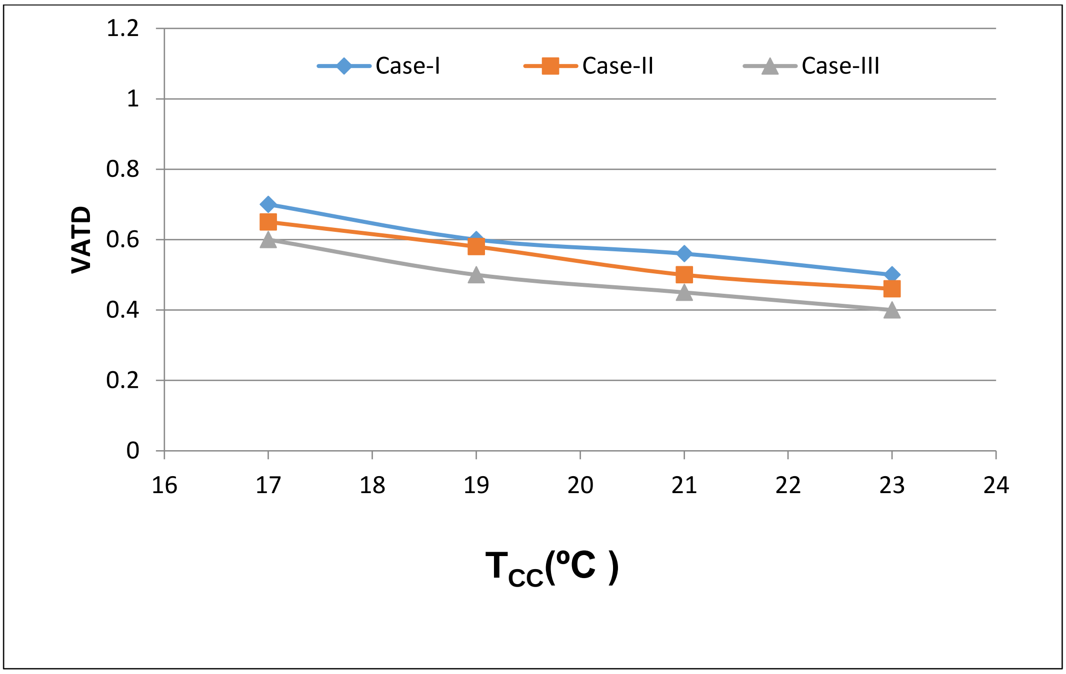

b- standing person

Fig.(5-6) Vertical air temperature difference profiles for sitting and standing person

Fig.(5-7) shows the relationship between the temperature of the cooled ceilings (T_{CC}) and the effectiveness of heat removal (ε_t) in three cases, where it was found that the temperature of the cooled ceilings increases with the increase in the cooling load treated by the cooled ceilings, and this leads to a decrease in the exhaust air temperature and then a decrease in the effectiveness of air temperature distribution according to equation (3-38). Effectiveness of heat removal (ε_t) describes the efficiency of the studied systems in removing heat inside the office room. In all cases and at each value (T_{CC}), the indicators of heat removal using (PV) for (case-II and case-III)were higher than those of (CC/MV) system (case-I). This means that the use of (PV) increases the exhaust temperature and speeds up the delivery of cold air to the human body and prevents tall thermal columns from reaching people. Where the values of the heat removal index ranged between (0.91 to 0.76), (0.93 to 0.79) at (T_{CC} = 0 ºC to 19 ºC) in the (case-I and case-III). The higher (PV) air flow rates led to an improvement in the heat removal index in (case-III) by (0.95-0.81) at (T_{CC} = 0 ºC and 19 ºC) than in the (case-II).

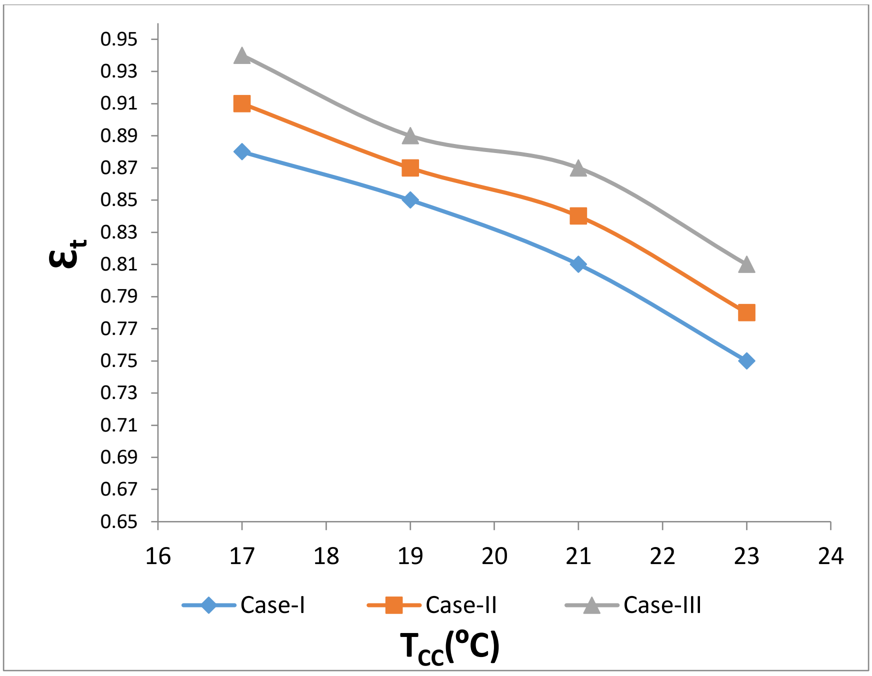

Fig.(5-7) Heat removal effectiveness profiles with (T_{CC}) for three case studies

5-1-3 Carbon dioxide decay results

Fig. (5-8) shows the results of measurements of average CO_2 concentrations over time at the breathing level of a seated and standing person (1.1 and 1.8 meters, respectively), with differing values (η) for three cases. All eight tests show differences in carbon dioxide concentration. Compared with (CC/MV), the time required to remove carbon dioxide from the office room was reduced by up to twice as much with the presence of the PV system (cases two and three). In addition, the (CO_2) concentration was (2.2–2.5) times lower with (PV) systems than with (CC/MV) systems at the respiratory level of the standing person and at the exhaust level. In addition, the (CO_2) concentration was (1 to 1.5) times lower and the (PV) flow rate was higher in(case III) than in (case II) at the breathing level of the seated and standing persons.

At the time, the carbon dioxide concentration ranged between (1000 and 700) ppm for three cases: (0 to 420 s), (0 to 250 s), and (0 to 180 s). During this time period, the cooling load value (η) had little effect on the decomposition of CO_2 concentration. This delay in (CO_2) removal increases the time it takes for fresh air to reach the breathing area (1.1 m). As the cooling load treated by the cooled ceiling increases over time, the concentration gradually decreases until it reaches the fresh air supply concentration. Air flows into the room area, and the carbon dioxide concentration decreases with time.

It is clear in Section 5.1.1 that the increase in the value of leads to a decrease in the temperature of the chilled ceiling and then a decrease in the air temperature by convection and movement to the bottom of the room, which hinders the removal of air from the exhaust and reduces the removal of carbon dioxide. For the three case studies, the maximum time required to remove (CO_2) from space is reached at (η = 80%) in each measurement holder, as shown in Fig. (5-8), clarifying the variation in CO_2 concentration with office room height for the three cases at (η = 0%, 25%, 50%, and 80%), respectively.

The (CO_2) concentration at altitude (1.8 m) is approximately greater (10 to 65 ppm) than the concentration at altitude (1.1 m), with load values (η) between (0 and 25%) for the two scenarios because the clean air reaches the (1.1 m) level first. While the difference in concentration between the two levels of the breathing zone (1.1 m and 1.8 m) may diminish at (η=80%), this is due to the cold air in the upper zone as a result of the lower ceiling temperature.

At any value of (η), the removal of carbon dioxide using the third case is faster by about (40 ppm/s) than using the second case. The reason is that increasing the flow rate leads to faster diffusion of new air and shortens the time required to remove carbon dioxide.

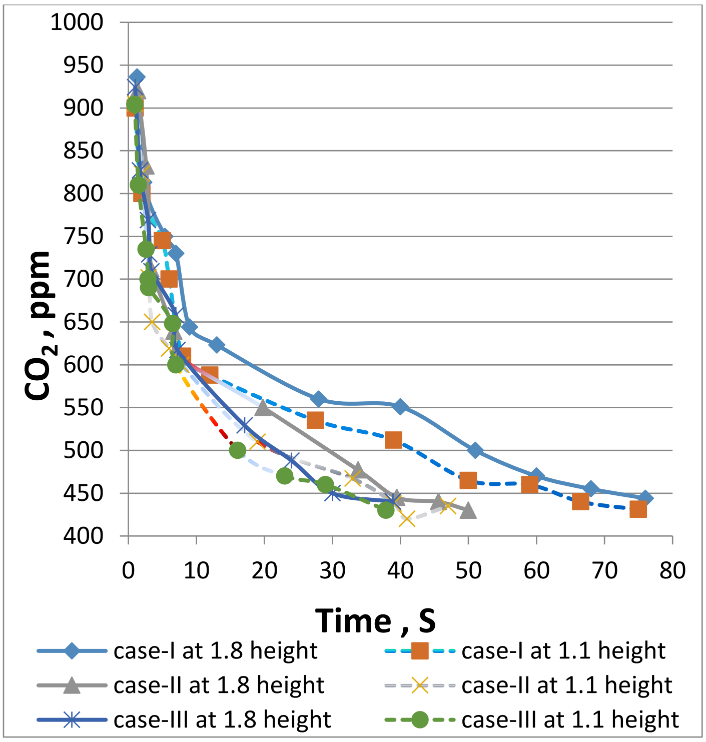

a- η=0%

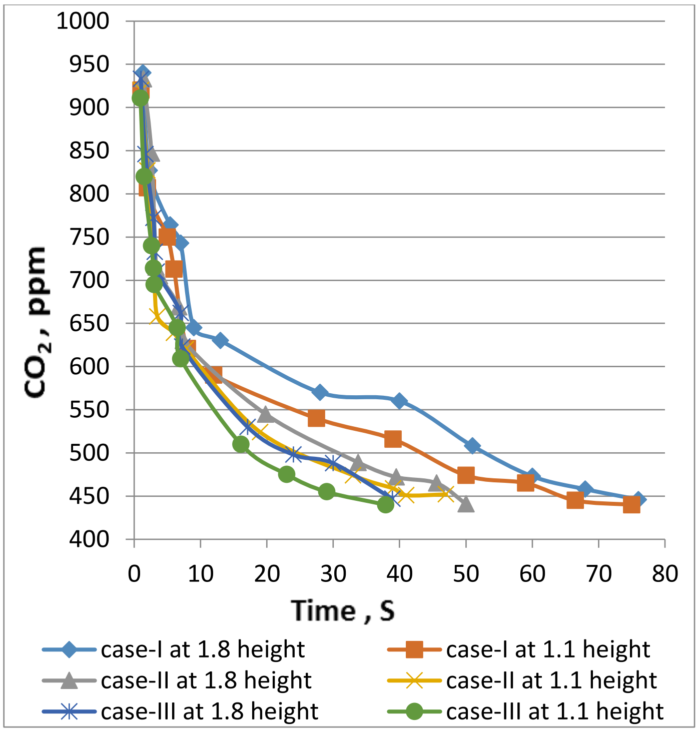

b- η =25%

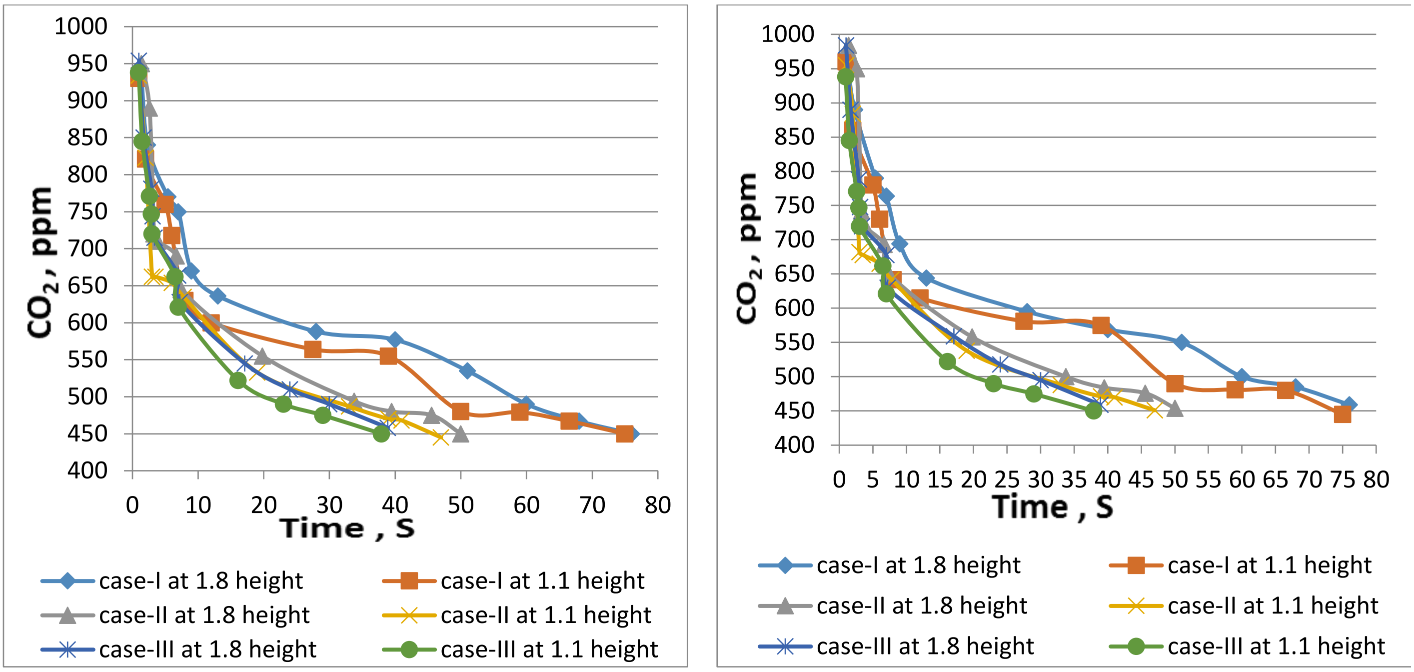

c- η=50% **d- η=80%**

Fig.(5-8) Average CO_2 concentration over time at breathing levels for sitting and standing person (1.1m and 1.8m) for the three cases at different (η)

5-1-4 Occupied density and occupant air exchange efficiency

The effectiveness of air exchange takes into account the fact that air has a variety of effects on ventilation. The impact is greater if the population is larger or stays longer. The occupant air exchange efficiency, which considers the spatio-temporal distributions of inhabitants, is able to provide a more accurate indication of the air quality in a space than conventional air exchange efficiency, which deals with the impact of air flow at various locations uniformly. To gauge a room's degree of thermal comfort, a similar concept can be used.

In all case studies, the longer people stay in the room, the less efficient the air change is for the occupants, which means if the residents stay longer or there are more of them, the effect is greater, as shown in

Figs.(5–9). In all cases, the efficiency of air exchange for occupants is higher than the efficiency of air exchange, and this means that fresh air replaces the air in the well of the occupied area, which leads to an improvement in air quality. Also, the longer the visiting person (the standing person) stays in the room, the less efficient the air change will be for the passengers due to the low rate of ventilation. This means that occupant air exchange efficiency better refers to room air conditions than standard air exchange efficiency, which addresses the effect of air flow at different locations in the same way to determine the room's thermal comfort level as mentioned in cases (II and III). As a result, increasing the (PV) air flow rate increases air exchange efficiency, which raises occupant air exchange efficiency in (case III) from (6.5 to 11.53 %) when compared to (case II).

The overall ventilation effect can be analyzed more comprehensively by using the passenger air exchange efficiency. As a result, the efficiency of air exchange for passengers increases in (cases II and III) from (22.25 to 25.11 %) and from (30.2 to 39.16 %) , respectively, when compared to (CC/MV), implying that personal ventilation improves air exchange efficiency and determines the level of comfort inside the room due to its unique characteristics.

Due to the low aeration rate, the results showed a high efficiency of air exchange (9 ACH). The air exchange efficiency of the inhabitants is higher than the air exchange efficiency due to the larger weight of the persons inhabiting the space. The findings demonstrate that the criteria for assessing the impact of ventilation can be improved by using the updated air exchange efficiency. In any other case, a system created to enhance indoor air quality may be useful.

Fig. (5–10) shows the relationship of air exchange efficiency for occupants (η_D) with different load values of (η) for the three case studies, where it was found that the temperature of the cooled ceilings increases with the increase in the cooling load treated by the cooled ceilings, and this leads to an increase in the age of the air and then a decrease in the efficiency of air exchange.

In all cases with the (PV) system, the air exchange efficiency for occupants (η_D) was higher than the (CC/MV) system by (0.22 to 24.4%), and (32 to 38.7%)at (η = 0 to 80%) as a result of reducing the mean air age up to (30 to 38%)at (η = 0 to 80%) at a seated and standing person breathing level. The air exchange efficiency (η_a, η_D) increases with a decline in average air age and an increase in PV air flow rate. According to Fig.(5-9) the highest air exchange efficiency (η_a, η_D) values in (CC/MVPV-2) are (70 to 67.5%), (99 to 90.25%) at (η = 0 to 80%), and with the air flow rate (7.5 l/s). In order to protect residents from direct pollution in the BZ and in the local microclimate, a flow rate of (7.5 l/s) is the optimum choice.

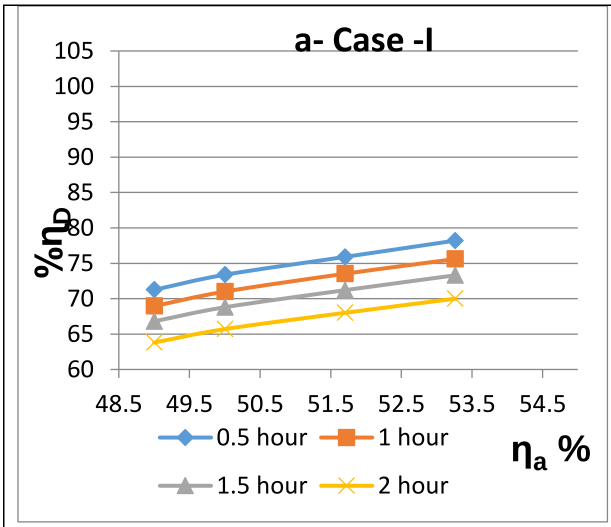

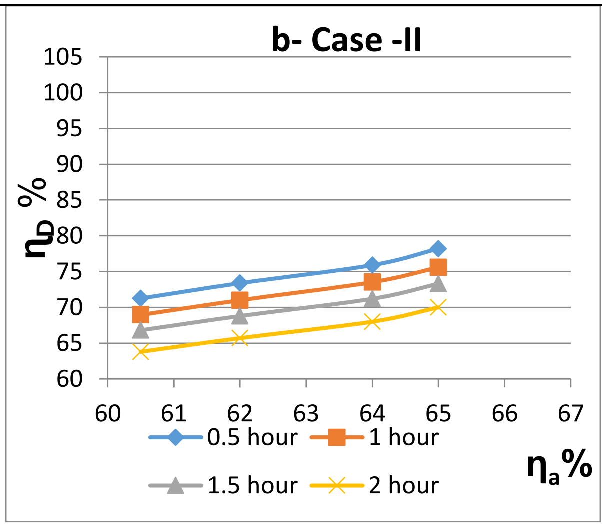

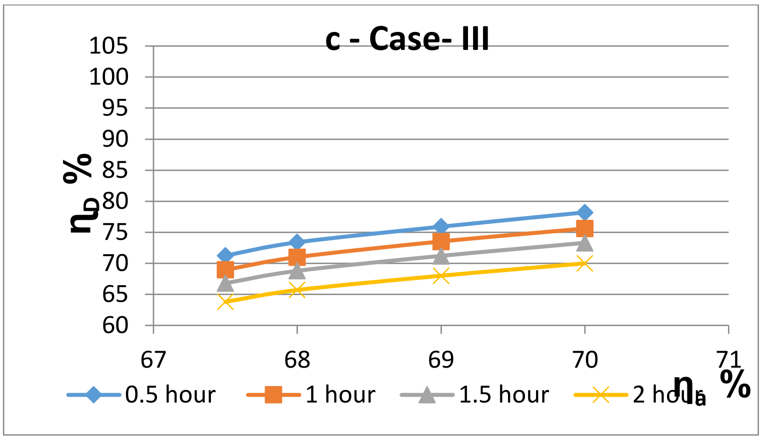

Fig.(5-9) Relationship between air exchange efficiency and occupant air exchange at different times

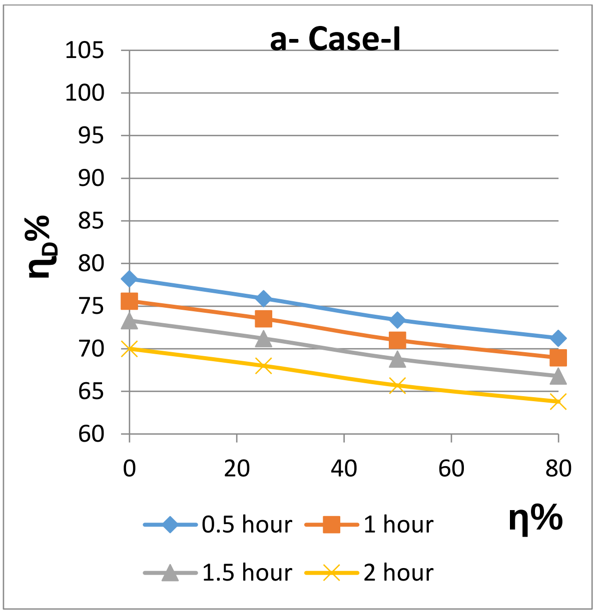

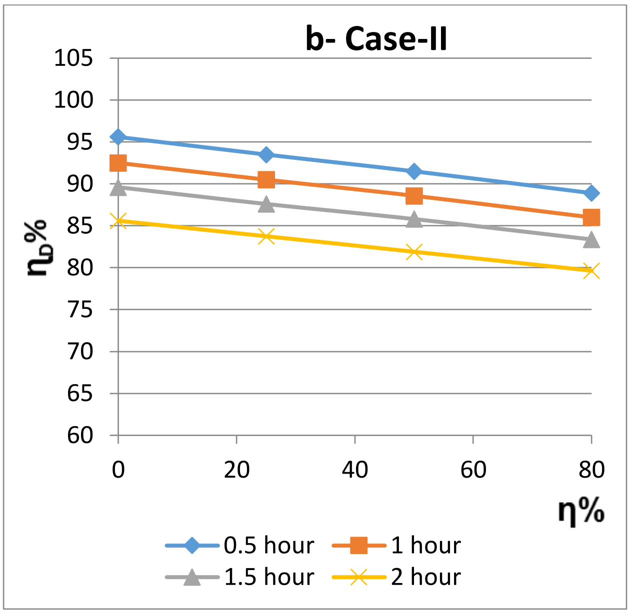

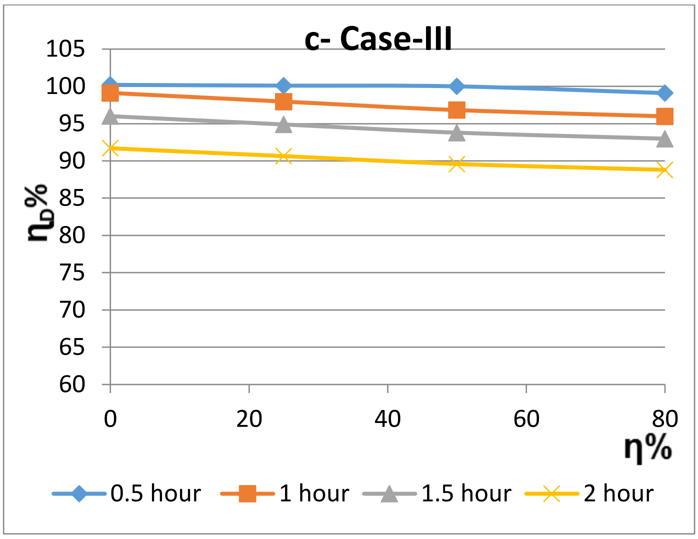

Fig.(5-10) Relationship between different values of (η) and occupant air exchange at different times.

5.2 Numerical Results

5.2.1 Validation of AIRPAK software

The results of the AIRPAK program for the three systems (CC/PVMV, CC/MV) were validated by an experimental study conducted by Lipczynska et al. **[6]**. in two office rooms and compared with the numerical results (with the k-RNG turbulence model). To determine the success of the (CFD) model in predicting the temperature of an area around an occupant, experimental results based on average values of vertical temperature gradients in that area and a ventilation effectiveness index were used as the basis for validation (IAQ). The climatic chamber (4.12 x 4.2 x 2.89 m), which was constructed to seem like an office with two workstations, was used for the experiments. The room had personal ventilation (PV) on each desk, a chilled ceiling, and mixing ventilation (MV,CC) and covered (75%) of its surface area. The office temperature was set to (26 and 28)°C, and when (PV/MV) was used, it was set to (25 °C, 7.5 l/s); (MV), the supply air temperature was (16°C), and the total heat load for the two rooms was (72, 66) W/m^2. The experimental and numerical results were found to be in good agreement, with a maximum relative error of (5.04%) obtained at a height of (2 m) and a maximum relative error of (4.53%) for the abdomen region as listed in Fig. (5-11).

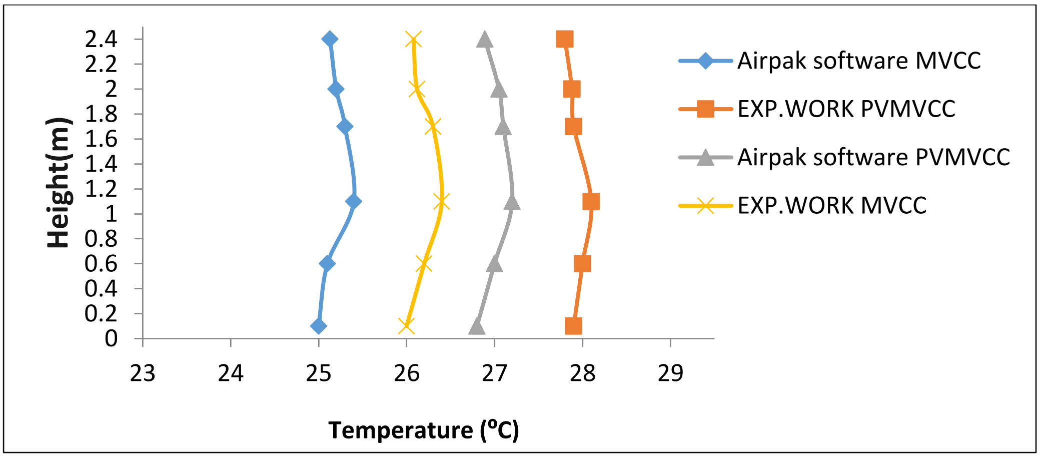

Fig.(5-11)Validation of the AIRPAK software with experimental data.

5.2.2 Numerical results of insulated office room for three case studies

Three case studies were designed for a thermally insulated office room using ANSYS AIRPAK software, where each case is separated into four tests based on the proportion of cooling load taken up by the chilled ceiling as mentioned in Chapter 4, Section (4.4). The boundary conditions for the numerical analysis were obtained based on the results of the numerical study. A numerical analysis was performed to provide more results on the assessment of thermal comfort and air age characteristics for the three cases in a thermally insulated office room using AIRPAK software .The main numerical results for insulated office (case-I, II and III) .

Table(5-2)Main numerical results for insulated office room (case-I, II and III)

Case	η %	T_{av} (ºC)	V_{av} (m/s)	MRT	RH_{av} (%)	ADPI (%)	PPD (%)	PMV	VATD (ºC)	ηa (%)	ε_t
Case I	0	24.25	0.142	25.5	57.2	59	17	0.74	0.8	60.25	0.925
	25	24.5	0.139	25.7	55.9	88.1	15.6	0.72	0.7	57.72	0.88
	50	24.8	0.133	25.8	55.7	86.5	15.2	0.66	0.63	56	0.827
	80	25.25	0.127	26.1	54.4	85.3	15	0.63	0.52	54	0.782
Case II	0	24	0.147	24.5	59	60	16.5	0.64	0.71	73	0.943
	25	24.31	0.154	24.8	58.1	86.8	16.3	0.61	0.6	71	0.89
	50	24.62	0.150	25.6	55.6	88.9	16	0.62	0.53	69	0.85
	80	25	0.133	25.8	55.2	87.6	14.6	0.59	0.41	67.15	0.806
Case III	0	23.75	0.154	24.2	57.3	63	14	0.55	0.63	75.36	0.965
	25	24.12	0.160	24.5	57.9	91.2	13.8	0.5	0.5	74.17	0.912
	50	24.5	0.158	25.2	58.2	89.9	13.4	0.49	0.42	73	0.878
	80	24.81	0.138	25.5	55.62	88.92	12.3	0.44	0.3	72.11	0.834

Fig.(5-12) displays numerically the contours of the mean local air age distribution of the insulated office room at different values of (η) for three cases at plane (z =1.25 m). This plane passes through the air supply diffuser and the human body. In the air supply diffuser, the age of air starts from zero and increases in the indoor area. The age of air increases with the height of the room and reaches its maximum above the diffuser location, which means that low air movement in this area leads to increased pollutants and discomfort to the occupants. Because of the exchange of hot air rising to the top and cold air coming from the chilled ceiling, the air temperature rises as the value of rises. It is noted that the increase in air velocity around the human body caused a decrease in the life of the air in this region as a result of the increase in air temperature caused by convection near the heat sources (person and computer).

The average air age values in each level of the office room increase with an increase in the processed cooling load from the chilled ceiling because the hot air rises from the lower area and the cold air descends from the upper area after it is cooled by the coolers due to the thermal load, which leads to a decrease in the speed of the air. Despite the fact that the air flow was constant in each test, the (IAQ) was higher for (CC/MVPV) than (CC/MV) .As a result, when the surface temperature of (PV) is higher, it provides the best (IAQ) .As a result of the use of (PV), the percentage of air age drops below a value of (0.34 %) . With the lowest PV air flow rate of (5 l/s) (as in CC/MVPV-2), compared with the (CC/MV) system, the probability of the mean age of the air was reduced by 25%. Higher (PV) airflow rates resulted in a (14%) improvement in occupant protection from cross infection. According to Table (5-2), the (CC/MVPV) system produced better (IAQ) than the (CC/MV) system.

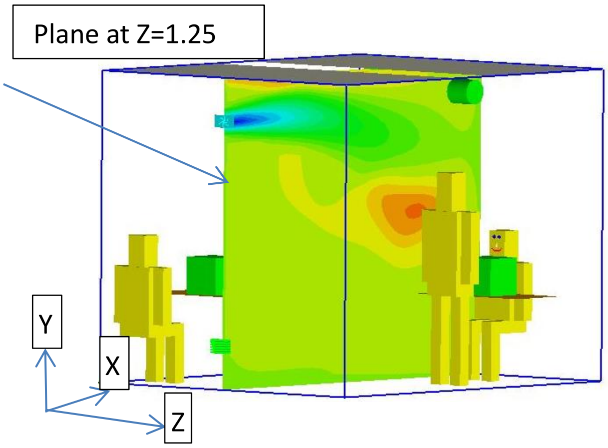

CC/MV(case-I)

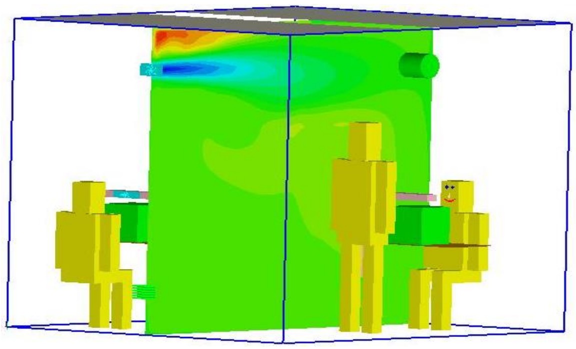

CC/MVPV(case-II,case-III)

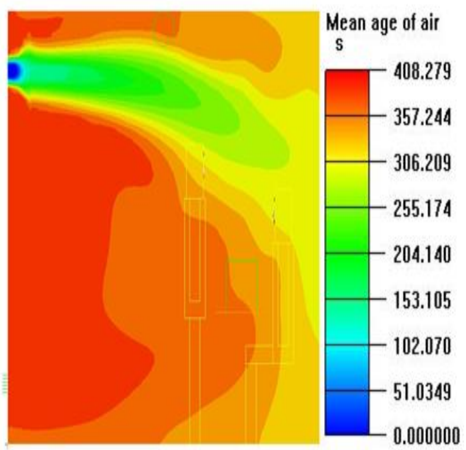

Case-I

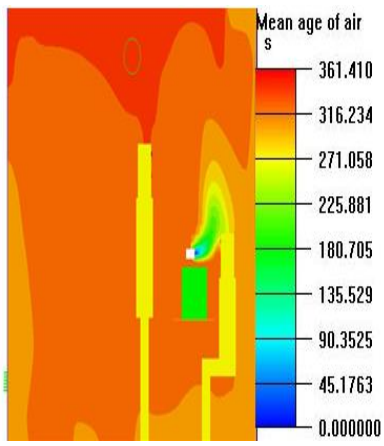

Case-II

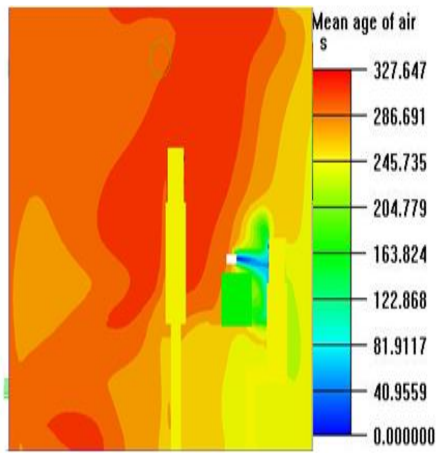

Case-III

a- η=0 %

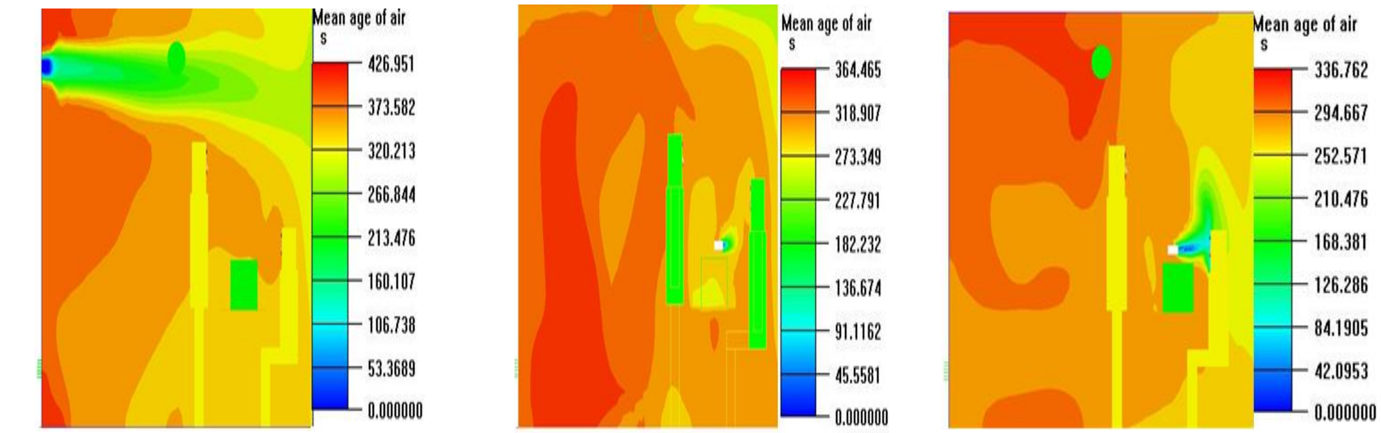

Case-I Case-II Case-III

b- η=25%

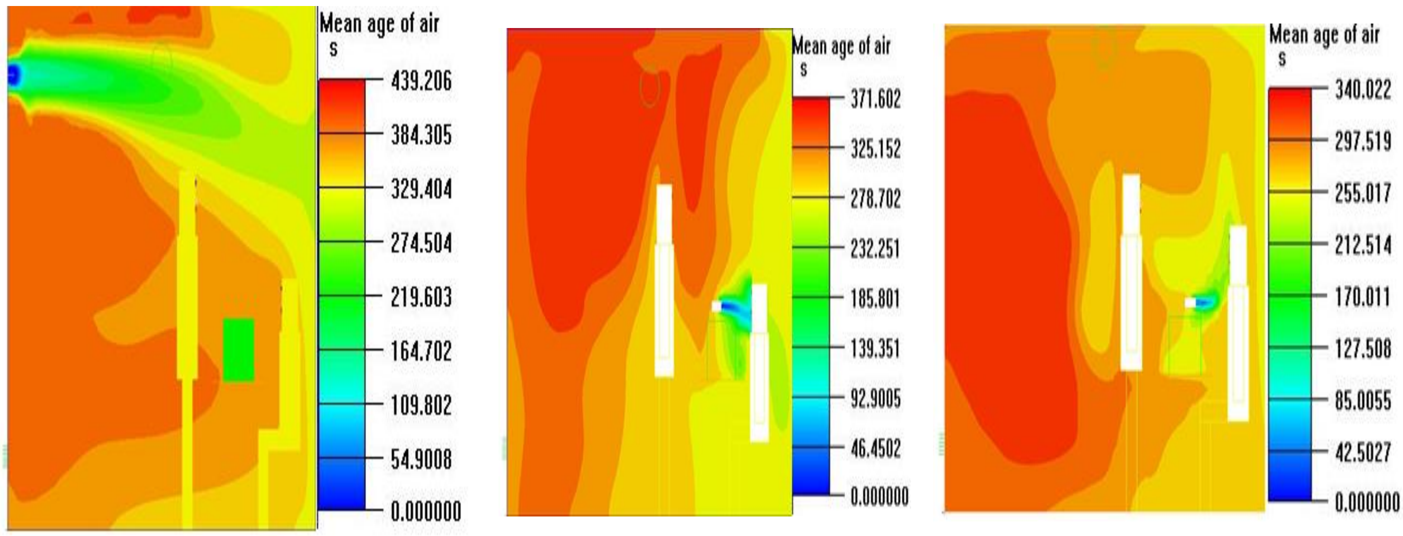

Case-I Case-II Case-III

c- η=50%

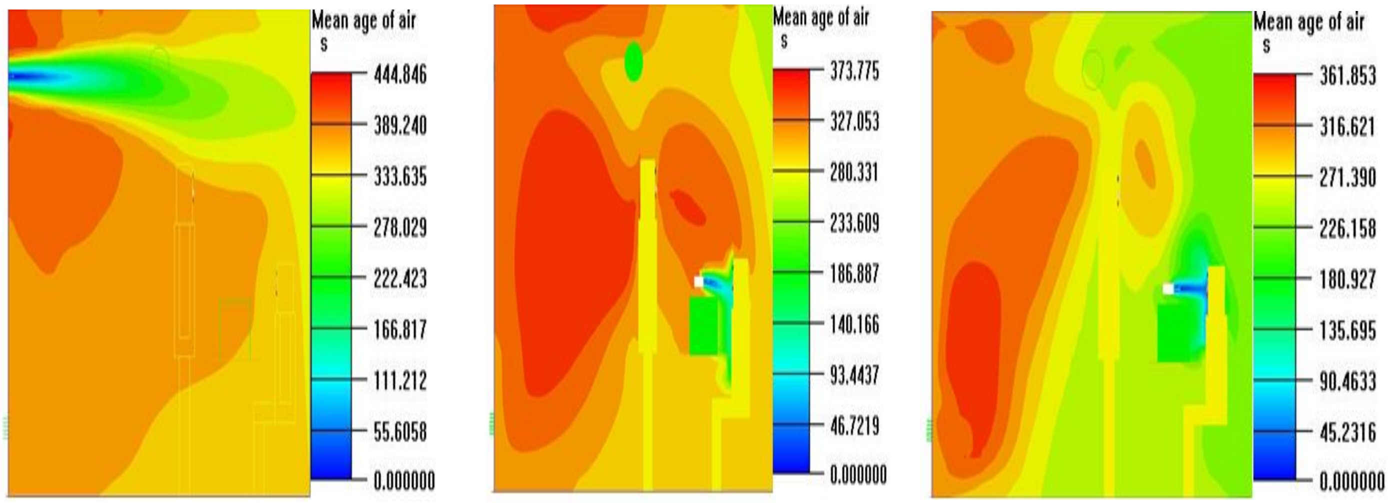

Case-I Case-II Case-III

d- η=80%

Fig.(5-12) Contours of mean age of air in plane (z =1.25m) with different values of (η) for the three case studies.

Fig. (5-13) shows the relationship of the efficiency of air exchange (η_a) with a different value of (η) under three cases, where it was found that the temperature of the cooled ceilings increases with the increase in the cooling load treated by the cooled ceilings, and this leads to an increase in the age of the air and then a decrease in the efficiency of air exchange.

Air exchange efficiency (η_a) describes how well the ventilation system delivers fresh air to the level of breathing. In all cases with PV, the air exchange efficiency (η_a) was higher than that of (CC/MV) by (0.24 to 0.3%) at (η=0 to 80%). Compared with (CC/MV), (PV) in the thermal dwarf produced higher air quality indices. Through the use of

(PV), the mean age of the air was reduced by up to (0.23 to 0.3),(0.22 to 0.29) at (η=0 to 80%) when compared with (CC/MV) at the sitting and standing person's breathing level. All of the systems checked gave the room a good deal of mixing. The efficiency of air exchange increases with the decrease in the average age of the air and the increase in the (PV) air flow rate. So the highest value (η_a) in (CC/MVPV) system by (75 to 72%) at (η =0 to 80%) at air flow rate (7.5 l/s) as shown in Fig. (5-13). As a result, air flow rate (7.5 l/s) is the best option to protect occupants from direct pollution in the (BZ) area and in the surrounding microclimate as listed in Table (5-2), using this average flow rate for optimum comfort and ventilation effectiveness .

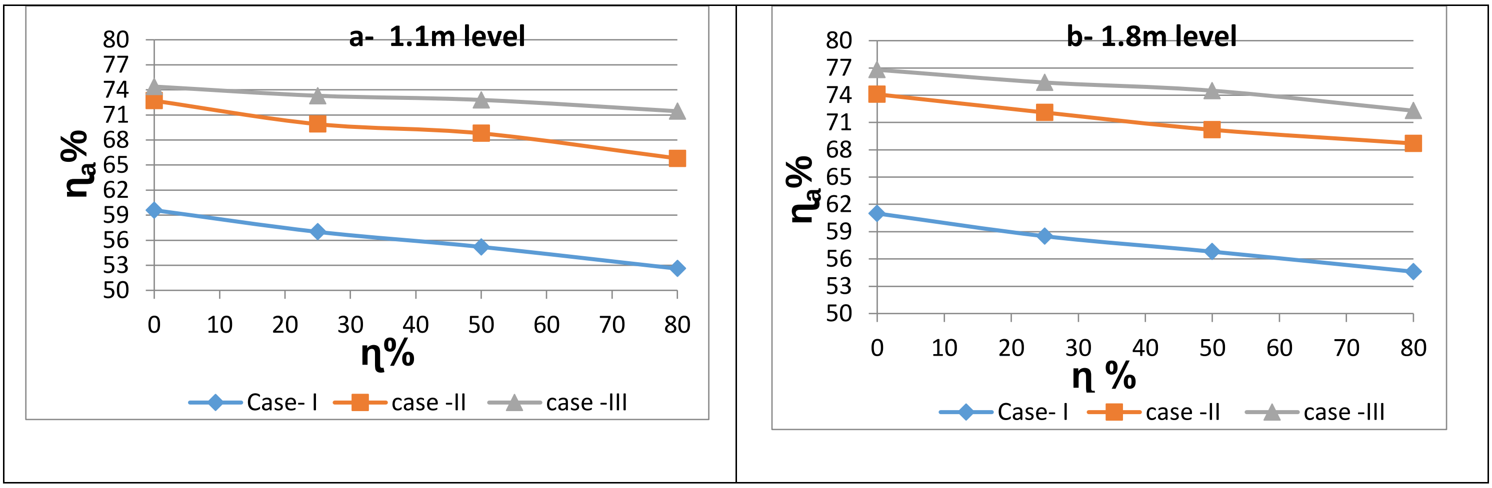

Fig.(5-13) Air exchange efficiency (η_a) profiles at (1.1m and 1.8m) levels for different values of (η) under three cases

Fig (5-14) shows the distribution level of air velocity vectors in a thermally insulated office room is shown numerically at the level (z = 1.25 m) for the three cases, where high air velocity values are produced from a rectangular (MV) diffuser that supplies air, it is installed in the upper part of the room wall (it is located in the middle of the south wall (0.3 m) below the ceiling), where the air enters with a high speed and momentum, (the air velocity inside is 2.5 m / s), and the cool fresh air from the diffuser mixes with the hot air as a result of gaining Heat from people, computers, etc., and this leads to an increase in the speed of air circulation in the room, which is evident in the area near and above heat sources (at a height of 1.1m). Air is expelled through the air outlet under the distributor (at a height of (0.3 m) from the floor of the room), due to the small size (exhaust grille) compared to the air supply area, the air outlet velocity is higher than inlet velocity (diffuser hole) As the air velocity decreases, the air velocity decreases in the area above the air supply diffuser and this leads to an increase in mean age of air in this area.

The vertical profiles of air velocity were consistent across all sites at different heights and in all cases. The highest air velocity recorded in all studied cases was between the manikin and the door wall, at a height of one foot (0.05 to 0.1m) as shown in Fig.(5-14). As shown in the visualization of the air velocity vector of the turbulent model, the middle section of the chamber acts as a separation point for the flow, after a small piece of backflow hits the opposite wall and flows downward, a larger portion of the flow is exhausted and the remaining portion heads upwards towards the ceiling and the room's circulation area is created in the middle with the movement it generates. Warm air exits the tested area through the exhaust grille, which results in a clockwise rotation and flow close to the objects because cold air has a greater density than hot air. The air velocity was often more uniform due to the air grille and the exhaust grill being on the same side so the air velocity was often more uniform.

The numerical results show a relationship between air velocity, air age and temperature, so that increasing the air supply velocity (ATD) lowers the temperature in the breathing area and lowers the average room temperature and shortens the age span of the air in the room although the increase in air velocity should not cause any inconvenience to the occupants of the space if the air velocity remains lower than (0.25 m /s). The lowest values of the average air velocity in the occupied area appeared in the case (CC / MV), this means that the use of (PV) led to an increase in air velocity and a significant decrease in the average air life in the breathing area and the perimeter of the room Which means that the air in the breathing area is replenished faster than it is (without using)

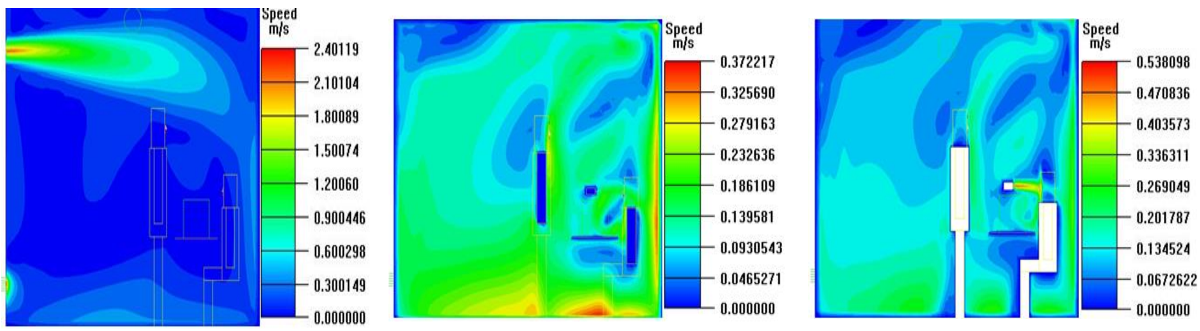

Case-I Case-II Case-III

a- η=0 %

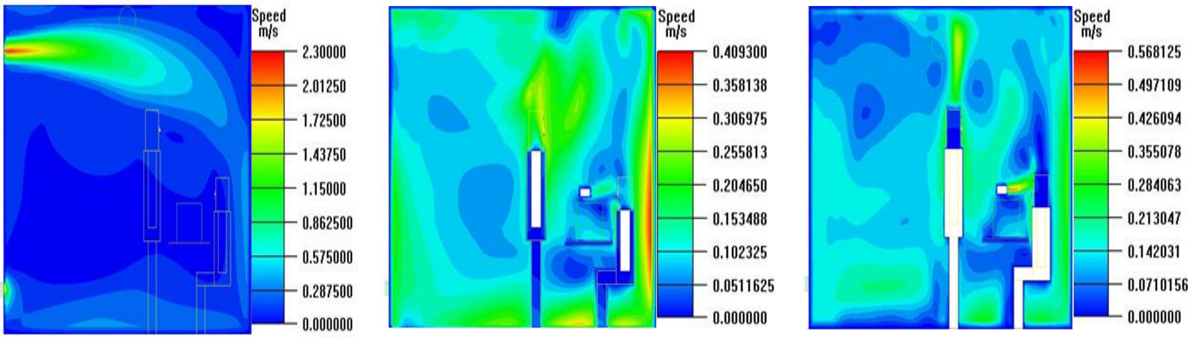

Case-I Case-II Case-III

b- η=25%

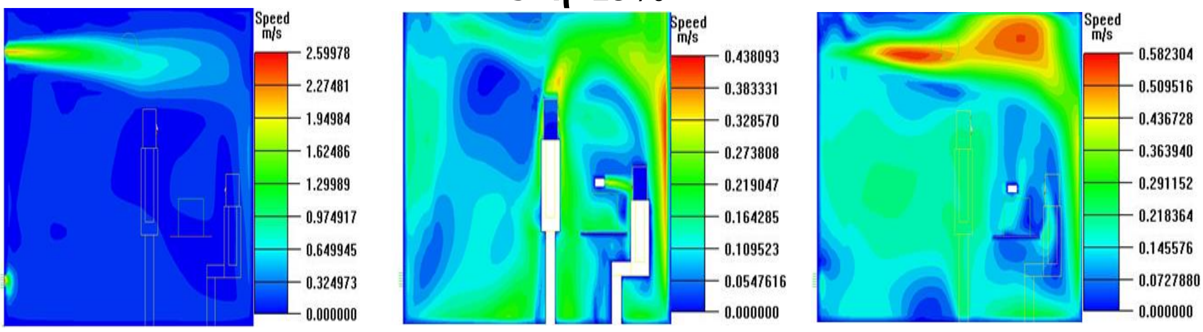

Case-I Case-II Case-III

c- η=50%

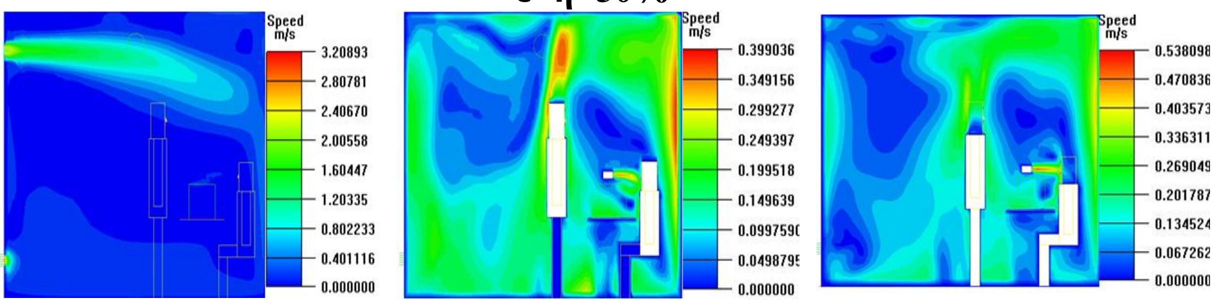

Case-I Case-II Case-III

d- η=80%

Fig(5-14) The contours of velocity at different (η) for three cases at (z=1.25m).

Air temperature distribution profiles with different (η) at (z =1.25) in the test chamber are shown in Fig.(5-15). It is noted that the effect of the cold air supply coming from the distributor located at the top of the room wall leads to the ceiling temperature being cooler than the room floor temperature. Due to the arrival of cold air streams from the personal ventilation devices (ATD) as well as the air supply diffuser, the air temperature begins to rise and then gradually decreases near the (MV device).The temperature difference between the head and the feet is less than (2°C), which is within the permissible range of ASHRAE standards.

When the air flow rate is increased, the average room temperature in the breathing area decreases and the increase in air velocity within the breathing area leads to a decrease in the overall room temperature as shown in Fig. (5-15).

The highest constant temperature values for a person sitting and standing (CC / MV) appeared, as well as the irregular distribution of temperature over parts of the entire body, such as the air temperature in the breathing area and lower parts of the body. The body rises while it decreases in the upper parts of the body. Therefore, the use of photovoltaic cells results in a cooling of the whole body and reduces the differences between the head and ankle compared to the case (CC / MV). Parts of the upper body (CC) are cooled due to increased radiation. It is noted that when (PV) is increased from (5 l / s to 7.5 l / s), (25% to 50%), the air temperature near the head decreases at (1.8 m) .This is due to the increased rate of supply of fresh air which provides more cooling . Therefore, the breathing zone in the case of (CC / MVPV) is characterized by a decrease in temperature with a good rise in the permissible air velocity within the recommended thermal comfort.

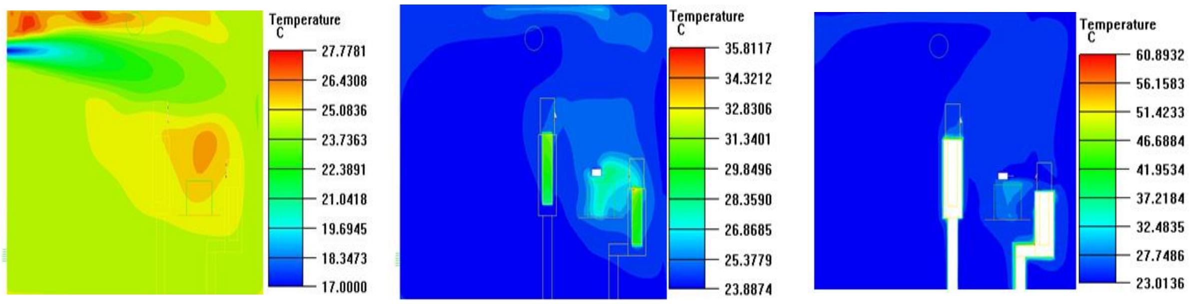

Case-I Case-II Case-III

a- η=0 %

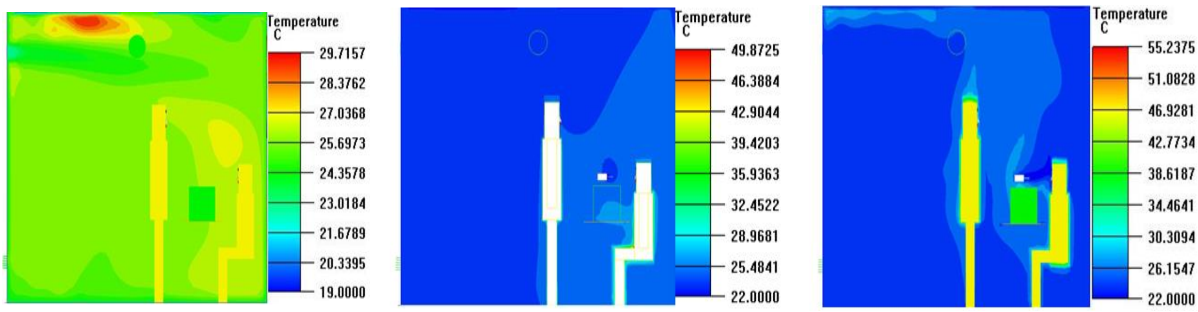

Case-I Case-II Case-III

b- η=25%

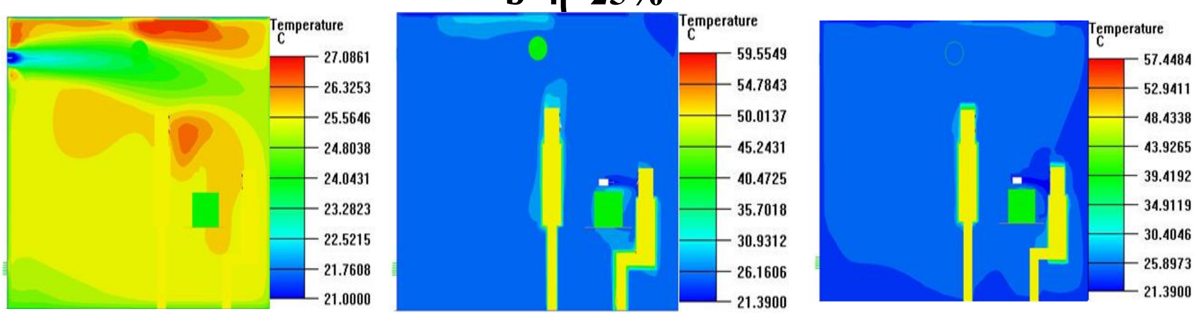

Case-I Case-II Case-III

c- η=50%

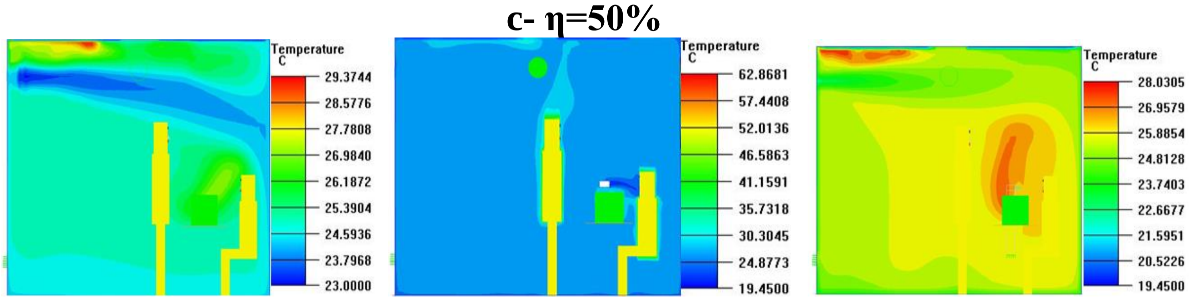

Case-I Case-II Case-III

d- η=80%

Fig.(5-15) The contours of air temperature distribution at different (η) for three cases at (z=1.25m)

Figs.(5-16) and (5-17) show relative air quality profiles, and thermal comfort indices (PMV and PPD) with different values (η) for three cases. It is noted in all cases that as the value of (η) increases, the (PMV and PPD) values decrease and converge with the comfort values defined by the (ASHRAE 2017) standard (-0.5 PMV 0.5 and PPD = 10%), due to increased heat loss from the body as a result of a decrease in the surface temperature of the radiator , which enhances radiative heat transfer between heat sources and the ceiling wall. In all cases it was seen that the values of (PMV and PPD) decreased from (0.25 to 0.30),(0.33% to 0.36%) with the (CC/MVPV) (case-II, case-III) compared to the (CC/MV) system (case-I), at (η=0 to 80 %) , which means that the introduction of cool (PV) air at warmer temperatures led to heat attenuation and improved thermal comfort than in (case I). The values of (PMV and PPD) decrease with the increase of the air flow rate from $(0.2 \text{ to } 0.34), (0.19\% \text{ to } 0.24\%)$ $\text{at}(\eta = 0 \text{ to } 80\%)$ in two cases (case-II,and case-III) , which means that the increase in the (PV) air flow rate leads to an increase in the turbulence near the person as well as the heat loss from the upper parts of the body caused by the (CC), which It leads to improved comfort and this can be seen in Figs.(5-16)and (5-17).

Fig.(5-18) shows results of (ADPI) analyses at different value of (T_{CC}) for the three cases (case-I, case-II and case-III) performed according to (ASHRAE 2017) . For all cases analyzed, ADPI achieves values greater than (80%), which is above the minimum values (ADPI) recommended by the ASHRAE standard for good indoor air mixing. It is noted in all cases that with an increase in the value of (η), the values of (ADPI) increase and this means that when the convection is removed from the cooled ceilings, it leads to better thermal comfort. Values of (ADPI) go down with system (CC/MV) so that use of (PV) in the (CCMV/PV) system for both airflow rate (5 l/s, 7.5 l/s) resulted in a higher (IAQ) in (BZ) due to continuous cleaning and mitigation of pollutants. This study shows that (PV) is able to create a uniform thermal environment and good air quality in the occupied area when combined with (CC) and may be higher than conventional (CC/MV).

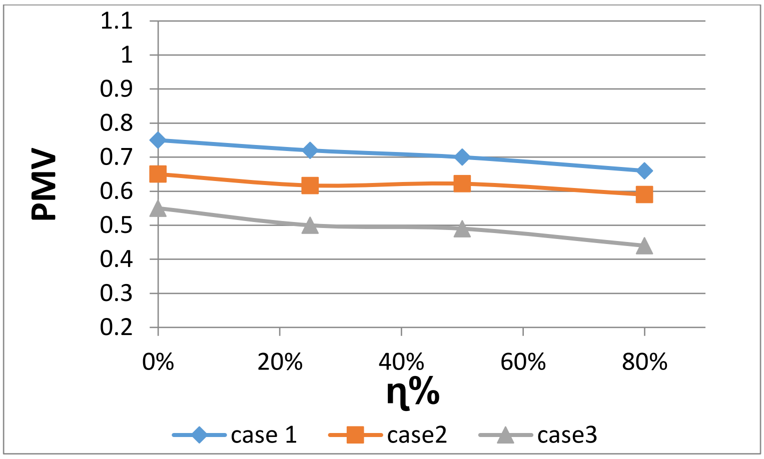

Fig.(5-16) Illustration of the (PMV) at varies (η) for three cases

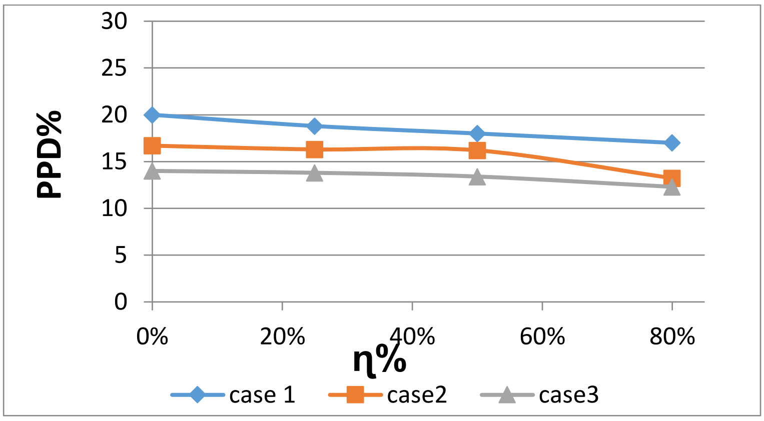

Fig.(5-17) Illustration of the (PPD) at varies (η) for three cases

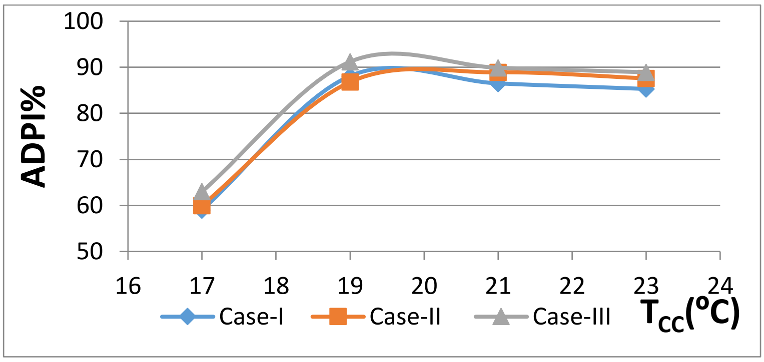

Fig.(5-18) (ADPI) profile with temperature of chilled ceiling (T_{CC}) for three cases

5.2.3 Occupied density and occupant air exchange efficiency

All studied cases demonstrate that the updated air exchange efficiency can be used to improve the ventilation effect assessment criterion. Otherwise, a system designed to improve indoor air quality can be useful. In all cases, the longer people stay in the room, the less air changes the occupants, as shown in Fig. (5-19). The overall ventilation effect can be analyzed more comprehensively using passenger air exchange efficiency. Therefore, the efficiency of air exchange for passengers increases in cases (case-II and case-III) from (13 to 20%), (18.3 to 26.2%) at (η= 0 to 80%) compared with (CC / MV) (case-I), this means that personal ventilation improves the efficiency of air exchange air and determine the level of comfort inside the room as a result of its unique characteristics due to the low rate of ventilation, the results showed a high efficiency of air exchange (9 ACH). However, because the weight of the occupied density inside the room is higher, the occupant air exchange efficiency is higher than the air exchange efficiency. In all cases, the efficiency of air change for passengers increases with the increase in the (PV) air flow rate. This means that fresh air replaces the air in the well of the occupied area faster, which leads to an improvement in air quality. As in the (case-III) , the efficiency of air exchange for occupants (η_D) increased by (3 to 5.4%) at (η=0 to 80%) compared with (case-II).

Fig.(5-20) shows the relationship of air exchange efficiency for occupants (η_D) with a different value (η) under the three cases, where it was found that the temperature of the cooled ceilings increases with the increase in the cooling load treated by the chilled ceilings, and this leads to an increase in the age of the air and then a decrease in the efficiency of air exchange.

In all cases with (PV), the air exchange efficiency for occupants (η_D) was higher than (CC/MV) system by (22.25 to 25.11%), (30.2 to 39.16) at (η = 0 to 80%) compared with the (CC / MV) system as a result of reducing the mean air age up to (0.23 to 0.3),(0.22 to 0.29) at (η = 0 to 80%) compared to (CC/MV) at a seated and standing person breathing level. The air exchange efficiency (η_a , η_D) increases with the decrease in the average air age and the increase in the (PV) air flow rate. So the highest value air exchange efficiency (η_a , η_D) in (CC / MVPV-2) by (75 to 72%),(99.5 to 93%) at (η = 0 to 80%) at the air flow rate (7.5 l / sec) as shown in Fig. (5-20). As a result, flow rate (7.5 l/s) is the best option for protecting occupants from direct pollution in the (BZ) and in the surrounding microclimate .

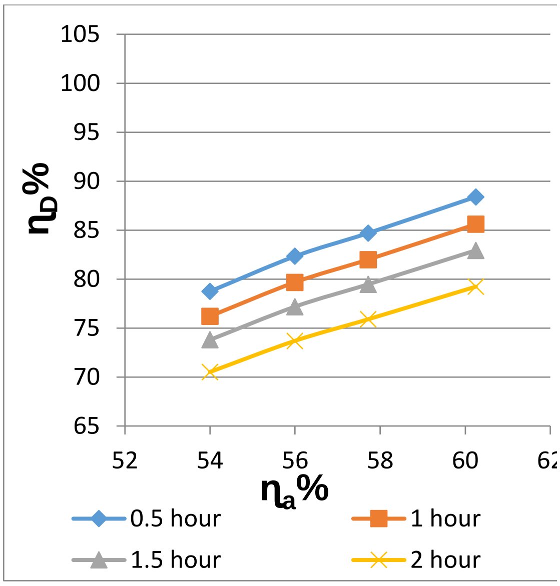

a- case-I

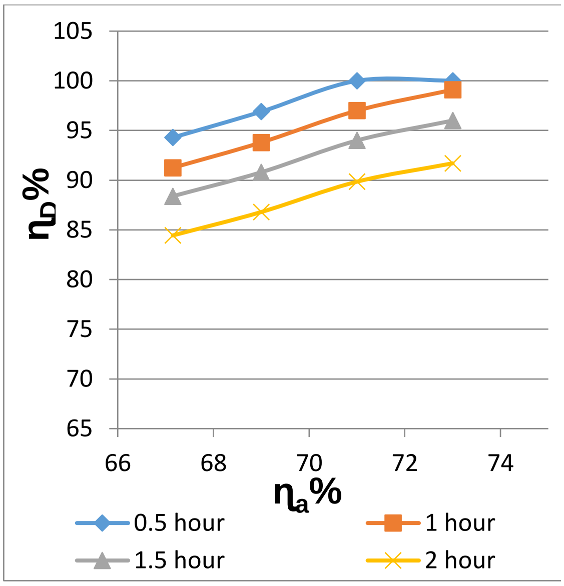

b- case-II

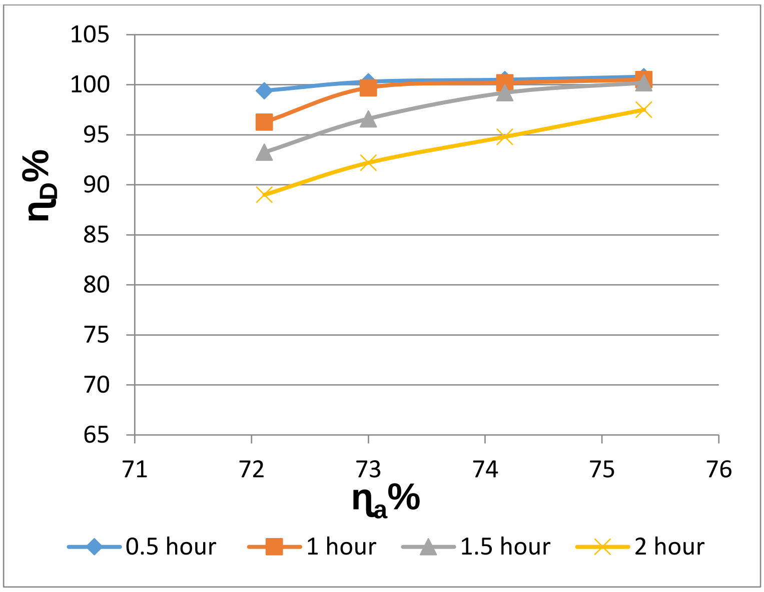

c- case-III

Fig.(5-19) Relationship between of air exchange efficiency and occupant air exchange at four times in three cases (case-I,II, and III)

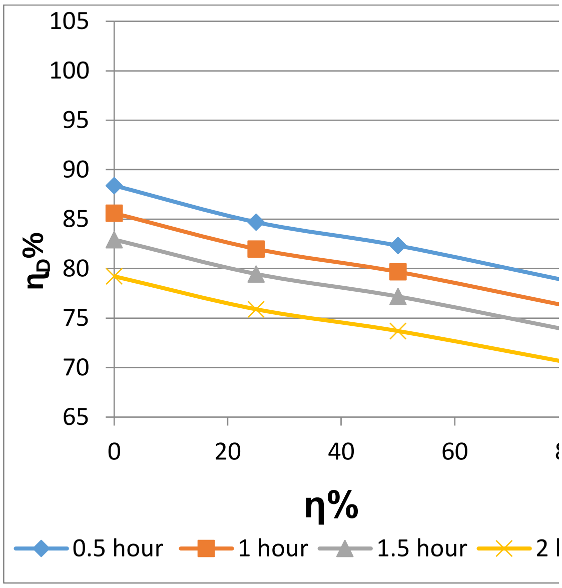

a- case-I

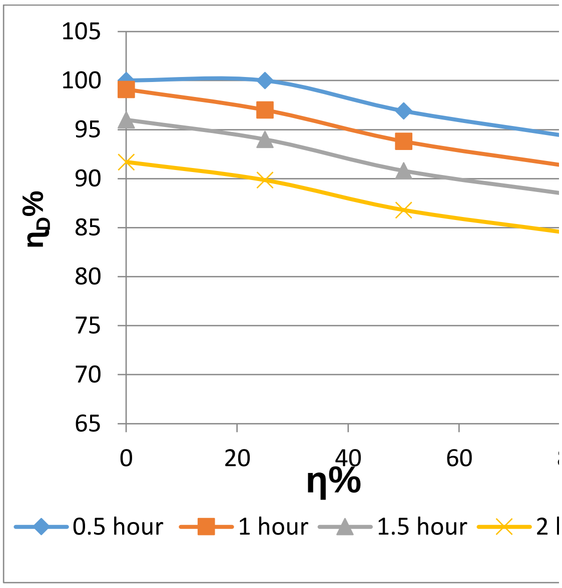

b- case-II

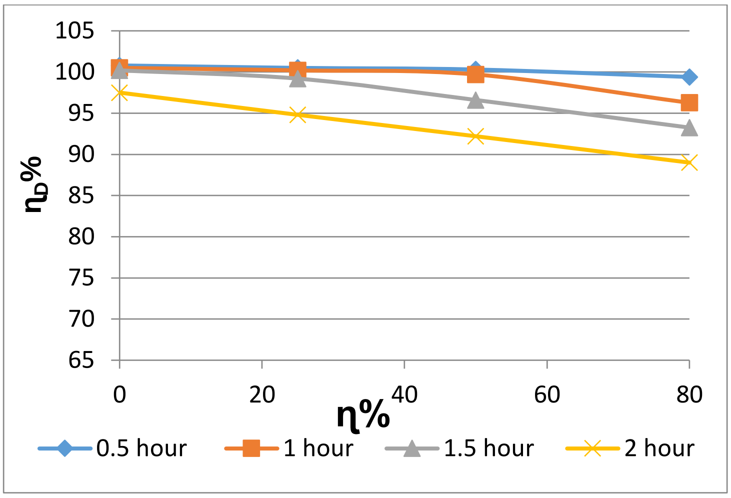

c- case-III

Fig.(5-20) Relationship between of different values of (η) and occupant air exchange at four time in three cases(case-I,II, and III)

5.3 Comparison Between Experimental and Numerical Results

The difference between the experiments measured results and those predicted by the (CFD) model occurs due to various reasons, including unexpected fluctuations in nature that lead to error during meter readings, irregularities in the temperature and speed of the air supply to the diffuser, and common defects in the operation of the (CFD) software.

The discrepancy between experimental and numerical results can be caused by a variety of factors, including measurement errors, irregularities in the temperature and speed of the air supply to the diffuser, and common defects in the operation of (CFD) software.

The three experiments determined parameters such as (local air age, temperature distribution with altitude, and CO_2 removal over time) for the tested office room on three measurement stands were used to calculate the average percentage error between experimental and numerical results according to Eq.(3-12).

5.3.1 Average percentage error for the local mean air age (LMA)

The average percentage error was determined in six points on three measurement stands with varying values of cooling load treated by chilled ceiling (η =0, 25, 50, and 80%) within the tested office room and each holder had two points at the breathing zone height (1.1 m and 1.8 m) for the seated and standing person for three cases as shown in Figs. (5-21) to (5-23) .The (LMA) distribution average percentage error between experimental and numerical data is obtained by using Eqn (3-12).

The percentage error between the experimental and numerical values in all cases was reasonable due to the irregularity of the air supply velocity and the (CO_2) supply from the diffusers, which was used to measure the local air age using the atomization method.

In Table (5-3), the percentage average error for the three cases are shown for various values of (η) (four tests in each case with (η =0, 25, 50, and 80%))

Table(5-3) Percentage average error between experimental and numerical results

for local air age in the three cases at different value of (η)

Case	**Test**	**η %**	**Average error %**
case - I	test -1	0	± 13.29
	test -2	25	±11.54
	test -3	50	±12.3
	test -4	80	±10.54

case - II	test -5	0	±13
	test -6	25	±11.26
	test -7	50	±11.09
	test -8	80	±11
case - III	test -9	0	±8
	test -10	25	±7.5
	test -11	50	±7.1
	test -12	80	±6.8

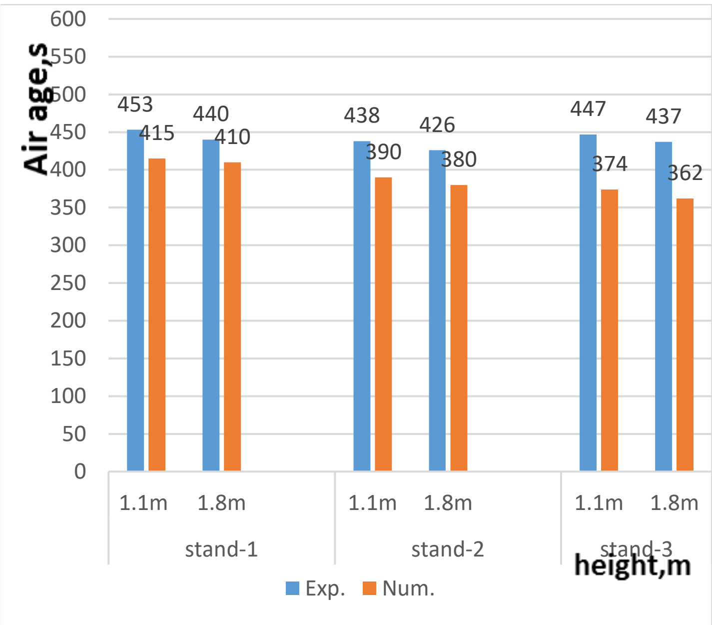

a- η =0 %

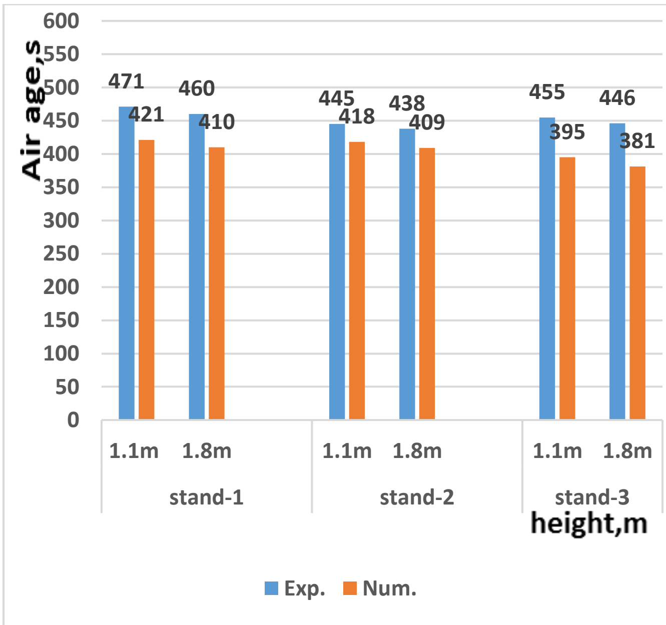

b- η =25 %

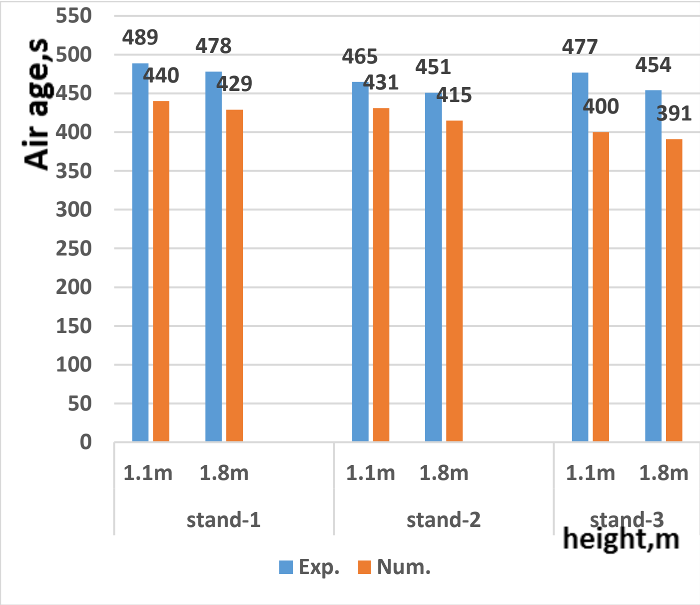

c- η =50 %

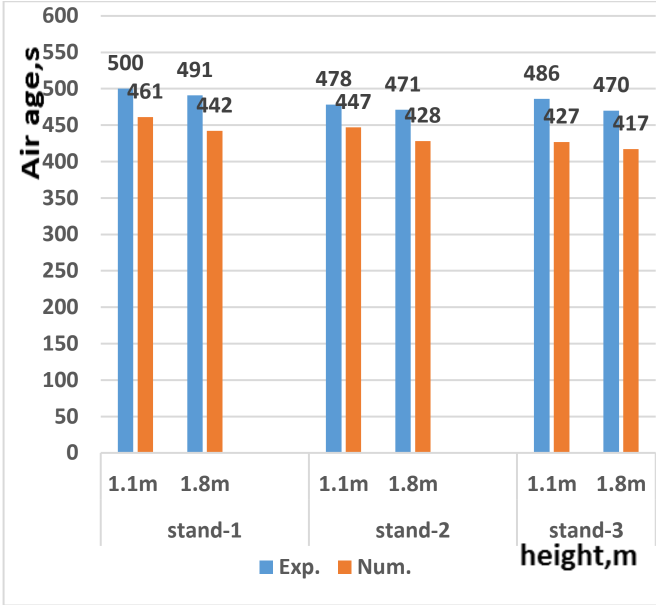

d- η =80 %

Fig.(5-21) Comparison between experimental and numerical results for (LMA) at different value of (η) for thee measurement stands in (Case-I) at high (1.1m and 1.8m).

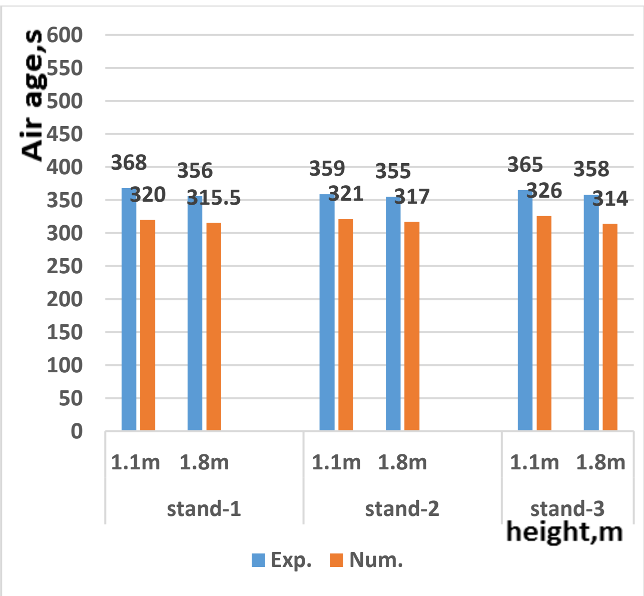

a- η =0 %

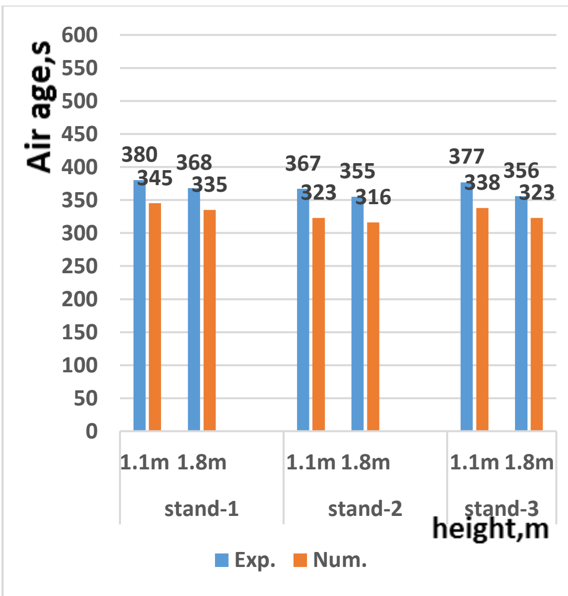

b- η =25 %

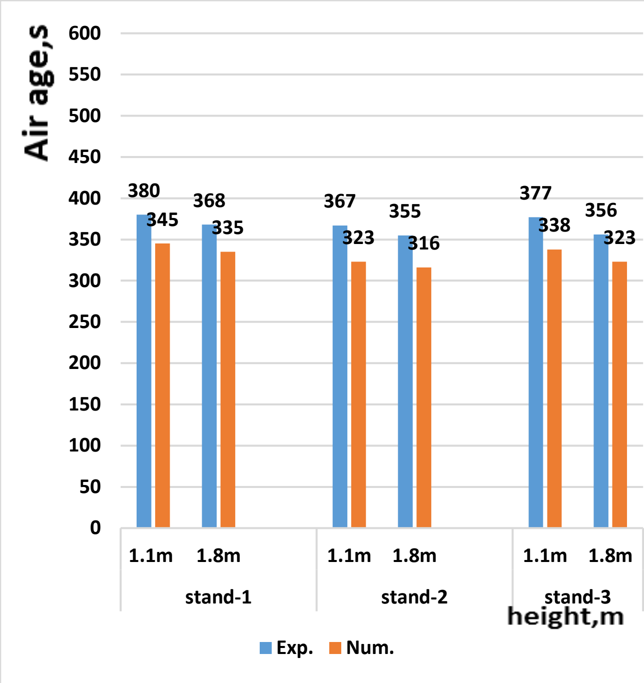

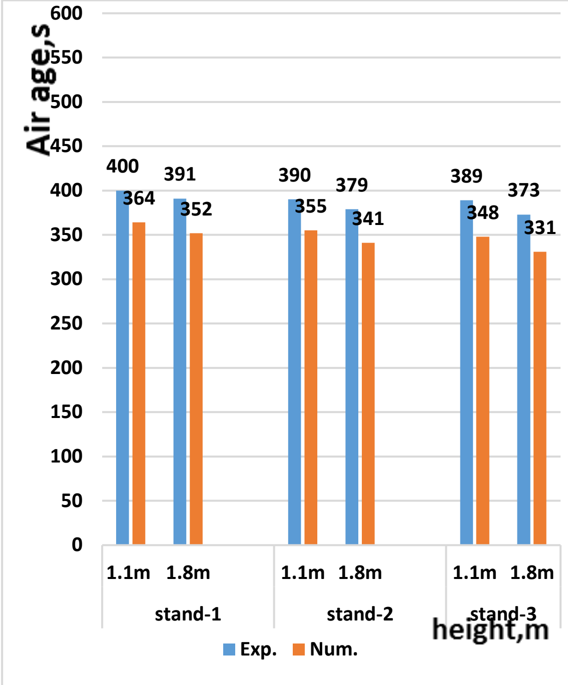

c- η =50 %

d- η =80 %

Fig.(5-22) Comparison between experimental and numerical results for (LMA) at different value of (η) for thee measurement stands in (Case-II) at high (1.1m and 1.8m).

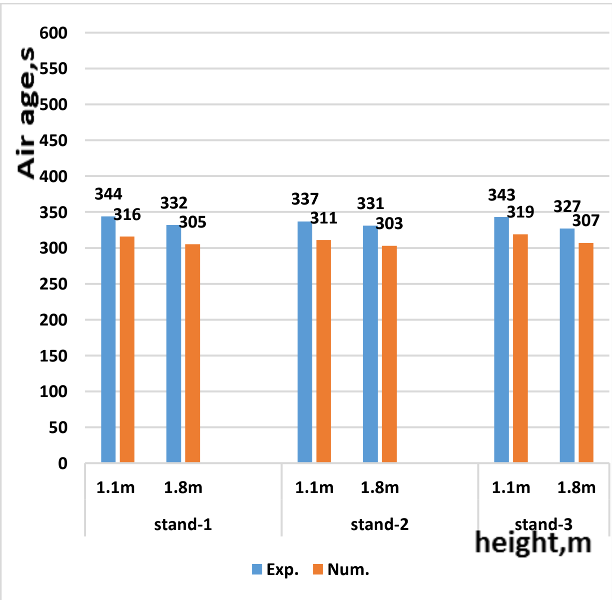

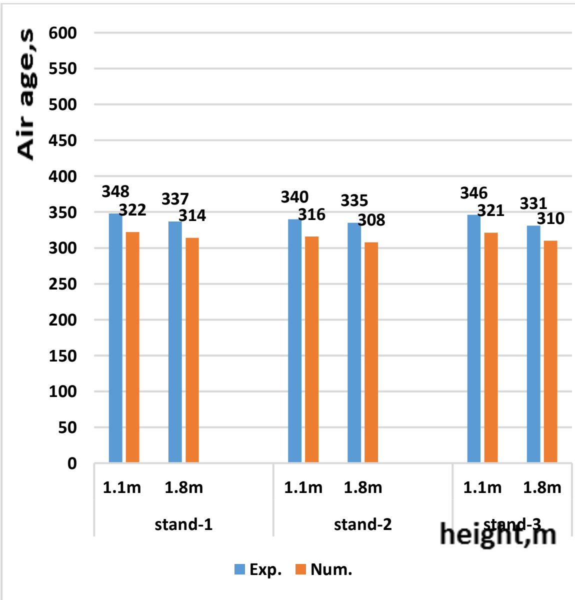

a- η =0 %

b- η =25 %

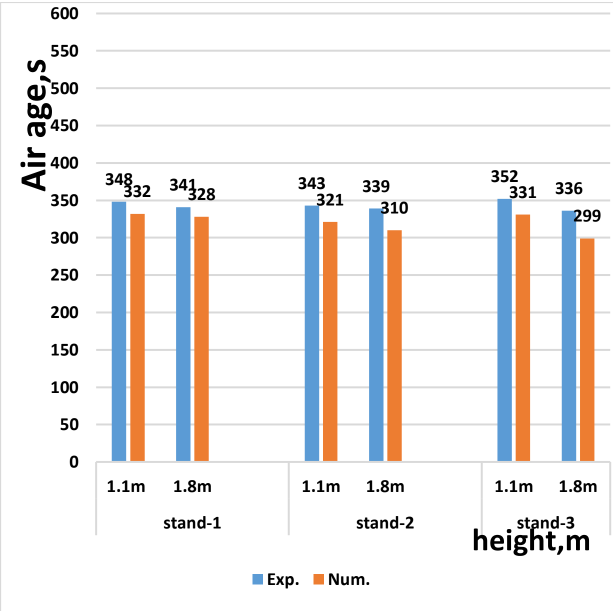

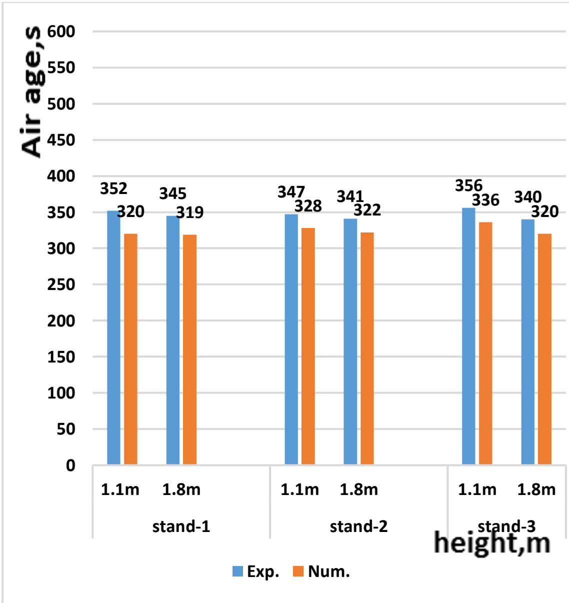

c- η =50 % **d- η =80 %**

Fig.(5-23) Comparison between experimental and numerical results for (LMA) at different value of (η) for thee measurement stands in (Case-III) at high (1.1m and 1.8).

5.3.2 Average percentage error for the temperature distribution

twenty one points on three measurement stands with varying values of cooling load treated by chilled ceiling (η =0, 25, 50, and 80%) were used within the office room and each holder had seven points at height (0.1, 0.4, 0.8, 1.1,1.4,1.8 and 2.4m) for the three cases as shown in Figs. (5-24) to (5-26) .The temperature distribution average percentage error between experimental and numerical data is obtained by using Eqn (3-12).

The percentage error between the experimental and numerical values in all cases was reasonable due to the irregularity in air supply velocity and temperature by supply diffuser. In Table (5-4), the percentage average error for the three cases are shown for various values of (η) (four tests in each case with (η =0, 25, 50, and 80%)) .

Table(5-4) Percentage average error between experimental and numerical results for temperature distribution in the three cases at different values of (η)

Case	**Test**	**η %**	**Average error %**
case - I	test -1	0	± 5.21
	test -2	25	±4.56
	test -3	50	±5
	test -4	80	±4.5
case - II	test -5	0	±4.38
	test -6	25	±4.12
	test -7	50	±4.08
	test -8	80	±4.14
	test -9	0	±4.21

case - III	test -10	25	±4.6
	test -11	50	±4.16
	test -12	80	±4

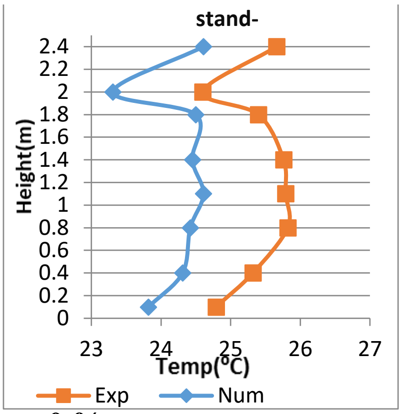

η =0 %

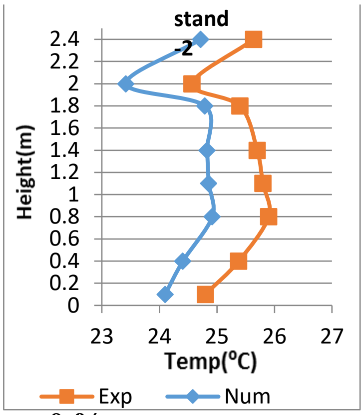

η =0 %

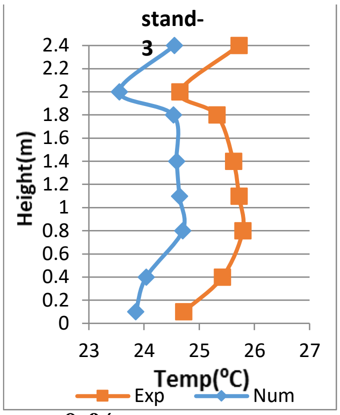

η =0 %

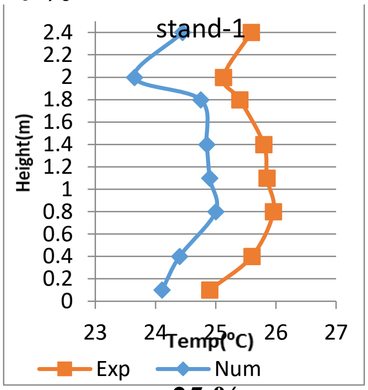

η =25 %

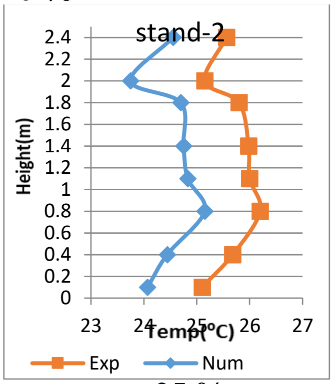

η =25 %

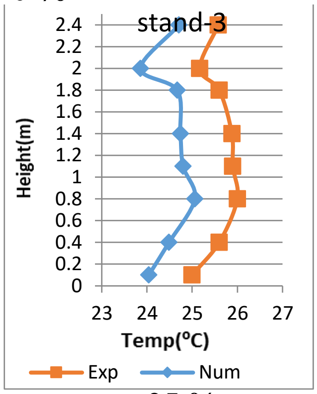

η =25 %

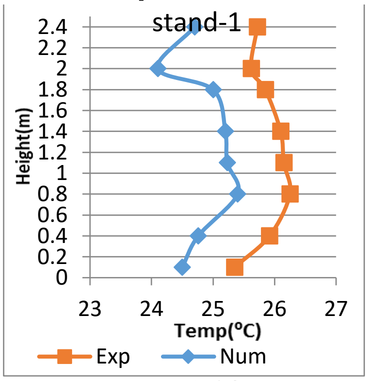

η =50 %

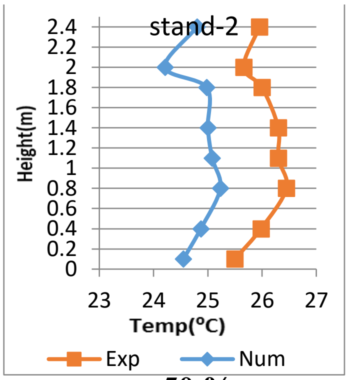

η =50 %

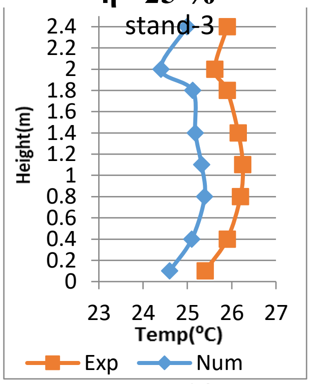

η =50 %

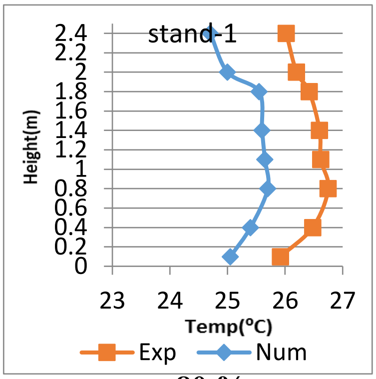

η =80 %

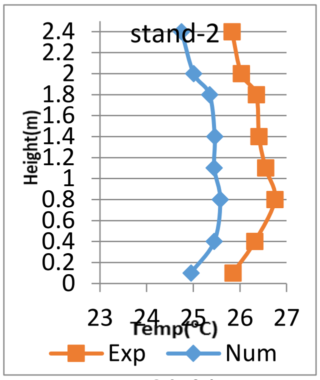

η =80 %

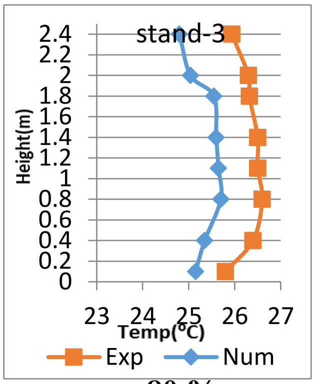

η =80 %

Fig.(5-24) Comparison between experimental and numerical results for temerature distribution with a heigh at different values of (η) for thee measurement stands in (Case-I)

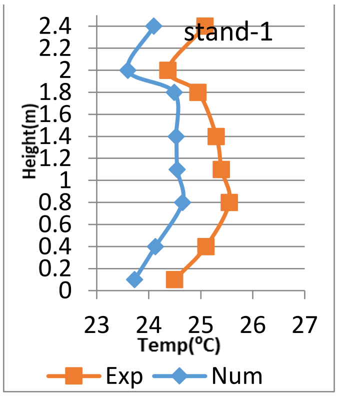

η =0 %

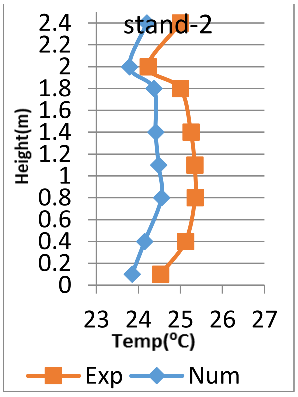

η =0 %

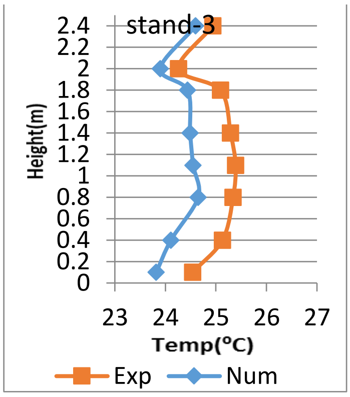

η =0 %

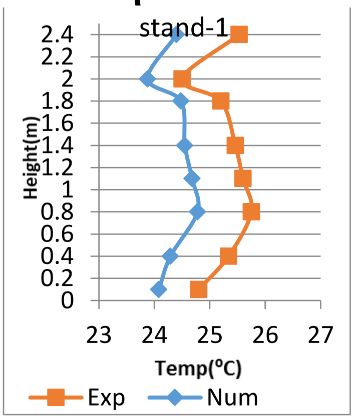

η =25 %

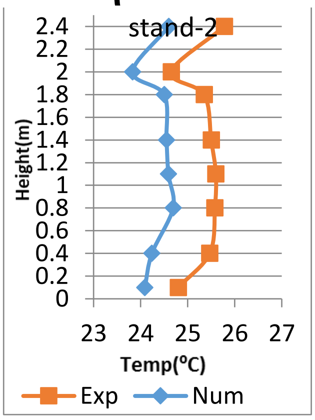

η =25 %

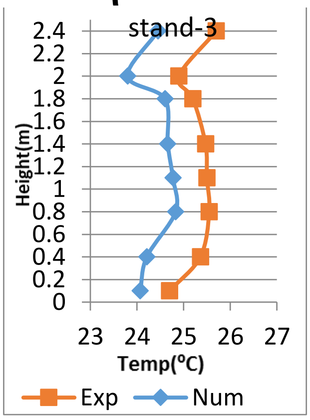

η =25 %

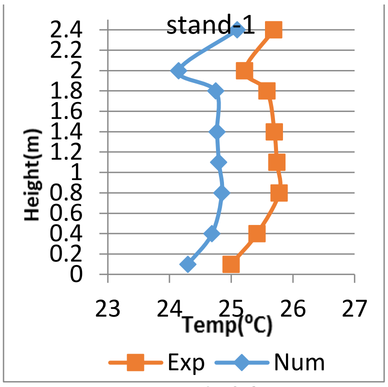

η =50 %

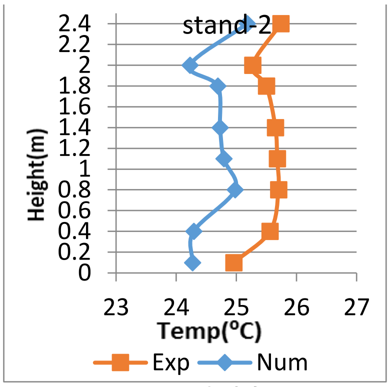

η =50 %

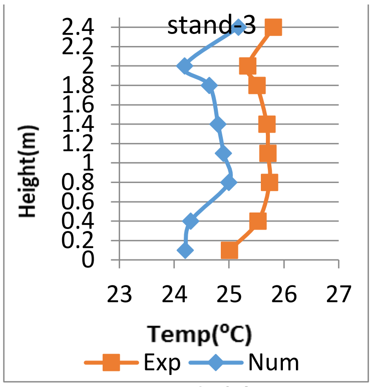

η =50 %

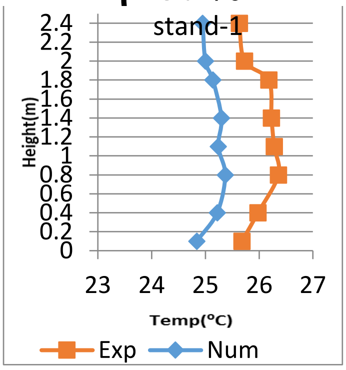

η =80 %

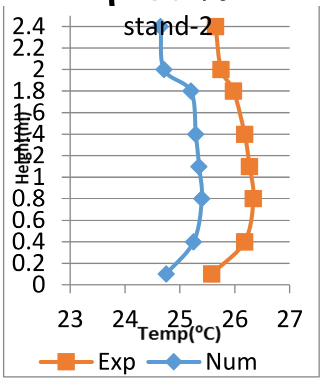

η =80 %

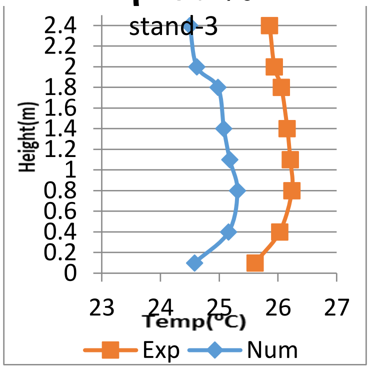

η =80 %

Fig.(5-25) Comparison between experimental and numerical results for temerature distribution with a heigh at different values of (η) for thee measurement stands in (Case-II)

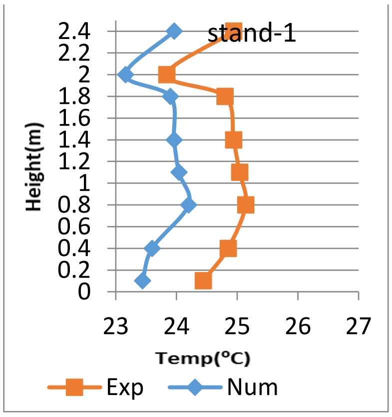

η =0 %

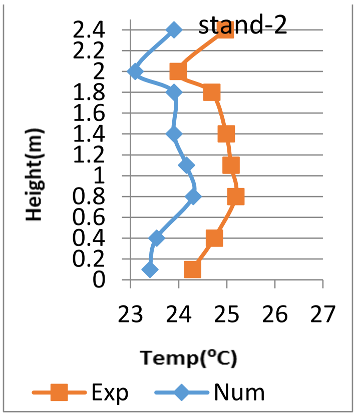

η =0 %

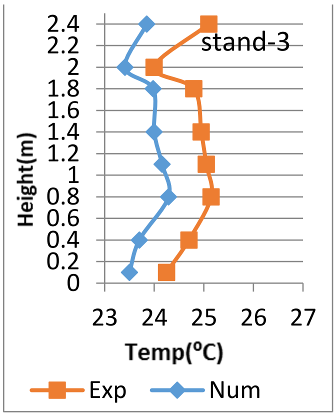

η =0 %

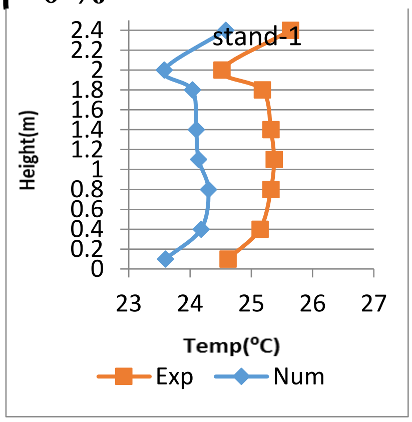

η =25 %

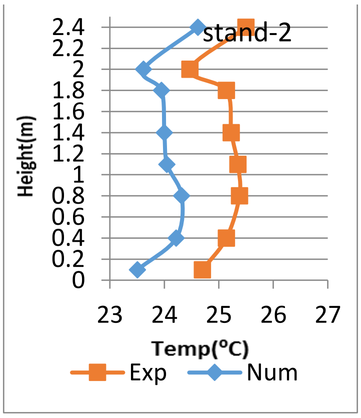

η =25 %

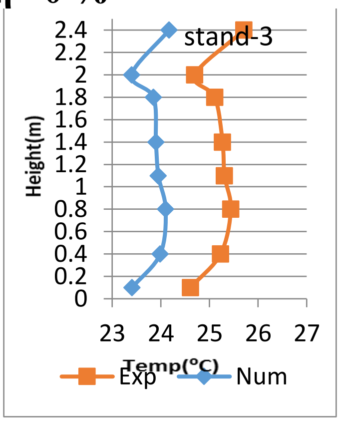

η =25 %

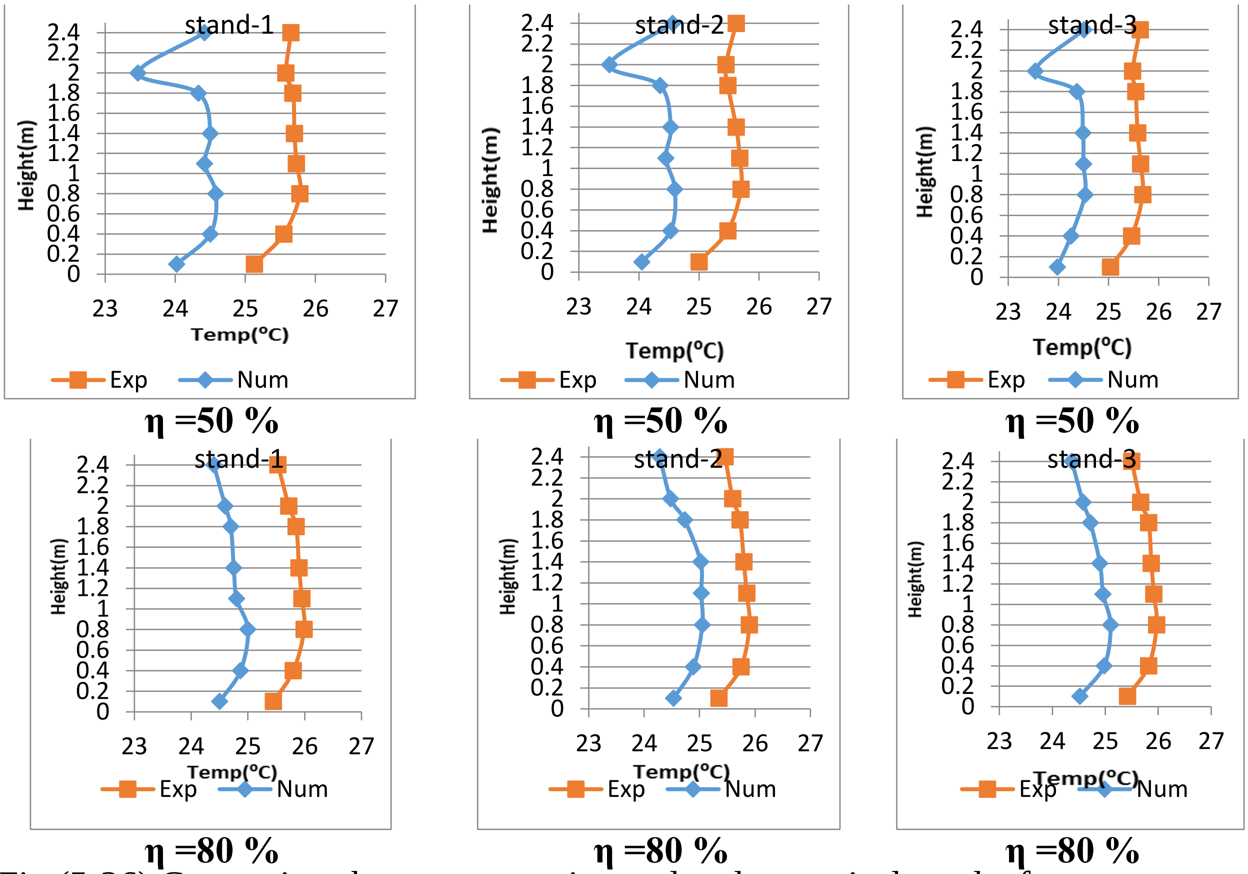

Fig.(5-26) Comparison between experimental and numerical results for temperature distribution with a heigh at different values of (η) for thee measurement stands in (Case-III)

5.3.3 Average percentage error for carbon dioxide decay

Six points on three measurement stands with varying values of cooling load treated by chilled ceiling (η =0, 25, 50, and 80%) were used within the office room and each holder had two points on the breathing area height (1.1 m and 1.8 m) for the seated and standing person as shown in Figs. (5-27) to (5-29) .The (CO_2) distribution average percentage error between experimental and numerical data is obtained by using Eqn (3-12). In Table (5-5), the percentage average error for the three cases are shown for various values of (η) (four tests in each case with (η =0, 25, 50, and 80%))

Table(5-5) Percentage average error between experimental and numerical results for Co_2 decay with time in the three cases at different value of (η)

Case	Test	η (%)	Average error (%)
case - I	test -1	0	± 7.4
	test -2	25	±6.36
	test -3	50	±5.35
	test -4	80	±5
case - II	test -5	0	±7.59
	test -6	25	±6.5
	test -7	50	±5.5
	test -8	80	±5.27
case - III	test -9	0	±6.7
	test -10	25	±6.2
	test -11	50	±5.26
	test -12	80	±4.85

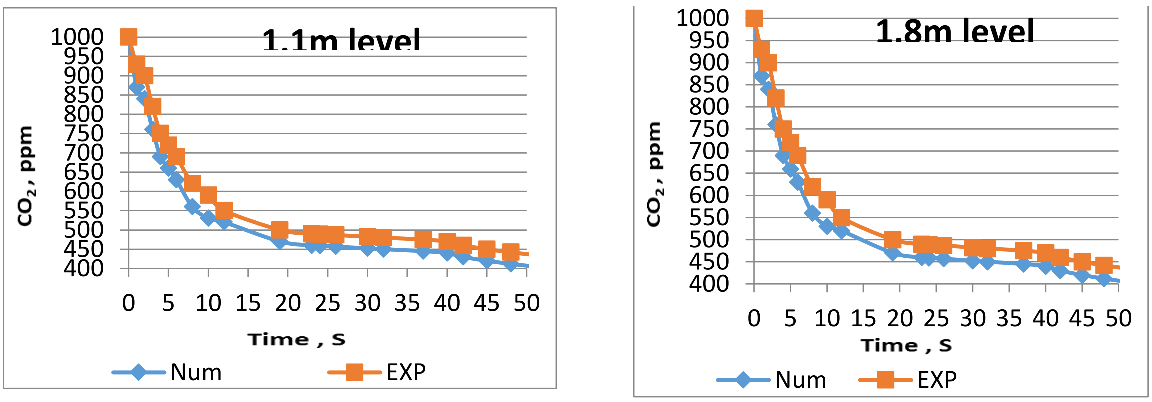

a- η = 0%

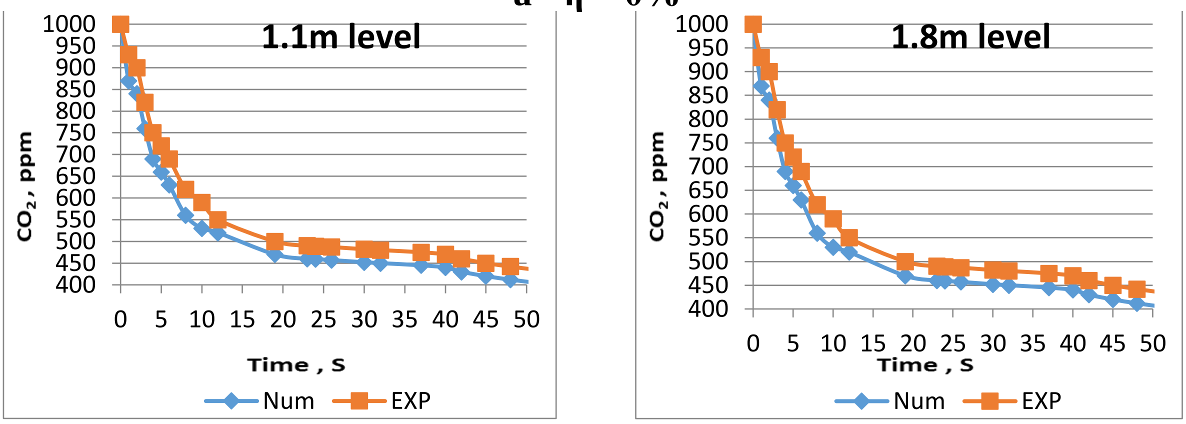

b- η = 25%

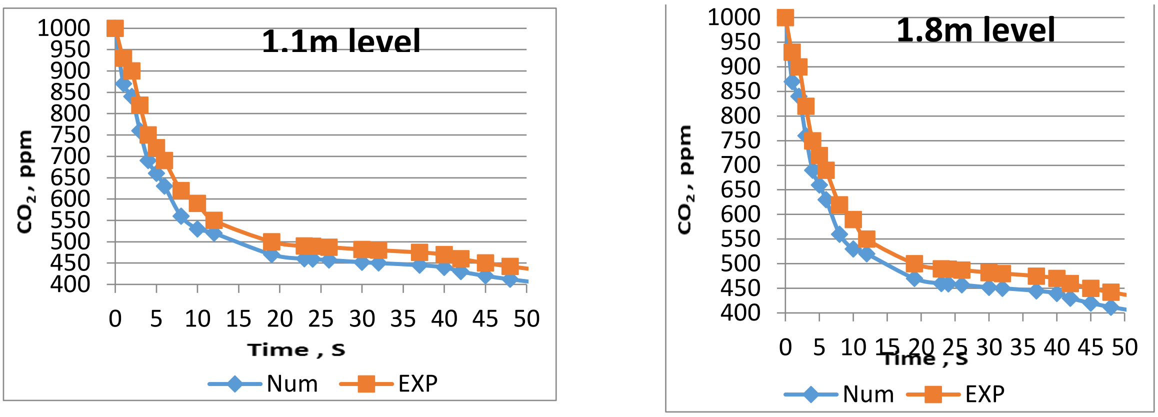

c- η = 50%

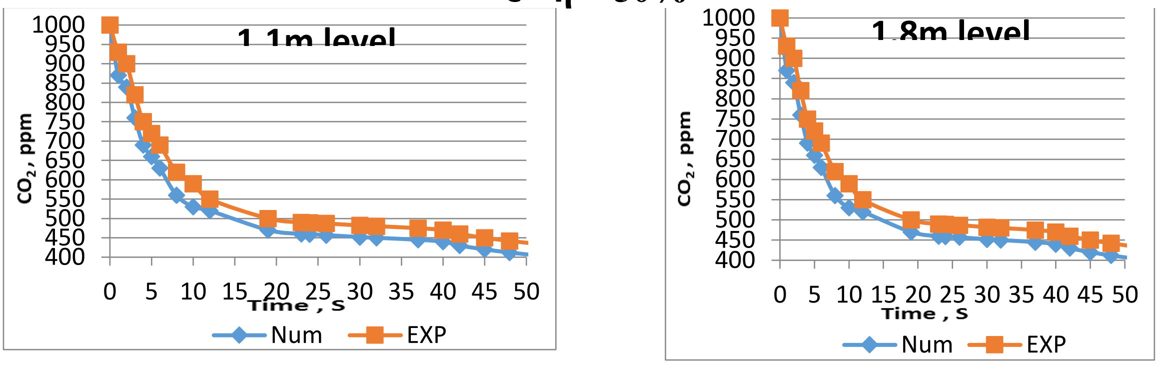

d- η = 80%

Fig.(5-27) Comparison between experimental and numerical results for CO_2 with time at avarage measurement stands in (Case-I)

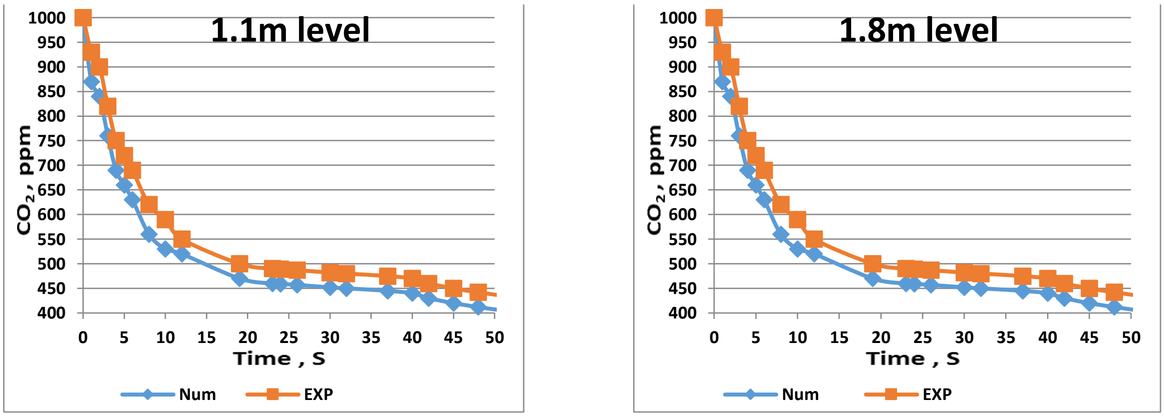

a- η = 0%

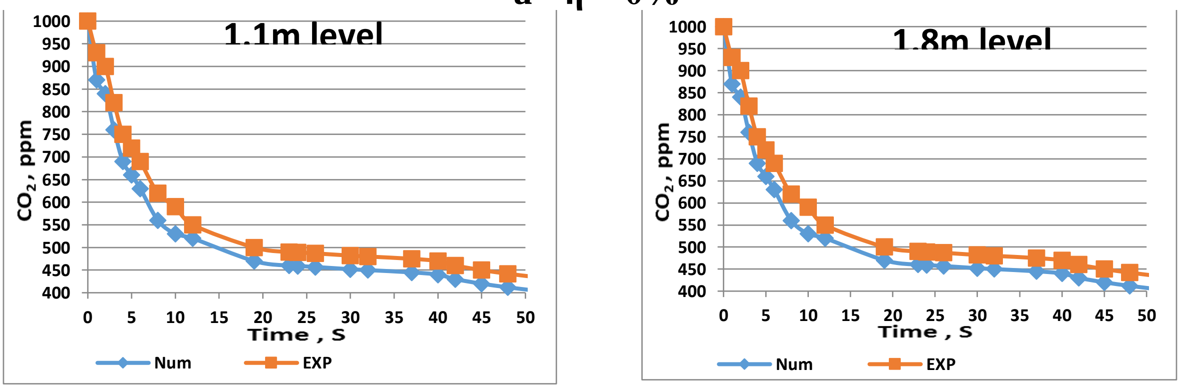

b- η = 25%

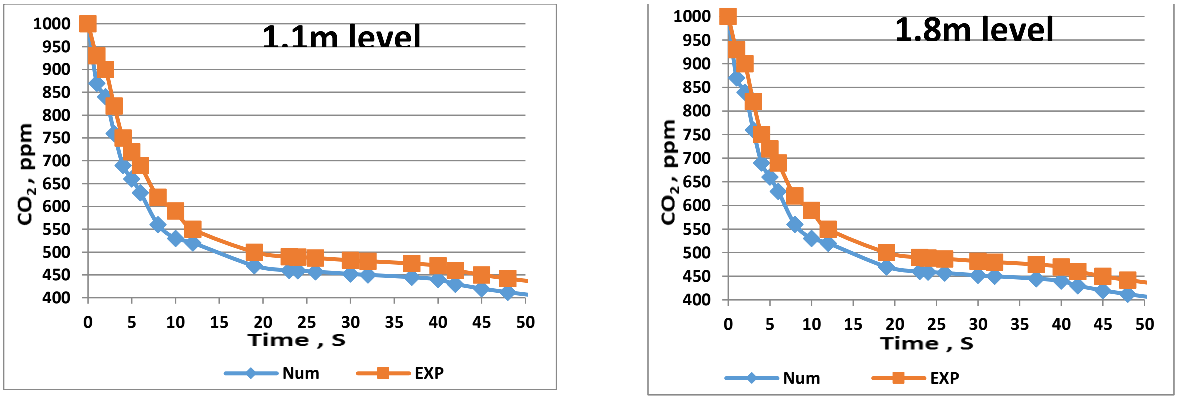

c- η = 50%

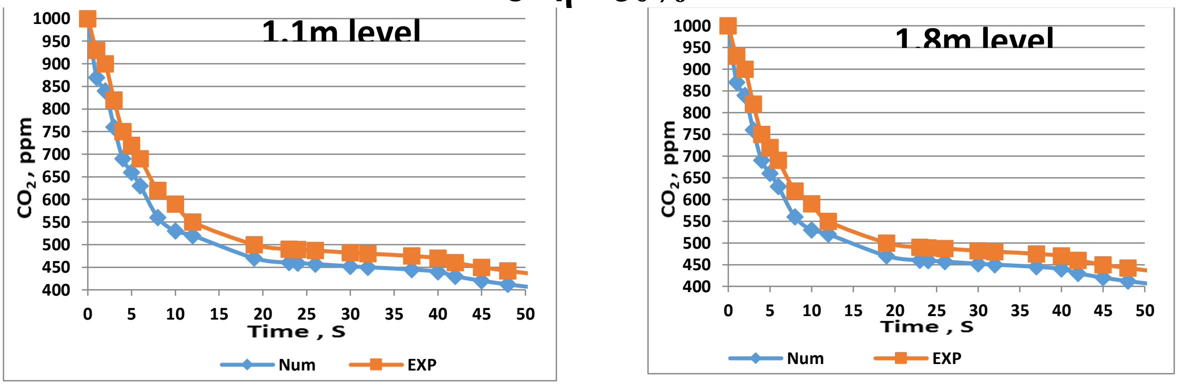

d- η = 80%

Fig.(5-28) Comparison between experimental and numerical results for CO_2 with time at avarage measurement stands in (Case-II)

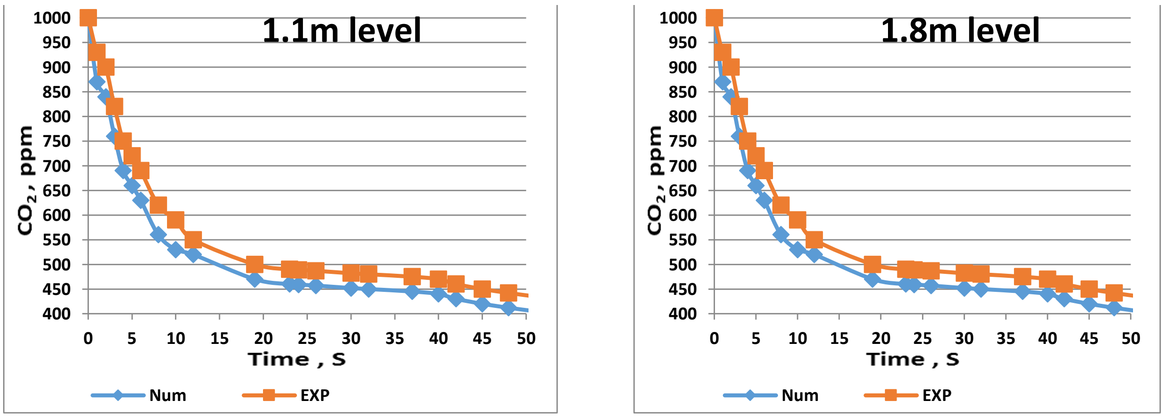

a- η = 0%

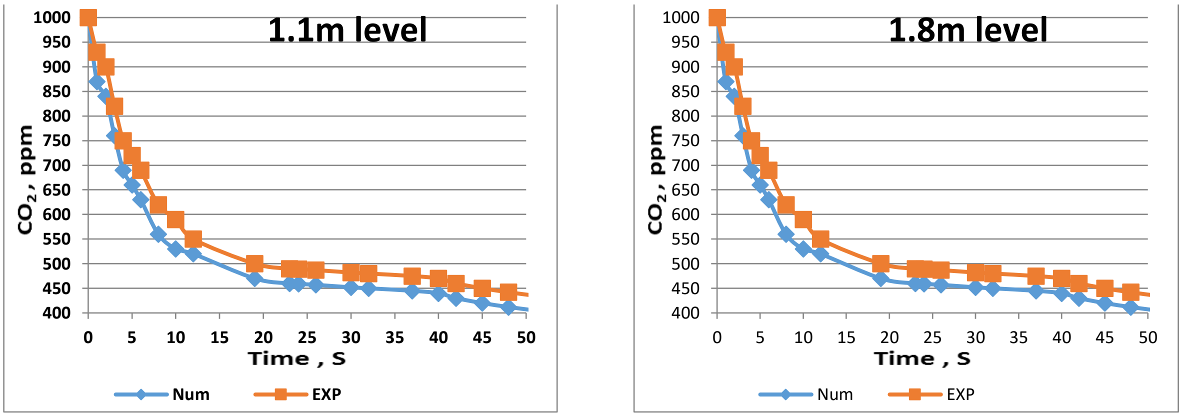

b- η = 25%

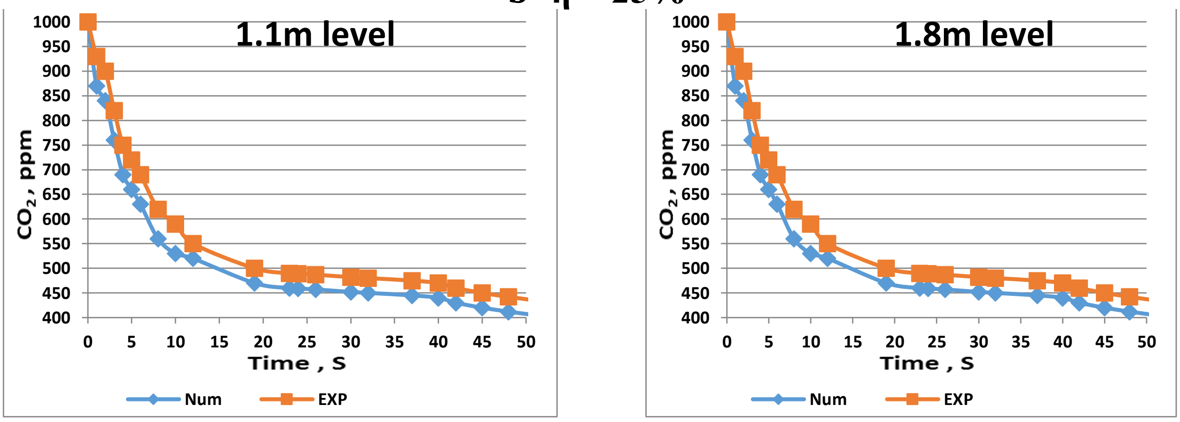

c- η = 50%

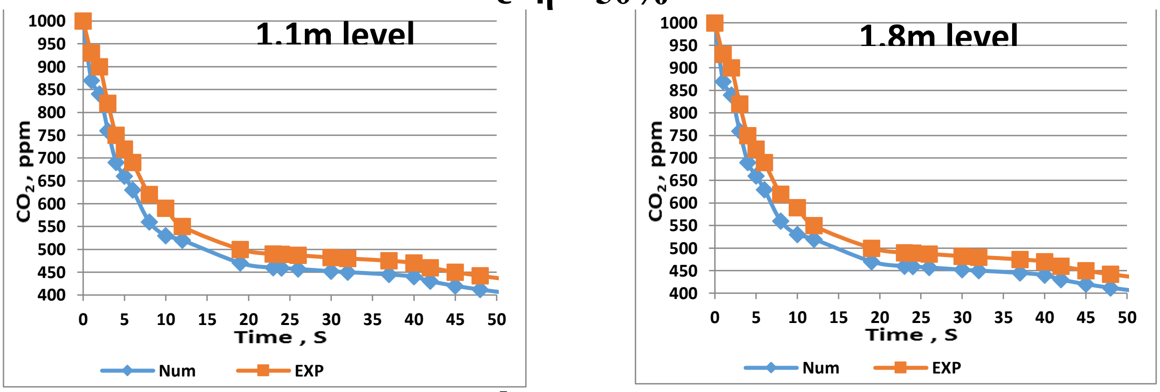

d- η = 80%

Fig.(5-29) Comparison between experimental and numerical results for CO_2 with time at avarage measurement stands in (Case-III)

5.4 Numerical Results for Meeting Room (Case-IV and V)

A meeting room with eight occupants under Hilla City (Iraq) climate at maximum summer temperature (47°C) was simulated using the (CC/MVPV) system and compared with the chilled ceiling and mixing ventilation (CCMV) by using AIRPAK software. The (CFD) model was used to evaluate the mean air age, temperature distribution, carbon dioxide concentration and thermal efficiency using AIRPAK software. Four tests were conducted for four different cooling load conditions treated with a chilled ceiling (0, 25 , 50 , 80%) with a total cooling load of (33, 66.17 and 105.8) W/m^2 of floor area. The cooled ceiling surface temperature ranged between (0, 23 , 21.39, 19)°C and the air temperature with mixing ventilation (17,19, 21, 23) °C at a constant supply air flow rate (240 l/s) with a PV air flow rate (7.5 l/s), and the room air temperature (25°C). The cases are designed according to the recommendations of the EN 15251 standard for indoor climates of conditions,. The operating conditions and main results parameters of two systems are listed in Table (5-6).

Table (5-6) Main numerical results for meeting room (case-IV and V)

Case	η %	T_{av} (°C)	V_{av} (m/s)	RH_{av} (%)	ADPI (%)	PPD (%)	PMV	VATD (°C)	η_a (%)	ε_t
Case IV	0	23.45	0.155	61	51	18	0.72	0.71	63. 5	0.953
	25	23.4	0.158	60.3	60.12	15.35	0.62	0.6	60.6	0.92
	50	23.71	0.15	57.25	62.45	15.07	0.59	0.5	57.5	0.88
	80	24.19	0.141	59	68	12.93	0.47	0.42	55.8	0.84
Case V	0	22.8	0.17	65	56	15.4	0.5	0.6	77.45	0.978
	25	23.16	0.165	62	64.3	13.3	0.45	0.5	75. 7	0.943
	50	23.4	0.16	61.2	69.5	12.9	0.4	0.4	74.5	0.895
	80	23.75	0.149	57.3	75	10.05	0.31	0.31	69	0.864

5.4.1 Mean air age and air exchange efficiency results

Fig. (5-30) show lines of average age of air distribution in an non-isolated meeting room for two cases (z = 2.25m) passing through the air distributor and the meeting attendees sitting at the same desk and connected to the non-isolated north and south walls with different values of (η). The average age of air is found to decrease with height. The highest values for the average age of air in the occupied area appeared in the case (CC/MV), this means that the use of (PV) led to a significant decrease in the average age of air in the breathing area and the periphery of the room (0.22 to 0.26%) at (η= 0 to 80%) compared with (CC/MV) , which means that the air in the breathing area is regenerated faster than it is (when the (PV) system is not used) which results in greater thermal comfort for the individual compared to the case (CC/MV).

The chilled ceiling has an effect on temperature because the average age of the air increases as the cooling load fraction treated by the chilled ceiling increases. This result illustrates the effect of cold air moving downwards due to convection from the chilled ceiling and meeting with hot air, resulting in a lower air velocity. In fact, the increased turbulence increases the mixing effect resulting in an increased diffusion of pollutants from carbon dioxide generation sources into the overall climate.

The highest value of air age was recorded in all cases above the location of the air distributor and near the windowless wall (red zone), which means that the decrease in air movement in these two areas leads to an increase in pollutants and discomfort for the occupants, and also due to heat radiation and convection through the windows, the temperature rises The air near the wall heats up with the windows, causing the maximum air age to be in the upper area near the wall. The age of the air in this region decreases due to the resulting decrease in air velocity. For the two cases, the minimum value of air life near the diffuser (blue zone) is due to the supply of cool fresh air by the mixed ventilation diffusers.

In each case, the decrease in the air age around those seated in the meeting results from an increase in the air temperature resulting from convection with the human body, which leads to a decrease in air density and an increase in the speed of air movement, and this leads to a decrease in the air age.

Fig.(5-31) presents the mean vertical air age of air profiles in separation with height for the two scenarios with different values (η). This number varies depending on the typical average age of air in different horizontal planes at different altitudes. With height, the average air age of a seated and standing person decreases. When (η) increases, the average air age in both cases increases with each value of (η). This is due to a decrease in air velocity due to the combination of warm air and a decrease in cooler air once it comes into contact with the surface of the cooled roof. Convection causes the air temperature to drop. In fact, the increased turbulence increases the mixing effect leading to an increased diffusion of pollutants from (CO_2) generating sources into the overall climate.

Fig.(5-32) illustrates the relationship between the air exchange efficiencies and (η) for two cases. Regardless of the case, the air exchange efficiency decreases with increasing (η) because the travel time of air particles from the air input to the air exit increases with increase (η) for the two cases because the chilled ceiling's cold air slows the air's velocity. The effectiveness of air exchange depends on the mean air age value, The air exchange efficiency increases with decreasing average air age from (0.22 to 0.24%) at (η = 0 to 80%) compared with (CC/MV). Therefore, the highest value of (ηa) in (CC/MVPV) at an air flow rate of (7.5 L/s) is (77.45 to 69%) in (η = 0 to 80%). As a result, the flow rate (7.5 L/sec) is the largest option for protecting the occupant from direct contamination in the (BZ) and in the surrounding microclimate as shown in Table (5-6).

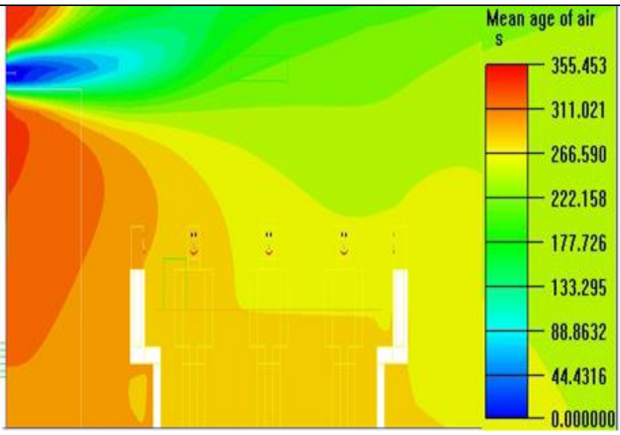

Case- IV

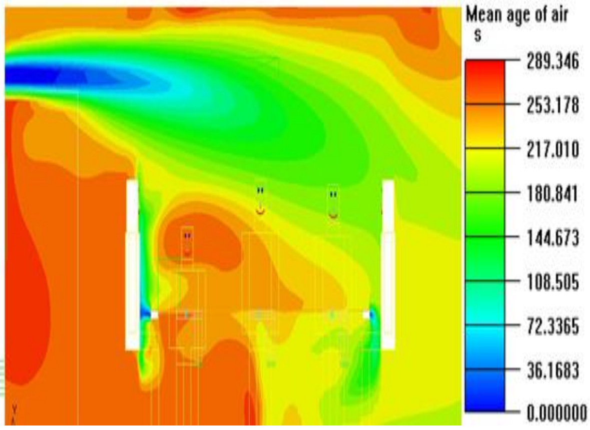

Case- V

a-η=0%

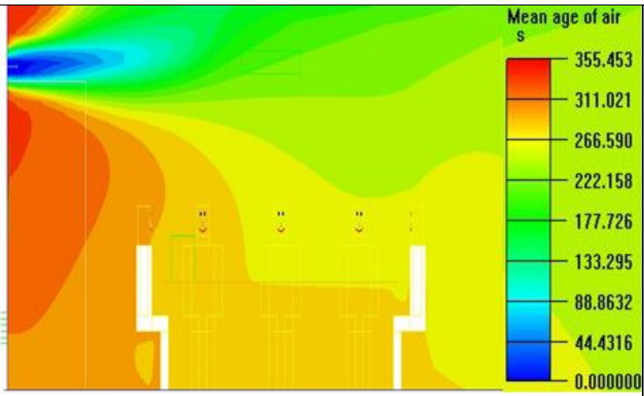

Case- IV

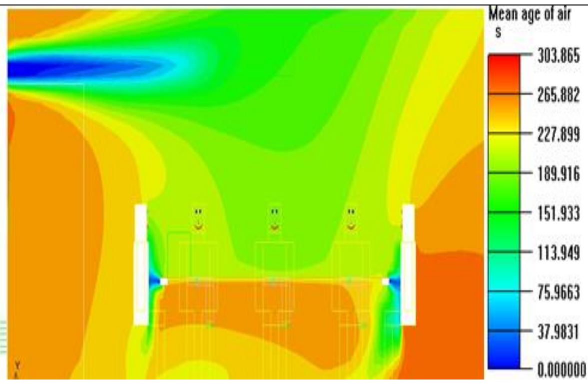

Case- V

b- η=25%

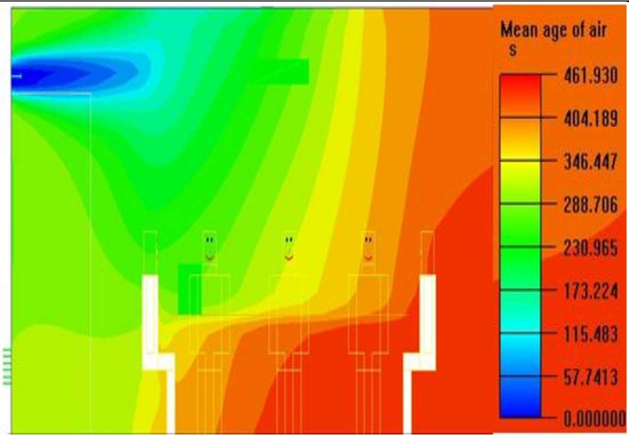

Case- IV

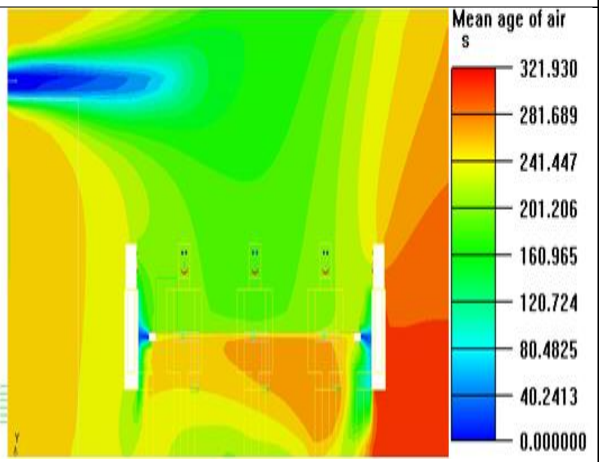

Case- V

c- η=50%

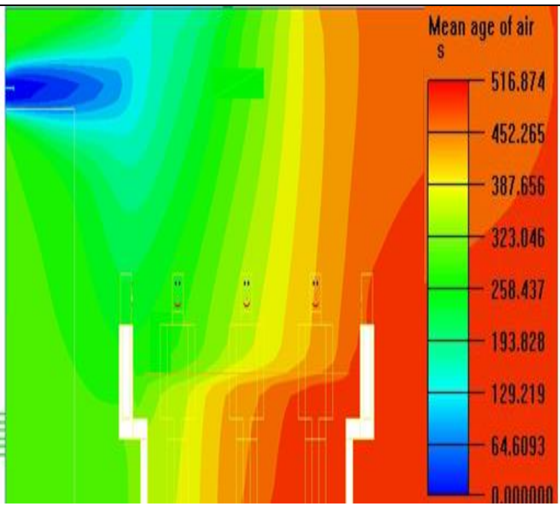

Case- IV

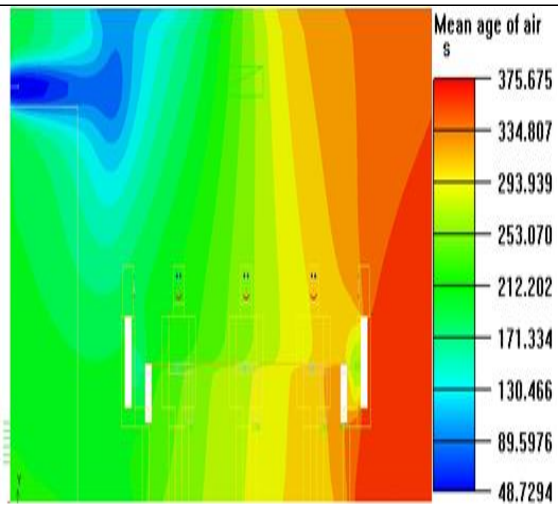

Case- V

d- η=80%

Fig(5-30) The air age contours at different (η) for two cases at plane (z=2.25m)

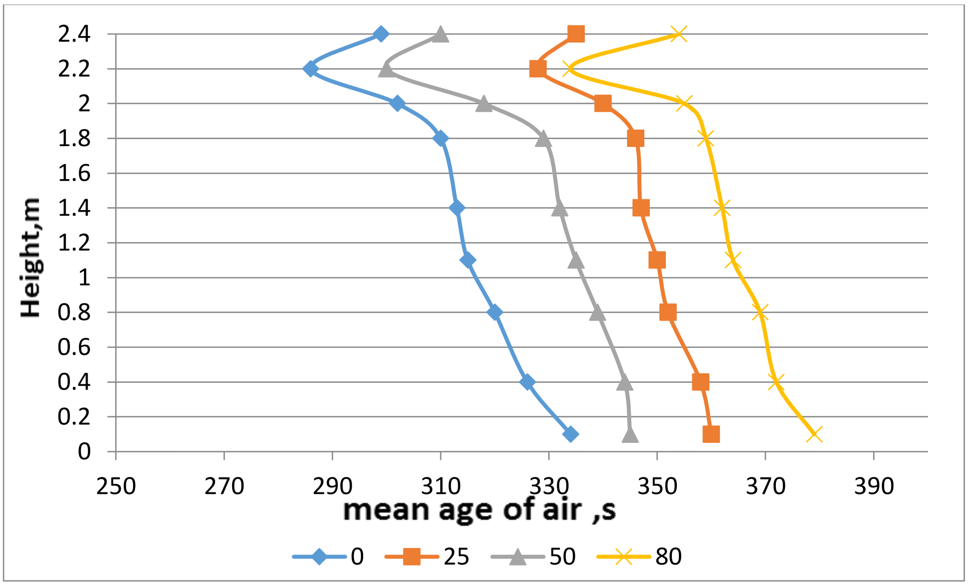

a- Case-IV

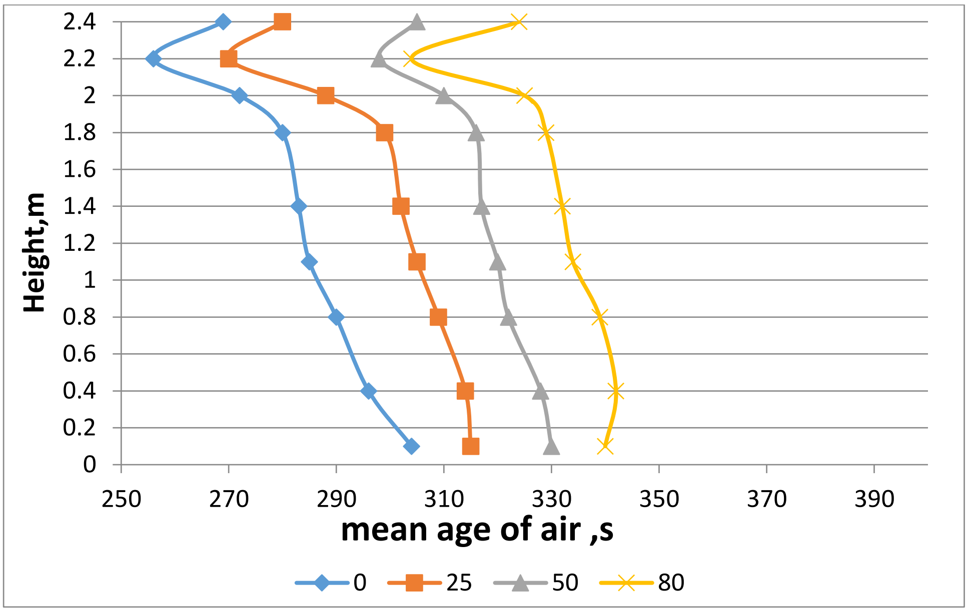

b- Case-V

Fig.(5-31) Mean age of air with heights (1.1m) for different values of (η) for two cases (case-IV and V).

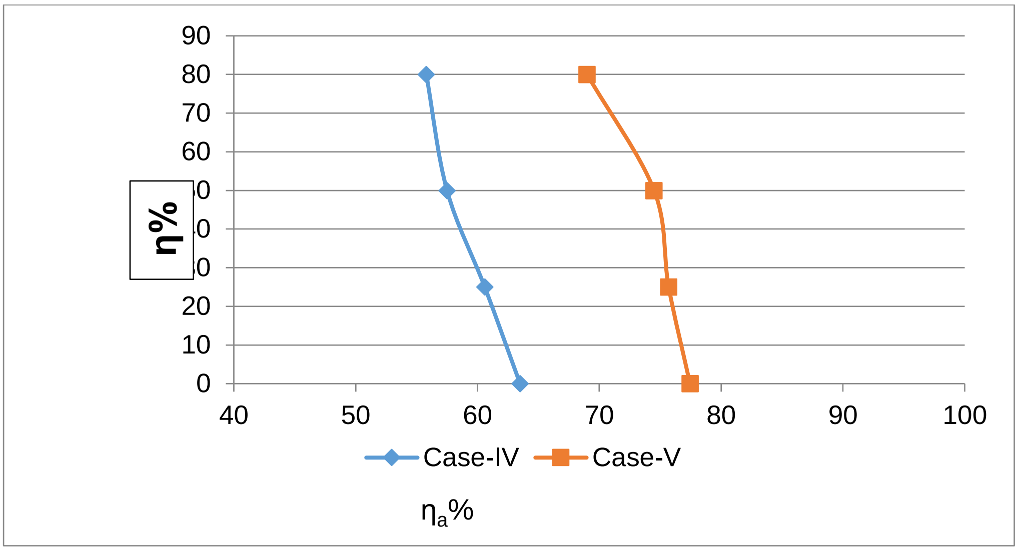

Fig.(5-32) Air exchange efficiency (η_a) profiles at (1.1m) levels for different values of (η) under two cases

5.4.2 Distribution of air temperature and velocity

Fig.(5-33) depicts the contours of the distribution of air temperature with different at (z = 2.25) m for two cases in the meeting room. Notes that the effect of the cold air supply coming from the diffuser positioned in the upper section of the room wall causes the temperature to drop with the height of the office room in all cases. The temperature differential between the head and the foot is less than (2 °C), which is within the ASHRAE standards' permissible range.

When there is an increase in the rate of airflow , the average room temperature decrease in the breathing zone and an increase in the speed of the air within a breathing zone resulted in a decrease in room temperatures in general as shown in Fig.(5-33). Because the air diffuser is situated towards the ceiling, the ceiling temperature is cooler than the room's floor temperature.

Fig.(5-35) presents the value of the temperature difference between the head and the foot for a seated and standing person decreases with the increase in the amount of cooling load treated by the chilled ceiling. Where the highest values of (VADT) appeared for a seated person with a system with (CC/MV) between (0.72 to 0.47)ºC at (η= 0 to 80%), the use of PV reduced the differences between head to foot of a seated compared to the (CC/MV) case by (0.44 to 0.56) at (η= 0 to 80%) . It is noted that when using the (PV) system, the air temperature near the head drops at (1.1m) due to the photovoltaic fresh air supply rate which provides more cooling. So the breathing zone in (CC/MVPV) is characterized by a decrease in temperature with a good rise in the permissible air velocity within the recommended thermal comfort limits. The temperature difference between the head to feet of the seated person decreases by

(0.26 to 0.73)°C at (η= 0 to 80%) with (CC/MVPV) between for the two cases. This means that the temperature difference between the head to feet level is the lowest in the third case study when compared to the rest of the cases due to the ability of the (CC/MVPV) system to deliver cold air faster to the human body.

Air temperature distribution profiles with different (η) at (z = 2.25) in the test chamber are shown in Fig.(5-33). For two cases, it is observed that the temperature increases with height, and with an increase (η), and the average room temperature increases with the increase in the temperature of the feed air due to the decrease in the cooling capacity of the air, it is noted that the temperature begins to rise when it passes through heat sources and moves up .As a result of the buoyancy effects, in general, the decrease in temperature returns with the height of the office room due to the cold air currents coming from the personal ventilators (ATD) as well as the air supply distributor (MV device) mounted on top of the room wall.

The lowest temperature inside the room is observed at a level (2.2 m) near to supply diffuser. Fig.(5-36) show the effectiveness of air temperature distribution for the two cases at various (η). In cases IV and V, the heat removal index values ranged between (0.953-0.84) and (0.978-0.86) at(η = 0 to 80%) . The use of PV air flow rates improved the heat removal index in (CC/MVPV) by (3 to 2.3)% at (η = 0 to 80%) compared to (CC/MV).

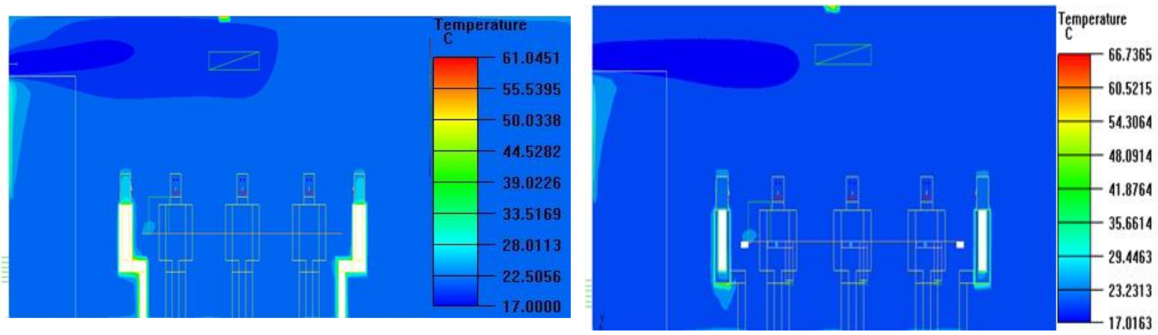

Case-IV Case-V

a- η=0 %

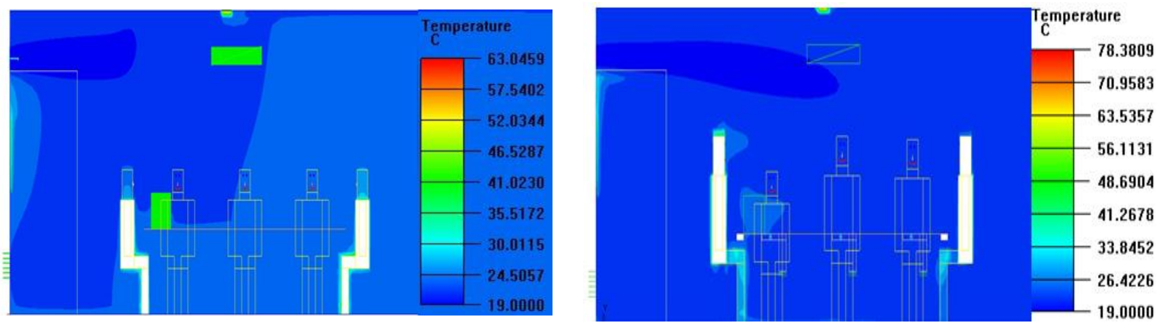

Case-IV Case-V

b- η=25%

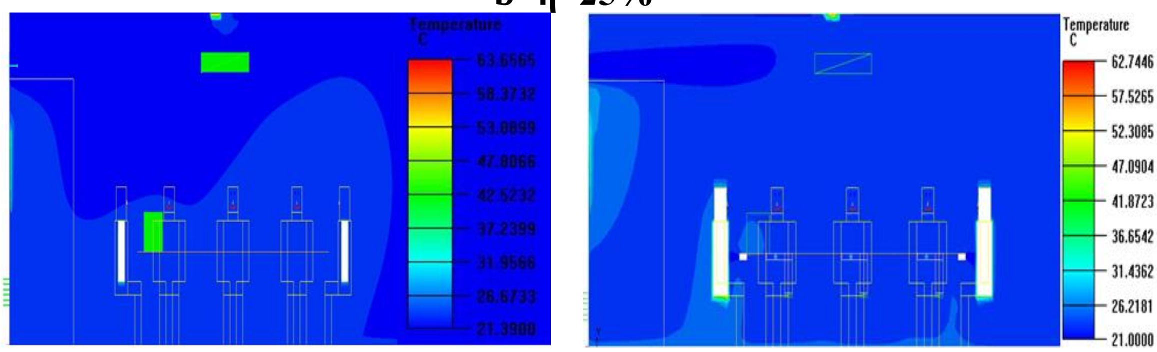

Case-IV Case-V

c- η=50%

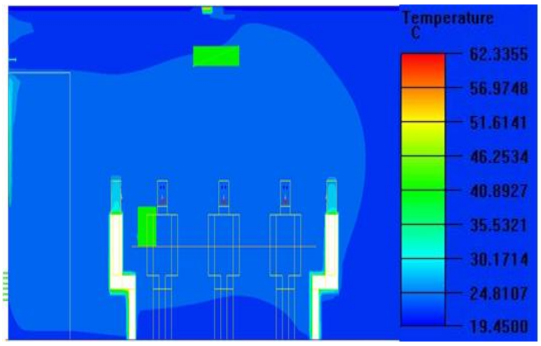

Case-IV

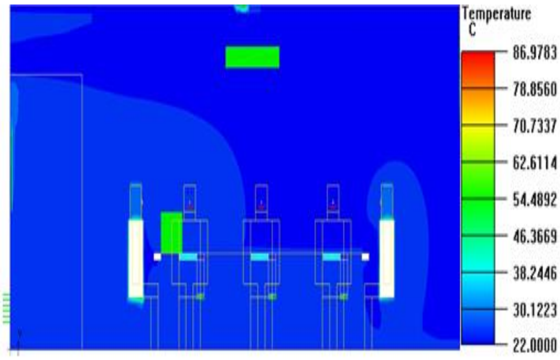

Case-V

d- η=80%

Fig.(5-33) The contours of distribution of air temperature at different (η) for two cases at (z=1.25m)

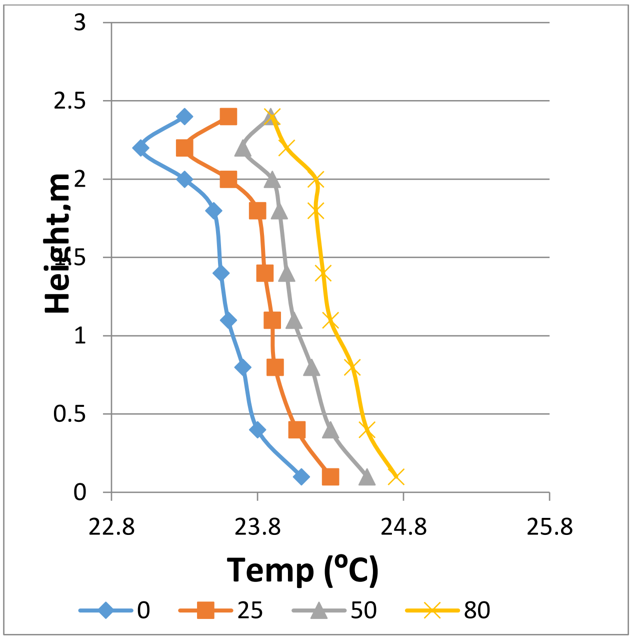

a- Case-IV

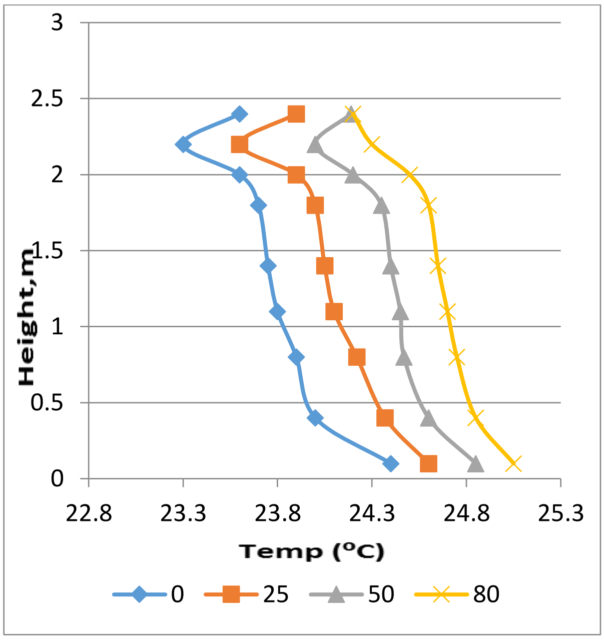

b- Case-V

Fig.(5- 34) Distribution of air temperature with height at various value of (η) for two cases(IV and V)

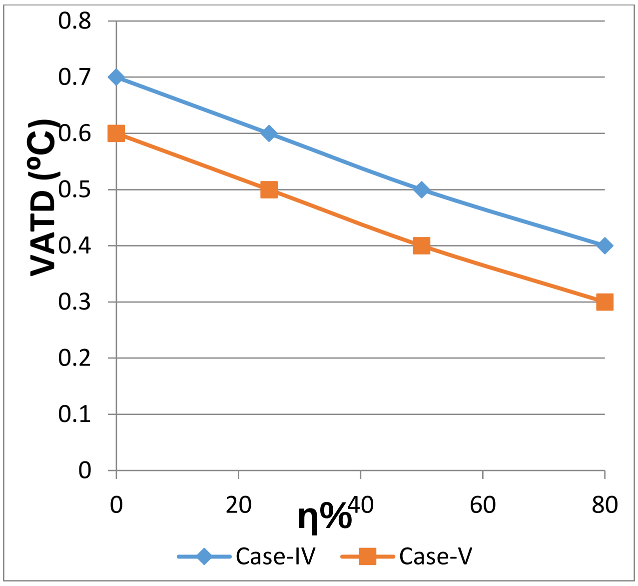

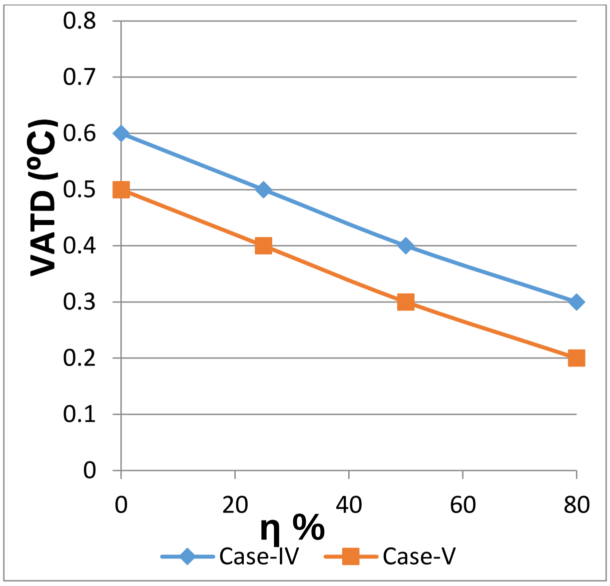

a- sitting person b- standing person

Fig.(5-35) Vertical air temperature difference profiles for sitting and standing person

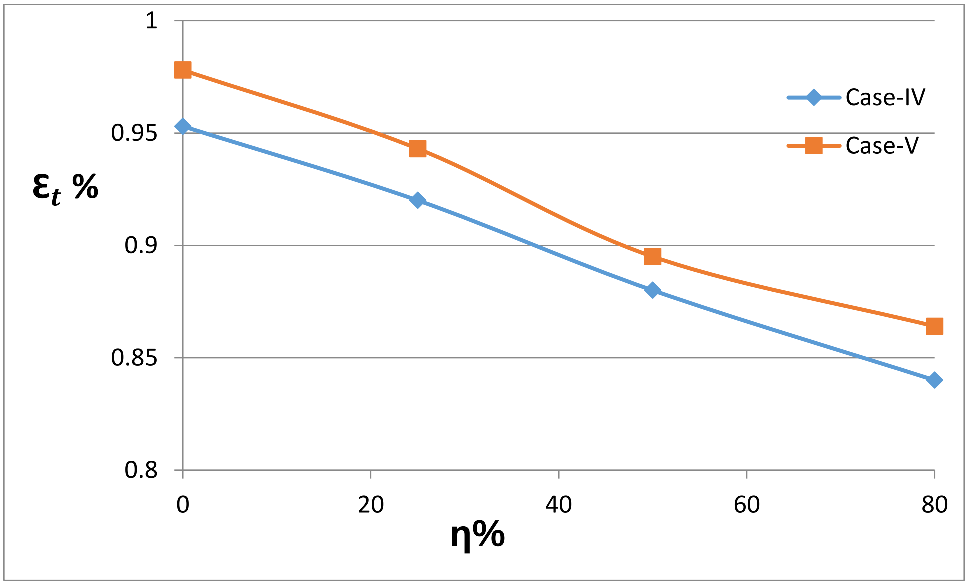

Fig.(5-36) Heat removal effectiveness profiles with (η) for two case studies

Figs.(5–37) show the air velocity distribution vector for the two cases on the plane (z = 2.25 m). The maximum air velocity of the supply diffuser, which is (2.5 m/s) in each case, After that, the velocity decreases until it reaches zero in the majority of the interior. The buoyancy force affects the cooled air near the air diffuser, but this effect decreases as the temperature of the air source increases. The heat from the heat sources is then replaced by cool, fresh air as it begins to exit the room through the exhaust grille. Due to air hitting the body surface wall and backflow, air circulation is restricted in the counterclockwise region between (ATD) and people. an increase in air temperature caused by heat transfer between sources.

The movement of air molecules can be divided into two categories: translational movement caused by the buoyant force caused by the temperature difference between the surrounding air and heat sources, and rotational movement caused by momentum and high-speed air entry from the diffuser. The diffuser, placed slightly below the ceiling of the room, allows air to flow parallel to the floor of the space, as shown in Fig.(5-37). Eventually, the air goes into the exhaust grille and is expelled from it.

Fig.(5-38) show the change in the mean distribution of air velocity with height for different values of for two cases (cases IV and V), respectively. The air velocity near the air supply diffuser (greater than 2 m) decreases with increase (η) due to increase in the temperature of the air source rises .The air velocity usually increases with height, and it is at a level of more than (1 m) due to the effect of heat sources on the rise in air temperature. After that, the heat from the heat sources is replaced by cool, fresh air when it passes through personal ventilation, and then the hot air begins to exit from the room through the exhaust grille. Due to the collision of air against the surface wall of the body and its reverse flow, air circulation is restricted in the counterclockwise area between the ATD and the person. The maximum value of air velocity is close to the air supply diffuser in two cases (cases IV and V), respectively equal to (0.84 and 0.54 m/s) at (η = 0%), and it continues to rise, reaching its peak near the ceiling at (η = 80%). This is due to the zone's strong convectional heat transfer rates between the air and the chilled ceiling, as well as the impacts of the exhaust grille's ceiling-mounted location.

The air velocity increases in the area near and above the heat sources as a result of the convective heat transfer that occurs between the supply of cooled air and the heat sources (more than 1.1 m). The cooled air near the ceiling, created by convection between the heated air and the cooled roof, causes a decrease in air velocity over the occupant, leading to an increase in the mean age of the air with an increase of ceiling, created by convection between the heated air and the cooled roof, causes a decrease in air velocity over the occupant, leading to an increase in the mean age of the air with an increase of (η).

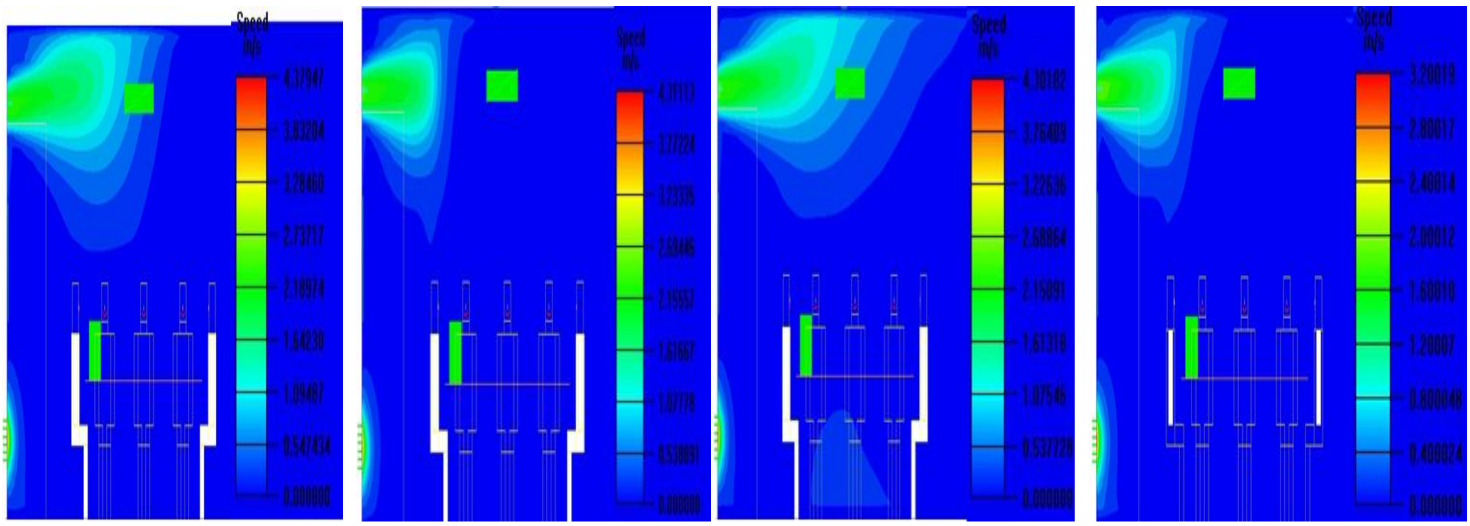

η=0 % **η=25 %** **η=50 %** **η=80 %**

a- Case-IV

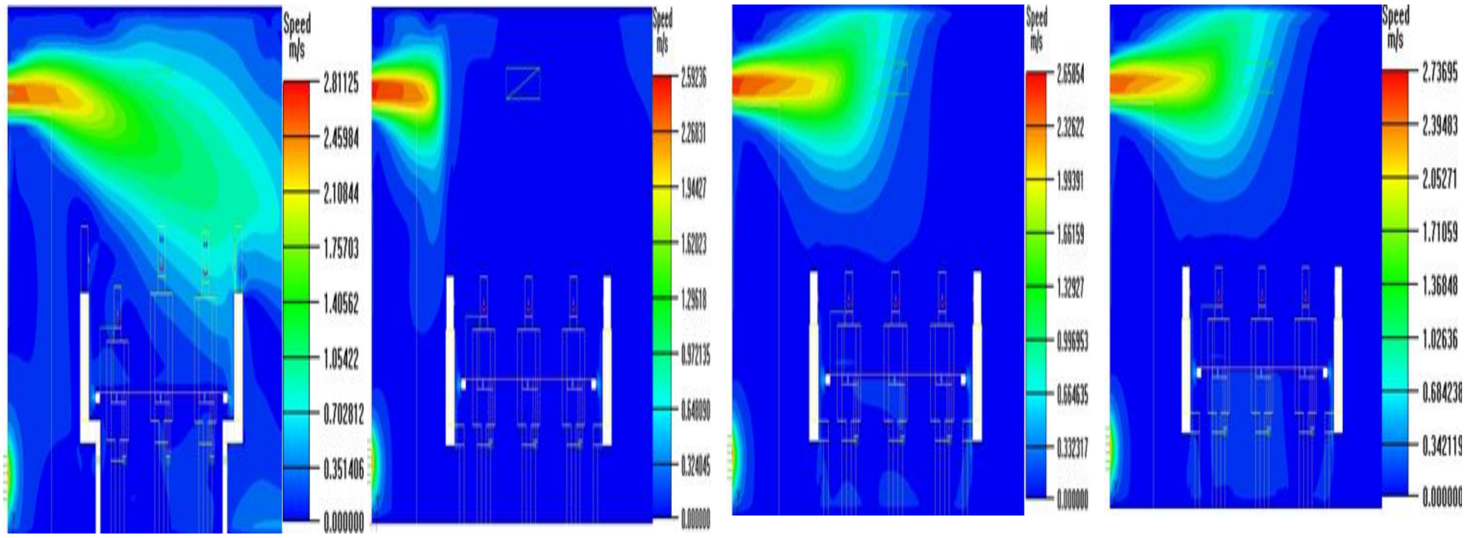

η=0 % **η=25 %** **η=50 %** **η=80 %**

b- Case-V

Fig(5-37) The contours of velocity vector at different (η) for two cases at (z=2.25m).

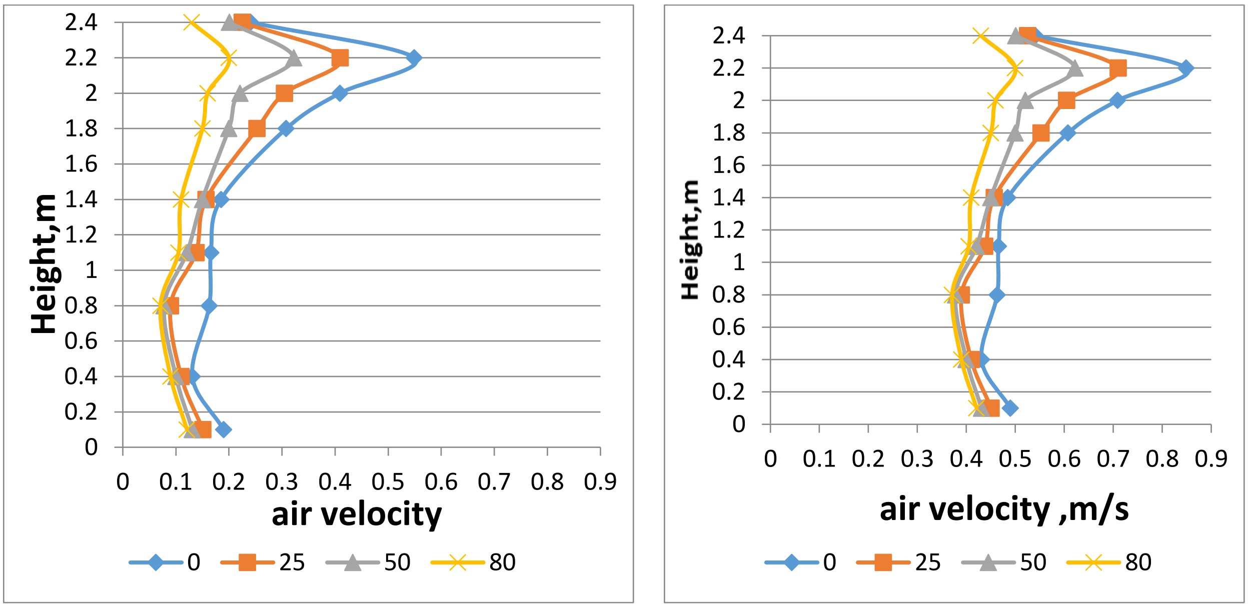

a- case-IV b- case-V

Fig.(5-38) Air velocity distribution with heights for different values of (η) for two cases (case-IV and V).

5.4.3 Thermal comfort and air quality results

In this part, three variables (PPD, PMV, and ADPI) are examined to give a good idea of the thermal comfort indicators in the occupied meeting room. The results of these factors were evaluated using the ASHRAE Standard (2013).

Figs.(5-40) and (5-41) show thermal comfort indices (PMV and PPD) with different values (η) for two cases. As the value of increases, the PMV and PPD values for the two cases decrease and improve, getting closer to the values specified for the ASHRAE 2013 standard (-0.5, PMV 0.5, and PPD 10%). The (CC/MVPV) with (CC/MV) decreases from (0.72 to 0.5),(0.47 to 0.31) at (0 to 80%), respectively, and the (PPD) decreases from (18 to 15.4%),(12.93 to 10.05) when the value of (η) increases from (0 to 80%), respectively. The values of (PMV and PPD) decrease with (CC/MVPV) (case-V) from (0.44 to 0.52%),(0.17 to 0.3)respectively at (η = 0-80%) compared with(CC/MV) (case-IV).This is because decreasing the temperature of the chilled ceiling surface leads to lower air temperatures in the overhead area, which improves heat transfer by heat sources by convection (PMV and PPD). due to increased heat loss from the body as a result of a decrease in the surface temperature of the radiator, which enhances radiative heat transfer between heat sources and the ceiling wall.

These results indicate that the increase (η) led to an improvement in the level of thermal comfort, but also show that these values exceed the parameters set by the AHREA criterion (-0.5 PMV 0.5 and PPD 10%). As the mean radian temperature (MRT) is higher as presented in the table, it approximates somewhat warmer weather as shown in Fig. (5-41). The values of (PMV and PPD) with the (CC/MVPV) system are lower than those with the (CC/MV) system, which means that the introduction of cool (PV) air at warmer temperatures led to heat attenuation and improved thermal comfort than in (Case IV).

to demonstrate how a cooled ceiling affects comfort in a climate like Hilla (Iraq).The level of distribution lines (PMV) of those sitting in the meeting is shown at the level of the breathing area (at a height of 1.1 m) for the two cases. The value of PMV rises near the windows for each case with different values (η) and ranges between (1.25 and 2.6) . This is because the hot summer weather in Hilla (Iraq) causes heat to be transmitted through conduction and radiation through the windows, and as a result, people sitting near the windows will feel uncomfortable. The occupied space was between (0.5 and 1.5m) away from a windowed wall. Thus, the range specified by the ASHRAE standard for cooled ceilings was not affected. The PMV value in the other parts far from the windows ranges between (0.28 and 1.22) in both cases, indicating that the climate is between normal and slightly warm at this level, and decreases with increasing value of (η).

Fig. (5-42) shows the relationship between (ADPI) with different values of (η) for the two cases (IV and V). According to the same logic used in the office room, it is noted in the two cases that as the value of (η) increases, the values of (ADPI) increase, and this means that when convection is removed in chilled ceilings, resulting in better thermal comfort. The (ADPI) values increase with the (CC/MVPV) system by (9.8 to 10.29) at (η = 0-80%) compared to the (CCMV) system, so that PV is used in the (CCMV/PV) system for air flow rate (7.5 l/s). It led to a higher (IAQ) in (BZ) due to the continuous cleaning and dilution of pollutants. According to this study, combining PV with CC can produce a consistent thermal climate and acceptable air quality in the inhabited space, and this combination may be more efficient than traditional CC and MV.

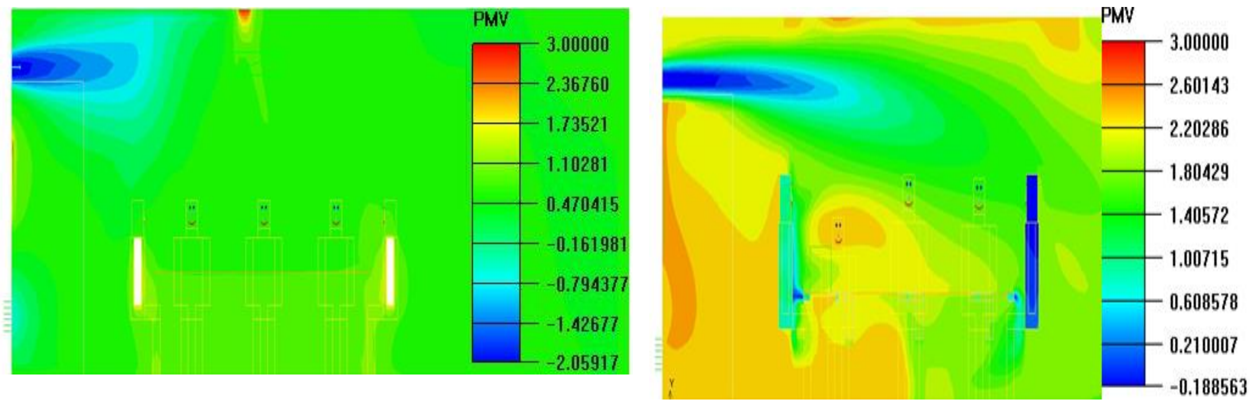

Case-IV Case-V

a- η= 0%

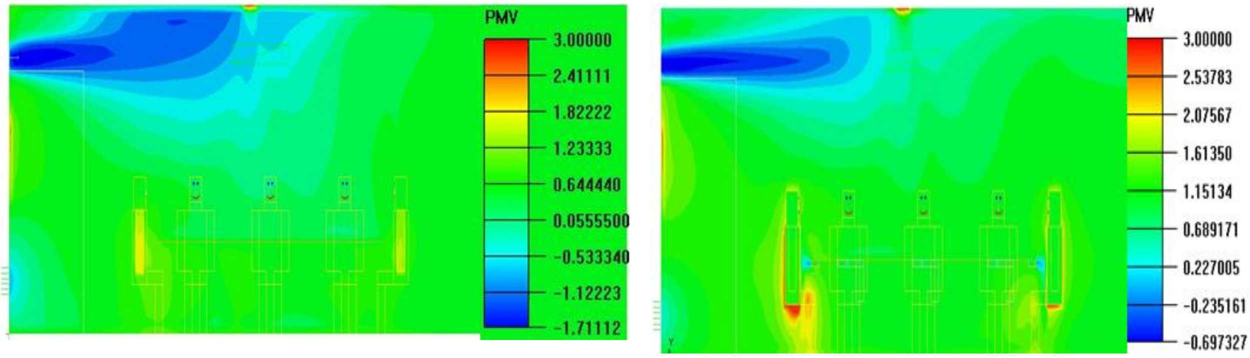

Case-IV Case-V

b- η= 25%

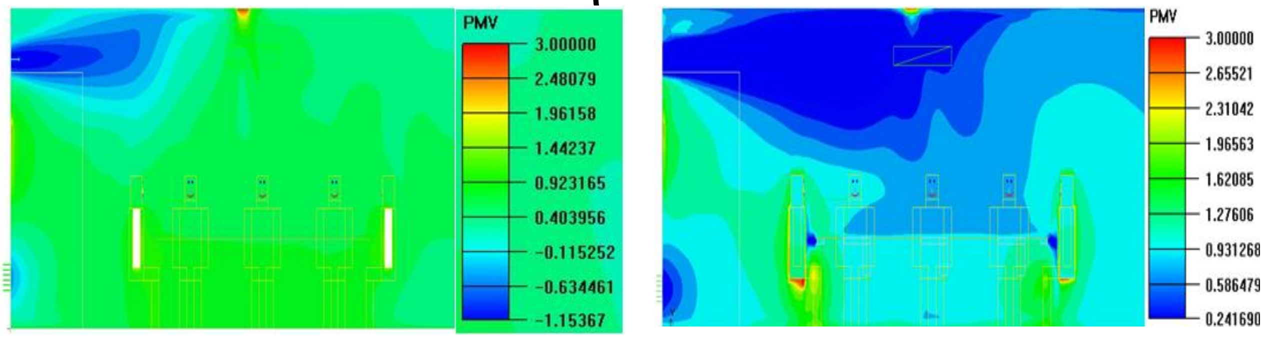

Case-IV Case-V

c- η= 50%

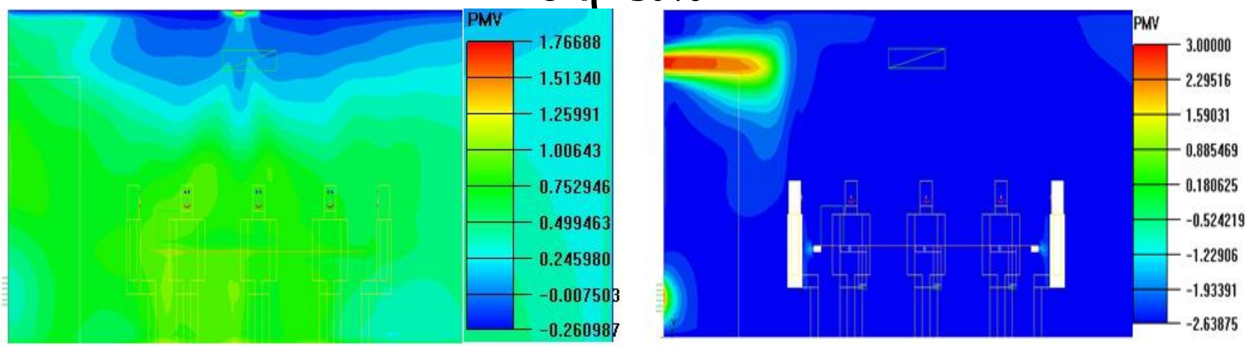

Case-IV Case-V

d- η= 80%

Fig.(5-39) PMV contours at plane (z=2.25m) with different (η) for the two cases

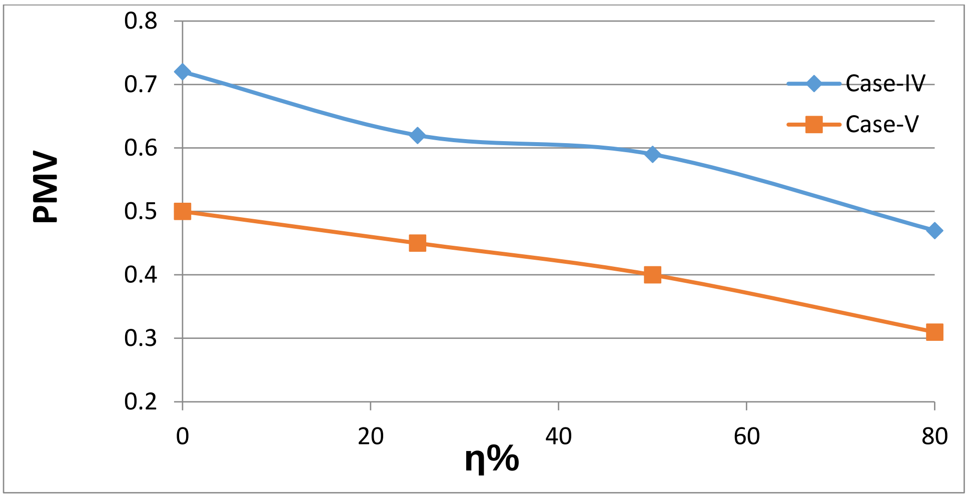

Fig.(5-40) Illustration of the (PMV) at varies (η) for two cases

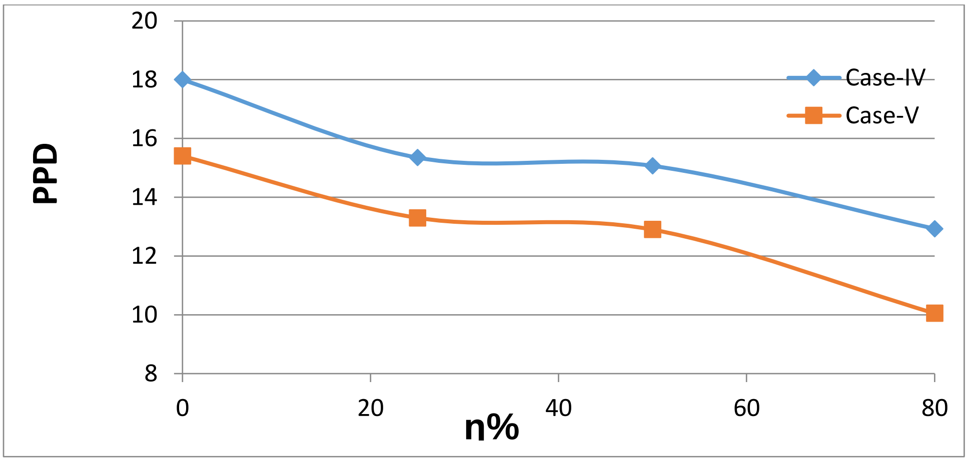

Fig.(5-41) Illustration of the (PPD) at varies (η) for two cases

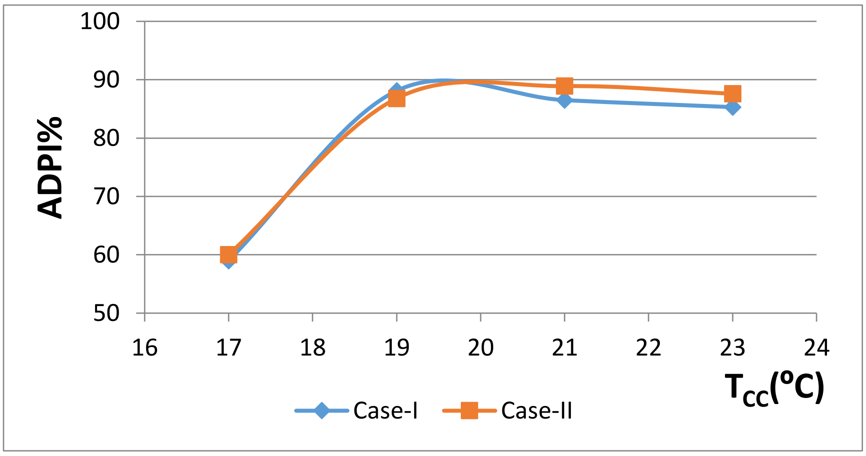

Fig.(5-42) (ADPI) profile with temperature of chilled ceiling (T_{CC}) for two cases

Fig. (5-43) show the decomposition of (CO_2) over time for states IV (CC/MV) and V (CC/MVPV) with different (η), from the initial concentration (1000 ppm) to the air supply concentration (400 ppm).`In both cases, the carbon dioxide content gradually decreases until it reaches the level of air supply. The results indicate that (CO_2) removal is affected very little by the increased load handled by a cooled roof at a constant air supply flow. Due to the higher cooling load, the higher flow of fresh air supply (460 l/s) quickly causes old air to be replaced with cool fresh air and exits the room through the exhaust grille more quickly and reduces the cooling effect of the roof.

When comparing the performance of the two systems, the (CO_2) concentration takes about (60 to 76) s at (η= 0 to 80%) with (CC/MV)system , while with (CC/MVPV) takes about (30 to 38.9) s at (η= 0 to 80%), for the two cases to reach the desired (CO_2) concentration (400 ppm). Also it is noted that the (CC/MVPV) system removes (CO_2) from the air approximately (32 s) faster when supplied with a constant air flow rate.

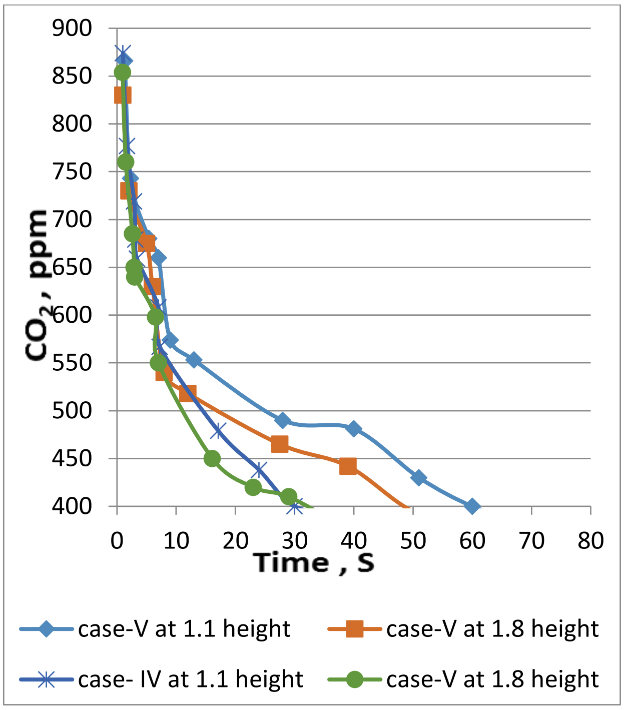

a- η=0%

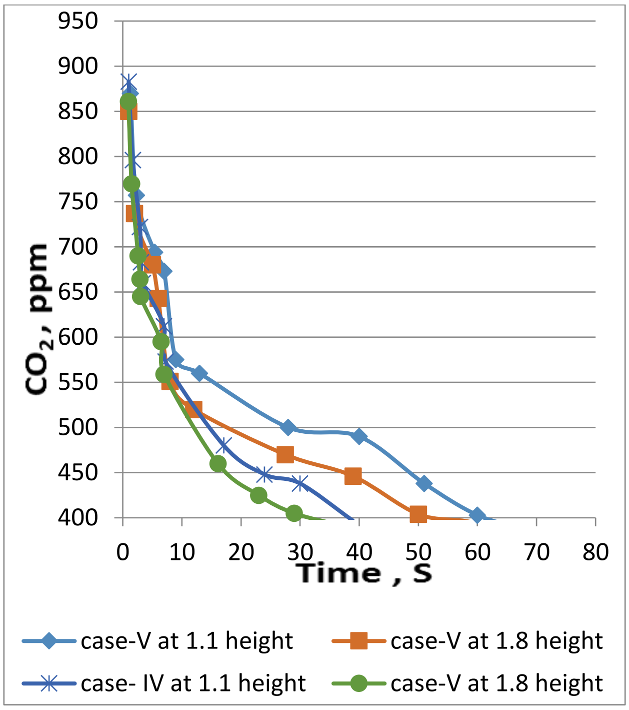

b- η= 25%

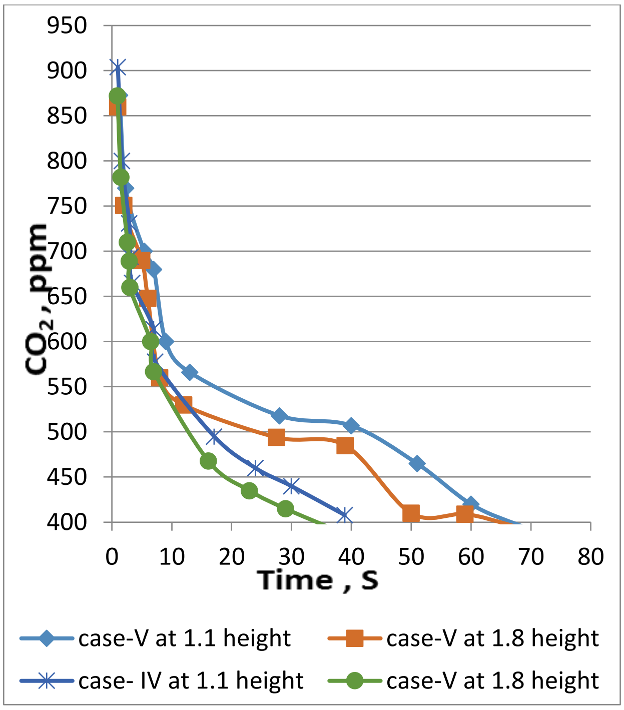

c- η= 50%

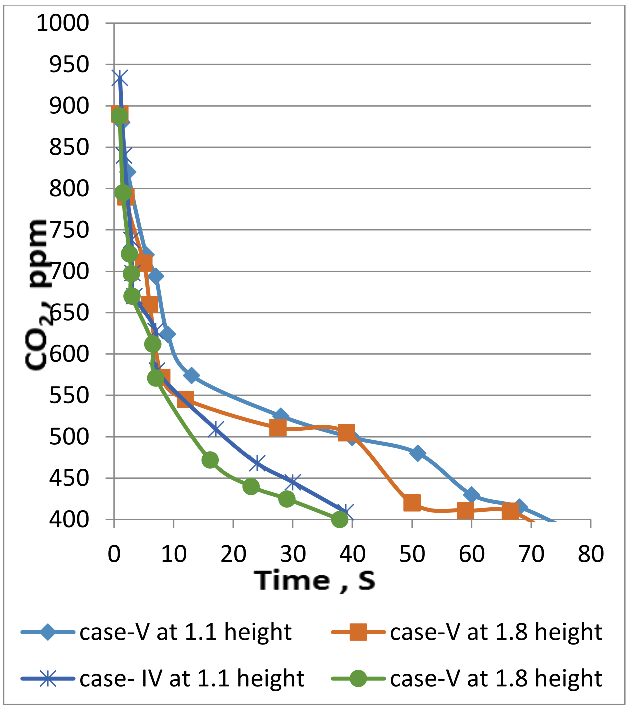

d-η= 80%

Fig.(5-43) Time required to remove carbon dioxide at breathing levels for sitting and standing person (1.1m and 1.8m) for the two cases at different (η)

5.4.5 Occupied density and occupant air exchange efficiency

In all case studies, the longer people stay in the room, the less efficient the air change is for the occupants, which means if the residents stay longer or there are more of them, the effect is greater, as shown in Figs.(5–9). The efficiency of air exchange for inhabitants is always higher than the efficiency of air exchange, which results in a replacement of the air in the well of the inhabited space with fresh air, improving the quality of the air. Compared to standard air exchange efficiency, which considers the impact of air flow at various locations in order to estimate the room's thermal comfort level, occupant air exchange efficiency more accurately describes the air conditions in a space (case-V). The overall ventilation effect can be analyzed more comprehensively by using the passenger air exchange efficiency. Therefore, the efficiency of air exchange for occupants increases in cases (case-V) from (22.25 to 25.11 %) and from (30.2 to 39.16 %) at (η) compared with (CC/MV), so that this means that (PV) improves the efficiency of air exchange and determines the level of comfort inside the room as a result of its unique characteristics.

Fig.(5–10) shows the relationship of air exchange efficiency for occupants (η_D) with different load values (η) for the three case studies, where it was found that the temperature of the cooled ceilings increases with the increase in the cooling load treated by the cooled ceilings, and this leads to an increase in the age of the air and then a decrease in the efficiency of air exchange.

The air exchange efficiency for occupants (η_D) in the (PV) system was higher than the (CC/MV) system by (0.22 to 21.4%) and (32 to 38.7%) at (η = 0 to 80%) compared to the (CC/MV) system as a result of reducing the mean air age up to 30 to 38% at breathing level for a seated person. As shown in Figs.(5-10), the air exchange efficiency (η_a,η_D) increases with decreasing average air age in (CC/MVPV) by (81 to

67.5%), (99 to 90.25%) at (η = 0 to 80%). Therefore, a flow rate of (7.5 l/s) is the optimum choice for shielding residents from direct pollution in the BZ and in the local microclimate.

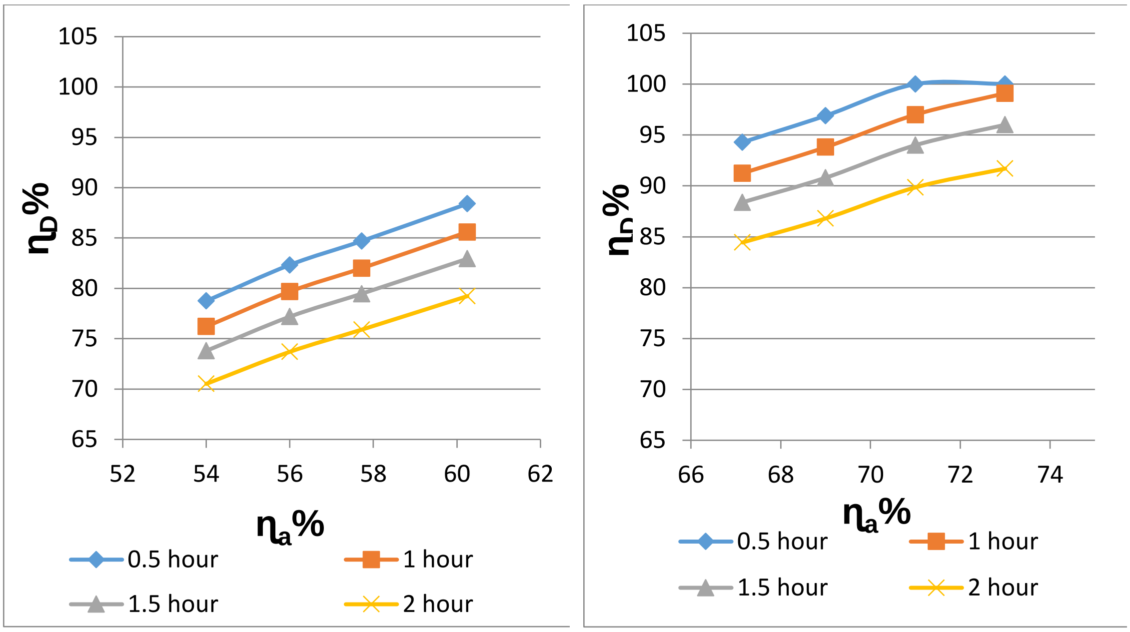

a- case-IV **b- case-V**

Fig.(5-19) Relationship between of air exchange efficiency and occupant air exchange at three times in two cases (case-IV and V)

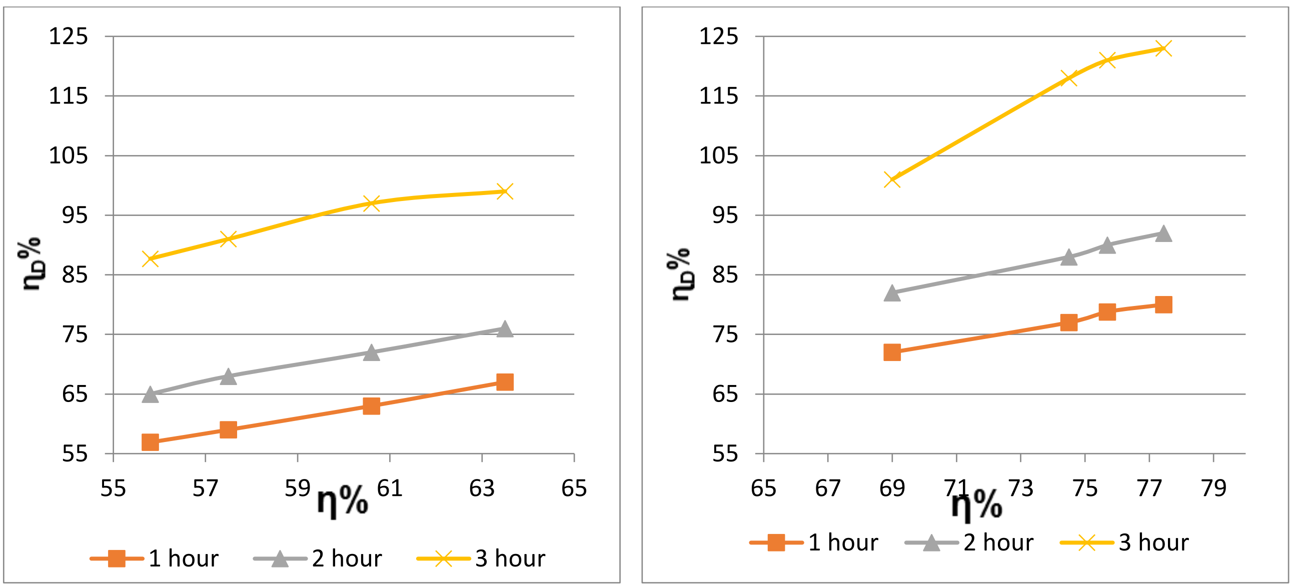

a- case-IV **b- case-V**

Fig.(5-20) Relationship between of different values of (η) and occupant air exchange at three time in two cases(case-IV and V)

CHAPTER SIX

CONCLUSIONS

&

SUGGESTIONS FOR FUTURE WORKS

Chapter Six

Conclusions and Suggestions for Future Works

6-1 General conclusions

1. For all cases, the average air age increases with altitude regardless of the increase in the cooling load treated by chilled ceiling (η).

2. The local air age increases with the increase in the cooling load treated with the cooled ceiling. The highest values of the average air life were in the case of (CCMV) compared to the case of (CCMV), and the lowest value of the air life was near the heat sources due to the high velocity of the air in this region.

3. When the air flow rate is increased, the average life of the air decreases as the part of the cooled ceiling treated cooling load increases.

4. The air exchange efficiency increases with the decrease in the average air life and the increase in the photovoltaic air flow rate of the (CCMV/PV) system at a rate of (7.5) l/sec.

5. The temperature difference between the head to feet of a seated or standing person is directly proportional to the temperature of the cooled ceiling and inversely proportional to the increase in the part of the cooling load treated by the chilled ceiling

6. The efficiency of the air temperature distribution decreases with the decrease in the temperature of the cooled ceiling and the increase in the cooling load fraction processed by the cooled ceiling, and the heat removal indicators using (PV) were higher than those of (CC/ MV).

7. The results of three case studies show that occupant air exchange efficiency is the best way to assess the effect of room ventilation.

8. This study shows that the proposed (CCMV/PV system) provides thermal comfort and higher air quality in the occupied area

6.1.1 Conclusion for the insulated office room

1. In all cases it was seen that the values of (PMV and PPD) decreased from (0.25 to 0.30),(0.33 to 0.36) respectively with the (CC/MVPV) compared to the (CC/MV) system at$(\eta = 0 \text{ to } 80\%)$, which means that use PV lead to improve thermal comfort than in (CC/MV). The values of (PMV and PPD) decrease with the increase of the air flow rate from $(0.2 - 0.34\%), (0.19 - 0.24\%)$respectively at $(\eta = 0 \text{ to } 80\%)$ in two cases (CC/MVPV-1 and(CC/MVPV-2) .
2. As a result of the use of (PV), the percentage of air age drops below a value of (0.34) %. With the lowest (PV) air flow rate of (5 l/s) (as in CC/MVPV-2) compared with (CC/MV), the probability of mean age of air was reduced by 25% . A value of (14%) improvement in occupant protection from cross infection was observed with higher (PV) airflow rates .
3. The heat removal effectiveness increased by (4-5.12%) at (η = 0-80%) in the (CC/MVPV) compared with (CC/MV). The higher (PV) air flow rates led to an improvement in the heat removal index in (CC/MVPV-2) by (319-3.6%)at (η = 0-80%) than in the (CC/MVPV-1) system.
4. The vertical air temperature difference (VATD) for the seated and standing person was between (0.8-0.3) and (0.7-0.4) at (η = 0-80%). The highest values for a seated and standing person were seen between (0.8-0.52) °C for a person standing with (CC/MV) system . The temperature difference between the head to feet of the seated person decreases by (0.63-0.3)°C with (CC/MVPV-2) between (0-80%) for the three case studies.

5. In all cases with (PV), the air exchange efficiency (η_a) was higher than that of (CC/MV) by (0.24 to 0.3%) at (η=0 to 80%). Through the use of (PV), the mean age of the air was reduced by up to (0.23 to 0.3),(0.22 to 0.29) at (η=0 to 80%) when compared with (CC/MV) at the sitting and standing person's breathing level. So the highest value (η_a) in (CC/MVPV) system by (75 to 72%) at (η =0 to 80%) at air flow rate (7.5 l/s).
6. In all cases with (PV), the air exchange efficiency for occupants (η_D) was higher than CC/MV system by (22.25 to 25.11%), (30.2 to 39.16) at (η = 0 to 80%) compared with the (CC / MV) system as a result of reducing the mean air age up to (0.23 to 0.3),(0.22 to 0.29) at (η = 0 to 80%) compared to (CC/MV) at a seated and standing person breathing level.
7. The highest value air exchange efficiency (η_a , η_D) in (CC / MVPV-2) by (75 to 72%),(99.5 to 93%) at (η = 0 to 80%) at the air flow rate (7.5 l / s) .

6.1.2 Conclusion for non- insulated meeting room

1. The values of (PMV and PPD) decrease with (CC/MVPV) (case-V) from (0.44 to 0.52%),(0.17 to 0.3)respectively at (η = 0 to 80%) compared with(CC/MV) (case-IV).
2. The use of (PV) airflow rates lead to decrease in the local air age by (22 to 26%) at (η = 0-80%) compared with (CC/MV) system .
3. The mean local air age is decreased by (8 to 14%),(8.6-16) at (η = 0-80%) with (PV) air flow rate compared with (CC/MV).
4. The heat removal effectiveness increased by (4-5.12%) at (η = 0-80%) in the (CC/MVPV) compared with (CC/MV). The higher (PV) air flow rates led to an improvement in the heat removal index in (CC/MVPV) by (3-3.6%)at (η = 0-80%) than in the (CC/MVPV).

5. The vertical air temperature difference (VATD) for the seated person was between (0.8-0.3) and (0.7-0.4) at (η = 0-80%). The highest values for a seated person were seen between (0.8-0.52) °C for a person seated with CCMV. The temperature difference between the head to feet of the seated person decreases by (0.63-0.3)°C with (CC/MVPV-2) between (0-80%) for the three case studies.
6. The air exchange efficiency (η_a) of (CC/MVPV) was higher than (CC/MV) by (0.22 to 0.24 %) at (η=0 to 80%). Compared with (CC/MV), PV in the thermal dwarf produced higher air quality indices .
7. In all cases with (PV), the air exchange efficiency for occupants (η_D) was higher than CC/MV system by (22 to 24%), (28 to 35) at (η = 0 to 80%) compared with the (CC / MV) system as a result of reducing the mean air age up to (0.2 to 0.28),(0.2 to 0.25) at (η = 0 to 80%) compared to (CC/MV) at a seated and standing person breathing level.

6.2 Suggestions for Future Works

To advance the current study , Future studies are advised as the following:

1. Studying thermal comfort conditions, indoor air quality, and ventilation efficiency in large spaces such as schools, universities, cinemas, theaters, and commercial centers under hot and dry climates.

2. An experimental study examining thermal comfort conditions under different shapes and types of personal peripheral ventilation devices (PV ATDs) at different occupant distances.

3. Examine the performance of the personal ventilation system in relation to shifts from the design site of the occupant because individuals move around and do not stay in one place for long periods of time.

4. Examination and comparison of the effectiveness of personal ventilation (PV ATDs) with angled desk fans (DF) and chair fans (CF) in busy office settings.

5. Studying the economic aspect of different forms and types of personal peripheral ventilation devices (PV ATDs, DF, and CF).

REFRENCES

References

[1] Seppanen O. , Fisk W.(2006). Some quantitative relations between indoor environmental quality and work performance or health, HVAC&R Res. 12 (4) 957-973.

[2] Wyon D., Wargocki P.(2013). How indoor environment affects performance, ASHRAE J. ,55 (3) , 46-52.

[3] Mustakallio, P., Kosonen, Risto, & Melikov, Arsen. (2016). The effects of mixing air distribution and heat load arrangement on the performance of ceiling radiant panels under cooling mode of operation. Science & Technology for the Built Environment 23(7), 1-15.

[4] Mustakallio, P. , Bolashikov, Z. , Rezgals, L. , Lipczynska, A. , Melikov, A. , & Kosonen, R. (2017). Thermal environment in a simulated double office room with convective and radiant cooling systems. Building & Environment, 123:88-100

[5] Zou L., Ruan F., Huang M., Liang L., Huang H., Hong Z., Yu J., Xia J., Guo Q., Yen H., Wu J.(2020). SARS-CoV-2 viral load in upper respiratory specimens of infected patients. The New England Journal of Medicine. 382:1177–1179.

[6] Ipinski T., Ahmad D. , Serey N. , Jouhara H.(2020). Review of ventilation strategies to reduce the risk of disease transmission in high occupancy buildings , International Journal of Thermo fluids, 7(8) :100045.

[7] Li X., Cao G., & Yang B. (2022). Occupant targeting ventilation brings clean air to occupants. REHVA Journal, 59(2), 30-35.

[8] Kazanci,O., Khovalyg, D., Lida, T., Uno, Y., Ukiana,T., Olesen, B.W.(2018). Expermental comparison of the thermal indoor environmental created by a radiant,and a combined radiant and convective cooling system .Proceeding-Roomvent&Ventilation 120, 223-228.

[9] Yang Zhang , Wenxuan Yu , Youli Li and Han Li (2020) .Comparative research on the air pollutant prevention and thermal comfort for different types of ventilation. Indoor and Built Environment,30(8), 1–14.

[10] Yang B., Melikov A., Kabanshi A., Zhang C., Bauman F., Cao G., Awbi H., Wigö H., Niu, J., Cheong D., Wai T.K., Sandberg M., Nielsen P., Kosonen R., Yao R., Kato S., Sekhar C., Schiavon S., Karimipanah T., Li X., Lin Z.(2019). A review of advanced air distribution methods-theory, practice, limitations and solutions. Energy and Buildings,202, 109359.

[11] Melikov A.K.(2020) COVID-19: Reduction of airborne transmission needs paradigm shift in ventilation, Building and Environment, 186 , 107336.

[12] Haider Latif, Goran Hultmark, Samira Rahnama, Alessandro Maccarini. (2022).Performance evaluation of active chilled beam systems for office buildings A literature review, Sustainable Energy Technologies and Assessments ,52(2),101999.

[13] Waterloo Air Products plc.(2012) An introduction to chilled beams and ceilings. Version1.

[14] Alan Kabanshi .(2017). Experimental study of an intermittent ventilation system in high occupancy spaces. University of Gävle, Faculty of Engineering and Sustainable Development ,PHD Thesis.

[15] Lipczynska A., Jan Kaczmarczyk J. ,Melikov A.(2021).The Energy-Saving Potential of Chilled Ceilings Combined with Personalized Ventilation, Energies , 14(4), 1133.

[16] Zhao B, Li X, Li D, Yang J .(2012). Revised air-exchange efficiency considering occupant distribution in ventilated rooms. " Air and Waste Management 53, 759–763.

[17] Khan Y., Bhandari, M., Math, J.(2017). Energy-saving potential of a radiant cooling system in different climate zones of India." Science and Technology for the Built Environment, 24(3).

[18] Franchesca G. ,Gonzalez O. ,Tomohito Matsuo Hikari Shimadera Akira Kondo . (2017). Use of local age of air to study the relation between ventilation efficiency and building configuration. Journal of Heat Island Institute International ,12-2 .

[19] Gao, S., Wang, Y., Zhang, S., Zhao, M., Meng, X., Zhang, L.,Jin, L. (2017) Numericalinvestigation on the relationship between human thermal c omfort and thermal balance under Radiant Cooling System. Energy Procedia, 105, 2879 2884.

[20] Szczepanik-Ścisło, N.(2018). Personal ventilation modeling using a CFD analysis . WSN,57 , 426-435.

[21] Liu J. , Li ,Z., Kim, M K, Zhu ,S. , Zhang, L. , Srebric ,J. (2019).A comparison of the thermal comfort performances of a radiation floor

cooling system when combined with a range of ventilation systems" , Indoor and Built Environment, 0(0) ,1–16 .

[22] Li Z. , Zhang D. , Li C .(2020). Experimental Study on Thermal Response Characteristics of Indoor Environment with Modular Radiant Cooling System. Energies , 13(19), 5012.

[23] Qin, S. Y. , Cui, X. , Yang, C. and Jin ,L. W.(2020). Thermal comfort analysis of radiant cooling panels with dedicated fresh-air system , Indoor and Built Environment, 0(0) : 1–13.

[24] Khalil, S., Ghali, K., Ghaddar, N. & Itani, M.(2020). Hybrid mixed ventilation system aided with personalised ventilation to attain comfort and save energy. " International Journal of Sustainable Energy 39(4), 1-18, Pages 964-981 .

[25] Katramiz, E., Assaad, D. A., Ghaddar, N. , Ghali, K. (2020) .The effect of human breathing on the effectiveness of intermittent personalized ventilation coupled with mixing ventilation. " Building and Environment ,174,106755.

[26] Ihab H .H., Azian H., Ahmad F.I.(2020) .CFD Analysis on Effect of Air Inlet and Outlet Location on Air Distribution and Thermal Comfort in Small Office , CFD Letters 12, 66-77.

[27] D Al Assaad, K. Ghali, N Ghaddar. (2020). Comparison of chilled ceiling and Mixing ventilation assisted by intermittent personalized ventilation: Thermal comfort and Energy savings. RE&PQJ, 18 ISSN 2172-038 X, No.17 .

[28] Itani, M. , Ghaddar, D. , Ghaddar,N. & Ghali,K.(2021) Model-based multivariable regression model for thermal comfort in

naturally ventilated spaces with personalized ventilation , Journal of Building Performance Simulation 14(1),78-93.

[29] Alsaad,H. , C.Voelker,C. (2021). Could the ductless personalized ventilation be an alternative to the regular ducted personalized ventilation . Indoor Air ,31,99-111.

[30] Lipczynska , A., Kaczmarczyk, J., Melikov, A. K.(2015). Thermal environment and air quality in office with personalized ventilation combined with chilled ceiling . "Building and Environment, 92, 603-614.

[31] Yuan Y, Zhoua X, Zhang X.(2015). Experimental study of heat performance on ceiling radiant cooling panel. Procedia Engineering, 121, 2176 – 2183.

[32] Lestinen, S. , Mustakallio, P., Kilpeläinen, S., Kosonen, R., Jokisalo, J., Koskela, H. , Arsen K. Melikov .(2019) .Experimental comparison of thermal conditions in office rooms: diffuse ceiling ventilation, chilled beam system and chilled ceiling combined with mixing ventilation", Science and Technology for the Built Environment.

[33] Wu X., Gao J., Wang H., Wang S. , Wang F. (2020) . Impact of chilled ceiling on indoor air distribution in a room with mixing ventilation. Science and Technology for the Built Environment,26 ,366-376.

[34] Tian Z., Yang L. and Wu X., Guan Z.(2020). A field study of occupant thermal comfort with radiant ceiling cooling and overhead air distribution system. Energy & Buildings ,223: 109949

[35] Xu C., Wei X., Liu L. , Su Li , Liu W. , Wang Y. , Nielsen P.V. (2020).Effects of personalized ventilation interventions on airborne infection risk and transmission between occupants. Building and Environment , 180 , 107008

[36] Chakroun W., Alotaibi S., Ghaddar N., GhaliK.(2020). Improved thermal comfort and sensation with occupant control of ceiling personalized ventilation system: A Lab Study . World Academy of Science, Engineering and Technology International Journal of Architectural and Environmental Engineering, 14(11).

[37] Auerswald S., Hörberg C., Pflug T., Pfa_erott J., Bongs C. , Henning H.M.(2020). Experimental investigation of the air exchange effectiveness of push-pull ventilation devices . Energies, 13, 5817.

[38] Mi-Su Shin, Ji-Su Choi and Kyu-Nam Rhee.(2021). Cooling capacity and energy performance of open-type ceiling radiant cooling panel system with air circulators . Energies, 14(1) , 5.

[39] Chludzinska M., Bogdan A. (2015) . The effect of temperature and direction of airflow from the personalized ventilation on occupants' thermal sensations in office areas . " Building and Environment , 85 : 277- 286.

[40] Ning B., Chen Y., Liu Hui. , Zhang S. (2016).Cooling capacity improvement for a radiant ceiling panel with uniform surface temperature distribution. Building and Environment, 102: 64 -72.

[41] Mahdi A.A., Hassan Z. (2016). Experimental and Numerical Study of Air Flow Diffusion and Contaminants Circulation in Room Ventilation Related with Iraqi Climate. International Journal of Mechanical Engineering and Applications 4, 24-42.

[42] Al Assaad D., Ghali K., Ghaddar N., Habchi C.(2017). Mixing ventilation coupled with personalized sinusoidal ventilation: optimal frequency and flow rate for acceptable air quality Energy and Buildings , 154,569-580.

[43] Al Assaad D., Ghali K., Ghaddar N (2018). Effectiveness of intermittent personalized ventilation assisting chilled ceiling for enhanced thermal comfort and acceptable indoor air quality. Building and Environment 144 , 9–22.

[44] Al Assaad D., Ghali K., Ghaddar N., Habchi C.(2018).Intermittent personalized ventilation coupled with mixing ventilation for occupant protection against active and passive contaminants and energy savings , International Conference on Renewable Energies and Power Quality RE&PQJ , 1(16), ISSN 2172-038 .

[45] Shi-Jie Cao , Hua-Yan Deng, Yelin Deng.(2018). Ventilation inlets design based on ventilation performance assessment using a dimensionless time scale, Indoor and Built Environment , 28: 116320.

[46] Yuan Y., Zhou X. & Zhang Xu .(2019).Numerical and experimental study on the characteristics of radiant ceiling systems. Building Research & Information, 47(8),912-927.

[47] Su X. , Zhang L. , Liu Z. , Luo Y., Lian J(2019) . A computational model of an improved cooling radiant ceiling panel system for optimization and design. Building and Environment, 163:106312.

[48] Imre Csáky, Tünde Kalmár and Ferend Kalmár . (2019). Operation testing of an advanced personalized ventilation system. " Energies, 12, 1596 .

[49] Jin W., Jing J., Jia L. , Wang Z.(2020) .The dynamic effect of supply water flow regulation on surface temperature changes of radiant ceiling panel for cooling operation. Sustainable Cities and Society, 52, 101765.

[50] Xie D., Wang C., Yu C., Wan Y.(2020) . Performance of capillary ceiling cooling panel on ceiling surface temperature and indoor thermal environment. Indoor and Built Environment, 29(6).

[51] Ye M., Serageldin A.A. and Nagano K(2020). CFD simulation on the thermal performance of a novel radiant ceiling cooling panel (RCCP) system with segmented and concave surface combined with forced ventilation. Energy Reports, 6,1519-1524.

[52] Khalil S., Ghali K., Ghaddar N. & M. Itani.(2020). Hybrid mixed ventilation system aided with personalised ventilation to attain comfort and save energy. " International Journal of Sustainable Energy 39(4), 1-18, Pages 964-981 .

[53] Zhang F., Guo H., Zhengxuan L., Zhang G.(2021). A critical review of the research about radiant cooling systems in China. Energy and Buildings, 235(52) :110756.

[54] Katramiz E., Assaad D. A., Ghaddar N., Ghali K. (2021). The effect of human breathing on the effectiveness of intermittent personalized ventilation coupled with mixing ventilation. " Building and Environment 174,106755.

[55] Al Assaad D., Ghali K., Ghaddar N (2018). Effectiveness of intermittent personalized ventilation assisting chilled ceiling in protecting occupants against active particles, Conference: ASME

Heat Transfer Summer Conference collocated with the ASME 13th International Conference on Energy Sustainability .

[56] Hussain Aziz Saheb Tarish(2021). Study the Indoor Air Quality by using Mixing and Personal Ventilation Systems in Iraq master Thesis.

[57] Fluent Inc. Airpak(3.0.16). User's Guide. Fluent Inc; 2007

[58] Gao, S., Wang, Y. A., Zhang, S. M., Zhao, M., Meng, X. Z., Zhang, L. Y., Jin, L. W. (2017). Numerical investigation on the relationship between human

thermal comfort and thermal balance under radiant cooling system. Energy Procedia, 105, 2879-2884.

[59] Liang, C., Li, X., Shao, X., & Li, B. (2020). Direct relationship between the system cooling load and indoor heat gain in a non-uniform indo environment. Energy, 191, 116490.

[60] B.F. Inc.(2010). Fluent User’s Guide in Fluent Incorporated Lebanon NH.

[61] Yakhot, V. S. A. S. T. B. C. G., Orszag, S. A., Thangam, S., Gatski, T. B., &Speziale, C. G. (1992). Development of turbulence models for shear flows by a double expansion technique. Physics of Fluids A: Fluid Dynamics, 4(7), 1510-1520.

[62] Shbeeb A. and Mahdi A. (2016) .Experimental and numerical investigation of displacement ventilation system with assessment of four turbulence models. Ms.Ctheses. Babylon University.

[63] Chen, Q. (1995). Comparison of different k-ε models for indoor air flow computations. Numerical Heat Transfer, Part B Fundamentals, 28(3), 353-369.

[64] Chong, J. L. S., Husain, A., & Tuan, T. B. (2005). Simulation of airflow in lecture rooms. In Proceedings of the AEESAP International Conference (pp. 7-8).

[65] ASHRAE. 2017. ANSI/ASHRAE Standard 55-2017, " Thermal Environmental Conditions for Human Occupancy ", Atlanta: American Society of Heating, Refrigerating and Air-conditioning Engineers.

[66] Accuweather,https://www.accuweather.com/ar/iq/baghdad/207375/julyweather/207375?year=2020

[67] J. P. Holman. Heat transfer. nine Edition. 1997.

[68] ASHRAE Fundamentals Handbook. 2013.

[69] EN 15251.(2007). "Indoor Environmental Input Parameters for Design and Assessment of Energy Performance of Buildings Addressing Indoor Air Quality, Thermal Environment, Lighting and Acoustics, European Committee for Standardization", Brussels.

[70] EN ISO 7730.(2007) "Ergonomics of the Thermal Environment - Analytical Determination and Interpretation of Thermal Comfort Using Calculation of the PMV and PPD Indices and Local Thermal Comfort Criteria", European Committee for Standardization, Brussels.

[71] Müller D., Kandzia C., Kosonen R., Melikov A., Nielsen P. (2013).Mixing Ventilation - Guidebook on Mixing Air Distribution

Design, Federation of European Heating, Ventilation and Air Conditioning Associations

[72] Gao, S., Wang, Y. A., Zhang, S. M., Zhao, M., Meng, X. Z., Zhang, L. Y., Jin, L. W. (2017). Numerical investigation on the relationship between human thermal comfort and thermal balance under radiant cooling system. Energy Procedia, 105, 2879-2884.

[73] J. P. Holman. Heat transfer. Tenth Edition. 2010.

[74] Hopfe C, Mcleod R. The passive house designer's manual. Routledge.2015.

[75] Iraqi cooling code, 2012.

[76] Koju, S. M. (2017). Thermal behavior of expanded polystyrene based lightweight concrete sandwich panel at various temperatures. Journal of Science and Engineering, 4, 47-52.

[77] Ayoub, M., Ghaddar, N., & Ghali, K. (2006). Simplified thermal model of spaces cooled with combined positive displacement ventilation and chilled ceiling system. HVAC&R Research, 12(4), 1005-1030.

[78] Wilkins, C., & Hosni, M. H. (2000). Heat gain from office equipment. ASHRAE Journal, 42(6), 33-39.

[79] Huang Shuguang (2011). Experimental and Numerical Study on Personalized Ventilation Coupled with Displacement Ventilation. Master Thesis.

[80] ASHRAE handbook. Heating, HVAC Systems and Equipment (SI). Panel heating and cooling; 2012.

[81] **Kaczmarczyk** J.**, Melikov** A. (2004). Human response to personalized ventilation and mixing ventilation. Indoor air **,14,17-29** .

[82] Melikov A.K.(2004). Personalized ventilation. . Indoor air **,14,157-167**.

[83] ASHRAE Fundamentals Handbook. 2009.

[84] ASHRAE Fundamentals of water system design. 1999

[85] Awbi, H. B. (2017). Ventilation for good indoor air quality and energy efficiency. Energy Procedia, 112, 277-286..

[86] ISO 16000–8: 2007. Indoor Air Part 8: Determination of Local Mean Ages of Air in Buildings for Characterizing Ventilation Conditions. Geneva, Switzerland: International Organization for Standardization

[87] Hormigos-Jimenez, S., Padilla-Marcos, M. A., Meiss, A., Gonzalez-Lezcano, R. A., & Feijó-MuÑoz, J. (2018). Experimental validation of the age-of-the-air CFD analysis: A case study. Science and Technology for the Built Environment, 24(9), 994-1003.

[88] Meiss, A., Feijó-Muñoz, J., & García-Fuentes, M. A. (2013). Age-of-the-air in rooms according to the environmental condition of temperature: A case study. Energy and buildings, 67, 88-96.

APPENDICES

Appendix-A

Appendix-A.1

Supply air temperature(T_s) and flow rate (Q_S) for (CC/MV and CMV/PV) system ((case-I,II and III)

In the case of MV, the initial supply air temperature and velocity of air supply for MV system were (17°C, 2.5 l/s) (according to ASHRAE.2011), to calculated supply air flow rate (Q_S):

$$CL_{MV} = qoe + ql + qex \qquad \text{....}(A-1)$$

$$CL_{MV} = (3q_{person}+2q_{Computer}) + ql$$

for insulated office room (q_{ex} = 0, q_l=100W, q_{oe}=445 W, ρ=1.2m^3/s and C_p=1.005kj/kg.^oC)

$$CL_{MV} = Qs \times cp \times \Delta T \qquad \text{....}(A-2)$$

$$Q_s = m^\circ \times \rho \qquad \text{....}(A-3)$$

After finding the air flow rate from the above equations, by fixed supply air flow rate at (46L/s) for each tests (to notice the change in air age for each test) and change supply air temperature (T_S) with varied the value of cooling load treated by mixing ventilation (CL_{MV}).

$$Q_S = Vx \times As \qquad \text{....}(A-4)$$

$$\text{where assume } Vx = 2.5, [101]$$

$$ACH = Q_S\,Vroom \times 3600 \qquad \text{....}(A-5)$$

Where: Vx: local air speed (m/s), As: Surface area of supply air diffuser (m^2), the area of exhaust grills is about (80 %) of the air supply unit area, [71].

Table(A-1) Calculated values for supply air flow rate and temperature for insulated office cases(case- I,II and III)

η (%)	CL_{MV} (W)	Q_S (m^3/s)	T_S (^oC)
0	445	0.046	17
25	333.75	0.046	19
50	222.5	0.046	21
80	89	0.046	23

Appendix-A.2

HAP PROGRAM RESULTS

Table (A-2) Results of cooling load for non-isolated meeting room by using from (HAP4.9) program

	DESIGN COOLING		
	COOLING DATA AT JulCOOLING OA DB / WB 47 °C / 22 °C		
ZONE LOADS	**Details**	**Sensible (W)**	**Latent(W)**
Window & Skylight Solar Loads	$3 m^2$	277	-
Wall Transmission	$15.5 m^2$	326	-
Roof Transmission	$0 m^2$	0	-
Window Transmission	$3 m^2$	211	-
Skylight Transmission	$0 m^2$	0	-
Door Loads	$2 m^2$	70	-
Floor Transmission	$0 m^2$	0	-
Partitions	$14.5 m^2$	302	-
Ceiling	$0 m^2$	0	-
Overhead Lighting	320 W	320	-
Task Lighting	0 W	0	-
Electric Equipment	210 W	210	-
People	8	600	0

Infiltration	-	0	0
Miscellaneous	-	0	0
>> Total Zone Loads	**-**	**2316**	**0**

Appendix-A.3

Occupied density and occupant air exchange efficiency

- **For insulated office room experimentally**

$$OD_i = \frac{\sum_{i=1}^{N} ID_i}{N} \qquad \text{....}(\mathbf{A-6})$$

$$\langle \tau \rangle_D = \sum_i \langle \tau \rangle_i D_i \qquad \text{....}(\mathbf{A-7})$$

N:Nunber of persons are stays
IDi: Individual OD_i

Number of occupants = 3 occupants
Time of occupants stay in office room = 8:00 am – 3:00 pm

N_1= 6 hour	8:00 am- 3:00 pm
N_2= 6 hour	8:00 am- 3:00 pm
N3= 5 hour	8:00 am- 3:00 pm
N_3= 0.5 hour	8:00 am- 9:00 am
N_3= 1 hour	9:00 am- 10:30 am
N_3= 1.5 hour	10:30 am- 12:30 pm
N_3= 2 hour	12:30 am- 3:00 pm

OD_{t1} at 8:00 am- 9:00 pm

$$OD_{t1} = \frac{\sum_{i=1}^{N} ID_i}{N} = \frac{\frac{1}{1}+\frac{0.5}{1}+\frac{0.5}{1}}{3} = 0.67$$

OD_{t2} at 9:00 am- 10:30 pm

$$OD_{t2} = \frac{\sum_{i=1}^{N} ID_i}{N} = \frac{\frac{1}{1.5}+\frac{1.5}{1.5}+\frac{1}{1.5}}{3} = 0.78$$

OD_{t3} at 10:30 am- 12:30 pm

$$OD_{t3} = \frac{\sum_{i=1}^{N} ID_i}{N} = \frac{\frac{1.5}{2}+\frac{2}{2}+\frac{1.5}{2}}{3} = 0.83$$

OD_{t4} at 12:30 am- 3:00 pm

$$OD_{t4}=\frac{\sum_{i=1}^{N} ID_i}{N}=\frac{\frac{2.5}{2.5}+\frac{2}{2.5}+\frac{2}{2.5}}{3}=0.87$$

Table (A-3)The results of occupant density and occupant air exchange at four times for three cases (case-I,II, and III)

Case	**ηa %**	**ηa)O.D% 0.5 hour**	**ηa)O.D% 1 hour**	**ηa)O.D% 1.5 hour**	**ηa)O.D% 2 hour**
CC/MV	0	%	69	64.17	61.9
CC/MV	25	78	67	62	60
CC/MV	50	75.7	64.9	60	58.1
CC/MV	80	73.5	63	58.46	56.42
CC/MVPV	0	98.6	85	78.5	76
CC/MVPV	25	96.49	83	77	74
CC/MVPV	50	94.44	81	75	72.48
CC/MVPV	80	90.39	77.6	73	69.9
CC/MVPV	0	100.2	89.52	84.5	81.5
CC/MVPV	25	100.1	89.52	83	80
CC/MVPV	50	100	88.48	82	79.2
CC/MVPV	80	99.1	87.7	81.3	78.5

- **For insulated office room numerically**

Table (A-4)The results of occupant density and occupant air exchange at four times for three cases (case-I,II, and III)

Case	**ηa %**	**ηa)O.D% 0.5 hour**	**ηa)O.D% 1 hour**	**ηa)O.D% 1.5 hour**	**ηa)O.D% 2 hour**
CC/MV	0	91.28	78.24	72.59	70
CC/MV	25	87.46	74.97	69.5	67.12
CC/MV	50	84.95	72.8	67.55	65.19
CC/MV	80	81.26	69.65	64.61	62.36
CC/MVPV	0	100.02	90.59	84	81.10
CC/MVPV	25	100	88.74	82	79.4
CC/MVPV	50	96.9	85.74	79.5	76.7

CC/MVPV	80	94.29	83	77	74.6
CC/MVPV	0	100.8	96	89.3	86.2
CC/MVPV	25	100.5	93.6	86.8	83.8
CC/MVPV	50	100.3	91	84.5	81.5
CC/MVPV	80	99.4	87.9	81.6	78.7

- **For non- insulated meeting room :-**

N : Nunber of persons are stays

IDi : Individual OD_i

Number of occupants = 8 occupants

Time of occupants stay in meeting room = 3 hours (10:00am-1:00pm)

OD_{t1} at one hour (10:00 am- 11:000 am)

$OD_{t1} = \frac{\sum_{i=1}^{N} ID_i}{N} = \frac{7}{8} = 0.87$

OD_{t2} at two hour (11:00 am- 12:00 pm)

$OD_{t2} = D_i = \frac{\sum_{i=1}^{N} ID_i}{N} = \frac{6}{8} = 0.75$

OD_{t3} at three hour (12:00 am- 1 pm)

$OD_{t3} = D_i = \frac{\sum_{i=1}^{N} ID_i}{N} = \frac{5}{8} = 0.62$

Table (A-5)The results of occupant density and occupant air exchange at three times for two cases (case-IV and V)

Case	ηa %	$\eta a)_{O.D}$% 1 hour	$\eta a)_{O.D}$% 1.5 hour	$\eta a)_{O.D}$% 2 hour
CC/MV	0	67	76	99
CC/MV	25	63	72	97
CC/MV	50	59	68	91
CC/MV	80	56.9	65	87.7
CC/MVPV	0	80	92	123
CC/MVPV	25	78.8	90	121
CC/MVPV	50	77	88	118
CC/MVPV	80	72	82	101

Appendix B
Deviation of Measuring Devices

B-1 Deviation of the thermocouple:

Thermocouples must be properly calibrated in order to verify the accuracy of the measured temperature readings. The difference between a mercury thermometer reading and a thermocouple reading was determined by placing both inside the mixture, which was made of pure water and crushed ice, and the results are shown in Table (B-1).

The least-squares method defines the average calibration curve of an instrument as a straight line that best matches the scattered data points. The straight line equation is:

$$T_O = mT_i + b \qquad \text{..........(B-1)}$$

m : The slope of a straight line

b : The Intercept with the (To) axis

$$m = \frac{n\sum(T_iT_o) - (\sum T_i)(\sum T_o)}{n\sum(T_i)^2 - (\sum T_i)^2} = 1.0014$$

$$\mathrm{b} = \frac{\sum T_o * \sum(T_i)^2 - \sum(T_iT_o) * (\sum T_i)}{n\sum(T_i)^2 - (\sum T_i)^2} = 0.0723$$

As shown below, the relation's residual percentage is(0.0973 %), where (n) is the total number of data points.

$$\delta = \sqrt{\frac{\sum(mT_i + b - T_o)^2}{n}} = 0.0973$$

The relationship between the temperature values of these two devices is depicted in Figure (B-1). A linear relationship fits the relationship as follows:

$T_{o.} = 1.0014T_i + 0.0723$ ....(B-2)

Table (B-1) The reading of temperatures with time for two device with the range of (0 to 47.6)

No.	Time sec.	Mercury thermometer (T_i) ºC	Thermocouple (T_o) ºC
1	0	0	0.05
2	5	3.5	3.7
3	10	6	6.2
4	15	8.4	8.33
5	20	10.88	11.01
6	25	13.1	13.33
7	30	15.5	15.35
8	35	18.32	18.43
9	40	20.56	20.61
10	45	23.2	23.31
11	50	25.6	25.72
12	55	28.2	28.4
13	60	31	31.13
14	65	34	34.08
15	70	36.44	36.6
16	75	38.2	38.28
17	80	40.3	40.48
18	85	44.4	44.53
19	90	47.6	47.72

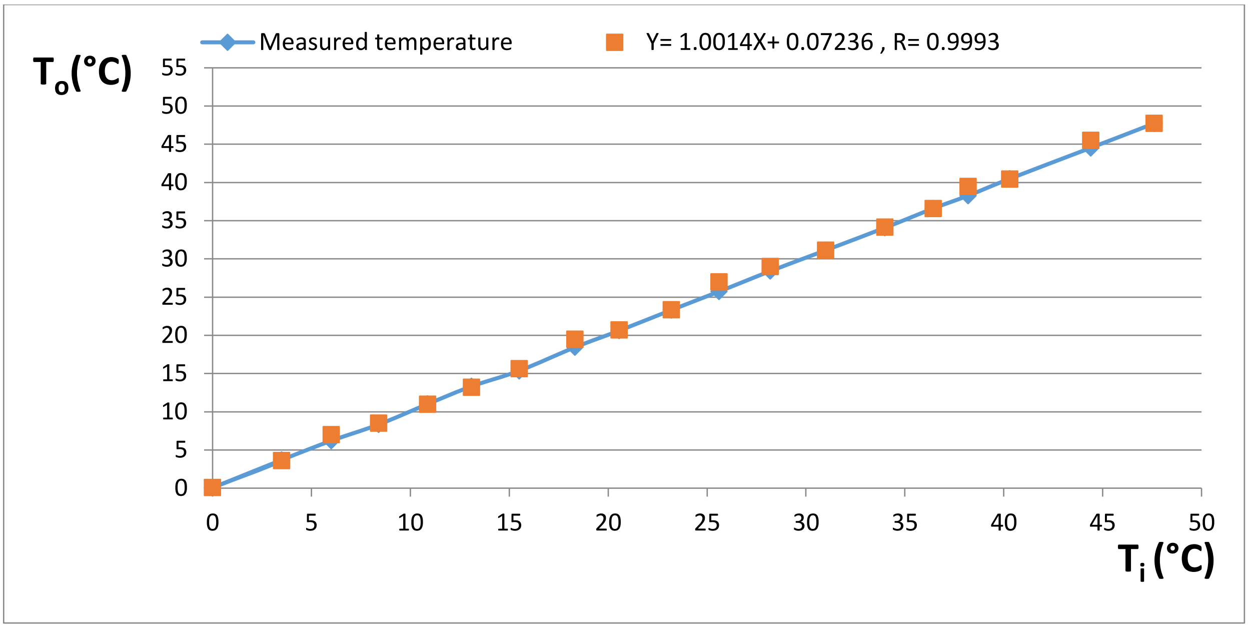

Fig (B-1) The calibration curve of thermocouple temperature reading.

B-1.1 The standard deviation and uncertainty

The standard deviation is a measure of how far the data has diverged from the mean , standard deviation is used to quantify the uncertainty of the data. The standard deviation of the thermocouple was estimated using equations (B-3) and (B-4),]88].

The thermocouple was placed in water at (25°C) to test the deviation for this study, where the measurements are repeated with the same amount (same temperature) to increase the accuracy of the measurements, and the time period for recording the temperature data of the thermocouple was within (45 s), as shown in the table (B-2). The standard deviation is found (0.116°C) by using the two equations at the same temperature as shown in Table (B-2).

$$T_m = \frac{\sum_{i=1}^{n} T_i}{n} \tag{B-3}$$

$$\sigma(T) = \sqrt{\frac{\sum_{i=1}^{n}(T_i - T_m)^2}{n-1}} \tag{B-4}$$

Table (B-2) Measured water temperatures with a thermocouple (at 25 °C)

Reading No.	Reading of thermocouple temperature
1	25.28
2	25.10
3	25.07
4	25.11
5	25.08
6	24.94
7	25.02
8	24.89
9	24.93
10	24.91
11	24.9
12	24.96
13	24.92
14	24.94
15	24.94

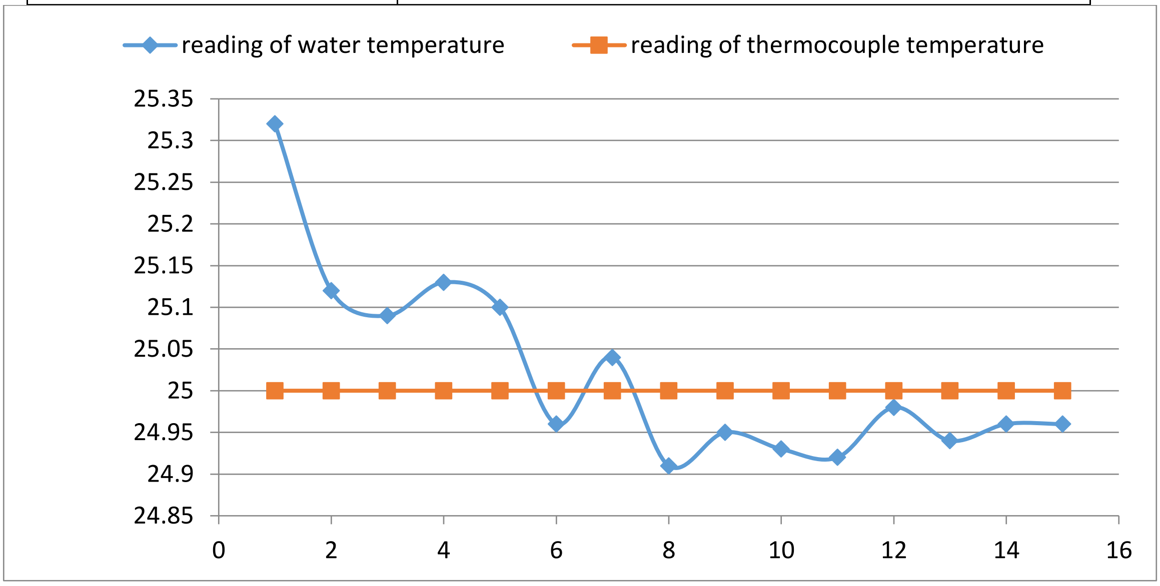

Fig (B-2) The deviation curve of thermocouple temperature reading.

B-2 Calibration of Flow Meter

The measuring cylinder and stopwatch were used to calibrate the flow meter. This method is based on how long it takes to fill a certain amount and how that compares to the flow meter measurement as shown in table

(B-3).The calibration of a flow meter is shown in Fig. (B-3). The standard deviation is (2.59 %).

Table(B-3) The reading of flow meter with flow water

Reading NO	Flow meter reading	Flow water reading
0	0	0
1	0.5	0.56
2	1	1.08
3	1.5	1.61
4	2	2.1
5	2.5	2.59
6	3	3.11
7	3.5	3.61
8	4	4.13
9	4.5	4.66
10	5	5.2

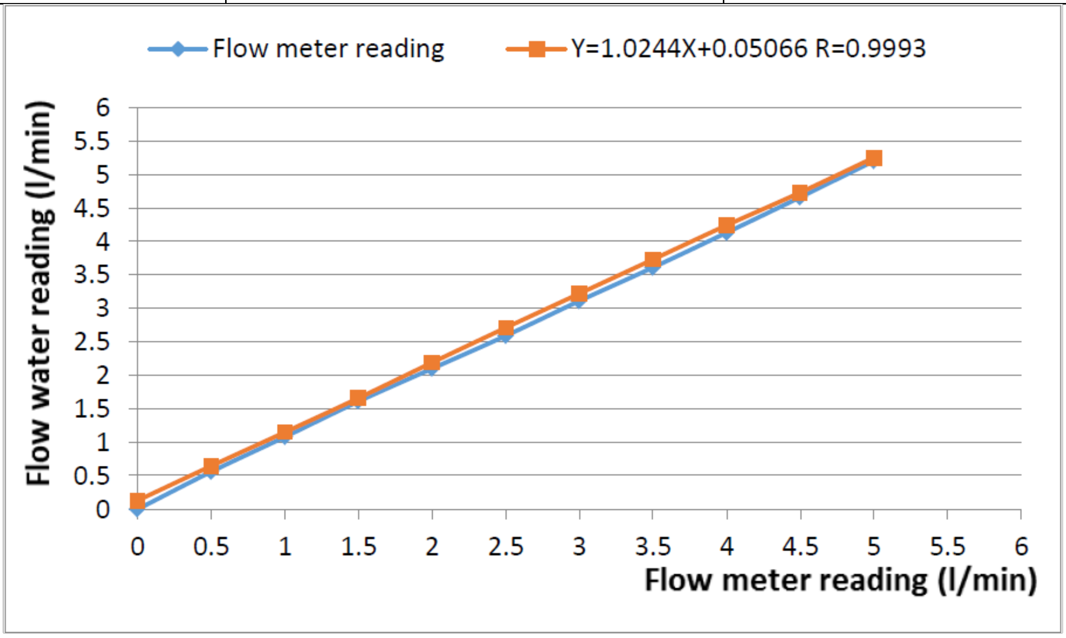

Fig.(B-3) Calibration curve of flow meter

B-3 Certificate of CO_2, Tem., RH data logger

Shenzhen BCTC Technology Co.,Ltd.
A.Floor 3, 44 Building, Tanglang Industrial Park B,
Taoyuan Street, Nanshan District, Shenzhen, China

BCTC

Certificate of Compliance

Certificate Number: BCTC-150403524

Applicant	:	**Dongguan Xintai Instrument Co., Ltd** No 149, Chunfeng Road, Longbeiling, Tangxia Town, Dongguan City, Guangdong, China
Manufacturer	:	**Dongguan Xintai Instrument Co., Ltd** No 149, Chunfeng Road, Longbeiling, Tangxia Town, Dongguan City, Guangdong, China
Product	:	**CO2/Temp./RH Data Logger**
M/N	:	**HT-2000**
Test Standard	:	**EN 55022: 2010** **EN 61000-3-2: 2014, EN 61000-3-3: 2013** **EN 55024: 2010** **EN 61000-4-2: 2009, EN 61000-4-3: 2006+A1:2008+A2:2010** **EN 61000-4-4: 2012, EN 61000-4-5: 2014** **EN 61000-4-6: 2014, EN 61000-4-8: 2010, EN 61000-4-11: 2004**

The EUT described above has been tested by us with the listed standards and found in compliance with the council EMC directive 2014/30/EU. It is possible to use CE marking to demonstrate the compliance with this EMC Directive. It is only valid in connection with the test report number: BCTC-150403524.

CE

SHENZHEN BCTC TECHNOLOGY CO., LTD.
APPROVED
Manager
Apr. 10, 2015

This certificate of conformity is based on a single evaluation of the submitted sample(s) of the above mentioned product. It does not imply an assessment of the whole product and relevant. Directives have to be observed.

Tel: 400-788-9558 0755-33019988 Http://www.bctc-lab.com Http://www.btc-lab.com

جمهورية العراق

وزارة التعليم العالي والبحث
العلمي

جامعة بابل / كلية الهندسة

قسم الهندسة الميكانيكية

استقصاء الظروف الحرارية وتشتت غاز ثاني اوكسيد الكاربون في غرف متعددة من خلال اعتماد السقف المبرد مع منظومة التهوية في مناخ مدينة الحلة

رسالة مقدمة الى قسم الهندسة الميكانيكية في جامعة بابل كجزء من متطلبات نيل درجة
الدكتوراه في الهندسة /الهندسة الميكانيكية/ قدرة

من قبل
ضحى راضي نايف عمران

بأشراف
أ.د. علاء عباس مهدي

1444هـ

2023 م

خلاصه البحث:

نظرًا للانتشار العالمي للأمراض والأوبئة ، فقد حظيت الحاجة إلى الحفاظ على جو داخلي نظيف باهتمام متزايد في السنوات الأخيرة . لذلك ، ستكون هناك حاجة لتقدير وتحديد المناطق التي تؤثر على تعرض الإنسان للملوثات بشكل واضح ، مع الأخذ في الاعتبار الكثافة السكانية المشغولة ، والتي تمثل الأهمية الأساسية لهذه الاطروحة . تمت دراسة سعة السقف المبرد مع تهوية الخلط ونظام التهوية الشخصية ومقارنتها بالسقف المبرد مع تهوية الخلط من حيث متوسط عمر الهواء وتوزيع درجة الحرارة وتركيز ثاني أكسيد الكربون والكفاءة الحرارية ، ومعايير الراحة الحرارية مثل مؤشر التنبؤ بالإحساس الحراري ، والنسبة المئوية المتوقعة لغير الراضين عن الظروف الحرارية ومؤشر أداء انتشار الهواء مع أفضل معدل تدفق للنظام المقترح مع مراعاة الكثافة المشغولة في غرفة مكتب معزولة حرارياً تجريبياً و عدديا في مناخ العراق - مدينة الحلة (مناخ حار وجاف) تم اختيارها كمنطقة بحثية لهذا النظام وتقع في وسط العراق على خطي طول (44.42 درجة مئوية) وخط عرض (32.46 درجة مئوية).

تم استخدام نموذج ديناميكيات السوائل الحسابية ثلاثية الأبعاد في غرفة مكتب معزولة حراريا تتسع لثلاثة أشخاص وفي غرفة اجتماعات تتسع لثمانية أشخاص ، تحت أحمال التبريد (445 واط) ، (2316 واط) على التوالي باستخدام برنامج AIRPAK. تم إجراء اثني عشر اختبارًا لأربعة أحمال تبريد مختلفة تمت معالجتها بالسقف المبرد (0 ، 25 ، 50 ، و 80٪ نسبة إلى إجمالي حمل التبريد) بثبوت معدل تدفق إمداد الهواء (46 لتر / ثانية) مع معدلين لتدفق الهواء الكهروضوئي (5 لتر / ثانية و 7.5 لتر / ثانية) للحالات الثلاث (الحالة الأولى ، الحالة الثانية والحالة الثالثة) التي تمت دراستها تجريبياً وتحليلها عديًا في غرفة مكتب معزولة حرارياً. تمت أيضًا دراسة ثمانية اختبارات عديًا في غرفة الاجتماعات لأربعة أحمال تبريد مختلفة تم معالجتها بسقف مبرد (0 ، 25 ، 50 ، 80٪) مع ثبوت معدل تدفق امداد الهواء (240 لتر / ثانية) ومعدل تدفق الهواء الكهروضوئي (7.5 لتر / ثانية) للحالتين (الحالة الرابعة والحالة الخامسة). تختلف درجة حرارة إمداد الهواء لكل حالة اعتمادًا على حمل التبريد المعالج بخلط التهوية و درجة حرارة هواء الغرفة (25 درجة مئوية). أجريت جميع الاختبارات التجريبية في يوليو في أغسطس وسبتمبر

تم اكتشاف أنه في جميع الحالات ، مع زيادة حمل التبريد المعالج بالسقف المبرد ، يزداد متوسط عمر الهواء مع الارتفاع. نتيجة استخدام التهوية الشخصية ، تنخفض نسبة عمر الهواء إلى أقل من (0.34٪) مقارنة بالسقف المبرد مع تهوية الخلط. لوحظ تحسن بنسبة (14٪) في حماية الركاب من العدوى المتصالبة مع ارتفاع معدلات تدفق هواء التهوية الشخصية. في جميع الحالات لوحظ أن قيم (مؤشر التنبؤ بالإحساس الحراري، والنسبة المئوية المتوقعة لغير الراضين عن الظروف الحرارية) انخفضت من (0.33٪ - 0.36) ، (0.25٪ -0.30) على التوالي مع السقف المبرد مع تهوية الخلط ونظام التهوية الشخصية مقارنة بالسقف المبرد مع نظام تهوية الخلط عند (80-0٪). زادت فعالية إزالة الحرارة بنسبة (٪ 4-5.12) عند (80-0٪) في السقف المبرد مع تهوية الخلط ونظام التهوية الشخصية مقارنة مع سقف مبرد مع تهوية مختلطة شوهدت أعلى قيم لشخص جالس واقف بين (0.8-0.52 درجة مئوية) لشخص واقف مع سقف مبرد مع نظام تهوية مختلط .أظهرت هذه الدراسة أن السقف المبرد مع تهوية مختلطة و نظام تهوية شخصي بمعدل تدفق (7.5 لتر / ثانية) يوفر راحة حرارية وجودة هواء أعلى في المنطقة

المحتلة بناءً على قيم كفاءة تبادل الهواء وكفاءة تبادل الهواء للركاب بنسبة (٪75 - 72) ، (٪99- 93) على التوالي عند (٪0-80) . ونتيجة لذلك ، فإن معدل التدفق (7.5 لتر / ثانية) هو الخيار الأفضل لحماية الركاب من التلوث المباشر في منطقة التنفس وفي المناخ المحلي المحيط. ، حيث نلاحظ أنه كلما طالت مدة الإقامة ، قل تغير الهواء في الشاغلين بسبب معدل التهوية المنخفض.